Computational Methods in String Theory and Applications to the Swampland Conjectures

Lorenz Schlechter

München 2021

Computational Methods in String Theory and Applications to the Swampland Conjectures

Lorenz Schlechter

Dissertation
an der Fakultät für Physik
der Ludwig–Maximilians–Universität
München

vorgelegt von
Lorenz Schlechter
aus Ravensburg

München, den 09.04.2021

Erstgutachter: Priv.-Doz. Dr. Ralph Blumenhagen
Zweitgutachter: Prof. Dr. Dieter Lüst
Tag der mündlichen Prüfung: 28.05.2021

Zusammenfassung

Das Ziel des Swampland Programms ist die Klassifizierung effektiver, zu Quantengravitationstheorien vervollständigbarer Theorien. Aufgrund der enormen Anzahl an möglichen Stringvacua, zusammengefasst in der sogenannten Stringlandschaft, sind die meisten der bisherigen Resultate des Programms Vermutungen. Jedoch existiert ein beständig wachsendes dichtes Netz aus Abhängigkeiten zwischen diesen Vermutungen.

Ein besseres Verständnis oder ein Beweis dieser Vermutungen würde die erlaubten Niederenergietheorien einschränken. Das Ziel dieser Arbeit ist deshalb die Entwicklung mathematischer Methoden, die explizite Tests der Swampland Vermutungen in stringtheoretischen Modellen ermöglichen. Insbesondere werden Perioden von Calabi-Yau Mannigfaltigkeiten auf numerischem und analytischem Weg berechnet. Darüber hinaus werden Methoden zur Berechnung von Calabi-Yau Metriken, Linienbündelkohomologien und Strebeldifferentialen behandelt.

Diese werden zur Überprüfung zweier Vermutungen eingesetzt, zum Test der Swampland Distanzvermutung sowie zum Test der dS Vermutung. Erstere besagt, dass eine effektive Theorie nur bis zu bestimmten Feldwerten gültig sein kann. Werden diese überschritten werden unendlich viele nicht berücksichtigte Zustände exponentiell leicht und die verwendete effektive Beschreibung bricht zusammen. Diese Vermutung wird durch eine explizite Berechnung von Distanzen zwischen effektiven Theorien in Calabi-Yau Moduliräumen getestet. Die dS Vermutung verbietet hingegen stabile Vacua mit positiver kosmologischer Konstante. Um diese Vermutung zu überprüfen, wird ein Teil der KKLT-Konstruktion explizit durchgeführt. Darüber hinaus wird die Validität der zugrundeliegenden effektiven Theorie in einem „warped throat“ analysiert. Neben diesen traditionellen Herangehensweisen werden exotischere Ansätze für die Konstruktion von dS Räumen untersucht. Dies umfasst Tachyonenkondensation sowie andere Raumzeitsignaturen.

Abstract

The goal of the swampland program is the classification of low energy effective theories which can be consistently coupled to quantum gravity. Due to the vastness of the string landscape most results of the swampland program are still conjectures, yet the web of conjectures is ever growing and many interdependencies between different conjectures are known.

A better understanding or even proof of these conjectures would result in restrictions on the allowed effective theories. The aim of this thesis is to develop the necessary mathematical tools to explicitly test the conjectures in a string theory setup. To this end the periods of Calabi-Yau manifolds are computed numerically as well as analytically. Furthermore, tools applicable to general string phenomenological models are discussed, including the computation of target space Calabi-Yau metrics, line bundle cohomologies and Strebel differentials.

These periods are used to test two conjectures, the refined swampland distance conjecture as well as the dS conjecture. The first states that an effective field theory is only valid up to a certain value of field excursions. If larger field values are included, the effective description breaks down due to an infinite tower of states becoming exponentially light. The conjecture is tested explicitly by computing the distances in the moduli space of CY manifolds. Challenging this conjecture requires the computation of the periods of different Calabi-Yau spaces. The dS conjecture on the other hand forbids vacua with positive cosmological constant. To test this conjecture, the KKLT construction is examined in detail and some steps of the construction are carried out explicitly. Moreover, the validity of the assumed effective theory in a warped throat is investigated. Besides these traditional approaches more exotic ones are followed, including the construction of dS theories using tachyons as well as modifying the signature of space time.

Contents

List of Figures

List of Tables

Chapter 1

Introduction

Over a century ago Einstein formulated his famous general theory of relativity, describing the observed gravitational effects to impressive precision. Since then experiments confirmed the predictions of the theory, culminating in the observation of gravitational waves by LIGO [6]. While the theory of general relativity describes the universe on a large scale, it was found that quantum field theories (QFT), especially non-abelian gauge theories, are well suited to describe the small scales appearing in atomic and particle physics. The standard model has tremendous success in predicting the scattering amplitudes of elementary particles. But while experiments have confirmed both theories to high precision, they contradict each other on a very fundamental theoretical level. The ground states in QFTs produce infinite vacuum energy. In the QFT itself this does not cause any problems, as only energy differences matter. But as the curvature of space-time couples to energy densities, the absolute value of the energy density plays and important role in the theory of general relativity. An infinite energy density would cause a gravitating universe to collapse to a point, something which is certainly not observed. On the other hand, trying to formulate Einstein gravity in terms of a QFT causes problems as the gravitational force, mediated by a massless spin 2 field, is a non-renormalizable force. The unification of gravity with quantum field theories is one of the unresolved problems in theoretical physics.

A possible way out of this situation is given by string theory. Originally string theory was developed to describe the strong interaction. It was observed that the hadronic spectrum follows so-called Regge trajectories, i.e. the mass squared of the hadrons is a linear function of the angular momentum of the hadrons. Such behaviour is a typical sign of spectra arising from strings. It is known today that the strong interaction is best described using quantum chromodynamics and later experiments showed that Regge trajectories are only approximately linear, which is why string theory is no longer a candidate theory for the strong interaction. But it was soon realized that the spectrum of closed strings naturally contains a massless spin 2 field, a graviton. This turned string theory into a quantum theory of gravity. Moreover, it has many favourable properties one would wish for a fundamental theory of everything. There is only a single free parameter, the tension of the string. Everything else, for example the coupling constants, the mass spectra and the field content, is predicted by the theory. The theory also enjoys a high amount of

symmetries, which allow to compute the partition functions as well as rendering the theory finite. The extended nature of the strings smooths the interactions such that the typical divergences plaguing QFTs are absent. The theory also includes even higher dimensional objects in form of so-called D-branes, which carry a gauge field on their world-volume and thereby allow for a geometric construction of non-abelian gauge theories. And finally, and probably most importantly, the theory even predicts the number of dimensions in which it can be consistently formulated. But this is the point where the nice features end. The mathematical consistency requires the theory to be formulated in more than 4 dimensions, either 26 for the original bosonic version or 10 for a supersymmetric variant. While there also exists a 4-dimensional variant, this turned out to describe pure self-dual gravity in a Euclidean space and does not look like our world at all. As only 4 dimensions are observed, it is necessary to somehow remove the additional 6 dimensions. To obtain a phenomenologically viable theory, one thus assumes that 6 of the 10 dimensions are compactified, i.e. their radii are taken to be too small to be observed by today's experiments. The masses, coupling constants and quantum numbers of the particles in the resulting 4-dimensional low energy effective theory are then determined by the properties of this 6-dimensional internal space. The problem with finding a theory describing our world is thus turned into the problem of finding the correct 6-dimensional geometry. The string equations of motion require this geometry to be Ricci flat, or equivalently to be a so-called Calabi-Yau(CY) space. The number of possible real 6-dimensional CY spaces is vast, at least of the order of several hundreds of millions. It is not even known if this number is finite. As each geometry corresponds to a different low energy effective theory, this gives rise to the so-called string landscape of possible theories. Due to the enormous amount of possibilities it is hopeless to try them all. Thus a mechanism which chooses the correct theory is needed, the so-called vacuum selection mechanism. When it became clear that such a mechanism is at least for the moment out of reach, the research in string phenomenology shifted away from constructing our world explicitly to restricting the possibilities. Despite the vastness of the landscape, it does not contain every possible low energy theory. The theories which are not contained in the landscape are said to lie in the swampland. While string theory is used as the prime example of a quantum theory of gravity, the swampland is assumed to be a general feature of quantum gravity independent of string theory itself. The assumption that string theory captures all relevant aspects and possible theories of quantum gravity is known as the string lamppost principle [7] or string universality. String theory gives explicit examples of consistent theories which are completely under computational control. But this control requires extended supersymmetry, as only in this case non-renormalization theorems hold. Non-supersymmetric string theories are much less understood. This could lead to a bias in the studied theories, thus it is important to construct new examples, including non-supersymmetric ones.

A theory which is in the swampland cannot be consistently coupled to quantum gravity in the UV. The aim of the swampland program is to find criteria when a low energy theory is in the swampland, or equivalently when it cannot be completed in the UV. It was initiated by the seminal work of Ooguri and Vafa [8, 9]. This paper introduced the swampland distance conjecture, which predicts an infinite tower of states to become

exponentially light when scalar fields take large trans Planckian values. This was only the first of many conjectures which are now known to form a tight web of interrelations. Many of these conjectures originate from black hole arguments [10], but were confirmed to hold in various string theoretic examples. While these conjectures are expected to hold in all theories of quantum gravity, we will focus on string theory, as this is the only theory of quantum gravity available to us developed far enough and providing sufficient computational control to test the conjectures.

The goal of this thesis is to challenge some of these conjectures in the string theory setting. To this end detailed computational methods necessary to construct explicit string models are developed. This reaches from the computation of so-called period integrals and finding Ricci-flat metrics in 6-dimensional spaces over computing partition functions of two-dimensional supersymmetric field theories to the construction of exotic string theories. This thesis is organized as follows:

After a short introduction chapter 2 begins with an overview of string theory, showing the plethora of possible string constructions as well as their interrelations and introduce the concept of compactification.

In chapter 3 methods for computing string theory vacua are developed. The main focus lies on the computation of the periods of CY manifolds in a symplectic basis. We start by constructing CY spaces in terms of hypersurfaces in toric varieties and complete intersections thereof. Using this formulation, the periods are computed on the complex structure or B-model side exploiting the properties of a system of differential equations, the so-called Picard-Fuchs (PF) system. To obtain the A-model periods the B-model periods are then mapped to the Kähler side using mirror symmetry. We develop an algorithm to compute analytic expressions for the periods at arbitrary points in the moduli space . This allows a computation of the periods close to conifold singularities in moduli space. The periods are expressed in terms of a local basis which gets mapped to the symplectic basis by a transition matrix. We show that the entries of this matrix can be expressed in terms of an ϵ-expansion of hypergeometric functions. The hypergeometric ${}_2F_1$ functions related to elliptic fibers are well studied, while the higher hypergeometric functions corresponding to shrinking divisors or CYs are much less understood. The same functions and expansions appear in the study of Feynman integrals, which allows us to use the rich literature in this area for our computations. We finally point out the connection to number theory and how the entries of the transition matrix are related to L-function values.

In the next section another possible description of CY spaces is introduced, which applies the gauged linear sigma models instead of the toric construction. These models allow the computation of the Kähler potential directly on the A-model side without referring to mirror symmetry. As this construction is not based on toric geometry, it is also possible to describe more exotic geometries which do not necessarily have a toric pendant. Since supersymmetric localization techniques are required for the computation of the partition function, the method is only applicable in $\mathcal{N} = 2$ supersymmetric theories. As the method results directly in expressions for the Kähler potential without determining the periods, it allows for a fast computation of the moduli space metric. Thus the GLSM approach is well suited for tests of the refined distance conjecture, but the supersymmetry requirement

prevents an application to flux vacua as these break parts of or all of the supersymmetry. In the next section of this chapter the state-of-the-art techniques for the computation of numerical CY metrics are discussed. This includes Donaldson's T-operator, minimization of the Calabi-energy as well as (holomorphic) neural networks. Knowledge of the target space metric is a requirement for the computation of the spectrum of the Laplacian. Furthermore, this would give a non-trivial test of of the results obtained by algebraic geometry.

Following this we discuss the computation of line bundle cohomologies. These are for example required for heterotic compactification. It is shown that by using machine learning techniques it is possible to determine analytic expressions for a given geometry in a fully automatized way if only a small sample of values are known. As this sample can be generated by the well-known CohomCalc algorithm, this solves the problem completely.

In the last section of this chapter we give a new method for computing analytic expressions for Strebel differentials of n-punctured spheres based on Belyi maps. There are existing algorithms for these computations, but for generic points in moduli space these become unmanageable. Thus only very few explicit examples are known. These differentials are relevant for the computation of closed string scattering amplitudes and solve a minimal area problem. Moreover, we point out a possible connection of this computation to the mirror map of CY manifolds, as the mirror map itself can be interpreted as a Belyi map.

After this mathematical chapter the swampland conjectures are introduced in chapter 4 and the refined swampland distance conjecture is discussed in detail. Using the moduli space metrics of the previous chapter, the range of validity of effective theories in CY moduli spaces is studied. The results are all in agreement with the refined distance conjecture. As the radii of the phases decrease with $h^{1,1}$, as has been seen in a 101-dimensional example, it is to be expected that the conjecture holds in general, although it is still unproven.

In chapter 5 we put our focus on the validity of the KKLT construction. This represents an explicit construction of 4-dimensional dS space in string theory. One of the swampland conjectures forbids the existence of such solutions. We find an explicit string theory setting in which the first ingredients of the construction are realized. I.e. we give a solution in which all complex structure moduli are stabilized close to a warped throat in form of a conifold, while the superpotential takes exponentially small values. Moreover, we show that light KK modes localized in the warped throat lead to corrections of the effective low energy theory. But these corrections are of the same functional form as the tree-level result, rendering these corrections only mildly dangerous and not fatal for the theory.

As the construction of dS space turns out to be difficult in the usual string lamppost of type II, F-theory or heterotic models, in chapter 6 we turn our attention to more exotic constructions which could lead to dS spaces. First we review the tachyon induced transitions between theories in different number of dimensions. Starting from non-supersymmetric tachyonic heterotic string theories, the transitions lead to stable dS vacua at late times, albeit with a linear dilaton background. Moreover, all known transitions seem to respect the cobordism conjecture. The obtainable stable dimensions correspond exactly to the allowed compactifications which do not suffer from a bubble of nothing instability. Similarly, the condensation of the bosonic bulk tachyon is studied. The endpoint of this condensation

is unclear, but using a supersymmetric embedding it can be shown that the previously known non-perturbative minimum is unstable in new directions arising from the addition of world-sheet fermions. As the number of dimensions and even the signature can change in tachyon condensations, we then ask the question if the dS conjecture holds also for different space-time signatures as well as for different world-sheet signatures. To this end Euclidean CFTs corresponding to open strings are developed and the phenomenology of these theories is studied. It turns out that for each non-standard target-space signature there is a single brane in the Euclidean CFT with a ghost-free gauge sector. As the orientifolds required to cancel the RR tadpole induced by these branes are exactly the orientifolds eliminating the dS solutions, the dS conjecture is extended to these more exotic theories. While it turns out that the studied theories do not give a loop-hole in the dS conjecture, the large amount of consistency in the a priori absurd theories shows that much more is possible in string theoretic constructions once one abandons the usual lamppost.

Finally, chapter 7 gives an outlook of possible future work, including new computational techniques for the hypergeometric periods, the computation of Pfaffians for the stabilization of Kähler moduli and the application of numerical CY metrics to the computation of the KK spectrum of warped throats.

This thesis is based on the following papers:

- **Small Flux Superpotentials for Type IIB Flux Vacua Close to a Conifold**
  Rafael Álvarez-García, Ralph Blumenhagen, Max Brinkmann, Lorenz Schlechter
  arXiv: 2009.03325[hep-th]

- **dS Spaces and Brane Worlds in Exotic String Theories**
  Ralph Blumenhagen, Max Brinkmann, Andriana Makridou, Lorenz Schlechter, Matthias Traube
  JHEP 06 (2020) 077 arXiv: 2002.11746 [hep-th]

- **Closed Bosonic String Tachyon Potential from the $\mathcal{N} = 1$ Point of View**
  Lorenz Schlechter
  arXiv: 1905.09621 [hep-th]

- **Swampland Variations on a Theme by KKLT**
  Ralph Blumenhagen, Daniel Kläwer, Lorenz Schlechter
  JHEP 05 (2019) 152 arXiv: 1902.07724 [hep-th]

- **Machine Learning Line Bundle Cohomologies of Hypersurfaces in Toric Varieties**
  Daniel Kläwer, Lorenz Schlechter
  Phys.Lett.B 789 (2019) 438-443 arXiv: 1809.02547 [hep-th]

- **The Refined Swampland Distance Conjecture in Calabi-Yau Moduli Spaces**
  Ralph Blumenhagen, Daniel Kläwer, Lorenz Schlechter, Florian Wolf
  JHEP 06 (2018) 052 arXiv: 1803.04989 [hep-th]

Chapter 2

Basics of String Theory

This thesis will be mainly focused on the application of computational methods to the problems arising in string theoretic models. We will start with a short review on the fundamentals of string theory. This chapter is based on the discussion in [11] and follows the notation therein. The first section begins by introducing bosonic string theory. This theory will turn out to be consistently formulated in 26 dimensions. To obtain a supersymmetric version of the theory, fermions living on the world-sheet will be added, which will reduce the number of dimensions to 10. As only 4 dimensions are observed in our world, the additional six dimension will be compactified to obtain a phenomenologically viable theory. It will turn out that the compactification space required for this is a Calabi-Yau(CY) manifold.

2.1 Conceptual Ideas

Before the construction of string theory is described in detail, some basic ideas appearing in the theory are discussed. This section is not mathematically rigorous and aims to give a reader unfamiliar with string theory an overview of the concepts.

The main problem of gravitational amplitudes lies in the point like interactions. A way out of this is to assume extended fundamental objects that "smear" the interaction. This removes the dangerous point-like interactions from the theory. The scattering amplitudes in a QFT computation are obtained by summing over the different Feynman diagrams. Each vertex of the diagram comes with one factor of the coupling constant g. Thus the sum over the Feynman diagrams corresponds to an expansion of the path integral in the coupling constant. Similar, string theory has a single parameter, the string coupling constant. The sum over Feynman diagrams gets replaced by a sum over possible world-sheet geometries. For closed strings, the relevant geometries are 2-dimensional surfaces without boundaries. These are characterized by a single topological number, the genus g, which, roughly speaking, counts the number of holes of the manifold. A n-loop contribution thus corresponds to a 2-dimensional manifold with n holes. The tree-level amplitude corresponds to the sphere, which has genus 0. The one-loop-level is given by the torus. For open strings the world sheet has a boundary. Thus the relevant geometries are a disc at

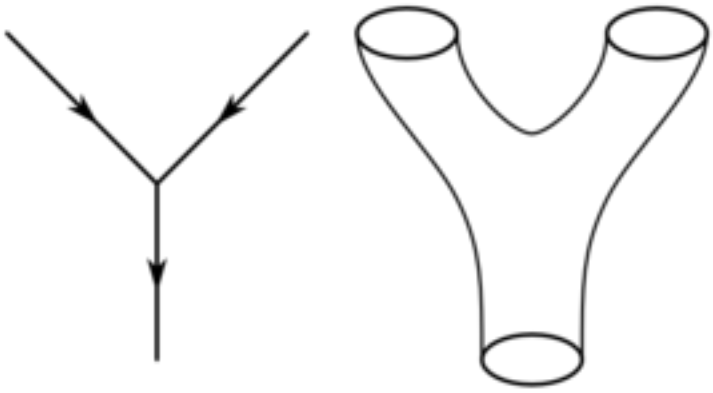

Figure 2.1: Comparison of a QFT amplitude on the left and a closed string amplitude on the right. There is no pointlike interaction in the string case.

tree-level and an annulus at one-loop-level. Intuitively the genus counts the number of holes in the surface. Figure 2.1 shows the two diagrams for a tree-level 3-point amplitude in a QFT as well as in string theory. Note that the string diagram is topologically a sphere with three holes or punctures. While summing over topologies may seem more complicated than summing Feynman diagrams, it also includes some simplifications. There is only a single tree-level diagram for an n-point amplitude in the closed string case, the sphere with n punctures. The tree-level n-point amplitude in a QFT computation can already include several Feynman diagrams. E.g. the 4-point amplitude consists out of 3 contributions, the s, t and u channels.

When computing a string scattering amplitude, one does not only sum over the different topologies, but one also has to integrate over all possible configurations, i.e. positions of the punctures. The symmetries of the sphere allow to fix 3 punctures. But starting from 4 punctures, there is additional freedom. The parameter space of n-punctured Riemann surfaces has interesting modular properties. These are the reason the amplitudes remain finite. A simple example of this is the 1-loop vacuum amplitude of string theory, given by a torus without punctures. This amplitude computes the cosmological constant of the theory. The detailed computation will be described in the next sections. Here we only state that the torus has a $\mathrm{SL}(2,\mathbb{Z})$ symmetry. As usual one integrates only over a fundamental domain of the symmetry group. In the case of $\mathrm{SL}(2,\mathbb{Z})$ this fundamental domain is the so-called Teichmüller space. This space can be chosen to exclude the origin, thereby removing the divergences.

In a QFT, divergences usually arise from momentum integrals of the form

$$\int_0^\infty \mathrm{d}^4k \frac{1}{(k^2-m^2)^n} \ , \tag{2.1}$$

where n is an integer. For $n \geq 2$ these integrals become divergent. If the theory would

have a symmetry

$$k \to \frac{1}{k} \,, \tag{2.2}$$

the integration should only be over the fundamental domain. In this case, there would be 2 fundamental domains, either from 0 to 1 or from 1 to ∞. Choosing the second one, the integral would become

$$\int_1^\infty \mathrm{d}^4 k \frac{1}{(k^2 - m^2)^n} \,, \tag{2.3}$$

which is finite.[1] Exactly the same happens in string theory, only that here the integral is two-dimensional and the fundamental domain is the Teichmüller space.

But this UV finiteness comes at a high cost. As the string is an extended object, it can be internally excited. It behaves exactly like a guitar string which can vibrate in all integer multiplicities of its eigenfrequency. This leads to an infinite tower of massive string states. Moreover, if the space-time geometry includes non-trivial circles, the string can wind around these. These winding modes have a mass proportional to the radius of the circle and also form an infinite tower of states. We will later see that exactly these infinite towers are necessary for the consistency of the theory, but at the same time it is important for phenomenological purposes to suppress the towers enough such that they cannot be seen in today's experiments. This turns out to be a formidable challenge.

As we have seen, choosing an extended object can lead to the removal of the typical UV divergences. String theory starts with the simplest choice for an extended object, a 1-dimensional string. One could ask the question why this is more natural than starting with point like particles or any d-dimensional object. But this is only the starting point of the theory. It turns out that open strings, depending on the boundary conditions, have to end on other extended objects, the so-called Dirichlet D-branes. These can be described equivalently by coherent states of closed strings or by the open strings ending on them. This is known as a open-closed duality. As D-branes of all possible dimensions exist, string theory is really not only a theory of strings. The advantage of taking a string as a starting point is that the world-volume traversed by a string during its lifetime is 2-dimensional. As 2-dimensional gravity is trivial, the world-sheet theory can be quantized consistently as will be described in the next section in detail. If one would start with a 2-dimensional brane or a higher dimensional object, gravity on the world volume would no longer be trivial and it is not clear how to quantize such a theory. There are signs that the true underlying theory is not really a string theory and that string theories are only describing certain limits of an underlying universal theory, often denoted M-theory. The meaning behind the M varies with context, examples include mysterious, membrane, matrix or metaplectic. They all mean a non-perturbative universal formulation of string theory, which is sadly still not available.

After this short conceptual section we now turn to a more rigorous formulation of the theory.

[1] For $n < 2$ one would choose the other fundamental domain to render the integral finite.

2.2 Bosonic String Theory

The basic idea of string theory is to formulate a theory of 1-dimensional objects, the strings. These can come in two varieties, open and closed. As we will see later, open strings are intrinsically related to gauge forces, while closed strings describe gravity and the geometry of space-time. While a particle traces out a one-dimensional world-line in space-time, a string traces out a two-dimensional world-sheet Σ. This world-sheet will be parameterized by the coordinates τ and σ, where $\tau \in (-\infty, \infty)$ parameterizes the time direction and $\sigma \in [0, l)$ describes the spatial extension of the string. Conventionally, the string length l is chosen to be 2π for closed strings and π for open strings. In this section we will assume that the world-sheet has Lorentzian signature $(1, 1)$. Later on we will drop this assumption and generalize the construction also to Euclidean world-sheets of signature $(0, 2)$, i.e. purely space-like.
To describe the movement of a string in a d-dimensional space-time, referred to as the target space, one introduces d scalar fields X^μ on the world-sheet. These bosons describe the position of the string in the target space-time, i.e. the usual coordinates become fields on the world-sheet. More abstractly these fields can also be thought of as maps from the world-sheet to the target space. Again for this section we will assume the target space to be a flat Minkowski space of signature $(1, d-1)$ with metric $\eta_{\mu\nu}$, another assumption we will loosen later on. The action to be extremized is the volume of the world sheet, the so-called Nambu-Goto action.

$$S_{NG} = -T \int_\Sigma \mathrm{d}A \,, \tag{2.4}$$

where T is the tension of the string. It is unknown how to quantize such an action due to the square roots appearing in explicit formulas for the surface area. Instead of working directly with (2.4), one introduces an auxiliary field on the world-sheet, the world-sheet metric $h^{\alpha\beta}$. Using this additional field it is possible to write down a classically equivalent action, the Polyakov action

$$S_p = -\frac{T}{2} \int_\Sigma \sqrt{-h} h^{\alpha\beta} \partial_\alpha X(\sigma,\tau)^\mu \partial_\beta X(\sigma,\tau)^\nu \eta_{\mu\nu} \mathrm{d}\sigma \mathrm{d}\tau \,. \tag{2.5}$$

This action is the true starting point of string theory. It is invariant under two local symmetries, coordinate reparameterizations as well as Weyl rescalings. Together, these can be used to eliminate all the degrees of freedom of the world-sheet metric. One possible gauge choice is the conformal gauge, in which the metric is set to the flat two-dimensional Minkowski metric:

$$h^{\alpha\beta} = \eta^{\alpha\beta} \,. \tag{2.6}$$

This is the step which is only possible for two-dimensional world-sheets, as there is enough freedom in 2 dimensions to completely gauge fix the metric. In $d \geq 3$ dimensions the reparameterizations and Weyl rescalings are no longer sufficient to achieve this. In the

conformal gauge, the Polyakov action (2.5) simplifies drastically:

$$S_p = \frac{T}{2}\int_\Sigma (\partial_\tau X(\sigma,\tau))^2 - (\partial_\sigma X(\sigma,\tau))^2 \mathrm{d}^2\sigma = T\int_\Sigma \partial_+ X(\sigma,\tau)\cdot\partial_- X(\sigma,\tau)\mathrm{d}^2\sigma\,, \tag{2.7}$$

where in the last equality the light cone coordinates $\sigma_\pm$ were introduced:

$$\sigma_\pm = \tau \pm \sigma\,. \tag{2.8}$$

From the variation of the Polyakov action follow the equations of motion in the usual way

$$\partial_+\partial_- X^\mu(\sigma,\tau) = 0\,. \tag{2.9}$$

These equations are solved by the following Ansatz for the scalar fields

$$X^\mu(\sigma,\tau) = X^\mu_L(\sigma_+) + X^\mu_R(\sigma_-)\,. \tag{2.10}$$

This implies that the free string consists out of two independent sectors, called the left- and right-moving sectors, which depend only (anti-)holomorphically on the world-sheet coordinates. Note that this separation of the two sectors holds only in the free theory, i.e. as soon as interactions between the world-sheet bosons X^μ are turned on, the two sectors mix. These interactions would correspond to a curved space-time. In this thesis we will always work in flat space, such that we will assume the independence of the two sectors.

The mode expansion of the left and right moving sectors depends on the boundary conditions. For closed strings these are the periodicity conditions

$$X^\mu(\sigma + l) = X^\mu(\sigma)\,. \tag{2.11}$$

The mode expansions compatible with this boundary condition are

$$X^\mu(\sigma_-) = \frac{1}{2}(x^\mu - c^\mu) + \frac{\pi\alpha'}{l}p^\mu\sigma_- + i\sqrt{\frac{\alpha'}{2}}\sum_{n\neq 0}\frac{\alpha^\mu_n}{n}e^{-\frac{2\pi}{l}in\sigma_-}\,, \tag{2.12}$$

$$X^\mu(\sigma_+) = \frac{1}{2}(x^\mu + c^\mu) + \frac{\pi\alpha'}{l}p^\mu\sigma_+ + i\sqrt{\frac{\alpha'}{2}}\sum_{n\neq 0}\frac{\overline{\alpha}^\mu_n}{n}e^{-\frac{2\pi}{l}in\sigma_+}\,. \tag{2.13}$$

In these expressions x^μ is the center-of-mass of the string, p^μ is the momentum and α^μ_n are the oscillators. We have also introduced the α' parameter, which is given by the inverse tension:

$$\alpha' = \frac{1}{2\pi T}\,. \tag{2.14}$$

While from a string theoretic perspective the bosons X are the basic fields, they have conformal dimension 0. Thus from a conformal field theory (CFT) point of view not

the bosons X are the elementary degrees of freedom but the currents ∂X. Defining the momentum p^μ as the zero mode oscillator,

$$\alpha_0^\mu = \overline{\alpha}_0^\mu = \sqrt{\frac{\alpha'}{2}} p^\mu \,, \tag{2.15}$$

the currents can be expressed in terms of the oscillators as

$$\partial_- X^\mu(\sigma_-) = \frac{2\pi}{l}\sqrt{\frac{\alpha'}{2}} \sum_{n=-\infty}^{\infty} \alpha_n^\mu e^{-\frac{2\pi}{l} in\sigma_-} \,, \tag{2.16}$$

$$\partial_+ X^\mu(\sigma_+) = \frac{2\pi}{l}\sqrt{\frac{\alpha'}{2}} \sum_{n=-\infty}^{\infty} \overline{\alpha}_n^\mu e^{-\frac{2\pi}{l} in\sigma_+} \,. \tag{2.17}$$

The mode expansions for open strings are constructed in a similar way. There are two possible boundary conditions, Neumann(N) and Dirichlet(D), which are given by

$$\text{Neumann}: \qquad \partial_\sigma X^\mu|_{\sigma=0,l} = 0 \,, \tag{2.18}$$

$$\text{Dirichlet}: \qquad \delta X^\mu|_{\sigma=0,l} = 0 \,. \tag{2.19}$$

A Dirichlet condition fixes the endpoint of the string in this direction. This would violate momentum conservation, unless there is an object which absorbs any incoming momentum. These objects are Dirichlet- or D-branes. The dimension of the brane is fixed by the number of Dirichlet boundary conditions of the open string.

As the boundary conditions at the two endpoints of the string do not need to be the same, there are four possible combinations of boundary conditions, NN, DD, DN and ND. For these four possibilities the respective mode expansions are

$$X^\mu_{NN}(\sigma,\tau) = x^\mu + \frac{2\pi\alpha'}{l} p^\mu \tau + i\sqrt{2\alpha'} \sum_{n\neq 0} \frac{\alpha_n^\mu}{n} e^{-\frac{\pi}{l} in\tau} \cos(\frac{n\pi\sigma}{l}) \,, \tag{2.20}$$

$$X^\mu_{DD}(\sigma,\tau) = x^\mu + \frac{1}{l}(x_l^\mu - x_0^\mu)\sigma + \sqrt{2\alpha'} \sum_{n\neq 0} \frac{\alpha_n^\mu}{n} e^{-\frac{\pi}{l} in\tau} \sin(\frac{n\pi\sigma}{l}) \,, \tag{2.21}$$

$$X^\mu_{ND}(\sigma,\tau) = x^\mu + \sqrt{2\alpha'} \sum_{r\in\mathbb{Z}+\frac{1}{2}} \frac{\alpha_r^\mu}{r} e^{-\frac{\pi}{l} ir\tau} \cos(\frac{r\pi\sigma}{l}) \,, \tag{2.22}$$

$$X^\mu_{DN}(\sigma,\tau) = x^\mu + \sqrt{2\alpha'} \sum_{r\in\mathbb{Z}+\frac{1}{2}} \frac{\alpha_r^\mu}{r} e^{-\frac{\pi}{l} ir\tau} \sin(\frac{r\pi\sigma}{l}) \,. \tag{2.23}$$

Note that the mixed boundary conditions have half-integer indices and thus no zero mode contribution. The zero modes for the NN and DD case are defined as

$$\text{NN}: \qquad \alpha_0 = \sqrt{2\alpha'} p^\mu \,, \tag{2.24}$$

$$\text{DD}: \qquad \alpha_0 = \frac{1}{\sqrt{2\alpha'}\pi}(x_l^\mu - x_0^\mu) \,. \tag{2.25}$$

In these cases different normalizations have been chosen for the oscillators to bring them exactly in this form. The reason is that one can now write down a single expression for the current $\partial_+ X$ in all cases:

$$\partial_+ X = \frac{\pi}{l}\sqrt{\frac{\alpha'}{2}}\sum_n \alpha_n^\mu e^{-\frac{\pi}{l}in\sigma_+} , \tag{2.26}$$

where the summation index n runs over the integers for NN and DN boundary conditions and over the half-integers for mixed boundary conditions. Note that there is only a single oscillator family, α_m. Also the anti-holomorphic current, $\partial_- X$, can be described by the holomorphic current if one doubles the range of the σ coordinate, i.e.

$$\partial_+ X^\mu = \pm\partial_- X^\mu(2l-\sigma) \qquad l < \sigma < 2l . \tag{2.27}$$

In all cases the oscillators fulfill the following commutation relations

$$[x^\mu, p^\mu] = i\eta^{\mu\nu} , \tag{2.28}$$
$$[\alpha_m^\mu \alpha_n^\nu] = [\overline{\alpha}_m^\mu \overline{\alpha}_n^\nu] = m\delta_{m+n}\eta^{\mu\nu} , \tag{2.29}$$
$$[\overline{\alpha}_m^\mu \alpha_n^\nu] = 0 . \tag{2.30}$$

This algebra, up to the numerical constant m which could in principle be absorbed into the mode definition, resembles the algebra of the usual harmonic oscillator. Thus the α_m with $m > 0$ are interpreted as annihilation operators, while the α_m with $m < 0$ are creation operators.

In addition to the equations of motions obtained from the variation of the free bosons, there are also the equations of motions from the variation of the world-sheet metric. After gauge fixing these become constraints on the solutions, known as the Virasoro-constraints. In light cone gauge they read

$$T_{++} = -\alpha'^{-1}\,\partial_+ X \cdot \partial_+ X = 0 , \tag{2.31}$$
$$T_{--} = -\alpha'^{-1}\,\partial_- X \cdot \partial_- X = 0 , \tag{2.32}$$

where T denotes the energy-momentum tensor. These constraints require the energy-momentum tensor to be traceless. This tensor transforms under a conformal transformation $w = f(z)$ as

$$T(w) = \frac{1}{f'^2}(T(z) - \frac{c}{12}\{f(z), z\}) , \tag{2.33}$$

where $\{\ ,\ \}$ denotes the Schwarzian derivative. c is the central charge of the theory and represents a conformal anomaly. As the conformal symmetry was used to gauge fix the metric, the total central charge of the theory should vanish. This is a very important constraint and will lead to the prediction of the number of space-time dimensions. The

Fourier modes L_n of the energy-momentum tensor are given by

$$L_n = -\frac{l}{4\pi^2}\int_0^l \mathrm{d}\sigma e^{-\frac{2\pi i}{2}n\sigma}T_{--} = \frac{1}{2}\sum_m \alpha_{n-m}\alpha_m \,, \tag{2.34}$$

$$\overline{L}_n = -\frac{l}{4\pi^2}\int_0^l \mathrm{d}\sigma e^{-\frac{2\pi i}{2}n\sigma}T_{++} = \frac{1}{2}\sum_m \overline{\alpha}_{n-m}\overline{\alpha}_m \,. \tag{2.35}$$

So far the discussion has been purely classical. When the theory is quantized, one encounters the problem of negative norm states in the spectrum due to the time direction. An example of such a state would be $|\psi\rangle = \alpha^0_{-1}|0\rangle$ with norm

$$\langle\psi|\psi\rangle = \langle 0|\,\alpha^0_1\alpha^0_{-1}\,|0\rangle = [\alpha^0_1, \alpha^0_{-1}] = \eta^{00} = -1 \,. \tag{2.36}$$

This is exactly the same problem encountered in the quantization of gauge fields. The gauge covariant formulation with D degrees of freedom for the gauge potential includes non-physical states which have to be removed. Either the theory is formulated using only D-2 degrees of freedom, i.e. one works in a transversal or Coulomb gauge, or all D degrees of freedom are used and additional ghost fields are included. The contribution of these fields effectively removes the unphysical directions.

To quantize the string theory the same two possibilities apply. First, one can only work with the d-2 transversal directions. This approach is called light-cone quantization. This directly removes all negative norm states as the time direction is no longer taken into account. Second, if one includes all directions one also has to include the Faddev-Popov ghost-fields arising from the gauge-fixing of the metric. This approach is known as covariant quantization. The ghosts arising from the gauge fixing of the metric form a first order fermionic bc system with central charge $c = -26$. Some properties of first order systems are summarized in appendix A.2. A free boson has a central charge of $c = 1$. Thus, for the total central charge to vanish in covariant quantization there have to be 26 bosons. As each boson describes a dimension, the number of dimensions is $d = 26$. For explicit computations it is often easier to use light-cone quantization, but for some arguments, like the above determination of the critical dimension, it is more useful to use covariant quantization. Moreover, the second quantization in terms of string field theory is mostly based on this approach. For now we will use the light cone theory.

In the quantized theory, the expressions for the Virasoro modes of the energy momentum tensor are replaced by their normal ordered versions. But due to the commutation relations (2.28) there is a normal ordering ambiguity in the zero mode of the energy-momentum tensor L_0:

$$L_0 = \frac{1}{2}\alpha_0^2 + \sum_{m=1}^{\infty} :\alpha_{-m}\cdot\alpha_m: + \frac{1}{2}\sum_{m=1}^{\infty}[\alpha^\mu_m, \alpha^\mu_{-m}] \,. \tag{2.37}$$

The infinite sum over the commutators can be evaluated as

$$\sum_{m=1}^{\infty}[\alpha_m^\mu, \alpha_{-m}^\mu] = (d-2)\sum_{m=1}^{\infty} m = (d-2)\zeta(-1) = -\frac{(d-2)}{12}\,. \tag{2.38}$$

In this evaluation we have applied a ζ-function normalization. As this function will appear quite often in this thesis we have summarized its properties in appendix A.17. The $(d-2)$ factor originates from the fact that each dimension contributes the same factor, but the time dimension comes with an opposite sign, canceling out the contribution from one space dimension. Using this the zero mode becomes

$$L_0 = \frac{1}{2}\alpha_0^2 + \sum_{m=1}^{\infty} : \alpha_{-m}\cdot\alpha_m : -\frac{(d-2)}{24}\,. \tag{2.39}$$

Using the modes of the energy-momentum tensor, we can rewrite the constraints (2.31) as

$$L_n\,|\text{phys}\rangle = \overline{L}_n\,|\text{phys}\rangle = 0 \qquad \forall n > 0\,. \tag{2.40}$$

$$L_0 + \frac{(d-2)}{24}\,|\text{phys}\rangle = 0\,. \tag{2.41}$$

$$\overline{L}_0 + \frac{(d-2)}{24}\,|\text{phys}\rangle = 0\,. \tag{2.42}$$

For the open string the constraints are the same, neglecting the constraints including the $\overline{L}$ modes. In principle we would have to ensure that also the negative modes annihilate the physical states, but that is actually impossible to achieve. But as $L_n = (L_{-n})^\dagger$ the above equations are sufficient to ensure the decoupling of of the negative modes. Another important constraint is the so-called level matching constraint for closed strings:

$$L_0 - \overline{L}_0\,|\text{phys}\rangle = 0\,. \tag{2.43}$$

This constraint is required for reparameterization invariance along the σ-direction of the string. Finally, using (2.39), we can compute the masses of the states:

$$\frac{\alpha'}{4}m^2 = \sum_{m=1}^{\infty} : \alpha_{-m}\cdot\alpha_m : -\frac{(d-2)}{24} = N - \frac{(d-2)}{24}\,, \tag{2.44}$$

where the mode number operator $N = \sum_{m=1}^{\infty} : \alpha_{-m}\cdot\alpha_m :$ was introduced in the second step. This formula implies that for $d > 2$ there is a tachyon in the spectrum. These tachyons will turn out to be present in most non-supersymmetric string theories. A tachyon in general implies that the chosen vacuum is not a minimum of the potential and thus unstable. The tachyon field then can "condense", i.e. roll down to the minimum of the potential, where it's mass becomes non-negative. While tachyon condensation is a non-perturbative effect and in general hard to study, it is by no means fatal for a theory. After all, the Higgs field of the standard model is a tachyonic field. Tachyon condensation in this case corresponds

to the electro-weak symmetry breaking. Tachyons will be discussed much more in detail in section 6.1.1.

As the case of $d = 2$ is uninteresting for phenomenology, we will for now accept the existence of the tachyon and fix a dimension $d > 2$. The central charge argument fixed this to $d = 26$ in the covariant quantization. The same can be seen in light-cone quantization as follows: The little group of a massless particle should be SO(d-1) and that of a massive particle SO(d-2). For $d = 26$, the normal ordering constant becomes -1 (-2) in the open (closed) case. The first excitation, α^{μ}_{-1} increases the mass by 1 (2), thus in both cases for $d = 26$ the first excitations are massless and form a representation of SO(24). For all other numbers of dimensions these states are massive and thus have the wrong little group. Thus $d = 26$ is the unique possible solution, in agreement with the vanishing of the central charge of the CFT. We have worked here only with Minkowskian world-sheets, but as it turns out, this critical dimension is actually independent of the chosen signature. [12]

The spectrum of the closed bosonic string consists at the massless level out of 26×26 massless fields. These can be organized into a symmetric tensor $g_{\mu\nu}$, the graviton, an antisymmetric tensor $B_{\mu\nu}$, the so-called Kalb-Ramond field, and a scalar field, the dilaton. In the open string case, there is besides the tachyon a massless gauge field. In both cases, open as well as closed, there is an infinite tower of massive fields.

Next let us compute the 1-loop partition function or cosmological constant. At 1-loop, the world sheet has the topology of a torus. Thus the partition function can be written as [13]

$$Z(\tau) = Tr(e^{-2\pi\tau_2 H} e^{2\pi i \tau_1 P}) \,, \tag{2.45}$$

where $\tau = \tau_1 + i\tau_2$ are the wick-rotated world sheet coordinates, which in this case correspond to the complex structure of the torus, H is the Hamiltonian and P the momentum. Expressing the Hamiltonian and momentum through the energy-momentum tensor, (2.45) becomes

$$Z(\tau) = Tr(q^{L_0} \overline{q}^{\overline{L}_0}) \,, \tag{2.46}$$

where the nome $q = e^{2\pi i\tau}$ was introduced. Note that we included the normal ordering constant in the definition of L_0. In most textbooks the central charge contribution is written out explicitly in this formula, resulting in an additional factor $q^{-\frac{c}{24}} \overline{q}^{-\frac{\bar{c}}{24}}$ in the trace. Inserting the explicit expressions for the zero modes (2.39) and representing the trace by a basis of Fock states, (2.46) becomes

$$Z(\tau) = Tr(q^{N_L - 1 + \frac{1}{2}\alpha_0^2} \, \overline{q}^{\overline{N}_R - 1 + \frac{1}{2}\alpha_0^2}) \,. \tag{2.47}$$

The trace over the zero modes results in a Gaussian momentum integral

$$\int \frac{\mathrm{d}^{24} p}{(2\pi)^{24}} \, e^{-\pi\alpha'\tau_2 p^2} = \frac{1}{(2\pi\sqrt{\alpha'})^{24}} \frac{1}{\tau_2^{12}} \,. \tag{2.48}$$

while the contribution of each oscillator is given by

$$\prod_{n=1}^{\infty} \frac{1}{(1 - q^n)} = \frac{q^{\frac{1}{24}}}{\eta(\tau)} \,. \tag{2.49}$$

The factors of $q^{1/24}$ cancel the central charge contribution. $\eta(\tau)$ is the Dedekind η-function defined as

$$\eta(\tau) = q^{\frac{1}{24}} \prod_{n=1}^{\infty}(1-q^n). \tag{2.50}$$

This is the first example of a modular function. Some of its properties are gathered in appendix A.4.1. Combining all contributions one arrives at the partition function

$$Z = \frac{1}{(2\pi\sqrt{\alpha'})^{24}\tau_2^{12}|\eta|^{48}} \ . \tag{2.51}$$

This function is modular invariant. Modular invariance is an important non-trivial consistency condition in string theory. The torus itself is modular invariant, thus every function defined on it should also be modular invariant. This is exploited heavily in the construction of supersymmetric string theory, where the modular invariance can be used as a guiding principle.

This finishes the discussion of the bosonic string. While the bosonic string has many promising features, especially the quantization of gravity, it also suffers from issues like the high-dimensionality and the omnipresent bulk tachyon. The next step of the construction is to introduce fermions on the world-sheet. This will reduce the critical dimension to $d = 10$ and at the same time allow the construction of tachyon-free supersymmetric theories.

2.3 Superstring Theory

In this section we will describe the web of ten-dimensional string theories and their low energy effective actions. We will use these later in compactifications to obtain phenomenologically interesting four-dimensional models. We will focus mostly on the closed string models, as the computations for the open string are very similar and will only give the results for the open string. The basic idea is to introduce fermions on the world-sheet, introducing supersymmetry. The effect of this is a reduced critical dimension and the appearance of space-time fermions in the perturbative spectrum.[2] The action for a complex fermion on the world sheet in light-cone gauge reads

$$S = \frac{i}{2\pi}\int \mathrm{d}^2\sigma \ \psi_+ \cdot \partial_-\psi_+ + \psi_- \cdot \partial_+\psi_- \ . \tag{2.52}$$

From this action follow the equations of motion

$$\partial_-\psi_+ = \partial_+\psi_- = 0 \ , \tag{2.53}$$

which are solved by

$$\psi_+(\tau,\sigma) = \psi_+(\sigma_+) \ , \tag{2.54}$$
$$\psi_-(\tau,\sigma) = \psi_-(\sigma_-) \ . \tag{2.55}$$

[2]The non-perturbative spectrum of the bosonic string already includes fermions in the form of bound states of D-branes [14], but the perturbative spectrum is purely bosonic.

As in the bosonic case the spectrum splits in a left- and a right-moving part. The two possible boundary conditions for fermions are[3]

$$\psi^\mu(\sigma) = \pm\psi^\mu(\sigma + l) \ . \tag{2.56}$$

The two possible sign choices give two sectors, known as the Ramond(R) sector (+) and the Neuveu-Schwartz(NS) sector (-). The two fields ψ_+ and ψ_- can have different boundary conditions, giving rise to in total four sectors, NSNS, RR, NSR and RNS. Again as in the bosonic case the fields can be expanded into modes as

$$\psi_-(\sigma_-) = \sqrt{\frac{2\pi}{l}} \sum_{r\in\mathbb{Z}+a} b_r^\mu e^{-2\pi i r\frac{\sigma_-}{l}} \ , \tag{2.57}$$

$$\psi_+(\sigma_+) = \sqrt{\frac{2\pi}{l}} \sum_{r\in\mathbb{Z}+a} \bar{b}_r^\mu e^{-2\pi i r\frac{\sigma_+}{l}} \ , \tag{2.58}$$

where $a = 0$ in the R sector and $a = 1/2$ in the NS sector. For the open string the boundary conditions relate the holomorphic and anti-holomorphic modes, such that again there is only half as many oscillators as for the closed string. The modes fulfill the algebra

$$\{b_r^\mu, b_s^\nu\} = \{\bar{b}_r^\mu, \bar{b}_s^\nu\} = \delta_{r+s}\eta^{\mu\nu} \ , \tag{2.59}$$

$$\{\bar{b}_r^\mu, b_s^\nu\} = 0 \ . \tag{2.60}$$

The Virasoro generators are given by

$$L_n = \sum_{r\in\mathbb{Z}+a} (r + \frac{n}{2}) b_{-r} \cdot b_{n+r} \ . \tag{2.61}$$

The critical dimension can be determined like in the bosonic case by demanding the vanishing of the total central charge. The central charge of a free fermion is $\frac{1}{2}$. Gauge fixing the superconformal symmetry results in two ghost systems, the fermionic bc system as well as a bosonic $\beta\gamma$ system. The latter has a central charge $c = 11$, such that the bc and $\beta\gamma$ together have a central charge of -15. Each dimension contributes $(1 + \frac{1}{2})$ to the central charge. Thus for $d = 10$ the total central charge vanishes.

Using light-cone quantization again, in the R sectors there is a normal ordering factor in the zero mode of the energy momentum tensor:

$$L_0 = \sum_{r\in\mathbb{Z}+a} r : b_{-r} \cdot b_r : -(d-2) \sum_{r=0+a}^{\infty} r\{b_r, b_{-r}\} \ . \tag{2.62}$$

In the R sector, $a = 0$ and the sum is again simply $\zeta(-1)$, but now with opposite sign compared to the bosonic case. Therefore, in the total L_0 which also includes the bosons

[3]These are not the only consistent choices, in general one can introduce any phase ϕ in the boundary condition $\psi^\mu(\sigma) = e^{i\phi}\psi^\mu(\sigma + l)$. These are known as twisted boundary conditions. For simplicity we ignore these for the moment.

the normal ordering constants cancel each other out. In the NS sector, we can rewrite the sum in terms of the shifted variable $r' = r - 1/2$ and use the closed form of the Hurwitz ζ-function, see (A.22):

$$\sum_{r=1/2}^{\infty} r = \sum_{r'=0}^{\infty}(r' + \frac{1}{2}) = \zeta(-1, 1/2) = -\frac{1}{12}(\frac{6}{4} - \frac{6}{2} + 1) = \frac{1}{24} \ . \tag{2.63}$$

Thus in the NS sector the total energy momentum tensor becomes

$$L_0^{\text{tot}} = \frac{1}{2}\alpha_0^2 + \sum_{m=1}^{\infty} : \alpha_{-m} \cdot \alpha_m : + \sum_{r=\frac{1}{2}}^{\infty} r : b_{-r} \cdot b_r : +(d-2)(-\frac{1}{12} - \frac{1}{24}) \ . \tag{2.64}$$

For $d > 2$ there is again a tachyon in the spectrum. We will come back to this issue in a moment. Let us first fix the dimension we are working in. By the same argument as in the bosonic case the massless states should form representations of the little group SO(d-2). In the open string case the first excited state is given by

$$b^{\mu}_{-1/2} \left|0\right\rangle \ , \tag{2.65}$$

where $|0\rangle$ denotes the ground state of the theory. This state has a mass

$$2\alpha' m = \frac{1}{2} - \frac{3(d-2)}{48} \ . \tag{2.66}$$

It becomes massless for $d = 10$, fixing the critical dimension in agreement with the CFT argument. The normal ordering constant in (2.64) simplifies in this case to $-\frac{1}{2}$. This theory as it stands is not consistent, as can be seen by examining the 1-loop terms. In the oriented case the world-sheet then has the topology of a torus. A torus has the property that functions defined on it are modular invariant. The 1-loop amplitudes of the full string spectrum fail to be modular invariant. This is remedied by projecting onto a subspectrum, known as the GSO-projection named after Gliozzi, Scherk and Olive. The different possible projections correspond to different ways to weight the spin structures in the path integral [15]. From a modern point of view they correspond to different choices of topological invariants on the world sheet, the SPT phases [16]. This allows for a complete classification of possible string theories in 10 dimensions, which completely agrees with the historically found GSO projections.

To see the different possibilities we first compute the partition functions for each sector separately. To shorten the notation we denote the NS sector with a + and the R sector with a -. The partition functions in each sector are

$$Z^{++} = \eta_{++}\frac{\theta_1^4(\tau)}{\eta^4(\tau)} \,, \tag{2.67}$$

$$Z^{+-} = \eta_{+-}\frac{\theta_2^4(\tau)}{\eta^4(\tau)} \,, \tag{2.68}$$

$$Z^{-+} = \eta_{-+}\frac{\theta_4^4(\tau)}{\eta^4(\tau)} \,, \tag{2.69}$$

$$Z^{--} = \eta_{--}\frac{\theta_3^4(\tau)}{\eta^4(\tau)} \,. \tag{2.70}$$

The total partition function is the sum of the $Z^{\pm\pm}$ together with the bosonic contribution. The phases $\eta_{\pm\pm}$ have to be chosen such that the total partition function is modular invariant. There are several ways how to achieve that, one possibility is

$$Z_{II}(\tau) = \frac{1}{4\tau_2^4|\eta|^{24}}|\theta_3^4 - \theta_4^4 - \theta_2^4 \pm \theta_1^4|^2 \,. \tag{2.71}$$

This gives the so-called type II string theories, the two possible sign choices correspond to the IIA and IIB theory. As $\theta_1 = 0$ this choice does not influence the partition function at all. This is a general feature of the difference between type IIA and IIB, while they look rather different from a space-time point of view, their CFT descriptions are very similar. The additional factor of $\tau_2^{-4}|\eta|^{-16}$ originates from the bosonic contributions.

This partition function can also be written as a trace over the Hilbert space. Anti-periodic boundary conditions are then represented by factors of $(-1)^F$, where F is the world-sheet fermion number. (2.71) then reads

$$Z_{II}(\tau) = Tr(e^{2\pi i\tau H_{NS}}\frac{1}{2}(1-(-1)^F)) - Tr(e^{2\pi i\tau H_R}\frac{1}{2}(1\pm(-1)^F)) + \text{leftmoving} \,. \tag{2.72}$$

Type IIB corresponds to choosing the same sign in the R sector for left and right movers, while IIA corresponds to opposite signs. Due to Jacobi's "absurd identity" the partition function vanishes, as required by supersymmetry. Using these GSO projections, we can construct the Hilbert space. Each state of the theory corresponds to a physical field in the ten-dimensional theory. The lowest lying state in the NS sector is the vacuum $|0\rangle$ with a mass of $-1/2$. Here and in the following we will give the mass squared in units of α'. This state is tachyonic and should be projected out. The NS vacuum gets assigned the fermion number 0[4], such that

$$\frac{1}{2}(1-(-1)^F)\,|0\rangle = 0 \,. \tag{2.73}$$

This choice projects the tachyon out. The ground state of the R sector is, due to the presence of the fermionic zero modes, a SO(8) spinor. There are two possible chiralities,

[4]This convention differs from the convention in [11] but is required for consistency

denoted $|a\rangle$ and $|\dot{a}\rangle$, which differ by one in fermion number. The GSO projections $(1 \pm (-1)^F)$ select therefore exactly half of these states at each level. The resulting massless spectra for type IIA and type IIB are:

$$\text{IIA} : [(1) + (28) + (35)]_{NSNS} + [(8) + (56)]_{RR} + 2 \cdot [(8) + (56)]_{RNS/NSR} \tag{2.74}$$

$$\text{IIB} : [(1) + (28) + (35)]_{NSNS} + [(1) + (28) + (35)]_{RR} + 2 \cdot [(8) + (56)]_{RNS/NSR} \tag{2.75}$$

The states have been split up into representations of SO(8). States in the NSNS and RR sector are bosons, while the states in the mixed sector represent fermions. In both theories there are 128 massless bosons and fermions, showing the supersymmetry. The NSNS sector consists in both theories out of a scalar dilaton d (1), an antisymmetric tensor $B_{\mu\nu}$ (28) and the graviton $g_{\mu\nu}$ (35). The RR fields correspond to p-form fields, in the case of IIB with even antisymmetric forms $C_0(1)$, C_2 (28) and a self-dual rank 4 tensor C_4 (35) and in the case of IIA to a vector $C_1(8)$ and a rank 3 antisymmetric tensor C_3 (56). These fields correspond to higher rank versions of gauge fields, thus they will not appear directly in the actions but in terms of their field strengths $F_{p+1} = dC_p$.

Low Energy Effective Theories

As the general string theories are hard to work with, one is interested in obtaining low energy effective actions. These are obtained by truncating the infinite string spectrum to the massless (or the first massive) level. The world-sheet theory has to be conformal, which implies that the beta-functions of all fields have to vanish. The resulting equations are known as the string equations. One then searches for a ten-dimensional action which encodes these equations as its equation of motion. For the type II strings, these correspond to the ten-dimensional supergravity theories. The actions of these theories consist out of the NS sector, the R sector as well as topological Chern-Simons (CS) terms:

$$S[\text{IIA/B}] = S_{\text{NS}} + S_{\text{R}}[\text{A/B}] + S_{\text{CS}}[\text{A/B}] \ , \tag{2.76}$$

where the NS-NS part is the same for type IIA and IIB. The respective terms in the action are given by

$$\begin{aligned}
S_{\mathrm{NS}} &= \frac{1}{2\kappa_{10}^2}\int \mathrm{d}^{10}x\sqrt{|\det G|}\; e^{-2\phi}\left[\mathcal{R}+4(\nabla\phi)^2-\frac{1}{2}|H_3|^2\right]\,,\\
S_{\mathrm{R}}[\mathrm{A}] &= -\frac{1}{2\kappa_{10}^2}\int \mathrm{d}^{10}x\sqrt{|\det G|}\left[\frac{1}{2}|F_2|^2+\frac{1}{2}|\tilde{F}_4|^2\right]\,,\\
S_{\mathrm{R}}[\mathrm{B}] &= -\frac{1}{2\kappa_{10}^2}\int \mathrm{d}^{10}x\sqrt{|\det G|}\left[\frac{1}{2}|F_1|^2+\frac{1}{2}|\tilde{F}_3|^2+\frac{1}{4}|\tilde{F}_5|^2\right]\,,\\
S_{\mathrm{CS}}[\mathrm{A}] &= -\frac{1}{4\kappa_{10}^2}\int B_2\wedge F_4\wedge F_4\,,\\
S_{\mathrm{CS}}[\mathrm{B}] &= -\frac{1}{4\kappa_{10}^2}\int B_2\wedge F_3\wedge F_5\,,
\end{aligned} \tag{2.77}$$

where $H_3 = dB_2$, $F_p = dC_{p-1}$, and $\tilde{F}_p = F_p - H_3\wedge C_{p-3}$. Using partial integration the Chern-Simons term in the last row can be equivalently written as

$$S_{\mathrm{CS}}[\mathrm{B}] = \frac{1}{8i\kappa_{10}^2}\int \frac{C_4\wedge G_3\wedge\overline{G}_3}{\mathrm{Im}(S)}\,, \tag{2.78}$$

where $G_3 = F_3 - \tau H_3$ and $S = C_0 + ie^{-\phi}$ is the axio-dilaton, such that

$$G_3\wedge\overline{G}_3 = 2i\mathrm{Im}(S)F_3\wedge H_3\,. \tag{2.79}$$

This shows that the three-forms H_3 and F_3 act as a source term for the C_4 field. Thus if we give these a vacuum expectation value (vev), so-called fluxes, these fluxes contribute to the tadpole for the C_4 field as

$$N_{flux} = \frac{1}{(2\pi)^4\alpha'^2}\int_X F_3\wedge H_3\,. \tag{2.80}$$

In addition to the fluxes, the C_4 field couples to D3 and O3 branes. Thus the total tadpole cancellation condition becomes

$$N_{\mathrm{D3}} - N_{\overline{\mathrm{D3}}} + N_{\mathrm{flux}} - \frac{1}{2}N_{\mathrm{O3}} = 0\,, \tag{2.81}$$

where N_{D3} is the number of D_3 branes and the same for anti-D3-branes as well as O-planes. Similar constraints exist for the higher form fluxes and branes. Note that the number of O-planes is fixed by the chosen orientifold, but the fluxes and number of branes are only restricted to be integer. These tadpole constraints play an important role in the construction of realistic theories, but in practice are not too hard to fulfill. Especially in F-theory compactifications there is an additional term related to the Euler characteristic of the compactification manifold. As these can take rather large values, these terms weaken the constraints considerably.

Frame Conventions

The Einstein-Hilbert terms in the low energy effective actions for the type II superstrings (2.77) are of the form

$$S_{\text{EH,string}} = \frac{1}{2\kappa_{10}^2} \int \mathrm{d}^{10}x \sqrt{|\det G|}\; e^{-2\phi}\mathcal{R}\,. \tag{2.82}$$

This is the form naturally arising in string theory, where the Ricci scalar $\mathcal{R}$ couples to the dilaton field. This form is known as the string frame. In the usual formulations of gravity the Einstein-Hilbert term is of the form

$$S_{\text{EH,Einstein}} = \frac{1}{2\kappa^2} \int \mathrm{d}^{10}x \sqrt{|\det G_E|}\mathcal{R}\,, \tag{2.83}$$

where κ is the gravitational coupling constant. The string frame action can be brought into Einstein frame by a Weyl rescaling of the metric,

$$G_{\mu\nu} \to G_{\mu\nu,E}\; e^{\phi/2}\;. \tag{2.84}$$

Another possibility is to first extract the vev from the dilaton field. As the dilaton corresponds to the string coupling constant the vev is denoted g_s. In this case one first defines a new field

$$\phi = \phi' + \phi_0\;. \tag{2.85}$$

and then performs the Weyl rescaling $G_{\mu\nu} \to G_{\mu\nu,E}\; e^{\phi'/2}$. This results in

$$S_{\text{EH,modifiedEinstein}} = \frac{1}{2\kappa_{10}^2 g_s^2} \int \mathrm{d}^{10}x \sqrt{|\det G_E|}\mathcal{R}\,. \tag{2.86}$$

This is known as the modified Einstein frame. The main difference is that the gravitational coupling constant has absorbed the g_s^{-2} factor.

Type 0 Theories

The type II theories were obtained by demanding modular invariance of the partition function. There is actually another consistent choice for the GSO projection corresponding to the type 0A/B theories with the partition function

$$Z_0(\tau) = \frac{1}{2\tau_2^4|\eta|^{24}} \left(|\theta_2|^8 + |\theta_3|^8 + |\theta_3|^8 \pm |\theta_1|^8\right)\;. \tag{2.87}$$

This choice of GSO projection corresponds to correlated spin structures between the left and right moving sectors. In contrast to the type II theories the partition function does not vanish, signaling a broken supersymmetry. Supersymmetry is even maximally broken as the type 0 theories do not include any fermions at all, the spectrum is purely bosonic. Like in most non-supersymmetric string theories, the spectrum includes a tachyon. This tachyon condenses in a chain of theories until they end up in a two dimensional theory,

either type 0 [17] or the bosonic string theory with a dilaton gradient [18]. This renders these theories rather uninteresting for phenomenological purposes. The existence of the 2-dimensional endpoint of tachyon condensation is mainly interesting for the larger picture of tachyon condensation, where most closed string tachyons end up.

Orbifolds and Orientifolds

Type II and type 0 still do not exhaust all possibilities for a modular invariant partition function. It is possible to obtain new partition functions from these by applying a construction known as orbifolding. In this procedure the spectrum of the theory is projected by a symmetry to construct another consistent theory. If the symmetry group acts on the target space side the resulting geometry is an orbifold. If the symmetry acts on the world-sheet instead, it is known as an orientifold. The spectrum obtained this way is in many cases no longer modular invariant. The restoration of modular invariance then forces the addition of so-called twisted sectors. An example of a symmetry which can be used is world-sheet parity of type IIB string theory. As the partition function is the same in the left and right moving sector, the two sectors can be exchanged without altering the theory. World sheet parity is defined as the transformation

$$\Omega : (\sigma, \tau) \to (l - \sigma, \tau) \ . \tag{2.88}$$

Including the operator $\frac{1+\Omega}{2}$ in the trace projects onto parity even states. The resulting theories are unoriented string theories. In the case of type IIB the result of the orientifold projection is type I string theory. Fixed points of the orientifold projection represent geometrical objects: orientifold planes, or for short O-planes. The dimension of these depend on the dimension of the locus fixed under the projection. This can be altered by including additional symmetry operators in the projection like shifts or reflections of target space coordinates. O-planes have opposite charges under the p-form fields compared to the D-branes and thus play an important role in the cancellation of overall charges and RR-tadpoles.

If a symmetry of the target space is used instead one obtains so-called orbifolds. If the symmetry acts non-freely this results in singular target spaces. But as strings are objects of finite extension they can resolve these singularities and still result in a sensible theory. In chapter 3 we will describe compactification geometries in detail and see that phases of certain solvable 2d superconformal models describe strings moving on orbifolds of Calabi-Yau spaces without producing any singularities.

As a simply toy example for an orbifold we take the complex plane. The complex plane $\mathbb{C}$ has as a subgroup of its symmetries a U(1) given by rotations around the origin. Thus it is possible to divide the complex plane by a $\mathbb{Z}_n$ operation by identifying

$$z = e^{\frac{2\pi i}{n}} z \ , \tag{2.89}$$

where z is the coordinate parameterizing the complex plane. The resulting space is an infinite real 2-dimensional cone where both edges are identified. There is a singularity

at the origin. If one would use such a geometry as a background for string theory, one would find a twisted sector localized at the origin. This sector is in general tachyonic, describing the decay of the orbifold back to the flat complex plane. This example is of course non-compact. In the case of a compact CY the orbifolds can be stable. Another important example of an orbifold is the K3 space, a complex 2-dimensional CY obtained by orbifolding the 4-torus.

Heterotic Theories

Another possible construction of consistent string theories is heterotic string theory. The left and right moving sectors of closed string theories are completely independent, thus nothing forbids choosing different theories for each of them. The heterotic superstrings are obtained by combining the bosonic string as a left-mover and the $\mathcal{N} = 1$ superstring as the right-mover (or vice versa). There is only one obvious problem with this construction: The critical dimension of the bosonic string is 26 while the superstring lives in 10 dimensions. The way out is to compactify the bosonic string on a 16-dimensional torus T^{16}. In the pure bosonic case one can choose any toroidal compactification, but for a heterotic theory the compactification has to be on an even self-dual lattice to ensure modular invariance of the combined theory. There are only two such lattices in 16 dimensions, the $E_8 \times E_8$ and $SO(32)$ lattices, giving rise to two supersymmetric heterotic string theories with the gauge groups corresponding to the lattices, $E_8 \times E_8$ and $SO(32)$.[5] It is important to note that the strings in a heterotic construction are necessarily closed, as there cannot be any boundary condition relating the left to the right-moving sector due to the different number of dimensions. The gauge sector arises from the isometries of the compactification lattice of the additional bosonic dimensions instead of the open string sector.

But this does not exhaust all possible heterotic theories. One can introduce twists or use the automorphism symmetry group of $E_8 \times E_8$ to generate new theories out of the above [19]. These constructions are best described by the free fermion description. The internal 16 bosonic dimensions are fermionized and therefore replaced by 32 free fermions. To each of these fermions one can assign different boundary conditions. Modular invariance restricts this choice slightly by demanding multiples of 8 fermions to have the same boundary condition. The resulting theories are listed in table 2.1. The same theories can be obtained by taking orbifolds of the supersymmetric heterotic string theories. E.g. the $O(16) \times O(16)$ theory is the $\mathbb{Z}_2$ orbifold of the $E8 \times E8$ theory where the $\mathbb{Z}_2$ corresponds to the automorphism group. This theory is the only tachyon free non-supersymmetric theory. All other non-supersymmetric heterotic theories are tachyonic. These tachyonic theories descend from the tachyonic $SO(32)$ theory. This is a non-supersymmetric theory, obtained by identifying the spin structures of the left and right moving sector in the free fermionic construction. This is in contrast to the usual supersymmetric theories, where the spin structures for the left- and right moving fermions are chosen independently. The system of the 32 left-moving fermions has a $\mathbb{Z}_2^5$ symmetry, where each $\mathbb{Z}_2$ factor acts on

[5] While the theory is commonly denoted $SO(32)$, this actually describes only the gauge algebra. The gauge group is given by it's double cover spin(32).

16 of the 32 fermions with a minus sign and on the other 16 as the identity. Gauging or equivalently orbifolding $n = 1 \dots 5$ of these symmetries results in the other tachyonic theories. It is interesting to note that the $O(16) \times O(16)$ theory has a positive cosmological constant. But despite the absence of tachyons, it still has a vacuum instability due to the dilaton and is thus no counter example to the dS conjecture.

gauge group	tachyons	massless fermions	gauge bosons
$SO(32)$	32	0	496
$O(16) \times E8$	16	256	368
$O(8) \times O(24)$	8	384	304
$(E7 \times SU(2))^2$	4	448	272
$SU(16) \times U(1)$	2	480	256
E8	1	496	248
$O(16) \times O(16)$	0	512	240

Table 2.1: Tachyonic heterotic strings in $d = 10$. Table adopted from [5].

$\mathcal{N} = 2$ Theories

So far we have included one world-sheet fermion per boson. Of course nothing prohibits larger amounts of super symmetry. In the case of an $\mathcal{N} = 2$ superconformal symmetry, one ends up with a ghost system consisting out of a bc system, two $\beta\gamma$ systems and an $\eta\xi$ system. The 2 $\beta\gamma$ systems originate in the gauge fixing of the supersymmetries, while the $\eta\xi$ system corresponds to the gauge fixed R-symmetry. Combined, these ghost systems have a central charge $c = -6$. To cancel that, one needs two complex bosons with their respective superpartners, each contributing $c = 3$. As both bosons in each pair have to have the same signature, this only allows for the signatures $(2, 2)$ or $(0, 4)$. Thus the phenomenologically interesting signature (1,3) is not possible. Moreover, it has been shown that this theory describes self-dual gravity and includes only a single perturbative degree of freedom, a tachyonic scalar, which corresponds to the Kähler deformation of the spacetime [20]. In non-critical versions of this theory one of the time dimensions is pure gauge, reducing the effective number of time dimensions to 1.

Nevertheless it is known that all string theories with less supersymmetry can be embedded into this theory [21]. The additional degrees of freedom (d.o.f.) of these theories are hidden in the non-perturbative sector of the $\mathcal{N} = 2$ theory. Going beyond $\mathcal{N} = 2$ leads to negative critical dimensions, rendering these theories uninteresting.

The Web of Theories

In figure 2.2 we summarize the string theories mentioned so far and all their interconnections in various dimensions. It is interesting to note that while the $\mathcal{N} = 1$ superstrings are all connected via dualities and tachyon transitions, the bosonic theory and the $\mathcal{N} = 2$

string theory are separated from this web. But the bosonic string theory is tachyonic, thus this tachyon should condense to some other theory. The endpoint of the tachyon condensation is not known, it was conjectured to lead to a type II string theory in 10 dimensions. Tachyons and especially the bosonic tachyon will be studied in chapter 6.

In addition to the tachyon condensations there exists another type of relations between different theories, so-called dualities. A duality is a symmetry of a theory which is not a symmetry of the Lagrangian. If we apply a duality transformation on a theory, we obtain a different theory which describes the same physical system. Important examples of dualities in string theory are the T and S dualities. T duality arises in compactifications on a circle and connects type IIA and IIB theories. A IIA theory compactified on a circle of radius R is equivalent to a type IIB theory compactified on a circle of radius 1/R. Physically, the duality exchanges the role of the winding and KK modes.

S duality is a non-perturbative duality acting on the axio-dilaton of type IIB theory, which plays the role of a gauge coupling parameter in string theory. The low energy effective 10-dimensional IIB SUGRA theory is invariant under $SL(2,\mathbb{R})$ transformations, which act on the axio-dilaton and the H and F fluxes, but leave the metric invariant. In the full string theory setting this symmetry gets broken to a discrete $SL(2,\mathbb{Z})$ symmetry due to an instanton contribution of D(-1) branes to the action. The $SL(2,\mathbb{Z})$[6] symmetry acts on the axio-dilaton $\tau = C_0 + ie^{-\phi}$ as

$$\tau \to \frac{a\tau + b}{c\tau + d}\,, \tag{2.90}$$

and on the fields H and F as

$$\begin{pmatrix} F' \\ H' \end{pmatrix} = \begin{pmatrix} a & b \\ c & d \end{pmatrix} \begin{pmatrix} F \\ H \end{pmatrix}\,. \tag{2.91}$$

S duality is generated by one of the generators of the group

$$S = \begin{pmatrix} 0 & -1 \\ 1 & 0 \end{pmatrix}\,. \tag{2.92}$$

Thus S-duality exchanges the F and H fluxes. Moreover, it exchanges the roles of the fundamental string and the D1-brane as well as the D5-brane and the NS5-brane[7]. This renders type IIB self-dual under S-duality. In contrast to this, type I string theory is related to the supersymmetric SO(32) heterotic string under S-duality.

[6]Note that the two transformation matrices A and -A produce the same transformation, thus the symmetry group is actually $PSL(2,\mathbb{Z}) = SL(2,\mathbb{Z})/\mathbb{Z}_2$.

[7]A NS5-brane is a 5-dimensional brane magnetically charged under the Kalb-Ramond field. They have to be included in the theory as they are the magnetic dual of the fundamental string. The name NS brane originates from the fact that they were first discovered as black hole SUGRA solutions which correspond to fields living purely in the NS sector.

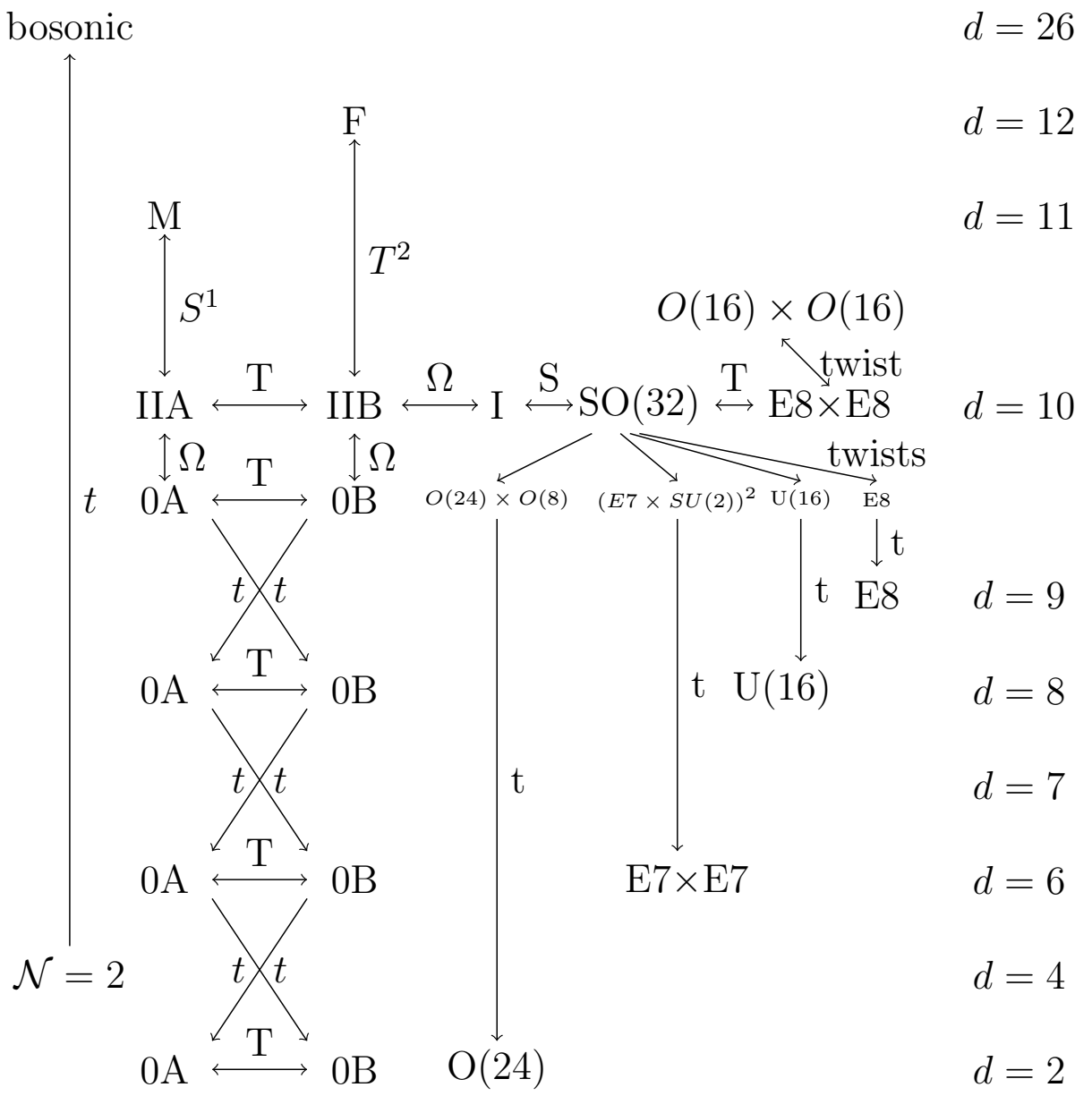

Figure 2.2: The web of string theories and their interconnections. Gauge groups represent heterotic strings, T- and S- denote the respective dualities and t denotes tachyon condensations. Geometric notations like S^1 or T^2 denote compactifications on the geometry.

M- and F-Theory

For completeness we mention two more string theoretic constructions of theories living in 11 and 12 dimensions, M- and F-theory. These theories are closely related to the 10-dimensional string theories. M theory arises as the strong coupling limit of type IIA string theory. From the 11 dimensional point of view, type IIA string theory is a circle compact-

ification of M theory, where the radius of the circle plays the role of the coupling constant of the type II theory. When the circle becomes very small, the theory is effectively 10 dimensional and described by weakly coupled type II strings. A non-perturbative formulation of M theory is not known, but it was proposed that the BFSS matrix model [22] gives a non-perturbative description. M theory is especially interesting as 11 dimensions is the maximal number of dimensions allowed by supergravity.

F-theory on the other hand is not really a 12 dimensional theory. It is obtained by interpreting the possible values of the axio-dilaton of type IIB as the complex structure of a 2-dimensional torus. The $\mathrm{SL}(2,\mathbb{Z})$ symmetry of type IIB is made manifest in the diffeomorphisms of the torus. The momenta for on-shell states in the additional dimensions are necessarily 0, such that the theory is effectively 10-dimensional. This is also required due to the signature, the theory has signature (2,10) and the additional time direction would cause problems if it would be a usual dimension.

M- and F-theory also enjoy some type of T-duality due to the T-duality of the underlying type II strings. M theory compactified on an elliptically fibered manifold X is equivalent to F theory compactified on $X \times S^1$ [23].

2.4 Compactifications

So far we have discussed string theory in the critical dimension of the superstring, $d = 10$. But in the real world only four dimensions are observed. Thus a way to get rid of the additional 6 dimensions is required. This is usually done by compactifying the extra dimensions. The internal space one compactifies on has to be a solution of the ten dimensional equations of motion. This gives the constraint that the internal manifold has to be Ricci flat, i.e. the Ricci tensor $R_{\mu\nu}$ has to vanish. The easiest possible choice fulfilling this constraint is a six-torus. But this results in an $\mathcal{N} = 8$ supersymmetric theory which is phenomenologically uninteresting. There are two ways out of this situation. One way is to take orbifolds of the torus, breaking some of the supersymmetries. Another possibility resulting in an $\mathcal{N} = 2$ supersymmetric theory is to compactify not on a torus but on a Calabi-Yau 3-fold. In this section we will go through some of the details of this construction.

2.4.1 Geometric Preliminaries

Before we describe the compactifications themselves, we give short review of (co)homologies of complex manifolds X to set the notation. We use ∂ for the boundary operator and d for the exterior derivative. Let a_p be a p-chain, i.e. a sum of p-dimensional submanifolds of X. Thus any p-chain can be written as $\sum_i c_i Y_i$ with $Y_i \subset X$ and c_i constants. Then the p-th homology group of X is defined as

$$H_p(X, G) = \frac{\{a_p | \partial a_p = 0\}}{\{\partial a_{p+1}\}} \ , \tag{2.93}$$

i.e. the chains without boundaries which are not boundaries themselves. The G denotes the group (or field) in which the coefficients c_i are defined. The dimensions of the homology groups are the Betti numbers b_p:

$$b_p = \dim(H_p(X, \mathbb{R})) \ . \tag{2.94}$$

The de Rham cohomology is defined in complete analogy but using the exterior derivatives and p-forms ω_p. The p-th de Rham cohomology group is defined as

$$H^p(X) = \frac{\{\omega_p | d\omega_p = 0\}}{\{d\omega_{p-1}\}} \ , \tag{2.95}$$

i.e. the closed p-forms which are not exact. By the Hodge decomposition theorem the p-cohomology group is isomorphic to the space of harmonic p-forms on X. On a complex manifold the cohomology can be refined a bit further using the $\overline{\partial}$ operator, resulting in the Dolbeault cohomology. The Dolbeault cohomology groups are defined by

$$H^{p,q}(X) = \frac{\{\omega^{(p,q)} | \overline{\partial}\omega^{(p,q)} = 0\}}{\{\overline{\partial}\omega^{(p,q-1)}\}} \ , \tag{2.96}$$

again the $\overline{\partial}$ closed forms which are not $\overline{\partial}$ exact. The dimensions of these groups are the Hodge numbers $h^{p,q}$. Also, like the de Rham cohomologies the Dolbeault cohomologies correspond to the harmonic (p,q)-forms on X. In the case of a Kähler manifold, which will always be the case for the compactifications we are interested in, the Hodge numbers have some symmetries, namely:

$$h^{p,q} = h^{q,p} \,, \tag{2.97}$$

$$h^{p,q} = h^{d-p,d-q} \,, \tag{2.98}$$

where d is the complex dimension of the manifold. Moreover, the only 0-forms are the constants, thus $h^{0,0} = h^{3,3} = 1$.[8] Using the symmetries, the remaining independent Hodge numbers are $h^{p,0}$, $h^{1,1}$ and $h^{2,1}$. If we demand that X is, in addition to being Kähler, a Calabi-Yau, there is a unique holomorphic (d,0)-form Ω_d, thus $h^{d,0} = 1$ and all $h^{p,0} = 0\,, 0 < p < d$. Therefore, in the case of a CY there are two unfixed Hodge numbers $h^{1,1}$ and $h^{2,1}$. $h^{1,1}$ parameterizes the Kähler deformations of the metric, while $h^{2,1}$ parameterizes the complex structure deformations. Some orientifolds include a holomorphic involution of the target space,

$$\sigma : X \to X \,. \tag{2.99}$$

It is important how the cohomology cycles transform under the involution to be able to determine which fields survive the projection. Thus it is in this case useful to further refine the cohomologies in even and odd parts under the transformation rule:

$$H^{p,q}(X) = H^{p,q}_{+}(X) \oplus H^{p,q}_{-}(X) \,. \tag{2.100}$$

The dimensions of $H^{p,q}_{+}(X)$ and $H^{p,q}_{-}(X)$ are denoted $h^{p,q}_{+}$ and $h^{p,q}_{-}$ respectively. For each Dolbeault cohomology class we choose a orthogonal basis. We follow the conventions of [24], i.e.

$$\{\omega_A\} \in H^{1,1}(X) \,, \tag{2.101}$$

$$\{\tilde{\omega}_A\} \in H^{2,2}(X) \,, \tag{2.102}$$

$$\{\alpha_\lambda, \beta^\lambda\} \in H^{2,1}(X) \,, \tag{2.103}$$

such that

$$\int_X \omega_A \wedge \tilde{\omega}^B = \delta^B_A \qquad \text{and} \qquad \int_X \alpha_\lambda \wedge \beta^\Sigma = \delta^\Sigma_\lambda \,. \tag{2.104}$$

The indices always run over the dimension of the cohomology groups, e.g. $A = 1 \ldots h^{1,1}$. To shorten the notation it is useful to assign the identity and the volume element to the 0 index, i.e. $\omega_0 = 1$ and $\omega^0 = \mathrm{d}vol_6$. In the case of an orientifold we use the following basis:

$$\{\omega_\alpha\} \in H^{1,1}_{+}(X) \qquad \{\omega_a\} \in H^{1,1}_{-}(X) \,, \tag{2.105}$$

$$\{\tilde{\omega}^\alpha\} \in H^{2,2}_{+}(X) \qquad \{\tilde{\omega}^a\} \in H^{2,2}_{-}(X) \,, \tag{2.106}$$

$$\{\alpha_\lambda, \beta^\lambda\} \in H^{3}_{+}(X) \qquad \{\alpha_i, \beta^i\} \in H^{3}_{-}(X) \,. \tag{2.107}$$

[8] This holds only for connected manifolds, but this will always be the case in our examples.

Note that we use upper case letters for the unsplit cohomology, lower case Greek letters for the even part and lower case Latin for the odd part. We can now expand the fields of the 10-dimensional effective actions in terms of four-dimensional fields and these bases.

2.4.2 Kaluza Klein Compactifications

Before we investigate the more complicated cases of CY compactifications, we present a famous historical example of a compactified theory developed long before string theory, the 5-dimensional Kaluza-Klein theory. This is a purely gravitational theory with one extra dimension in form of a circle. The theory was proposed by Kaluza in 1921 [25] and turned into a quantum theory by Klein in 1926 [26]. Klein proposed that the 5th dimension should be periodic. There are actually two theories which are named Kaluza-Klein theory. The first theory is a theory of a full five-dimensional metric, which results in a 4-dimensional theory of gravity and electromagnetism as well as matter fields. This unification of electromagnetism and gravity is known as the Kaluza-Klein miracle. The idea was extended by Witten to include the full standard model gauge group $SU(3) \times SU(2) \times U(1)$ by increasing the number of dimensions to 11, but the resulting matter representations do not match the observed particles [27].

Second, there is the theory where the 5-dimensional metric assumes the form $\mathcal{M}^4 \times S^1$, where $\mathcal{M}^4$ is a general 4-dimensional manifold, e.g. Minkowski space. This theory ignores some d.o.f. of the full theory and the matter energy momentum tensor has to be added by hand. But this version is closer to the situation in string theory, where mostly a $\mathcal{M}^4 \times CY^3$ spacetime is assumed. In the following we use capital Latin letters for 5-dimensional indices and lower case Greek letters for 4-dimensional indices. The purely gravitational action is given by

$$S = M_5 \int \mathrm{d}^5x\sqrt{-g}R_5 = M_5 \int_0^{2\pi} r\mathrm{d}x_5 \int \mathrm{d}^4x\sqrt{-g}R_4 \,. \tag{2.108}$$

Here g is the determinant of the metric and R is the Ricci scalar. Integrating over the circular dimension of radius r, the 4-dimensional action is obtained as

$$S = M_5 2\pi r \int \mathrm{d}^4x\sqrt{-g}R \,. \tag{2.109}$$

This shows that the four dimensional Planck scale depends on the internal volume, here simply given by the circumference of the circle. This implies that the internal dimensions have to be compact, as an infinite volume would correspond to an infinite Planck scale and thus to a decoupling of gravity. To obtain matter in the 4-dimensional theory one can either add matter fields into the 5-dimensional theory or relax the constraint that the spacetime metric is block-diagonal. For simplicity we will add a scalar field ϕ of mass m in the 5-dimensional theory. Its action then reads

$$S = \int \mathrm{d}^5x\sqrt{-g}\left(\partial^M\phi\partial_M\phi + m^2\phi^2\right) \,. \tag{2.110}$$

The field can then be expanded into its eigenmodes along the circular direction:

$$\phi(x^M) = \frac{1}{2\pi r} \sum_{n\in\mathbb{Z}} \phi_n(x^\mu) e^{inx_5/r} \,. \tag{2.111}$$

The normalization $\frac{1}{2\pi r}$ has been chosen such that the resulting 4-dimensional fields are canonically normalized. Inserting this expansion into the action and performing the integration in the x_5 direction, one obtains:

$$S = \sum_{n\in\mathbb{Z}} \int \mathrm{d}^4x \sqrt{-g} \left(\partial^\mu \phi_n \partial_\mu \phi_n^\dagger + \left(\frac{n^2}{r^2} + m^2 \right) \phi_n^\dagger \phi_n \right) \,. \tag{2.112}$$

This is an action for an infinite tower of massive states, known as the Kaluza-Klein tower. The fields are thus often denoted as the KK-modes of the original higher dimensional field. If the higher dimensional field is massless, the zero mode in the lower dimensional theory is also massless. In many cases it is sufficient to study these zero modes and ignore the massive states, which are then integrated out. This toy model incorporates most properties of the higher dimensional compactifications of string theory. The situation there is complicated by the fact that the volumes of the different cycles of a CY are hard to compute and there are many more moduli than a single radius. Moreover, a string can also wind around the circle. This gives in addition to the KK modes a second infinite tower of states, whose mass scales with the radius of the circle.

2.4.3 Preliminaries: Calabi-Yau Geometry

Before we describe the phenomenology, we first develop the necessary tools to describe the geometry. A Calabi-Yau(CY) can be defined in many different but equivalent ways. It is a complex Kähler manifold for which any of the following conditions hold

- the metric is Ricci-flat,
- it has SU(d) holonomy,
- the first Chern class vanishes.

Sometimes the stronger constraint that the CY has trivial canonical bundle is demanded. As we are interested in compact CY manifolds, these are equivalent. In the non-compact case the triviality of the canonical bundle implies the above constraints, but the opposite is not true.

That these manifolds are solutions of string theory can be seen in two ways. First, as already mentioned, the one-loop β function for the graviton of type II string theory is given by

$$\beta^G = \alpha'(R_{\mu\nu} - \frac{1}{4} H_\mu^{\rho\sigma} H_{\nu\sigma\rho} + 2\nabla_\mu \nabla_\nu \Phi) + \mathcal{O}(\alpha'^2) \,, \tag{2.113}$$

where Φ is the dilaton, H is the 3-form field strength of the Kalb-Ramond field and $R_{\mu\nu}$ is the Ricci tensor. If one assumes the dilaton and Kalb-Ramond field to be constants, the Ricci flatness constraint follows directly. Note that this is only taking into accounts effects linear in α' and a non-zero H-flux also breaks the constraint. Thus for phenomenological applications one often assumes the so-called dilute flux limit, where the volume of the CY is taken to be large such that the backreaction of the fluxes on the geometry can be neglected.[9]

Another way to derive the CY constraint is supersymmetry. The supercharge of a $\mathcal{N} = 1$ supersymmetric theory in ten dimensions is given by a Majorana-Weyl spinor living in the **16** representation of SO(1,9). Splitting the spacetime into a 4- and a 6-dimensionl part, $\mathcal{M}^{10} \to \mathcal{M}^4 \times \mathcal{M}^6$ splits this representation into representations of SO(1,3) and SO(6) as follows:

$$16 \to (2_L, \overline{4}) + (2_R, 4) \ . \tag{2.114}$$

Thus the Weyl representation splits into a total of 8 spinors in four dimensions. Imposing the Majorana constraint halves that number, resulting in a $\mathcal{N} = 4$ supersymmetric theory. This assumed a $\mathcal{N} = 1$ spacetime supersymmetric theory, i.e. a type I string theory. Type II theories have double the amount of supercharges, thus these theories result in a $\mathcal{N} = 8$ 4-dimensional theory. These are phenomenological not interesting. Thus more structure of the internal manifold is assumed. SO(6) is isomorphic to SU(4), which has a natural maximal subgroup of SU(3). Thus if one chooses a manifold with holonomy group SU(3), the **4** of SO(6) decomposes under this subgroup as

$$4 \to 3 + 1 \ , \tag{2.115}$$

and similar for the $\overline{4}$. Supersymmetry requires a covariantly constant spinor. This requirement especially includes that the spinor does not transform under the holonomy group, i.e. it is a singlet of the SU(3). For each chirality, i.e. 4 and $\overline{4}$ of SO(6), there is one covariantly constant spinor. This implies the number of supercharges is divided by 4 when compactifying on a manifold with SU(3) holonomy. For type I theories this corresponds to $\mathcal{N} = 1$ supersymmetry and for type II to $\mathcal{N} = 2$.

If one had chosen SU(2) holonomy instead, the **4** would decompose as

$$4 \to 2 + 1 + 1 \ , \tag{2.116}$$

resulting in 2 covariantly constant spinors per **4** or equivalent half the amount of supersymmetry. For type II this would lead to a $\mathcal{N} = 4$ theory. Of course, as stated above, manifolds of SU(N) holonomy are CY manifolds. Thus demanding the correct amount of supersymmetry also fixes the compactification geometry to be a CY.

CY spaces in 1 or 2 complex dimensions have been completely classified. In 1 dimension there is only the torus T^2, in 2 dimensions there is only the $K3$ manifold, which is an orbifold of T^4. Finally, in 3 dimensions there is an enormous amount of CY manifolds and it is not even known if the number of them is finite.

[9] Using GLSM models with torsion, it is possible to obtain exact solutions with non-zero H-flux. These solutions correspond to non-flat manifolds known as Fu-Yau manifolds [28].

A Toy Example: The Elliptic Curve

As a first very simple example of a CY space we take the two-torus represented as $\mathbb{C}/\mathbb{Z}^2$. Due to historical reasons genus 1 curves, i.e. tori, are also called elliptic curves. The torus arises by taking the complex plane $\mathbb{C}$ and identifying points of a lattice, i.e.

$$z \sim z + m\lambda_1 + n\lambda_2 \qquad \forall n, m \in \mathbb{Z} \; . \tag{2.117}$$

Here the λ_i are constants parameterizing the manifold. But different values of the λ_i give the same lattice. If

$$\begin{pmatrix} \lambda_1' \\ \lambda_2' \end{pmatrix} = A \begin{pmatrix} \lambda_1 \\ \lambda_2 \end{pmatrix} \; , \tag{2.118}$$

with an invertible integer matrix A the lattices are equivalent. Moreover, $w = \frac{z}{\lambda_1}$ defines an analytic map to another elliptic curve with $\lambda_1 = 1$. Thus all elliptic curves are isomorphic to an elliptic curve with $\lambda_1 = 1$. The other parameter then is given by $\tau = \frac{\lambda_2}{\lambda_1}$. It represents the complex structure of the torus. Of course sending any λ to $-\lambda$ does not change the lattice, so we can restrict the space of τ to be the upper half plane. The equivalent lattices of (2.118) act on the complex structure τ as follows:

$$\tau \to \frac{a\tau + b}{c\tau + b} \; , \tag{2.119}$$

with the matrix $\begin{pmatrix} a & b \\ c & d \end{pmatrix} \in SL(2, \mathbb{Z})$. The symmetry group $SL(2, \mathbb{Z})$ is also known as the modular group. This will play an important role in this thesis, some properties of this group and modular functions are summarized in appendix A.4. The moduli space of elliptic curves thus corresponds to the upper half plane mod $SL(2, \mathbb{Z})$ transformations. This space is the so called Teichmüller space, shown in figure 2.3. Note that this is the same group as the duality group of the axio-dilaton in type IIB. That the fundamental domain does not include the origin is the reason for the absence of IR singularities in string theory.

The elliptic curve inherits the flat metric of $\mathbb{C}$, therefore the tangent bundle is trivial and the space is a Calabi-Yau. In fact tori are the only example of 1-dimensional Calabi-Yau spaces.

A torus has only a single closed form, $\mathrm{d}z$. We can integrate this form over the line segments a between z and $z + 1$ and b between z and $z + \tau$. This gives the *periods*

$$\omega_a = \int_a dz = 1 \; , \tag{2.120}$$

$$\omega_b = \int_b dz = \tau \; . \tag{2.121}$$

The important relation here is that the periods are closely connected to the complex structure τ. In fact we can compute the complex structure from the periods:

$$\tau = \frac{\omega_b}{\omega_a} \; . \tag{2.122}$$

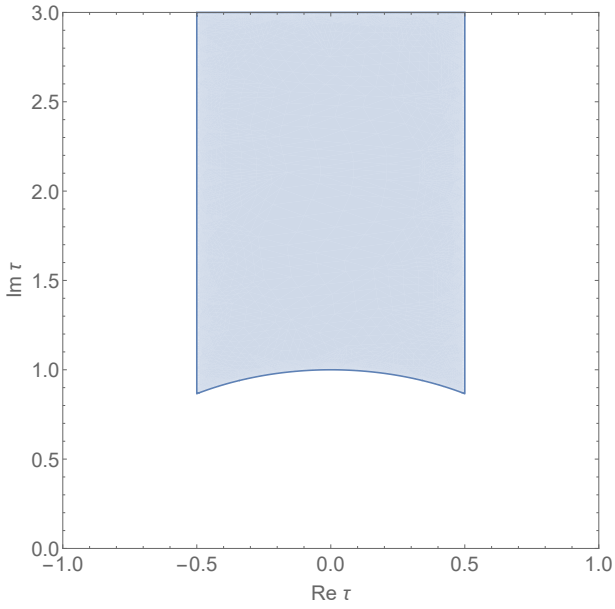

Figure 2.3: A plot of the Teichmüller space. It extends infinitely in the imaginary direction.

This is the first (trivial) example of a mirror map. In principle the Calabi-Yau 3-folds necessary for string theory will work exactly in the same way. The line segments (1-cycles) a and b are replaced by 3-cycles γ_α, the holomorphic 1-form dz is replaced by the unique holomorphic 3-form Ω_3 such that the periods become

$$\omega_\alpha = \int_{\gamma_\alpha} \Omega_3 \ . \tag{2.123}$$

The mirror maps are then given by ratios of these periods

$$t_a = \frac{A^{a\alpha}\,\omega_\alpha}{\omega_0} \ . \tag{2.124}$$

Here appears a slight complication compared to the torus. The numerator of the mirror map is a linear combination of all periods. The vector A can be fixed using monodromy considerations. If the basis of 3-cycles γ_α is chosen in a specific way, the mirror map simplifies to

$$t_a = \delta_{a,\alpha}\frac{\omega_\alpha}{\omega_0} \ , \tag{2.125}$$

which is of the same form as in the case of the elliptic curve. How to choose this basis will be discussed in detail in the next chapter. Moreover, while the integrals in (2.120) can be performed analytically, in the case of CY 3-folds they can in many cases only be performed in a power series approximation. The whole third chapter is dedicated to the computation of the periods in an as large as possible generality. For now we will simply assume that we can compute the periods of the CY we are interested in.

2.4.4 Calabi-Yau Compactifications

In this section we will put the results of the previous sections together to obtain explicit formulas for the low energy effective 4-dimensional theories in the case of a compactification on a CY manifold. To this end the fields of the low energy effective SUGRA action are expanded into 4-dimensional fields and the basis elements of the cohomology of the internal space defined in section 2.4.1. For example, the 4-form field C_4 is expanded as

$$C_4 = D_2^A \wedge \omega_A + V^\kappa \wedge \alpha_\kappa - U_\kappa \wedge \beta^\kappa + \rho_A \tilde{\omega}^A \ , \tag{2.126}$$

where D_2 is a two-form field, V and U are vector fields and ρ is a scalar field. Note that C_4 is a bit of a special case due to the self-duality constraint of F_5, such that only half of the fields are actually present. One can choose to either eliminate D_2 or ρ_A and either V^κor U_κ. In case of orientifold compactifications one expands the fields in either the even or odd basis of the cohomology, such that the combined cycle and field is invariant under the symmetry. After inserting these expansions into the action, the 6-dimensional internal integral can be performed and one obtains a 4-dimensional effective action. The expressions are rather lengthy, for type II orientifolds with O3/O7 and O5/O9 planes they can be found in [29]. We refrain from giving them here but instead directly use that the resulting 4-dimensional theory of a flux compactification is a $\mathcal{N} = 1$ supersymmetric theory. Such a theory is completely defined by a Kähler potential K, a superpotential W and the gauge kinetic function. The superpotential for a CY flux compactification was worked out in [30] by comparing the general expression for a 4-dimensional theory to the result from the compactification of the 10-dimensional theory, resulting in

$$W = \int_X G \wedge \Omega = G \, \Sigma \, \Pi \ , \tag{2.127}$$

where G is the combination of three-form fluxes

$$G = F + iSH \ , \tag{2.128}$$

and Σ is the symplectic pairing matrix while Π are the periods in the integral symplectic basis. S is the axio-dilaton and F and H are the fluxes, given by integrals of the three-forms $H_3 = \mathrm{d}B_2$ and F_3 over the cycles of the symplectic basis, i.e.

$$F = \begin{pmatrix} \int_{A^a} F_3 \\ \int_{B_a} F_3 \end{pmatrix} \ , \quad H = \begin{pmatrix} \int_{A^a} H_3 \\ \int_{B_a} H_3 \end{pmatrix} \ . \tag{2.129}$$

The Kähler potential is independent of the fluxes and depends only on the periods and the axio-dilaton [31],

$$K = -2\log(\mathcal{V}) - \log(S + \overline{S}) = -\log(\Pi\Sigma\overline{\Pi}) - \log(S + \overline{S}) \ , \tag{2.130}$$

where $\mathcal{V}$ is the volume of the CY. From this potential one obtains the Kähler metric

$$G_{i,\bar{j}} = \partial_i \partial_{\bar{j}} K \ , \tag{2.131}$$

where $i = 1, \ldots, h^{1,1}$. Finally, the gauge kinetic function M_{ij} is given in terms of the periods as [29]

$$M_{ij} = \overline{F}_{ij} + 2i\frac{\mathrm{Im}(F_{ik})X^k\mathrm{Im}(F_{jl})X^l}{X^n\mathrm{Im}(F_{nm})X^m} \ . \tag{2.132}$$

In this equation all indices run over the range $0 \ldots h^{2,1}$. The X^k represent the A-cycle periods, and F_{nm} are the derivatives of the B-cycle periods F_j:

$$F_{ij} = \partial_{X^i} F_j \ . \tag{2.133}$$

Note that the notation in terms of F originates from the fact that due to special geometry, the period vector and therefore the Kähler potential can be expressed in terms of $h^{2,1}$ special coordinates and a holomorphic function of these coordinates, the prepotential F. These coordinates are obtained by introducing a homogeneous coordinate system for the A-cycle periods: $z^i = \frac{X^i}{X^0}$, while the B-cycle periods are then given by the derivative of this prepotential with respect to the special coordinates, i.e.

$$\Pi = \begin{pmatrix} 1 \\ X^1 \\ X^2 \\ \ldots \\ X^{h^{2,1}} \\ \frac{\partial F}{\partial X^1} \\ \frac{\partial F}{\partial X^2} \\ \ldots \\ \frac{\partial F}{\partial X^{h^{2,1}}} \\ 2F - \sum_{i=1}^{h^{2,1}} \frac{\partial F}{\partial X^{h^{2,1}}} \end{pmatrix} \ . \tag{2.134}$$

The periods and the prepotential are thus in one-to-one correspondence. We will mainly focus on the computation of the periods in this thesis and derive the prepotential from these and mainly use the prepotential as a mean to summarize the results.

Given the Kähler as well as the superpotential, it is possible to explicitly compute the scalar potential of the theory:

$$V = e^K \left(G^{i\bar{j}} W_i W_{\bar{j}} - 3|W|^2 \right) \ . \tag{2.135}$$

In this formula W_i are Kähler covariant derivatives of the superpotential and $G^{i,\bar{j}}$ is the inverse Kähler metric.

Both, the superpotential as well as the Kähler potential depend on the choice of fluxes and the periods of the CY. While the fluxes, up to tadpole cancellation conditions and the requirement of them being integer, can be chosen freely, the periods are fixed by the geometry. The next chapter is focusing on methods to compute the periods, which then allows the computation of the 4-dimensional effective theory.

Chapter 3

Mathematical Tools

In this chapter we focus on the development of mathematical tools which will be applied in string theoretic settings in the later chapters. We start with the construction of CYs and the computation of their periods. For the construction we will use Batyrev's mirror polytope construction [32]. Then we will compute the periods using two different methods. First we apply a geometric method using Picard-Fuchs (PF) operators and solving the PF system locally. Second, we will use gauged linear sigma models to compute the Kähler potential directly and extract the periods from the potential. Depending on the application both approaches have their advantages and disadvantages. Then we turn to numerical algorithms for CY metrics as well as line bundle cohomologies.

3.1 Construction of Calabi-Yau manifolds

We will describe the CY as a hypersurface in a toric variety. A toric variety is a generalization of (weighted) projective space. An n-dimensional projective space is obtained by taking n+1 copies of the affine plane, $\mathbb{C}^{n+1}$, removing the origin and identifying points under the rescaling

$$\mathbb{C}^\star : \quad \{x_1, x_2, \ldots, x_{n+1}\} \to \{\lambda^{k_1} x_1, \lambda^{k_2} x_2, \ldots, \lambda^{k_{n+1}} x_{n+1}\}, \qquad \lambda \neq 0 \, . \tag{3.1}$$

The exponents k_i, $i = 1, \ldots, n+1$ are called weights. There is a bit of an abuse of notation common in this field by using the symbol $\mathbb{C}^\star$ for the group action as well as for the complex plane without the origin, $\mathbb{C}^\star = \mathbb{C}/\{0\}$. It should be clear from the context which one is meant. The weighted projective space is then defined as

$$\mathbb{P}^n_{k_1,k_2,\ldots,k_{n+1}} = \frac{\mathbb{C}^{n+1} - \{0\}}{\mathbb{C}^\star} \, . \tag{3.2}$$

This space is free of singularities as long as the weights have no common divisor except 1. Otherwise they have only quotient singularities which can be resolved by blowing them up. Allowing for more than one $\mathbb{C}^\star$ action, possibly with different weights, results in so-called

toric varieties. An algebraic torus is a group which is isomorphic to $\mathbb{C}^{\star m}$ for any integer m. A d-dimensional variety V is obtained as

$$V_\Sigma = \frac{\mathbb{C}^n - F_\Sigma}{\mathbb{C}^\star_\Sigma} \,. \tag{3.3}$$

F_Σ in this case is a subset of C^n defined by the coordinate hyperplanes. This space contains an algebraic torus $T = \frac{\mathbb{C}^{\star n}}{\mathbb{C}^{\star n-d}}$ of dimension d which is the origin of the name toric variety. The Σ indicates that these objects will be defined using a fan Σ of strongly convex rational polyhedral cones to describe them.

Before we go into details of the construction we note that there are in principle two ways of constructing a toric variety. One possibility is to use a fan, allowing the construction of normal varieties, the other is the application of a reflexive polyhedron, allowing the construction of projective varieties. As long as the variety of interest is both normal and projective, the different methods result in the same geometry and it does not matter which is applied [33]. This will be the case for all varieties in this thesis, therefore we will work mostly with fans and describe how to obtain a fan from a reflexive polytope Σ. Given a reflexive polyhedron, there are two ways to obtain a fan. First, a fan is obtained by interpreting the facets (dimension 1 faces) of the polyhedron as a cone and their collection as the fan. In this case the coordinates of the fan's vertices and the polyhedron coincide. The only difference then is that the origin is an integral point of the polytope and not an element of the vectors spanning the 1-dimensional cones.[1] We will refer to this fan as the fan over faces. Second, one can take the in-pointing normals of the cone's faces and interpret the collection of these as a fan. This gives the normal fan. This fan coincides with the fan over the cones of the dual polyhedron. To minimize possible confusion we assign to each polyhedron the fan over its faces, not the normal fan. The dual is denoted by a star $\star$. Polyhedra are denoted by Δ, while fans are denoted by Σ. Pictorially the relations can be described as follows:

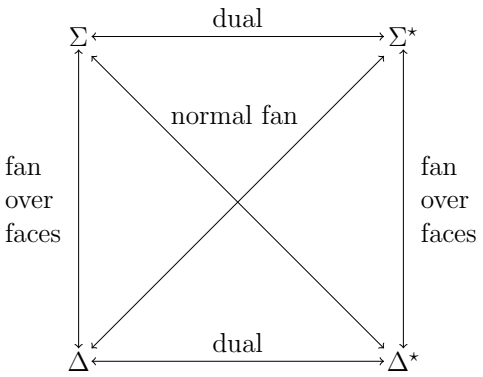

Figure 3.1: The relations between fans and cones.

[1] This fact will be important for a correct counting of the exponents of the monomials when we write down the monomial-divisor map.

To complicate things even further, in the construction of Calabi-Yau manifolds the polyhedra and their duals are sometimes interpreted in a space with one more dimension and lying in a hypersurface at distance 1 from the origin. We will use $\overline{\Delta}$ to denote the polyhedra in n+1 dimensions to distinguish them from the polyhedra in n dimensions. The dual polytope is defined by

$$\Delta^\star = \{m \in \mathbb{Z}^r | \langle m, v\rangle \ \geq -1, \forall v \in \Delta\} \ . \tag{3.4}$$

In the case of the interpretation in one higher dimension this changes to

$$\overline{\Delta}^\star = \{\overline{m} \in \mathbb{Z}^{r+1} | \langle \overline{m}, \overline{v}\rangle \ \geq 0, \forall \overline{v} \in \overline{\Delta}\} \ . \tag{3.5}$$

Reflexive polyhedra in 3 and 4 dimensions have been completely classified with the result that there are 4319 different 3-dimensional polyhedra [34] and 473,800,776 four-dimensional ones [35].

A fan Σ of strongly convex rational polyhedral cones is a collection of cones with the following properties:

- The intersection of any two cones is a face.
- All faces of the elements in Σ are in Σ .
- Any angle between two cones is less than π (strongly convex).
- There is only a finite number of cones in the fan (polyhedral).
- The cones are defined over a lattice $N \sim \mathbb{Z}^r$ (rational).

A face is a d-dimensional cone, which is the boundary of a (d+1)-dimensional cone. We denote by $\Sigma(i)$ the i-dimensional cones of Σ. The dimension of the fan will be denoted by r. There is a correspondence between the cones of the fan and submanifolds of the toric variety. Every fan includes the zero fan, the only element of $\Sigma(0)$, which corresponds to the whole toric variety. The elements of $\Sigma(1)$ correspond to divisors while the elements of $\Sigma(2)$, i.e. two-dimensional cones, correspond to co-dimension 2 submanifolds. This scheme continues, i.e. elements of $\Sigma(i)$ represent submanifolds of co-dimension i. Especially, elements of $\Sigma(r)$ represent points.

As the fan is rational, we can find an integral basis for the generators of the 1-dimensional cones, $\{v_a\}$, $a = 1 \ldots n$. I.e. each generator $v_a \in \Delta(1)$ is a vector in $\mathbb{Z}^r$. The components of this vector are denoted $v_{a,j}$, $a = 1 \ldots n$, $j = 1, \ldots, r$. To each v_a one assigns a complex coordinate x_a. All x_a together parameterize an affine space $\mathbb{C}^n$. The number of elements in $\Sigma(1)$, denoted n, then corresponds to the dimension of the affine space $\mathbb{C}^n$ in (3.3). The set F_Σ corresponds to the fixed points of the action of $(\mathbb{C}^\star_\Sigma)$. This set is encoded in the fan as follows. Take any subset S of $\Sigma(1)$ whose elements do not span a cone in Σ. $V(S)$ is defined as the subspace of $\mathbb{C}^n$ obtained by setting the coordinates

assigned to the elements of S to zero, $x_a = 0$. F_Σ is then the union of all $V(S)$. Finally the group $\mathbb{C}^\star_\Sigma$ is defined as the kernel of the map ϕ:

$$\phi : (\mathbb{C}^\star)^n \to (\mathbb{C}^\star)^r \ , \ (t_1, \ldots, t_n) \to (\prod_{i=1}^{n} t_i^{v_{i,1}}, \prod_{i=1}^{n} t_i^{v_{i,2}}, \ldots, \prod_{i=1}^{n} t_i^{v_{i,r}}) \ , \tag{3.6}$$

and

$$\mathbb{C}^\star_\Sigma = \mathrm{Ker}(\phi) \ . \tag{3.7}$$

As this construction is very abstract we will apply it to an example, the line bundle $\mathcal{O}(-3)$ over $\mathbb{P}^2$. The reason for choosing this example is the importance of line bundles over projective spaces for the construction of CY spaces. E.g. the quintic is constructed as a hypersurface in $\mathcal{O}(-5)$ over $\mathbb{P}^4$. But this case includes a 5-dimensional polyhedron which is hard to visualize, thus we show the $\mathcal{O}(-3)$ example, whose construction is fundamentally the same as the construction of $\mathcal{O}(-5)$.

We start with the description of the base $\mathbb{P}^2$. The fan of this space is spaned by the vertices

$$\begin{aligned} v_1 &= \{1, 0\}, \\ v_2 &= \{0, 1\}, \\ v_3 &= \{-1, -1\}. \end{aligned}$$

The resulting fan is shown in figure 3.2. Note that in this fan there are in total 7 cones. The origin or the 0 cone, 3 1-dimensional cones given by the v_a and 3 two-dimensional cones in between these. As we have 3 1-dimensional cones, the affine space described by

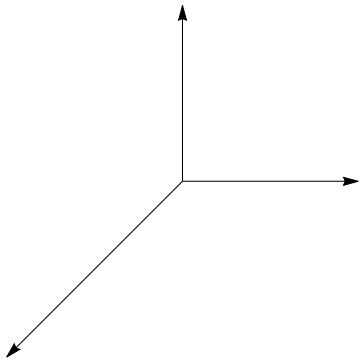

Figure 3.2: The fan for $\mathbb{P}^2$.

this fan is $\mathbb{C}^3$. The next step is to look for subsets of $\Delta(1) = \{v_1, v_2, v_3\}$ which do not span a cone in Σ. The only such subset is the whole $\Delta(1)$, resulting in a single fixed point, the origin. The fixed point set is thus $F_\Sigma = \{\{0, 0, 0\}\}$. The map ϕ is now given by

$$\phi : (\mathbb{C}^\star)^3 \to (\mathbb{C}^\star)^2 \ , \ (t_1, t_2, t_3) \to (t_1\, t_3^{-1}, t_2\, t_3^{-1}) \ . \tag{3.8}$$

The kernel is parameterized by a single coordinate t, such that $\phi(t,t,t) = (1,1), t \neq 0$. The space spaned by t is $\mathbb{C}^\star$, thus $\mathbb{C}^\star_\Sigma = \mathbb{C}^\star$. The toric variety defined by the fan is therefore

$$V_\Sigma = \frac{\mathbb{C}^3 - \{\{0,0,0\}\}}{\mathbb{C}^\star} = \mathbb{P}^2 \ . \tag{3.9}$$

Any $\mathbb{P}^n$ can be constructed this way by taking the vertices $v_i = e_i, i = 1, \ldots, n$ with e_i the usual orthonormal basis vectors of $\mathbb{C}^n$ and $v_{n+1} = -\sum_{i=1}^{n} v_i$. A line bundle above a projective space is obtained by increasing the dimension of the fan by 1 and adding one additional vertex. The additional vertex has the coordinates $v_0 = \{0,0,\ldots,0,1\}$. The original vertices are all given by $v_a = \{v_a, 1\}$. For the example of $\mathcal{O}(-3)$ the vertices are

$$\begin{aligned} v_1 &= \{1,0,1\}, \\ v_2 &= \{0,1,1\}, \\ v_3 &= \{-1,-1,1\}, \\ v_0 &= \{0,0,1\}. \end{aligned}$$

The resulting fan is shown in figure 3.1. The 1-dimensional cones do not span all of $\mathbb{R}^3$, thus the resulting variety is non-compact, as expected for a line bundle. Furthermore there are now 4 vertices, resulting in an four dimensional affine space $\mathbb{C}^4$. The only subset of $\Delta(1)$ not

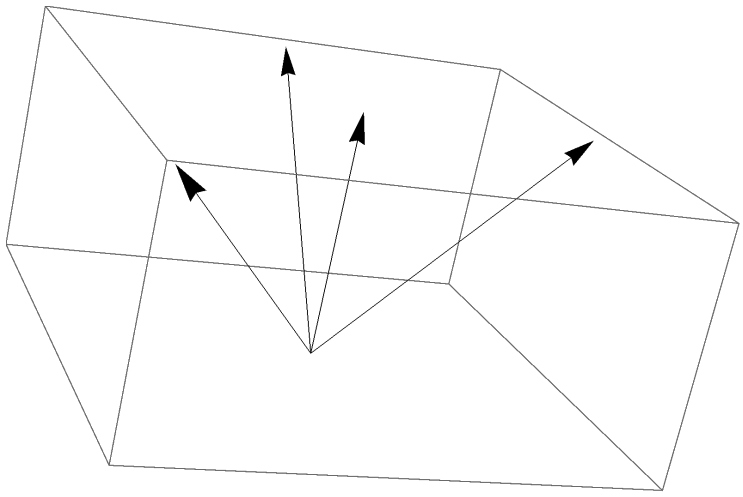

Figure 3.3: The fan for $\mathcal{O}(-3)$.

spanning a cone is $\{v_1, v_2, v_3\}$, thus the fixed point set is given by $F_\Sigma = \{x_1 = x_2 = x_3 = 0\}$. The map ϕ is

$$\phi : (\mathbb{C}^\star)^4 \to (\mathbb{C}^\star)^3 \ , \ (t_1,t_2,t_3,t_4) \to (t_1\, t_3^{-1}, t_2\, t_3^{-1}, t_1 t_2 t_3 t_4^{-1}) \ . \tag{3.10}$$

The kernel of this map is (t,t,t,t^{-3}) which is isomorphic to $\mathbb{C}^\star$, hence again $\mathbb{C}^\star_\Sigma = \mathbb{C}^\star$.

Furthermore, the direct product of weighted projective spaces is described by the product of the fans. For example, if one wants to construct $\mathbb{P}^n \times \mathbb{P}^m$ with the respective n and m dimensional fans Δ_n and Δ_m, the fan for the product space is obtained by taking vertices in $\mathbb{R}^{n+m}$. The vertices are the same as in Δ_n or Δ_m with the additional coordinates set to zero.

The line bundles are then constructed as before by adding additional dimensions and vertices, one for each weighted projective space. This finishes the construction for the ambient spaces of any complete intersection Calabi Yau. The last ingredient needed is the description of the hypersurface. These are defined by a polynomial equation in the ambient coordinates. As the ambient space is projective the defining polynomials have to be homogeneous. Moreover, they have to be invariant under the action of $\mathbb{C}^\star$ used to construct the ambient variety. For the CY condition to be fulfilled, the degree of the polynomials has to be the sum of the weights of the projective space. The polynomials are encoded in the integral points of the dual fan. The map assigning the monomials to the points of the dual fan is known as the monomial-divisor map [36]. It is given by

$$P = \sum_{i=0}^{M} a_i \prod_{j=1}^{r} x_j^{\langle \overline{v}_j, \overline{m}_i \rangle} = \sum_{i=0}^{M} a_i \prod_{j=1}^{r} x_j^{\langle v_j, m_i \rangle + 1} \ . \tag{3.11}$$

Here M is the number of integral points in the dual polyhedron $\Delta^\star$. The coordinate vectors of the integral points are denoted $m_i,\ i = 1, \ldots, M$. The name of the map originates in the interpretation of the polyhedron as a fan, where the elements m_i of $\Sigma^\star(1)$ correspond to divisors of the variety. The a_i parameterize the deformations of the complex structure of the mirror manifold. But this is an over-paramterization, as coordinate redefinitions leave the polynomial invariant. Therefore, from the M a_i, r can be fixed by reparameterizations. The physical deformations are encoded in the relations between the vertices of the fan Σ. One can choose any basis for the lattice of relations L. We will denote the elements of this basis as $l_a, a = 1, \ldots, \dim(L)$. Thus the dimension of the lattice equals the number of complex structure moduli, $h^{2,1} = \dim(L)$. It has been shown in [37] that there is a unique choice of coordinates centered around the large complex structure(LCS) point, given by

$$x_a = \prod_{i=1}^{r} a_i^{l_{a,r}} \ . \tag{3.12}$$

For the Kähler side, Batyrev showed [32] that the following formula holds:

$$h^{1,1}(\Delta) = h^{r-2,1}(\Delta^\star) = l(\Delta^\star) - (r+1) - \sum_{codim \Theta^\star = 1} l'(\Theta^\star) + \sum_{codim \Theta^\star = 2} l'(\Theta^\star) l'(\Theta) \ . \tag{3.13}$$

Here the functions l and l' count the number of integral points on the face and on the interior respectively. Θ and its dual $\Theta^\star$ are faces of a fixed codimension. For a CY 3-fold the dimension of the reflexive polyhedra is $r = 4$, thus this formula relates $h^{1,1}$ of a reflexive polyhedron to $h^{2,1}$ of its dual. This is the first example of mirror symmetry.

We will not use this formula as there are easier ways to determine the dimensions of the moduli spaces, but we will heavily exploit the resulting mirror symmetry to replace the complicated Kähler side computations by easier computations on the complex structure side. In the third section of this chapter we will introduce gauged linear sigma models, which allow the computation to be performed directly on the Kähler side.

3.1.1 An Example: The (Mirror) Quintic

In this section we will apply the methods described so far to the easiest example of a CY 3-fold, the mirror of a quintic hypersurface in $\mathbb{P}^4$. The quintic itself has 1 Kähler modulus and 101 complex structure moduli. Thus the mirror has 1 complex structure deformation, which by the mirror map corresponds to the single Kähler modulus of the quintic. So while we will compute everything for the mirror quintic, in the end we will have described the Kähler side of the quintic itself. From now on we will simply write the quintic and it should be obvious form the context if we refer to the quintic or its mirror. The fan for $\mathbb{P}^4$ is spanned by

$$v_{i,j} = \begin{pmatrix} 1 & 0 & 0 & 0 \\ 0 & 1 & 0 & 0 \\ 0 & 0 & 1 & 0 \\ 0 & 0 & 0 & 1 \\ -1 & -1 & -1 & -1 \end{pmatrix} . \tag{3.14}$$

The dual fan of this is spanned by

$$m_{i,j} = \begin{pmatrix} 4 & -1 & -1 & -1 \\ -1 & 4 & -1 & -1 \\ -1 & -1 & 4 & -1 \\ -1 & -1 & -1 & 4 \\ -1 & -1 & -1 & -1 \end{pmatrix} . \tag{3.15}$$

Note that the dual fan interpreted as a polyhedron includes the origin as an integral point. Now we extend the dimension of the fan by 1 and include the origin, to obtain

$$\overline{v}_{i,j} = \begin{pmatrix} 1 & 0 & 0 & 0 & 1 \\ 0 & 1 & 0 & 0 & 1 \\ 0 & 0 & 1 & 0 & 1 \\ 0 & 0 & 0 & 1 & 1 \\ -1 & -1 & -1 & -1 & 1 \\ 0 & 0 & 0 & 0 & 1 \end{pmatrix} . \tag{3.16}$$

These vertices have exactly one linear dependence, $\sum_{i=1}^{5} v_i - 5v_6 = 0$, thus

$$l_1 = \{1, 1, 1, 1, 1, -5\} . \tag{3.17}$$

The monomial divisor map can be written using either $v_{i,j}$ or $\overline{v}_{i,j}$ with the same result. From (3.11) follows the polynomial

$$P = a_1 x_1^5 + a_2 x_2^5 + a_3 x_3^5 + a_4 x_4^5 + a_5 x_5^5 + a_6 x_1 x_2 x_3 x_4 x_5 = 0 \; . \tag{3.18}$$

As we have 5 coordinate reparameterizations we can set the first 5 a_i to 1 and denote the last $a_6 = 5\psi$ to bring the defining polynomial to the usual form mostly used in the literature

$$P = x_1^5 + x_2^5 + x_3^5 + x_4^5 + x_5^5 + 5\psi x_1 x_2 x_3 x_4 x_5 = 0 \; . \tag{3.19}$$

As the ambient space is just $\mathbb{P}^4$ it has no singularities. Therefore, the quintic is only singular when the defining polynomial fails to be transversal, i.e.

$$P = \partial_i P = 0 \; \forall \; i = 1, \ldots, 5 \; . \tag{3.20}$$

These equations have only a solution in the case $\psi = 1$, where the manifold develops a conifold singularity. For all other values of ψ the manifold is smooth. Note that the simple value for the conifold position is the reason to choose $a_6 = 5\psi$. This coordinate choice is centered around the so-called Landau-Ginsburg point at $\psi = 0$. The LCS coordinate as given by (3.12) is

$$x = \frac{a_1 a_2 a_3 a_4 a_5}{a_6^5} = \frac{1}{5^5 \psi^5} \; . \tag{3.21}$$

3.1.2 Constructing General CICYs

To set the notation for the next sections we finally give the description of a general CICY. We use the notation

$$\left[\begin{array}{c|cccc} \mathbb{P}_{w_1^{(1)} w_2^{(1)} \ldots w_{n_k+1}^{(1)}} & d_1^{(1)} & d_2^{(1)} & \ldots & d_p^{(1)} \\ \mathbb{P}_{w_1^{(2)} w_2^{(2)} \ldots w_{n_k+1}^{(2)}} & d_1^{(2)} & d_2^{(2)} & \ldots & d_p^{(2)} \\ \ldots & \ldots & \ldots & \ldots & \ldots \\ \mathbb{P}_{w_1^{(k)} w_2^{(k)} \ldots w_{n_k+1}^{(k)}} & d_1^{(k)} & d_2^{(k)} & \ldots & d_p^{(k)} \end{array} \right] \; . \tag{3.22}$$

This describes a complete intersection of hypersurfaces in k projective spaces. The dimension of the m-th projective space is denoted n_m and the weight of its coordinates by $w_i^{(m)}$, $i = 1, \ldots, n_m + 1$, $m = 1, \ldots, k$. The degree of the coordinates of the i-th projective space in the j-th polynomial is denoted $d_j^{(i)}$, $j = 1, \ldots, p$, $i = 1, \ldots, k$. The degrees are taken to be positive integers.[2]

The ambient space of a complete intersection is the direct product of weighted projective spaces, thus the polytope describing the ambient spaces are also given by the direct product of the polytopes for each factor. In the case of k ambient spaces

$$\Delta = \Delta_1 \times \Delta_2 \times \ldots \times \Delta_k \; . \tag{3.23}$$

[2]It is possible to generalize this construction by allowing for the entries to take negative integers [38].

Δ then is a polytope in $\mathbb{R}^{n_1} \times \mathbb{R}^{n_2} \times \ldots \times \mathbb{R}^{n_k}$. The $v_{i,j}$ are the same as before. To describe the hypersurfaces another dimension is added to the polytope, one for each polynomial. For p polynomials we thus add another $\mathbb{R}^p$. The vertices of Δ are grouped into p sets and assigned the coordiantes $\{\vec{e}_p, v_{i,j}\}$ in $\mathbb{R}^p \times \mathbb{R}^{n_1} \times \mathbb{R}^{n_2} \times \ldots \times \mathbb{R}^{n_k}$. Here $\vec{e}_p$ is the unit vector in the p-th direction. How the vertices are grouped does not influence the resulting geometry. The resulting dual vertices $v^\star$ have the following relations:

$$l_i = \{-d_1^{(i)}, \ldots, -d_p^{(i)}, 0, \ldots, 0, w_1^{(i)}, \ldots, w_{n_i+1}^{(i)}, 0, \ldots, 0\} \ , \quad i = 1 \ldots k \ . \tag{3.24}$$

Note that while there is one relation per defining polynomial this does not directly imply that the number of moduli equals the number of equations, as some of the l_a can be linearly dependent.

3.2 Periods of CY Manifolds

As we now have a description of the CY itself, we turn to the computation of its periods. This whole section assumes for simplicity a CY 3-fold, but most of the formulas have straightforward generalizations for CY d-folds. The periods are defined as integrals of the unique holomorphic 3-form Ω over 3-cycles γ_i which form a symplectic basis of $H^3\{X, \mathbb{Z}\}$. The integral representation of the periods is then

$$\Pi = \int_{\gamma_i} \Omega \ . \tag{3.25}$$

Ω can be expressed in terms of the defining polynomial of the hypersurface:

$$\Omega = \frac{\mathrm{d}x_1 \mathrm{d}x_2 \mathrm{d}x_3}{\partial_4 P} \ . \tag{3.26}$$

Often a symplectic basis is not known a priori. In this case one first calculates any basis of periods ω_i and then transforms them into the symplectic basis. As the periods fulfill a linear system of differential equations, the transformation can be described by a matrix m:

$$\Pi = m \ \omega \ . \tag{3.27}$$

The determination of the matrix m is then the most involved step in the computation. There are two ways to approach the integral in (3.25). First one can develop the integrand into a Taylor series and integrate order by order. Second one can determine a system of differential equations fulfilled by the periods. Here we will follow the second approach. The first approach was historically used in [39–42] to compute the periods of the quintic and generalized to any hypersurface in weighted projective spaces.

The method described in this section will be based on solutions to a special system of differential equations introduced by Gel'fand, Kapranov and Zelevinsky(GKZ) [43]. It was shown by Batyrev in [32] that the periods as defined in (3.25) fulfill a GKZ system of

equations. This system is defined in terms of two differential operators, $\mathcal{D}_l$ and $\mathcal{Z}_j$. The first type of operators is given by the lattice of relations L. To each basis vector l one assigns an operator $\mathcal{D}_l$:[3]

$$\mathcal{D}_l = \prod_{l_i>0} (\partial_{a_i})^{l_i} - \prod_{l_i<0} (\partial_{a_i})^{-l_i} \ . \tag{3.28}$$

The second type of operator depends on the vertices themselves:

$$\mathcal{Z}_j = \sum_{i=0}^{n} \overrightarrow{v}^{\star}_{i,j} a_i \partial_{a_i} - \beta_j \ . \tag{3.29}$$

The number of $\mathcal{Z}$ operators equals the dimension of the fan, i.e. $j = 1, \ldots, r$. β is a vector, which is in the case of the period system given by $\beta = \{-1, 0, \ldots, 0\}$ [32]. The periods are annihilated by both types of operators, i.e.

$$\mathcal{D}_l \Omega_i = \mathcal{Z}_j \Omega_i = 0 \qquad i = 0, \ldots, 2h^{2,1} + 1 \, . \tag{3.30}$$

The $\mathcal{Z}_j$ part of the system restricts the coordinates to the physical complex structure coordinates. As described in the last section the a_i over-parameterize the space of complex structure deformations. The coordinates x_a given in (3.12) are exactly chosen such that

$$\mathcal{Z}_j f(x_a) = 0 \ , \tag{3.31}$$

for any function f of the coordinates x_a. The remaining PF operators can be written in terms of the weights $w_i^{(a)}$ of the a-th weighted projective spaces and the degrees of the polynomials $d_j^{(a)}$ [44]:

$$\begin{aligned} \mathcal{D}_a = & \prod_{j=1}^{n_a+1} \Big(w_j^{(a)} \theta_a \Big) \Big(w_j^{(a)} \theta_a - 1 \Big) \cdots \Big(w_j^{(a)} \theta_a - w_j^{(a)} + 1 \Big) \\ & - \prod_{j=1}^{p} \Big(\sum_{i=1}^{k} d_j^{(i)} \theta_i \Big) \cdots \Big(\sum_{i=1}^{k} d_j^{(i)} \theta_i - d_j^{(a)} + 1 \Big) x_a \ . \end{aligned}$$

Again, as for the lattice relations the operators do not all have to be independent. Note that there are as many differential operators as there are complex structure coordinates. This is due to the fact that on the mirror side the only Kähler moduli the toric construction sees are the sizes of the weighted projective spaces. Interestingly, most known CYs have a so-called favorable embedding where the number of Kähler moduli equals the number of ambient projective spaces [45].

[3] In general it can happen that these operators do not generate the full differential system. In this case additional operators need to be added. This does not happen for the models studied in this thesis. For the details of the computation in these cases see [37].

3.2.1 Local Solutions

A solution to the GKZ system (3.30) around the LCS point was constructed in [37]. This solution is based on a so-called fundamental period $\omega_0(\rho_i)$. The solution corresponds to the derivatives of this period with respect to the indices ρ_i evaluated at $\rho_i = 0$. These indices are merely an organizing principle to write down the solution. The fundamental period for a complete intersection CY is given by

$$\omega_0 = \sum_{n=0}^{\infty} c_n x^{n+\rho} \, . \tag{3.32}$$

Here and in the following we apply a multi-index notation to simplify the notation, i.e. $x^n = x_1^{n_1} x_2^{n_2} \dots x_{h^{21}}^{n_{h^{21}}}$ and $\sum_{n=0}^{\infty} = \sum_{n_1=0}^{\infty} \sum_{n_2=0}^{\infty} \dots \sum_{n_{h^{21}}=0}^{\infty}$. The expansion coefficients are [44]

$$c_n = \frac{\prod_{j=1}^{p} \Gamma\left(1 + \sum_{i=1}^{k} (n_i + \rho_i) d_j^{(i)}\right)}{\prod_{i=1}^{k} \prod_{j=1}^{n_i+1} \Gamma\left(1 + w_j^{(i)} (n_i + \rho_i)\right)} \, , \tag{3.33}$$

where we applied the notation from section 3.1.2. The full basis of periods is obtained by acting with the following differential operators on the fundamental periods:

$$\begin{aligned} D_{1,i} &= \frac{1}{2\pi i} \partial_{\rho_i} \, , \\ D_{2,i} &= \frac{1}{2} \frac{K_{ijk}}{(2\pi i)^2} \partial_{\rho_j} \partial_{\rho_k} \, , \\ D_3 &= -\frac{1}{6} \frac{K_{ijk}}{(2\pi i)^3} \partial_{\rho_i} \partial_{\rho_j} \partial_{\rho_k} \, , \end{aligned} \tag{3.34}$$

where the K_{ijk} are the classical triple intersection numbers and $i = 1 \dots, h^{2,1}$. The period vector is then

$$\omega_{\text{LCS}} = \left. \begin{pmatrix} \omega_0 \\ D_{1,i}\, \omega_0 \\ D_{2,i}\, \omega_0 \\ D_3\, \omega_0 \end{pmatrix} \right|_{\rho_i = 0} \, . \tag{3.35}$$

We will refer to this basis as the hypergeometric basis, as performing one of the sums in the fundamental period explicitly results in a hypergeometric function.

At other points in the moduli space a local basis can be obtained order by order by making an Ansatz for the periods as

$$\omega = \sum_{j=0}^{3} \sum_{n=0}^{\infty} c_n x^n \log(x)^j \, . \tag{3.36}$$

This Ansatz represents the most general polynomial of degree 3 in the logarithms of the coordinates and of infinite degree in the coordinates. If the exponents of the logarithms

at the LCS are known, one can compute the exponents at any point in moduli space by performing a coordinate change to coordinates centered around the point in moduli space one is interested in [46]. This reduces the required computational time, as the sum over j can be restricted to the values needed. In low moduli examples this is actually not necessary and the Ansatz can be solved by brute force and the lowest order equations determine the logarithms.

An important technical detail is the correct determination of the coordinates. (3.12) gives the coordinates around the LCS point. The structure of the $\mathcal{Z}$ operators shows that inverting the exponents of all a_i simultaneously in (3.12) gives another solution. This is the opposite point in moduli space, in many cases this represents the Landau-Ginzburg(LG) point in moduli space.[4] In the case of the quintic example, the ψ coordinate is exactly this second solution. For any other point in moduli space it is a priori unclear what coordinates to choose. The other possible intersections of divisors in moduli space are points of tangency, i.e. the divisors do not intersect normal. To remedy this situation one has to perform a blow up of the moduli space, carefully keeping track of the coordinates in this process.

3.2.2 Computation of the Transition Matrix

What remains to do is to compute the transition matrices. Around the LCS point these have been first computed by Candelas et al. in [40]. The basic idea is that one can compute the classical prepotential at the LCS point due to the fact that there are no instanton corrections at this point. There are only the classical intersection numbers as well as a 1- and a 4-loop contribution. The 4-loop term turns out to be related to the Euler characteristic χ, while the 1-loop term contributes subleading, i.e. quadratic and linear, terms. Thus the prepotential at the LCS point is given by[5]

$$F = -\frac{K_{ijk}}{6} t^i t^j t^k + \frac{1}{2} a_{ij} t^i t^j + b_i t^i + \frac{\zeta(3)\chi}{(2\pi i)^3} \,. \tag{3.37}$$

This prepotential corresponds to the periods vector

$$\Pi = \begin{pmatrix} 1 \\ t_i \\ \partial_i F \\ F \end{pmatrix} \,. \tag{3.38}$$

Here we already use homogeneous coordinates, i.e. we divided by Π_0, of course one can also work in inhomogeneous coordinates. The constants b_i are topological and can be computed

[4] There exist models e.g. $\mathbb{P}^5[3\,3]$ which do not have a LG point but instead there is a symmetry of the model $\Pi(x) = \Pi(x^{-1})$, in this case there is another LCS point. The geometric interpretation of the phase does not influence the computations, the coordinates and periods are still valid.

[5] This is exact up to 4-loops. For a CY 3-fold there are no further corrections. For a CY d-fold there are higher α' corrections resulting in further corrections of the form $\zeta(2n+1)c_{2n}$ where c_{2n} denotes the Chern classes.

as [37]:

$$b_i = -\frac{1}{24}\int_X c_2 J_i \ , \tag{3.39}$$

where J_i is the Kähler form corresponding to the i-th parameter. The a_{ij} are not related to topological numbers and do not influence the geometry. The shift symmetry $t \to t+1$ forces $\mathrm{Im}(a_{ij}) = \mathrm{Im}(b_i) = 0$. Acting with this symmetry on the period vector and demanding that the action corresponds to a symplectic transformation fixes the a_{ij}. As the form of Π at the LCS point is thus fixed, one can easily determine the transition matrix by solving the equation

$$\Pi = m\ \omega \ . \tag{3.40}$$

At other points in the moduli space one does not know the prepotential a priori, thus another way is needed to compute the transition matrix. The form of the matrix is restricted by the monodromies of the periods as well as the symplectic form. Both methods reduce the degrees of freedom. At the point of maximal monodromy, which is the LCS point, the monodromies are enough to completely fix the transition matrix. But at other points the monodromies are not sufficient. Thus one uses the knowledge of the periods at the LCS and analytically continues these periods to other points in moduli space. The phenomenologically interesting points are intersections of singular divisors. These correspond to one of the following: LCS points (i.e. large volume), Landau-Ginzburg points corresponding to a point-like target space which receives quantum corrections, hybrids between the two possibilities, i.e. a fibration of a LG model over a geometric fibre, or conifold points. In terms of coordinates, the LCS point corresponds to all $x_i = 0$. The LG point, if existent, then corresponds to all $x_i = \infty$.[6] Hybrid phases are obtained when some $x_i = 0$ and some $x_j = \infty$. Finally, at the phase boundaries for real values of the coordinates there are the conifold points. We normalize our coordinates such that the conifolds are located at $x_i = 1$ if all other x_i are either 0 or ∞. Analytic continuation to the LG or hybrid phases can be performed explicitly using the Mellin-Barnes representation of the periods. The periods around the LG point can be written as an infinite sum

$$\omega = \sum_{n=0}^{\infty} c_n x^n \ . \tag{3.41}$$

Here we are for the moment only interested in one coordinate which we denote x, the dependence on all other coordinates is absorbed into the coefficients c_n. The sum can be rewritten as an integral

$$\omega = \int_\gamma \frac{d\nu}{2i\sin(\pi\nu)} c_\nu (-x)^\nu \ , \tag{3.42}$$

where the path γ connects $-i\infty$ with $i\infty$ such that it does not intersect any poles. For small x we can close the contour to the right. The sum over residues then picks up the poles from the sin function at $\nu \in \mathbb{N}_0$, resulting exactly in the sum (3.41). For large x the

[6] We will call the point $x_i = \infty$ LG point even if it is another LCS point to be able to easily distinguish the points in moduli space. In all explicit examples in this thesis it will be an actual LG point.

contour has to be closed to the left, leading to another infinite series description of the same period, now convergent for $x > 1$. The exact form of this period depends on c_n. This procedure can be repeated for each coordinate separately, allowing to express the periods around the center of each phase. The general expressions become rather involved and we will not give them here. They can be found in [42].

This method converges well when applied to computations deep in the phases of the models, but it is not possible to compute periods close to the phase boundaries. At the boundaries all series representations converge rather badly. In practice, numerical computations are only reliable for x (or $1/x$) smaller than 0.9. The solution for this problem is to use a local basis centered around the conifold and to compute the transition matrix from this basis to the LCS basis, whose transition matrix to the symplectic basis is known. The transition matrix is usually computed numerically by choosing a point at which both bases, the LCS and local basis, converge. This point is normally taken to be exactly the midpoint, i.e. $x = 1/2$. This approach was taken e.g. in [47, 48] to construct explicit vacua. While this method allows to compute rather good approximations to the periods, it does not give analytic results. As these are required in some applications, we will now give a second method developed in [46] to compute the transition matrices analytically. While the idea of using the LCS basis and a local basis around the conifold remain the same, we will use the hypergeometric structure of the LCS periods to obtain an explicit expansion around $x_i = 1$. Comparing the coefficients of this basis with the coefficients of the local basis fixes the transition matrix uniquely. This method works for all moduli except one fixed at the LCS. Figure 3.4 shows the different bases and how they are connected.

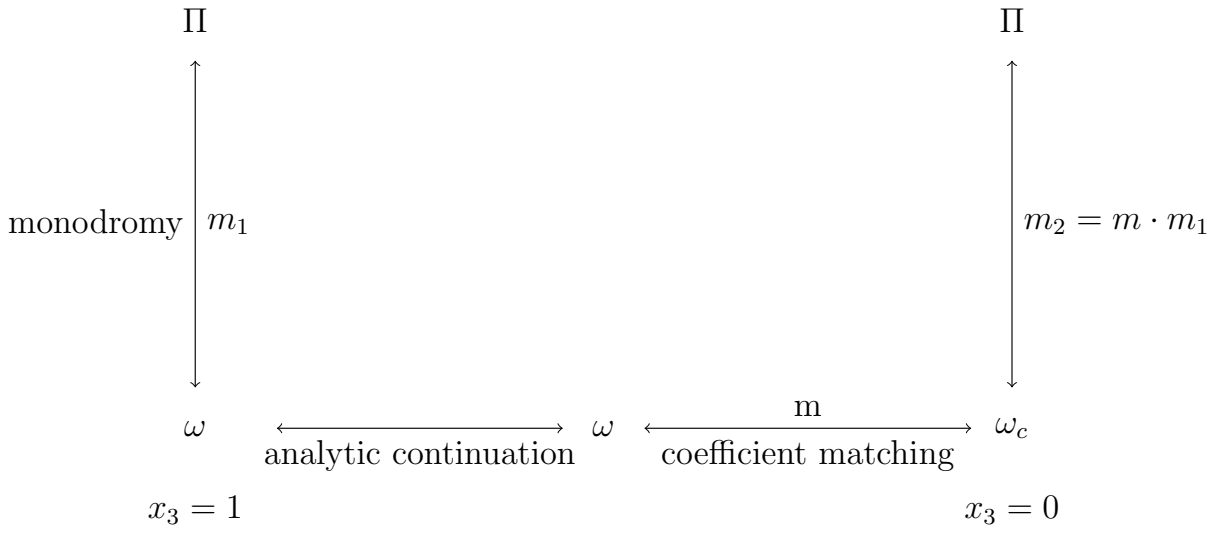

Figure 3.4: The different bases involved in the computation and the relations between them.

The critical step in this method is the analytic continuation. The periods are given at

the LCS as infinite sums of hypergeometric type. This means that (3.32) can be rewritten as infinite sums of hypergeometric functions of one variable:

$$\omega_0 = \sum_{\substack{n_i=0 \\ i\neq j}}^{\infty} \prod_{\substack{i=0 \\ i\neq j}}^{h^{2,1}} x_i^{n_i+\rho_i} x_j^{\rho_j} f(n_i,\rho_i)\ {}_pF_q(\vec{a};\vec{b};x_j)\ , \tag{3.43}$$

Here $f(n_i,\rho_i)$ denotes a combination of hypergeometric functions which does not depend on the moduli. This will result in finite polygamma contributions to the period which pose no problem for the analytic continuation. The exact form of the hypergeometric ${}_pF_q$ function depends on the model in question. It follows from the data of the l-vectors as follows. For shrinking curves the parameters p and q are given by

$$p = \sum_{k,l_k^{(z)}<0} |l_k^{(z)}|\,, \quad q = \sum_{k,l_k^{(z)}>0} |l_k^{(z)}| - 1\,, \tag{3.44}$$

i.e. p is the sum of the negative entries of the charge row vector $l^{(z)}$, and q is the sum of the positive entries of the same row(minus 1). Due to the CY-condition these sums have to be equal and $p = q + 1$. The entries of $l^{(z)}$ appear inversely in the parameters $\vec{a}$ of the hypergeometric function. The exact form of the hypergeometric function is model dependent. Note that due to possible cancellations in the hypergeometric function the effective p can be smaller. Also, the fundamental period can have larger p if the fibration structure is complicated. But in these cases the hypergeometric functions simplify after taking the limit $\rho \to 0$.

We know assume that we can compute an expansion of the fundamental period (3.43) around $\rho_i = 0$. I.e. we expand

$$\omega_0 = \sum_{k_i=1}^{3} \prod_{i=1}^{h^{2,1}} \rho_i^{k_i} F_{i,j}(x) + \mathcal{O}(\rho_i^4)\ . \tag{3.45}$$

This expansion is known as the ϵ-expansion of a hypergeometric function. The origin of this name lies in the computation of Feynman amplitudes in dimensional regularisation, where the amplitudes are expanded around $4-\epsilon$ dimensions. The indices ρ_i play in our case the role of ϵ. The periods are then given by linear combinations of the $F_{i,j}(x)$. If we are able to expand these functions around $x_j = 1$ we can compare the result to the local basis. Note that the expansion in the $x_i, i \neq j$, i.e. in the moduli which are still in the LCS, is trivial as the fundamental period is already written as a power series in these coordinates. Also, as the transition matrix is only $2(h^{2,1}+1) \times 2(h^{2,1}+1)$ dimensional, we only need a finite amount of terms to uniquely fix the transition matrix. As the form of the hypergeometric function is crucial for the computations which will follow, we will give here some examples. For simplicity we take 1-moduli examples and denote the single coordinate by x.

The simplest case is the charge vector $l = \{1, 1, -2\}$. This charge vector describes 2 points given by the vanishing of a polynomial in $\mathbb{P}^2$, i.e. a 0-dimensional manifold. This is

of course only a toy example, but it already carries all the details of the more complicated higher dimensional examples and is exactly solvable. As the sum of the negative entries is 2, the corresponding fundamental period is a ${}_2F_1$ function. The entries of the charge vector appear inversely in the parameters, thus the parameters are multiples of 1/2. The exact form in this case is

$$\omega_0 = x^\rho \, {}_2F_1(1, \frac{1}{2} + \rho_1; 1 + \rho_1; 4x) \; . \tag{3.46}$$

As the hypergeometric function has only half-integer parameters it can be ϵ-expanded using the HypExp2 package [49]. The result can be expressed in terms of logarithms and poly-logarithms:

$$\begin{aligned}
{}_2F_1(1, \frac{1}{2} + \rho_1; 1 + \rho_1; 4x) = {} & \frac{1}{\sqrt{1-4x}} + \frac{\rho_1 \, 2 \log\left(\frac{1-\sqrt{1-4x}}{\sqrt{1-4x}+1} + 1\right)}{\sqrt{1-4x}} + \\
& \frac{\rho_1^2 \, 2 \left(\mathrm{Li}_2\left(-\frac{1-\sqrt{1-4x}}{\sqrt{1-4x}+1}\right) + \log^2\left(\frac{1-\sqrt{1-4x}}{\sqrt{1-4x}+1} + 1\right)\right)}{\sqrt{1-4x}} + \\
& \frac{\rho_1^3 \, 2 \log\left(\frac{2}{\sqrt{1-4x}+1}\right) \left(2 \log^2\left(\frac{2}{\sqrt{1-x}+1}\right) - 3 \log\left(\frac{4x+2\sqrt{1-4x}-2}{4x}\right) \log\left(\frac{2}{\sqrt{1-4x}+1}\right) + \pi^2\right)}{3\sqrt{1-x}} + \\
& \frac{\rho_1^3 \, 2 \left(-6\mathrm{Li}_3\left(\frac{1-\sqrt{1-4x}}{\sqrt{1-4x}+1} + 1\right) - 3\mathrm{Li}_3\left(-\frac{1-\sqrt{1-4x}}{\sqrt{1-4x}+1}\right) + 6\zeta(3)\right)}{3\sqrt{1-4x}} + \mathcal{O}(\rho^4) \; .
\end{aligned}$$

Note the appearance of $\zeta(3)$ in the ρ^3 term. This will turn out to be the origin of the $\zeta(3)$ term in the prepotential. Moreover, each term includes a factor of ${}_2F_1(1, \frac{1}{2}; 1; 4x) = (1-4x)^{-1/2}$. Thus the expansion can be written as

$${}_2F_1(1, \frac{1}{2} + \rho_1; 1 + \rho_1; 4x) = \; {}_2F_1(1, \frac{1}{2}; 1; 4x)(1 + c_1(x)\rho + c_2(x)\rho^2 + c_3(x)\rho^3) \; . \tag{3.47}$$

The functions appearing in the coefficients c_i are much simpler than the original hypergeometric functions. These functions appear e.g. in the mirror map. Note that this behaviour is general and does not only appear in this simplex example.

Inserting the ϵ-expansion in (3.46) and taking the derivatives with respect to ρ as defined in (3.35) gives the period vector. As we are dealing with a 1-parameter model, the mirror map is simply

$$e^{2\pi t} = q = e^{\left(\frac{\omega_1}{\omega_0}\right)} = e^{x c_1(x)} = \frac{4x}{\left(\sqrt{1-4x}+1\right)^2} \; . \tag{3.48}$$

Expanding the right hand side around $x = 0$ we obtain the series

$$q = x + 2x^2 + 5x^3 + 14x^4 + 42x^5 + 132x^6 + 429x^7 + 1430x^8 + \mathcal{O}\left(x^9\right) \; . \tag{3.49}$$

The coefficients are known as the Catalan numbers. They are all integers as it is expected for a mirror map around the LCS point. The integrality of the coefficients is in practice a very useful tool. If no closed form is available for the ϵ-expansion, one can still compute these numbers by numerically evaluating the series expansion in a computer algebra program like Mathematica. This provides a very fast way to compute Gromov-Witten invariants as well as a crosscheck for computations.

For applications it is also important to invert the mirror map. In this case this can be done algebraically with the result

$$x = \frac{q}{(1+q)^2} \,. \tag{3.50}$$

As a second example we take the charge vector $l = \{1, 1, 1, 1, 1, -5\}$. This corresponds to the quintic hypersurface in $\mathbb{P}^4$. In this case the fundamental period is

$$\omega_0 = x^\rho \, {}_5F_4(1, \frac{1}{5}+\rho_1, \frac{2}{5}+\rho_1, \frac{3}{5}+\rho_1, \frac{4}{5}+\rho_1; 1+\rho_1, 1+\rho_1, 1+\rho_1; 5^5 x) \,. \tag{3.51}$$

This hypergeometric function is highly unbalanced, i.e. there are more rational parameters in the $\vec{a}$ parameters than in the $\vec{b}$ parameters. Most of the mathematical literature focuses on balanced hypergeometric functions. Denoting the degree of unbalance, i.e. the number of rational parameters in $\vec{a}$ minus the number of rational parameters in $\vec{b}$, by s, shrinking curves correspond to $s \leq 2$, shrinking divisors to $s \leq 3$ and shrinking CYs to $s = 4$. In the case of half-integer parameters the hypergeometric functions correspond to sums of central binomial coefficients with exponent s, i.e. sums of the form

$$\sum_{n=0}^{\infty} f(n) \left(\frac{\binom{2n}{n}}{4^n} \right)^s x^n \,. \tag{3.52}$$

Evaluation of these sums for $s = \pm 1$ is standard by now. The cases s=2 and s=3 have been recently started to be studied by mathematicians, see e.g [50–52] and references therein. For the case s=4 only special cases are known, mostly related to Ramanujan-like representations of π. This is the reason we mostly focus on shrinking curves in this thesis and will only comment on the cases of shrinking divisors or CYs. As the example of the quintic is of the s=4 type, the ϵ-expansion is not known. But the series expansion can still be computed numerically with the result

$$q = e^{\left(\frac{\omega_1}{\omega_0}\right)} = x\left(1 + 770x + 1014275x^2 + 1703916750x^3 + 3286569025625x^4\right) + \mathcal{O}\left(x^6\right) \,, \tag{3.53}$$

which agrees with the mirror map found originally in [39]. There are in total 13 1-parameter hypersurfaces in a single projective space. The fundamental periods for all of them can be written as

$$\omega_0 = \, {}_5F_4(1, a_1+\rho, a_2+\rho, a_3+\rho, a_4+\rho; 1+\rho, 1+\rho, 1+\rho, 1+\rho; x) \,. \tag{3.54}$$

The quintic example above corresponds to $a = \{1/5, 2/5, 3/5, 4/5\}$. The full list of possible values of the a_i can be found in [53]. Here we will just focus on two more examples, the four quadrics in $\mathbb{P}^7$ with all $a_i = 1/2$ and the codimension 2 hypersurface $\mathbb{P}^7_{111112}[3\,4]$. In the first case the l-vectors are given by [37]

$$l = \begin{pmatrix} -2 & 1 & 1 & 0 & 0 & 0 & 0 & 0 & 0 \\ -2 & 0 & 0 & 1 & 1 & 0 & 0 & 0 & 0 \\ -2 & 0 & 0 & 0 & 0 & 1 & 1 & 0 & 0 \\ -2 & 0 & 0 & 0 & 0 & 0 & 0 & 1 & 1 \end{pmatrix} . \tag{3.55}$$

The resulting fundamental period is

$$\omega_0 = {}_5F_4(1, \frac{1}{2}+\rho, \frac{1}{2}+\rho, \frac{1}{2}+\rho, \frac{1}{2}+\rho; 1+\rho, 1+\rho, 1+\rho, 1+\rho; x) . \tag{3.56}$$

The resulting mirror map is

$$q = x(1 + 64x + 7072x^2 + 991232x^3 + 158784976x^4 + 27706373120x^5) + \mathcal{O}\left(x^7\right) . \tag{3.57}$$

While the ϵ expansion of all of these models is unknown, we still can obtain some information about the periods. It was observed in [54] that the ϵ-expansion in the case of a one parameter CY fulfills the following. If we write

$$\omega_0 = \sum_{j=0}^{3} \rho^j F_j(x) , \tag{3.58}$$

then the following holds:

$$\frac{F_j(1)}{L(g,s)} \in \mathbb{Q} . \tag{3.59}$$

Here g are Hecke eigenforms of $\Gamma_0(N)$, where N in the known examples is in the range [4,864] and s is an integer. We have gathered some definitions and details on modularity and L-functions in the appendix. Note that while this observation holds in all models which where tested, it is not proven. Furthermore, for critical values of a modular form g it holds that

$$\frac{L(g,2k)}{L(g,2k-2)} = \text{algebraic number} \cdot \pi^s , \tag{3.60}$$

as well as

$$\frac{L(g,2k+1)}{L(g,2k-1)} = \text{algebraic number} \cdot \pi^s , \tag{3.61}$$

for some integers k and s [55]. Finally, the derivatives of a hypergeometric function with respect to its argument only change the parameter values by integers, i.e.

$$\frac{\mathrm{d}}{\mathrm{d}x}\, {}_pF_q(\vec{a}; \vec{b}; x) = \frac{\prod_{i=1}^{q} a_i}{\prod_{i=1}^{p} b_i}\, {}_pF_q(\vec{a}+1; \vec{b}+1; x) . \tag{3.62}$$

As the complexity of a hypergeometric function only depends on its degree of unbalance, the derivatives can also be expressed in terms of L-values. These three observations would imply that the entries of the transition matrix can be expressed in terms of 2 different L-values, one even and one odd. But of course only the last one is proven at the time of writing.

The appearance of L-values in the transition matrix to the conifold is a general phenomenon. In the case of elliptic curves the L-values simplify and can be evaluated directly. Returning to the example of four quadrics, the fundamental period can be written as

$$F_0 = \frac{16}{\pi^2} L(f, 2) \ , \tag{3.63}$$

where $f = \eta(2\tau)^4\eta(4\tau)^4$ is a weight 4 modular form of $\Gamma_0(8)$. There is no known expression for this modular form in terms of Γ-functions. But the ratios of the periods have very simple expressions, i.e.

$$\frac{F_3(1)}{F_1(1)} = \frac{1}{8\pi^2} \tag{3.64}$$

and

$$\frac{F_2(1)}{F_0(1)} = \frac{1}{4\pi^2} \ . \tag{3.65}$$

An even simpler example is the one parameter complete intersection $\mathbb{P}^7_{1,1,1,1,1,2}[3,4]$ which corresponds to the parameters $a_i = \{1/3, 2/3, 1/4, 3/4\}$. In this case the weight 4 modular form of $\Gamma_0(9)$ is

$$f(\tau) = \eta(3\tau)^8 \ . \tag{3.66}$$

The leading orders of the ϵ expansion are given by

$$F_1(1) = -\frac{3\sqrt{3}\Gamma(\frac{1}{3})^9}{16\pi^5} \ . \tag{3.67}$$

$$F_2(1) = \frac{9\Gamma(\frac{1}{3})^9}{8\pi^4} \ . \tag{3.68}$$

$$F_3(1) = -\frac{3\sqrt{3}\Gamma(\frac{1}{3})^9}{\pi^3} \ . \tag{3.69}$$

In the ratios of $F_j(1)$ the Γ-functions cancel out, thus they represent algebraic numbers times multiples of π as expected. But the fundamental period seems not to follow this simple scheme and actually we could not find a closed form in terms of Γ-functions for the fundamental. Comparing these expressions to the known L-values of $f = \eta(3\tau)^8$ [54]

$$L(f, 2) = -\frac{\Gamma(\frac{1}{3})^9}{96\pi^4} \ , \tag{3.70}$$

and

$$L(f, 3) = -\frac{\Gamma(\frac{1}{3})^9}{144\sqrt{3}\pi^3} \ , \tag{3.71}$$

it is easy to verify that the conjectures (3.59) and (3.61) hold.

3.2.3 Example: $\mathbb{P}^4_{112812}[24]$

Finally, we give the main example of [46], $\mathbb{P}^4_{1,1,2,8,12}[24]$. It will be used in the next chapter to construct explicit vacua. The geometry represents a 3-parameter elliptic fibration. It's l-vectors are given by

$$l = \begin{pmatrix} -6 & 3 & 2 & 0 & 0 & 0 & 0 & 1 \\ 0 & 0 & 0 & 0 & 1 & 1 & 0 & -2 \\ 0 & 0 & 0 & 1 & 0 & 0 & -2 & 1 \end{pmatrix} . \tag{3.72}$$

We use the coordinates x_i, $i = \{1, 2, 3\}$ where the i labels the row of the l-matrix. We can write the fundamental period in 3 different ways in terms of hypergeometric functions, one for each coordinate. These correspond to

$$\omega_0 = \sum_{n_2=0}^{\infty} \sum_{n_3=0}^{\infty} x_1^{\rho_1} x_2^{n_2+\rho_2} x_3^{n_3+\rho_3} f_1 \, {}_3F_2(1, \frac{1}{6} + \rho_1, \frac{5}{6} + \rho_1; 1 + \rho_1, 1 + \rho_1 - 2\rho_3 - 2n_3; 432x_1)$$

$$\omega_0 = \sum_{n_1=0}^{\infty} \sum_{n_3=0}^{\infty} x_1^{n_1+\rho_1} x_2^{\rho_2} x_3^{n_3+\rho_3} f_2 \, {}_3F_2(1, -\frac{n_3}{2} + \rho_2 - \frac{\rho_3}{2}, \frac{1}{2} - \frac{n_3}{2} + \rho_2 - \frac{\rho_3}{2}; 1 + \rho_2, 1 + \rho_2; 4x_2)$$

$$\omega_0 = \sum_{n_1=0}^{\infty} \sum_{n_2=0}^{\infty} x_1^{n_1+\rho_1} x_2^{n_2+\rho_2} x_3^{\rho_3} f_3 \cdot$$
$$ {}_3F_2(1, -\frac{n_1}{2} - \frac{\rho_1}{2} + \rho_3, \frac{1}{2} - \frac{n_1}{2} - \frac{\rho_1}{2} + \rho_3; 1 + \rho_3, 1 + \rho_3 - 2(n_2 + \rho_2); 4x_3)$$

They are all equivalent, the difference being only which infinite sum has been resumed into a hypergeometric function. The f_i denote again some coordinate independent combination of Γ functions. As these are rather long and are easily treatable in computer aided computations we only give f_1:

$$f_1 = \frac{\Gamma(\rho_2 + 1)^2 \Gamma(\rho_1 - 2\rho_3 + 1) \Gamma(\rho_3 + 1) \Gamma(-2\rho_2 + \rho_3 + 1) \Gamma(n_2 + \rho_2 + 1)^{-2}}{\Gamma(-2n_3 + \rho_1 - 2\rho_3 + 1) \Gamma(n_3 + \rho_3 + 1) \Gamma(-2n_2 + n_3 - 2\rho_2 + \rho_3 + 1)}.$$

These different ways of writing the fundamental period nicely represent the fibration structure of the manifold. Keeping the other moduli fixed at the LCS values, i.e. $x_i = 0$, only the leading terms of the remaining sums, i.e. $n_i = 0$ contribute. In these cases the hypergeometric functions reduce in the latter two cases to the function in our example (3.46). This allows the computation of the ϵ-expansion and therefore of the transition matrix analytically. The matching of the coefficients in the expansion around the conifold uniquely fixes the transition matrix. The exact expressions for the local basis used are given in the

appendix A.7. The resulting transition matrix is

$$m_2 = \begin{pmatrix} 1 & 0 & 0 & 0 & 0 & 0 & 0 & 0 \\ \frac{id}{2\pi} & -\frac{i}{2\pi} & 0 & -\frac{i}{2\pi} & 0 & 0 & 0 & 0 \\ \frac{i\log(2)}{\pi} & 0 & -\frac{i}{\pi} & 0 & 0 & 0 & 0 & 0 \\ 0 & 0 & 0 & \frac{i}{\pi} & 0 & 0 & 0 & 0 \\ \frac{a_7}{2} & \frac{-11\log(2)-6\log(3)}{2\pi^2} & -\frac{d}{2\pi^2} & \frac{1-3\log(2)}{2\pi^2} & \frac{1}{4\pi^2} & 0 & \frac{1}{2\pi^2} & 0 \\ a_6 & -\frac{d}{2\pi^2} & 0 & 0 & 0 & \frac{1}{4\pi^2} & 0 & 0 \\ a_7 & \frac{-11\log(2)-6\log(3)}{\pi^2} & -\frac{d}{\pi^2} & 0 & 0 & 0 & \frac{1}{\pi^2} & 0 \\ a_8 & b & c & 0 & 0 & -\frac{i\log(2)}{4\pi^3} & -\frac{id}{2\pi^3} & \frac{i}{6\pi^3} \end{pmatrix}, \tag{3.73}$$

where

$$\begin{aligned} a_6 &= \frac{4\pi^2 + 25\log^2(2) + 9\log^2(3) + 30\log(2)\log(3)}{4\pi^2}\,, \\ a_7 &= \frac{23\pi^2 + 180\log^2(2) + 54\log^2(3) + 198\log(2)\log(3)}{6\pi^2}\,, \\ a_8 &= \frac{i\left(726\zeta(3) - 325\log^3(2) - 54\log^3(3) - 540\log^2(2)\log(3)\right)}{12\pi^3}\,, \\ &\quad + \frac{\left(-297\log(2)\log^2(3) + 127\pi^2\log(2) + 69\pi^2\log(3)\right)}{12\pi^3}\,, \\ b &= \frac{i\left(-23\pi^2 + 180\log^2(2) + 54\log^2(3) + 198\log(2)\log(3)\right)}{12\pi^3}\,, \\ c &= \frac{i\left(-4\pi^2 + 25\log^2(2) + 9\log^2(3) + 30\log(2)\log(3)\right)}{4\pi^3}\,, \\ d &= 5\log(2) + 3\log(3)\,. \end{aligned}$$

While these expressions are rather long and non-rational, the important part is that all entries are known analytically, such that the cancellation of the irrational factors in the following steps is manifest.

Applying this matrix to the local solution around the conifold gives an expression for the periods in the symplectic basis to arbitrary order. The periods themselves, especially those corresponding to the β-cycles, are too long to be presented here, instead they are listed in the appendix A.7. After dividing by the fundamental period, the α-periods which represent the mirror map take the form

$$\begin{pmatrix} 1 \\ \frac{\log(x_1)}{2\pi i} - \frac{31ix_1}{72\pi} + \frac{ix_3}{4\pi} + \frac{5ix_1\sqrt{x_3}}{72\pi} - \frac{5ix_1x_2\sqrt{x_3}}{1152\pi} + \frac{ix_2\sqrt{x_3}}{32\pi} - \frac{i\sqrt{x_3}}{2\pi} + \frac{3i\log(3)}{2\pi} + \frac{5i\log(2)}{2\pi} + \cdots \\ \frac{\log(x_2)}{2\pi i} + \frac{x_3}{\pi i} - \frac{i\log(x_3)}{\pi} + \frac{i\log(2)}{\pi} + \cdots \\ \frac{5ix_2\sqrt{x_3}x_1}{576\pi} - \frac{5i\sqrt{x_3}x_1}{36\pi} - \frac{ix_2\sqrt{x_3}}{16\pi} + \frac{i\sqrt{x_3}}{\pi} + \cdots \end{pmatrix}.$$

Changing the x_3 coordinate to $x_3 = x_3^2$ and defining

$$\begin{aligned} q_{U^1} &= 864\, e^{2\pi i U^1} = x_1 + \cdots , \\ q_{U^2} &= \frac{4}{(\frac{\pi}{i}Z)^4}\, e^{2\pi i U^2} = x_2 + \cdots , \\ q_Z &= (\tfrac{\pi}{i}Z) = x_3 + \cdots \end{aligned} \tag{3.74}$$

allows us to invert the mirror map order by order. The numerical factors in the expressions for q_{U^1} and q_{U^2} arise from the chosen coordinates. A choice for the normalization of the coordinates is possible such that these are absent. The resulting mirror map is given by

$$x_1 = q_{U^1} - q_{U^1}q_Z - \frac{31q_{U^1}^2}{36} + \cdots , \tag{3.75}$$

$$x_2 = q_{U^2} + \frac{5}{9}q_{U^1}q_{U^2}q_Z - \frac{q_{U^2}^2}{4} - \frac{5}{9}q_{U^1}q_{U^2} + \cdots , \tag{3.76}$$

$$x_3 = q_Z + \frac{5}{36}q_{U^1}q_Z - \frac{5}{192}q_{U^1}q_{U^2}q_Z + \frac{1}{16}q_{U^2}q_Z + \cdots . \tag{3.77}$$

Moreover, the hypergeometric representation allows us to compute the mirror maps around the conifold exactly in the conifold coordinate. At $x_1 = x_2 = 0$ the conifold modulus on the Kähler side is given by

$$\begin{aligned} 2\pi i Z &= \log(1-x_3^2) - 2\log(2) + 2\,\mathrm{HPL}\left[-1; \frac{1-x_3}{1+x_3}\right] \\ &= -2\,\mathrm{arctanh}(x_3)\ . \end{aligned}$$

In this case the harmonic polylogarithm (HPL) actually reduces to a simple logarithm, but in higher orders more complicated HPLs of higher weight appear. In the appendix A.4.1 we give the basic definitions of harmonic polylogarithms. The mirror maps can be written purely in terms of a sum of these at any order in x_1 and x_2. Finally, inserting the mirror map into the periods allows us to write down the prepotential around the conifold as

$$\begin{aligned} \mathcal{F} = &-\frac{4}{3}(U^1)^3 - U^2(U^1)^2 + \frac{23}{6}U^1 + U^2 - \frac{120i}{\pi^3}e^{2i\pi U^1} - \frac{35496i}{\pi^3}e^{4\pi i U^1} \\ &- \frac{Z^3}{4} - 2(U^1)^2 Z - U^2U^1Z - U^1Z^2 + \frac{23}{12}Z + \frac{120}{\pi^2}e^{2i\pi U^1}Z \\ &+ Z^2\left(\frac{i\log(2\pi Z)}{2\pi} - \frac{3i}{4\pi} + \frac{1}{4}\right) + \frac{121i\zeta(3)}{4\pi^3} + \text{higher order}\,. \end{aligned} \tag{3.78}$$

Note that all polynomial terms involving U^1 or U^2 are rational. The only non-rational terms are the quadratic Z^2 term and the constant $\zeta(3)$ term shown in the last row. We also observe that the linear terms related to the U^i are all given by the same topological numbers as they are in the LCS regime. The same holds for the manifold $\mathbb{P}^4_{1,1,2,2,6}[12]$. Together with the observation that the topological numbers at a conifold transition are given by sums of the LCS topological numbers [56], this gives rise to the following conjecture: all coefficients in the prepotential around the conifold except the quadratic terms are rational numbers. While we cannot prove this for the general case, it seems to be a rather frequent property.

If one would try to compute the analytic transition matrix to the conifold at $x_1 = 1$, one would encounter the ϵ-expansion of

$$ {}_2F_1(\frac{1}{6} + \rho_1, \frac{5}{6} + \rho_1; 1 + \rho_1; 432x) \ . \tag{3.79} $$

This function turns out to be much harder to treat than the first case. One complication is the singularity of the fundamental period at $x = 1$. This does not influence the physical quantities as these only depend on the derivatives of f in the combination f'/f, such that these divergences cancel out. Moreover, the ϵ-expansion is not known. But as it is only an elliptic curve or respectively only a ${}_2F_1$ function, one can use a generalized version of Euler's reflection formula to expand this function around $x = 1$ by rewriting it in terms of a Meijer G function [57]:

$$ {}_2F_1(a, b; c, x) = \frac{\Gamma[c]}{\Gamma[a]\Gamma[b]\Gamma[c-a]\Gamma[c-b]} G^{2,2}_{2,2}(a, b; c-b-a, 0; 1-x) \ . \tag{3.80} $$

Changing the coordinate $x \to 1 - x$ and expanding around 0 gives the required expansion.

3.3 Gauged Linear Sigma Models

After having computed the periods on the complex structure side and applying the mirror map we will take a completely different approach in this section. This will allow for a direct computation of the periods on the Kähler side. In his seminal paper Witten introduced the so-called gauged linear sigma models (GLSM) [58]. These models are 2-dimensional $\mathcal{N} = 2$ supersymmetric field theories. He showed that due to the supersymmetry it is possible to compute many properties of an IR theory using a much simpler UV theory whose RG-flow ends in the IR theory. Due to the high amount of supersymmetry these models are solvable using supersymmetric localization, which leads to exact expressions for the partition functions [59, 60]. The important formula allowing to compute the periods is the observation that the sphere partition function of a GLSM is in one to one correspondence with the Kähler potential of a CY [61]:

$$ Z_{S_2} = e^{-K} \ . \tag{3.81} $$

We will first describe the GLSM construction itself and how it relates to the geometric formulation used in the last section. Then we will describe the algorithm of [61] to compute the periods. Finally we will give some example computations for the quintic and $\mathbb{P}^4_{11222}[8]$.

3.3.1 The Gauged Linear Sigma Model

The GLSM is a two-dimensional $\mathcal{N} = 2$ supersymmetric gauge theory. Such theories consist out of chiral multiplets as well as vector multiplets. We will only be interested in hypersurfaces in toric varieties, thus we will only consider abelian GLSMs, i.e. the gauge group G will be $U(1)^s$ with an integer s. Each $U(1)$ factor will represent a (weighted) projective space, thus the number of gauge factors exactly equals the number of Mori cone generators, $s = h^{1,1}$. The charges of the chiral fields under the $U(1)$ factors correspond to the weights.

As before we want to describe a D-dimensional complex projective space with D+1 coordinates z_i with weights k_i. The N homogeneous polynomials describing the hypersurfaces have degrees d_i, $i = 1, \ldots, N$, i.e. the geometry we are interested in is:

$$\mathbb{P}^D_{k_1,\ldots,k_{D+1}}[d_1, \ldots, d_N]\,. \tag{3.82}$$

To achieve this one closely follows the geometry description. First one describes the ambient toric variety. For each of the D+1 coordinates one introduces a chiral multiplet Φ_m with $m = 1, \ldots, D+1$ and the s vector multiplets V_j describe the action of the toric symmetry by which the variety is quotiented. This results in a non-compact variety. Then the polynomial constraints are included by adding a chiral multiplet Σ_n for each of the N polynomials. The chiral multiplets carry the $U(1)$ charges shown in table 3.83.

	Φ_1	Φ_2	$\ldots$	Φ_{D+1}	Σ_1	$\ldots$	Σ_N
$U(1)_1$	$Q_{1,1}$	$Q_{2,1}$	$\ldots\ldots$	$Q_{D+1,1}$	$Q_{D+2,1}$	$\ldots$	$Q_{N+D+1,1}$
$U(1)_2$	$Q_{1,2}$	$Q_{2,2}$	$\ldots\ldots$	$Q_{D+1,2}$	$Q_{D+2,2}$	$\ldots$	$Q_{N+D+1,2}$
$\vdots$	$\vdots$	$\vdots$	$\vdots$	$\vdots$	$\vdots$	$\vdots$	$\vdots$
$U(1)_s$	$Q_{1,s}$	$Q_{2,s}$	$\ldots\ldots$	$Q_{D+1,s}$	$Q_{D+2,s}$	$\ldots$	$Q_{N+D+1,s}$

(3.83)

These charges are in one-to-one correspondence with the l-vectors encoding the relations of the polytope in the last section, i.e. the generators of the Mori cone. The dimension of the resulting compact hypersurface is $d = D + 1 - N - s$. Note that the hypersurface is described in a different manner compared to the geometric construction on the B-model side. The toric variety which is used by the GLSM is not simply the projective space of the hypersurface one started with. As a simple example of this we use $\mathbb{P}_{11222}[8]$. As described earlier this corresponds to an octic surface in a complex 5-dimensional space with one projection. The GLSM description of the same surface is given by a surface in a 6-dimensional variety with 2 projections which are represented by the gauge group $U(1) \times U(1)$. It is always possible to use a symplectic quotient of a single affine space

$(\mathbb{C}^n/(\mathbb{C}^\star)^m)$ to describe any toric variety, no matter how many factors of projective space it contains [58]. The GLSM uses exactly this description.

But a GLSM is much more general than the toric formalism. If one chooses non-abelian gauge groups, it is also possible to construct determinantal CYs or purely non-geometrical spaces which do not posses a geometrical phase. Thus we will change the point of view now slightly and will assume the GLSM as the fundamental construction, only taking the charges (l-vectors) for specific constructions as an input if necessary. If we want to construct a general GLSM corresponding to a CY we only have the following constrains:

The CY condition is related to the vanishing of the mixed gravitational - abelian gauge anomalies, which are proportional to the sum of the gauge charges

$$\sum_{i=1}^{D+1} Q_{i,j} = 0\,. \tag{3.84}$$

In addition there exists a superpotential

$$W = \sum_{n=1}^{N} P_n(\Phi)\,\Sigma_n\ , \tag{3.85}$$

which is linear in the Σ_n and the polynomials P_n are chosen such that W carries vanishing charges. Moreover, one associates R-charges R_i to the chiral fields such that the superpotential has R-charge 2. The superpotential only depends on the complex structure, given by the deformations of the polynomials. Therefore the A-model partition function is independent of the superpotential itself as it can only depend on the Kähler parameters. The superpotential only restricts the value of the R-charges. This does not uniquely fix the R-charges, but the remaining freedom corresponds to a rescaling of the partition function or equivalently a Kähler transformation of the Kähler potential. Thus the remaining freedom does not influence any physical observables.

3.3.2 The Partition Function

The partition function for an abelian gauge group $G = U(1)^s$ can be written as [59, 60]

$$Z_{S^2}(\xi,\bar{\xi},Q,R) = \sum_{m_1\in\mathbb{Z}} \dots \sum_{m_s\in\mathbb{Z}} \int_{-i\infty}^{i\infty} d\sigma_1\ \dots \int_{-i\infty}^{i\infty} d\sigma_s\ Z_{\text{class}}\ Z_{\text{gauge}}\ Z_{\text{chiral}}\ , \tag{3.86}$$

where the purely imaginary integration contour for the scalar fields σ_i is chosen to simplify the expressions. For an abelian gauge group $Z_{\text{gauge}} = 1$ is trivial. The classical contribution is

$$Z_{\text{class}} = \prod_{j=1}^{s} e^{-4\pi r_j\sigma_j + i\theta_j m_j}\ , \tag{3.87}$$

and the contribution from the 1-loop determinants of the chiral fields are given by

$$Z_{\text{chiral}} = \prod_{i=1}^{M} \frac{\Gamma\left(R_i/2 + \sum_{j=1}^{s} Q_{i,j} \cdot (\sigma_j - m_j/2)\right)}{\Gamma\left(1 - R_i/2 - \sum_{j=1}^{s} Q_{i,j} \cdot (\sigma_j + m_j/2)\right)} \,. \tag{3.88}$$

Thus given the Q- and R-charges, the partition function depends only on the complexified FI-parameters $\tau = r_j + i\theta_j$. Depending on the signs of the τ_j the contour of the integral in (3.86) can be closed to the right or to the left. The classical contribution Z_{class} ensures that the contributions at infinity are suppressed. Thus the integrals can be written as as sum of residues of gamma functions. As a Γ function is only singular at negative integer arguments, the choice of FI parameters determines which Γ functions contribute to the sum. The resulting sums are exactly of hypergeometric type. Rewriting the partition function for general charges poses a difficult problem and has only been solved for 1-parameter models in [62]. The reason for the complexity of the evaluation in multi-parameter models lies in the definition of multivariate residues. A detailed explanation of the evaluation can be found in the appendix of [63] which applies a method developed in [64]. Here we only give a short review of the method.

Before we go into details on the evaluation method we explicitly evaluate the example of the quintic. This will show the necessity of a systematic method in the multivariate case. We have $h^{1,1} = 1$, thus the gauge group is U(1). The ambient space is described by 5 chiral fields with U(1) charge 1. The CY constraint then enforces the addition of another chiral field with charge -5 to cancel the gravitational anomaly. This corresponds to the addition of the line bundle in the toric construction. The charge vector is thus given by

$$Q = \{-5, 1, 1, 1, 1, 1\} \,, \tag{3.89}$$

which is the same as the l-vector in the toric description given in (3.17). The R-charges of the fields in the superpotential need to add up to 2. The easiest choice for this is [7]

$$R = \{2, 0, 0, 0, 0, 0\} \,. \tag{3.90}$$

The partition function then becomes

$$Z_{S_2} = \sum_{m \in \mathbb{Z}} \int_{-i\infty}^{i\infty} \mathrm{d}\sigma \, e^{-4\pi r\sigma + i\theta m} \frac{\Gamma[\sigma - \frac{m}{2}]^5 \Gamma[1 - 5(\sigma - \frac{m}{2})]}{\Gamma[1 - \sigma - \frac{m}{2}]^5 \Gamma[5(\sigma + \frac{m}{2})]} \,. \tag{3.91}$$

The Γ functions in the nominator have poles at

$$(i)\ \sigma = \frac{m}{2} - k_1 \qquad \text{and} \qquad (ii)\ \sigma = \frac{m}{2} + \frac{k_1 + 1}{5} \qquad k_1 \in \mathbb{N}_0 \,. \tag{3.92}$$

[7] This choice is singular in the sense that the integration contour intersects poles of the Γ functions. In more complicated examples this can lead to problems, but in the explicit evaluation of this example the choice does not cause any problems and shortens the equations.

For $r < 0$ the contour can be closed to the left. Thus only zeroes where σ takes negative values will contribute. This results in constraints on the values of m which contribute. In the case (i) $m < 2k_1$ and in the case (ii) $m < -\frac{2k_1+2}{5}$. These are all possible poles. But the Γ functions in the denominator can cancel some of these poles. As there is a pole of order five in case (i) the only possible cancellation can come from the $\Gamma[1-\sigma-\frac{m}{2}]^5$ term. Thus if a solution to the equation

$$1-\sigma-\frac{m}{2} = 1-m+k_1 = -k_2 \ , \tag{3.93}$$

exists for non-negative k_2 the corresponding m will not contribute. Rewriting this as

$$m = 1+k_1+k_2 \leq 1+k_1 \tag{3.94}$$

shows that only $m \leq k_1$ will contribute. A similar argument shows that all poles of the case (ii) are canceled. Thus we can write the partition function as

$$Z = \sum_{k=0}^{\infty}\sum_{m\leq k}\oint_{\epsilon=0} \mathrm{d}\epsilon (z\overline{z})^{\epsilon} z^k \overline{z}^{m-k} \frac{\Gamma[-k+\epsilon]^5\Gamma[1+5k-5\epsilon]}{\Gamma[1+k-m-\epsilon]^5\Gamma[5(m-k+\epsilon)]} \ , \tag{3.95}$$

where we have defined $z = e^{-2\pi r+i\theta}$. To bring this into a more symmetric form we introduce a new summation variable $l = m-k$ and apply the reflection formula

$$\Gamma[x] = \frac{\pi}{\sin(\pi x)\Gamma[1-x]} \tag{3.96}$$

to all Γ functions which are singular at $\epsilon = 0$. This results in

$$Z = \sum_{k=0}^{\infty}\sum_{l=0}^{\infty}\oint_{\epsilon=0} \mathrm{d}\epsilon (z\overline{z})^{\epsilon} z^k \overline{z}^{l} \pi^4 \frac{\sin(5\pi\epsilon)}{\sin(\pi\epsilon)^5} \frac{\Gamma[1+5l-5\epsilon]\Gamma[1+5k-5\epsilon]}{\Gamma[1+l-\epsilon]^5\Gamma[1+k-\epsilon]^5} \ . \tag{3.97}$$

Defining

$$f(\epsilon) = \sum_{n=0}^{\infty} \frac{\Gamma[1+5n-5\epsilon]}{\Gamma[1+n-\epsilon]^5} z^n = \frac{\Gamma[1-5\epsilon]}{\Gamma[1-\epsilon]^5}\, {}_5F_4(1, \frac{1}{5}-\epsilon, \frac{2}{5}-\epsilon, \frac{3}{5}-\epsilon, \frac{4}{5}-\epsilon; 1-\epsilon, 1-\epsilon, 1-\epsilon; 5^5 z) \ ,$$

the partition function takes its final simple form

$$Z = \oint_{\epsilon=0} \mathrm{d}\epsilon (z\overline{z})^{\epsilon} \pi^4 \frac{\sin(5\pi\epsilon)}{\sin(\pi\epsilon)^5} |f(\epsilon)|^2 \ . \tag{3.98}$$

Note that the hypergeometric function appearing in $f(\epsilon)$ is exactly the same as the one in the fundamental period (3.51). The different prefactors appear due to the unfixed normalization of the partition function. Evaluating the integral of the partition function in this form is simple. To be able to express the result compactly we define the "period" vector $\omega = \{f(0), f'(0), f''(0), f'''(0)\}$. With this definition the partition function is

$$Z = \overline{\omega}\, \sigma\, \omega \ , \tag{3.99}$$

where

$$\sigma = \begin{pmatrix} \frac{50\pi^2}{3}\log(z\overline{z}) - \frac{5}{6}\log(z\overline{z})^3 & -\frac{50\pi^2}{3} + \frac{5}{2}\log(z\overline{z})^2 & -\frac{5}{2}\log(z\overline{z}) & \frac{5}{6} \\ -\frac{50\pi^2}{3} + \frac{5}{2}\log(z\overline{z})^2 & -5\log(z\overline{z}) & \frac{5}{2} & 0 \\ -\frac{5}{2}\log(z\overline{z}) & \frac{5}{2} & 0 & 0 \\ \frac{5}{6} & 0 & 0 & 0 \end{pmatrix} . \tag{3.100}$$

For the LG phase, i.e. $r > 0$, a similar computation leads to the result

$$\begin{aligned} Z_{\text{LG}} =& \frac{1}{5}\sum_{l=0}^{3}(-1)^l\,(z\bar{z})^{-\frac{l}{5}}\,\frac{\Gamma^5\left(\frac{1+l}{5}\right)}{\Gamma^2(l+1)\,\Gamma^5\left(\frac{4-l}{5}\right)}\cdot \\ & \left|{}_5F_4\left(\tfrac{1+l}{5},\ldots,\tfrac{1+l}{5},1;\tfrac{2+l}{5},\ldots,\tfrac{5+l}{5};-\tfrac{1}{5^5 z}\right)\right|^2 . \end{aligned} \tag{3.101}$$

Note that the 1 in the first parameter set is canceling a 1 in the second parameter set such that the functions are actually only ${}_4F_3$ functions, the ${}_5F_4$ is just used for notational convenience.

It is possible to extract the periods as well as the Gromov-Witten invariants from the LCS partition function. The method was developed in [61] and involves the following steps:

- Extract the coefficient of $\zeta(3)$.
- Perform a Kähler transformation such that the coefficient becomes $\frac{\chi}{4\pi^3}$. This fixes the normalization.
- Identify the $\log(\overline{z}_n)\log(\overline{z}_m)$ terms with $\frac{i}{8\pi^2}K_{lnm}t^l$
- The flat coordinates are $t_l = \frac{\log(z_l)}{2\pi i} + t_l^{(0)} + f_l(z)$. This is fixed up to the constants $t_l^{(0)}$.
- The remaining constants are fixed by demanding positivity of the lowest order Gromov-Witten invariants.
- Inverting the mirror map and computing the q-expansions allows the read-off of the Gromov-Witten invariants.

Thus if the classical intersection numbers K_{lnm} as well as the Euler characteristic χ are known one can determine the genus 0 Gromov-Witten invariants. Moreover, the partition function allows for a fast evaluation of the Kähler potential, avoiding the computation of the transition matrices completely. But as should be clear after the example, the evaluation of the partition function by hand involves many steps and is inconvenient. Additionally, the complexity increases drastically with the dimension of the moduli space. Thus a more algorithmic approach which can be fully automated is necessary. This approach was developed in [65]. In the algorithm the divisors are sorted in a geometric way, uniquely determining which contribute in a certain phase to the residue count. Then the poles are

extracted using a variation the reflection formula (3.96). Finally the residue is transformed into a form treatable by Cauchy's residue formula. This approach works only in the resonant case, i.e. if the sum of the upper a parameters of the hypergeometric function equal the sum of the lower b parameters. As this condition is exactly the CY condition, the method is always applicable in our cases of interest.

We will now go through each of these steps in detail. We follow the original work and first treat the two-dimensional case before describing the general d-dimensional procedure. We will use $\mathbb{P}_{11222}[8]$ as an example. This manifold is one of the most often used two parameter models, details of its GLSM evaluation can be found e.g. in [2, 62, 66]. The charge matrix is given by

$$Q = \begin{pmatrix} 1 & 1 & 1 & 0 & 0 & 1 & -4 \\ 0 & 0 & 0 & 1 & 1 & -2 & 0 \end{pmatrix} . \tag{3.102}$$

Moreover, the defining polynomial can be obtained by the toric construction to be

$$P = x_1^8 + x_2^8 + x_3^4 + x_4^4 + x_5^4 - 8\psi x_1 x_2 x_3 x_4 x_5 - 2\phi x_1^4 x_2^4 . \tag{3.103}$$

The superpotential of the GLSM is $\Sigma_0 P$ and has to have R charge 2, thus the following R charges are assigned to the fields

$$R = \begin{pmatrix} \frac{2-q_1}{4} & \frac{2-q_1}{4} & \frac{2-q_1-4q_2}{4} & \frac{2-q_1-4q_2}{8} & \frac{2-q_1-4q_2}{8} & q_2 & q_1 \end{pmatrix} . \tag{3.104}$$

These are only fixed up to the choice of two parameters q_1 and q_2. These can take any value as long as all R-charges remain positive. In principle even choosing 0 is possible, but this will lead to singular divisors at 0, causing problems for numerical algorithms. The different choices correspond to Kähler transformations and thus do not influence the result. With this choice the partition function (3.86) becomes

$$Z = \sum_{m_1 \in \mathbb{Z}} \sum_{m_2 \in \mathbb{Z}} \int_{-i\infty}^{i\infty} \mathrm{d}\sigma_1 \int_{-i\infty}^{i\infty} \mathrm{d}\sigma_2 \, z_1^{-\frac{m}{2}-\sigma_1} \overline{z}_1^{\frac{m}{2}-\sigma_1} z_2^{-\frac{m}{2}-\sigma_2} \overline{z}_2^{\frac{m}{2}-\sigma_2} Z_0 Z_1 Z_2^2 Z_3^3 , \tag{3.105}$$

where the Z_i correspond to the 1-loop determinants of the chiral fields. With the chosen charges they read explicitly

$$Z_0 = \frac{\Gamma[\frac{q_1}{2} - 4(-\frac{m_1}{2} + \sigma_1)]}{\Gamma[1 - \frac{q_1}{2} + 4(\frac{m_1}{2} + \sigma_1)]} , \tag{3.106}$$

$$Z_1 = \frac{\Gamma[\frac{q_2}{2} - \frac{m_1}{2} + \sigma_1 - 2(-\frac{m_2}{2} + \sigma_2)]}{\Gamma[1 - \frac{q_2}{2} - \frac{m_1}{2} - \sigma_1 + 2(\frac{m_2}{2} + \sigma_2)]} , \tag{3.107}$$

$$Z_2 = \frac{\Gamma[-\frac{m_2}{2} + \frac{1}{8}(2 - q_1) + \sigma_2]}{\Gamma[1 - \frac{m_2}{2} + \frac{1}{8}(q_1 - 2) - \sigma_2]} , \tag{3.108}$$

$$Z_3 = \frac{\Gamma[-\frac{m1}{2} + \frac{1}{16}(2 - q_1 - 4q_2) + \sigma_1]}{\Gamma[1 - \frac{m_1}{2} + \frac{1}{16}(q_1 - 2 + 4q_2) - \sigma 1]} . \tag{3.109}$$

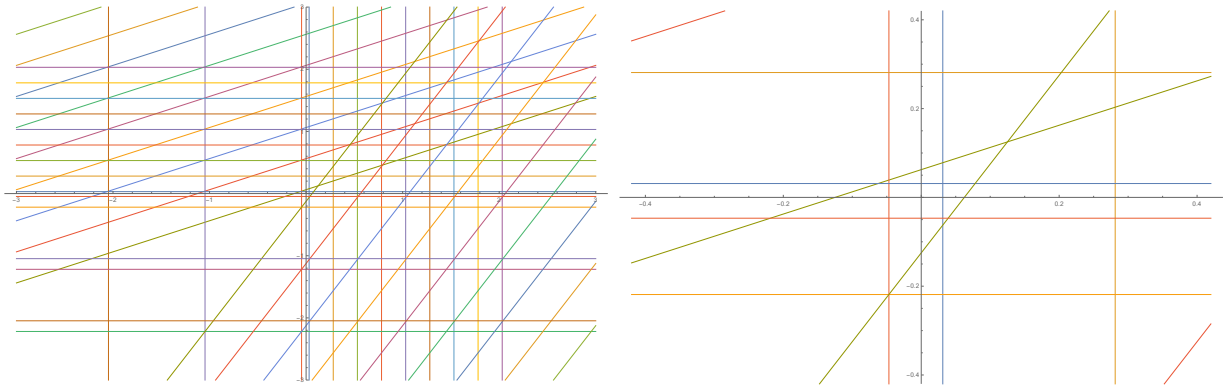

(a) (b)

Figure 3.5: The divisor structure for $\mathbb{P}_{11222}[8]$ at two different scales. On the left hand side the cones are clearly visible. On the right hand side the region around the origin is shown, making the polyhedron around the origin visible.

The zeroes of the polynomials inside the Γ functions define divisors in the σ-plane. Figure 3.5 shows the structure of these divisors for fixed values of m_i and q_i. This shows that there are no divisors in a small polyhedron around the origin as well as the cone structure.

The first step in the evaluation is the determination of the cones corresponding to the different phases of the GLSM. To this end one draws a line l through the origin of the σ-plane. Of course there are infinitely many possible lines, but the procedure will still only result in finitely many phases. As long as the slope of the line does not cross any slope of a divisor the result will not change. Moreover, for each line there will be two resulting cones, one on each side of the line. The line should also not be taken parallel to any of the divisors to ensure the existence of intersections.

As the partition function consists out of two integrals, only intersections of two divisors will contribute to it. A pole is included in a phase when the two divisors intersect the line l at different sides of the origin. This rather strange looking definition is necessary to exclude so-called spurious poles and at the same time defines the cones.

The side on which the divisor intersects l depends on the values the summation variables m_i take. This constraints the values for which the divisors contribute and reproduces the conditions on the summation range worked out before by hand. Working this out for the example gives the following phase picture:

Knowing the contributing factors, one can perform the same transformations as in the 1-dimensional case. The singularities are first brought to the origin by the transformation

$$\sigma_i \to \epsilon_i + f(\vec{m}, \vec{k}) \ , \tag{3.110}$$

where $f(\vec{m}, \vec{k})$ are the roots of the contributing polynomials. Then the singularities are extracted from the Γ function by using the reflection formula

$$\Gamma[x-k] = (-1)^k \frac{\Gamma[1+x]\Gamma[1-x]}{x\Gamma[1+k-x]} \ .$$

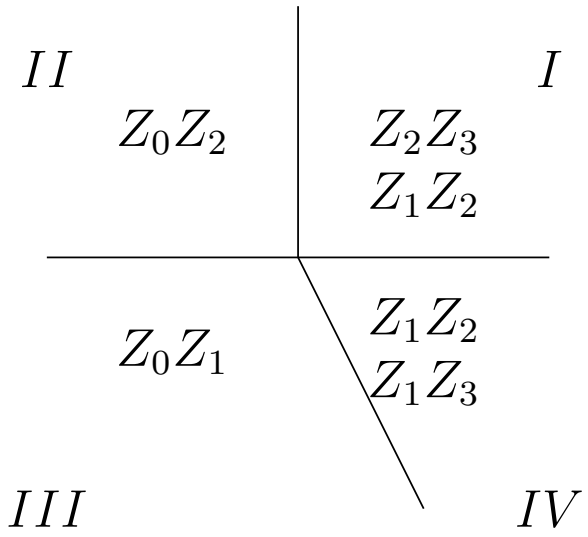

Figure 3.6: The four GLSM phases and the contributing pairs in the partition function for $\mathbb{P}_{11222}[8]$. I corresponds to the geometric phase while III is the LG phase.

Note that the only singularity on the right hand side is in form of the x^{-1}, all Γ-functions are regular at $x = 0$. In phase II, only Z_0 and Z_2 contribute. These have vertical and horizontal divisors. Applying the reflection formulas to this pair, the partition function is of the form

$$\mathrm{Res}_{\epsilon_1=0,\epsilon_2=0}\frac{h(\epsilon_1,\epsilon_2)}{\epsilon_1^n\epsilon_2^m}\ , \tag{3.111}$$

where n and m are integers given by the exponents of the contributing Z_i in the partition function and $h(\epsilon_1, \epsilon_2)$ is a combination of Γ functions which is regular at the origin. These residues can be directly evaluated using Cauchy's residue theorem, i.e.

$$\mathrm{Res}_{\epsilon_1=0,\epsilon_2=0}\frac{h(\epsilon_1,\epsilon_2)}{\epsilon_1^n\epsilon_2^m} = \frac{1}{\Gamma[n]\Gamma[m]}\frac{\partial^{n+m-2}h(\epsilon_1,\epsilon_2)}{\partial^n\epsilon_1\partial^m\epsilon_2}\bigg|_{\epsilon_1=0,\epsilon_2=0}\ . \tag{3.112}$$

This finishes the computation in phase II. In the other phases, each pair has a contribution of Z_1, which leads to structures of the form

$$\mathrm{Res}_{\epsilon_1=0,\epsilon_2=0}\frac{h(\epsilon_1,\epsilon_2)}{\epsilon_1(\epsilon_1-2\epsilon_2)}\ . \tag{3.113}$$

This complicates the computation slightly due to the appearance of linear combinations of the ϵ_i in the denominator. This can be transformed into a residue which can be evaluated by Cauchy as above by application of the transformation theorem [67], i.e.

$$\mathrm{Res}\left(\frac{h(\epsilon_1,\epsilon_2)}{\epsilon_1^n\epsilon_2^m(\epsilon_1+a\epsilon_2)^p(\epsilon_1+b\epsilon_2)^q}\right) = \mathrm{Res}\left(\frac{h(\epsilon_1,\epsilon_2)\det(A)}{\epsilon_1^r\epsilon_2^s}\right)\ , \tag{3.114}$$

where n, m, p, q, r and s are integers, $h(\epsilon_1, \epsilon_2)$ is a regular function at $\epsilon_1 = \epsilon_2 = 0$ and A is an analytic 2x2 matrix. The condition for this theorem are the following. Define two vectors f and g, where

$$g = \{\epsilon_1^r, \epsilon_2^s\} \qquad f = \{f_1, f_2\} \ . \tag{3.115}$$

The f_i are products of the elements of the denominator of the residue one wants to evaluate, i.e products of $(\epsilon_1 + a\epsilon_2)^p$,$(\epsilon_1 + b\epsilon_2)^q$, ϵ_1^n and ϵ_1^m. The assignment to f_1 and f_2 is based on the intersection of the divisor they originate from with the line l as well as whether the cone lies to the left or to the right of l. If the cone lies to the left of l,f_1 includes the ones intersection the left side, f_2 the ones intersecting the right side. If the cone lies to the right exactly the opposite is applied. Finally the matrix A is determined by the equation $Af = g$.[8] This equation does not have an analytic solution for all values of r and s, restricting the values these integers can take. But different values of r and s leading to solutions result in the same residue, thus taking small values simplifies the computation.

For the LG phase above we have $f = \{\epsilon_1, \epsilon_1 - 2\epsilon_2\}$. The simplest g that works is $g = \{\epsilon_1, \epsilon_2\}$. Solving for A results in

$$A = \begin{pmatrix} 1 & 0 \\ \frac{1}{2} & -\frac{1}{2} \end{pmatrix} \ . \tag{3.116}$$

Thus the residuum (3.113) becomes simple $-\frac{1}{2}h(0,0)$. The absence of derivatives is typical for LG phases. The resulting expression consists of 4 infinite summations. This is already useful for numerical evaluation, but can be simplified by redefining the summation variables. This computation was performed in [62] with the result

$$\begin{aligned} Z_{LG} = \frac{1}{8}\sum_{\delta=1}^{3} \Bigg(& (-1)^{\mathrm{Gr}_0} \frac{\widehat{\Gamma}_{\delta,0}(0)}{\widehat{\Gamma}^*_{\delta,0}(0)} I_{\delta,0}(z_1, z_2, 0) I_{\delta,0}(\overline{z}_1, \overline{z}_2, 0) \\ & + (-1)^{\mathrm{Gr}_1} \frac{\widehat{\Gamma}_{\delta,1}(0)}{\widehat{\Gamma}^*_{\delta,1}(0)} I_{\delta,1}(z_1, z_2, 0) I_{\delta,1}(\overline{z}_1.\overline{z}_2, 0) \Bigg) \ . \end{aligned} \tag{3.117}$$

Here $\mathrm{Gr}_\kappa = \delta + \kappa + 3\left\lfloor \frac{\delta}{4} \right\rfloor + 2\left\lfloor \frac{\delta+4\kappa}{8} \right\rfloor$ encodes the signs obtained by the transformations, $I_{\delta,i}(z_1, z_2, \epsilon)$ is the Givental I function [68]

$$\begin{aligned} I_{\delta,\kappa}(z_1, z_2, 0) = & \frac{1}{\Gamma\left(\left\langle \frac{\delta}{4} \right\rangle\right)^3 \Gamma\left(\left\langle \frac{\delta+4\kappa}{8} \right\rangle\right)^2} \\ & \sum_{l=0}^{\infty}\sum_{p=0}^{\infty} (-1)^p e^{\frac{z_1}{4}(4p+\delta-1)} e^{\frac{z_2}{8}(8l+\delta-1+4\kappa)} \frac{\Gamma\left(p+\frac{\delta}{4}\right)^3 \Gamma\left(l+\frac{\delta+4\kappa}{8}\right)^2}{\Gamma(4p+\delta)\,\Gamma(1+2l-p+\kappa)}, \end{aligned} \tag{3.118}$$

The I functions are closely related to the periods and together with the gamma class form the geometric ingredients of the partition function. In these expressions the brackets denote

[8] What is considered left and right of the line, i.e. the orientation of the line, contributes an overall sign and the choice does not matter as long as the same convention is chosen for all contributing pairs.

expressions modulo 1, i.e. $\langle x \rangle = x - \lfloor x \rfloor$. Finally the gamma class is given by

$$\widehat{\Gamma}_{\delta,\kappa}(0) = \Gamma\left(\left\langle \frac{\delta}{4} \right\rangle\right)^3 \Gamma\left(\left\langle \frac{\delta + 4\kappa}{8} \right\rangle\right)^2 , \tag{3.119}$$

The gamma class in the denominator is obtained from the gamma class in the nominator by reflecting the gamma function inside the bracket, i.e. setting $\langle x \rangle \to \langle 1 - x \rangle$. In the example this corresponds to

$$\widehat{\Gamma}^*_{\delta,\kappa}(0) = \Gamma\left(\left\langle 1 - \frac{\delta}{4} \right\rangle\right)^3 \Gamma\left(\left\langle 1 - \frac{\delta + 4\kappa}{8} \right\rangle\right)^2 . \tag{3.120}$$

Note that the ratio of gamma classes is exactly like the structure of Γ-functions appearing in the partition function. There are 6 different Givental functions appearing in (3.117), interpreting this as a period vector $\omega = \{I_{1,0}, I_{2,0}, I_{3,0}, I_{1,1}, I_{2,1}, I_{3,1}\}$ and denoting the rations of gamma classes as

$$\gamma(i,j) = \frac{\widehat{\Gamma}_{i,j}(0)}{\widehat{\Gamma}^*_{i,j}(0)} , \tag{3.121}$$

we can write the partition function compactly as

$$Z_{LG} = \overline{\omega} M \omega , \tag{3.122}$$

with the pairing matrix

$$M = \frac{1}{8} \begin{pmatrix} \gamma(1,0) & 0 & 0 & 0 & 0 & 0 \\ 0 & \gamma(2,0) & 0 & 0 & 0 & 0 \\ 0 & 0 & \gamma(3,0) & 0 & 0 & 0 \\ 0 & 0 & 0 & -\gamma(1,1) & 0 & 0 \\ 0 & 0 & 0 & 0 & -\gamma(2,1) & 0 \\ 0 & 0 & 0 & 0 & 0 & -\gamma(3,1) \end{pmatrix} .$$

Note that the $\gamma(i,j)$ are only numbers independent of the coordinates and ω is holomorphic while $\overline{\omega}$ is anti-holomorphic. As the moduli space metric is given by the derivatives of the Kähler potential, which itself is given by

$$K = -\log(Z) , \tag{3.123}$$

this leads to an simple expression for the moduli space metric

$$g_{i\bar{j}} = \partial_i \partial_{\bar{j}} K = -\frac{\overline{\omega} M \partial_{\bar{j}} \overline{\omega} \partial_i \omega M \omega}{(\overline{\omega} M \omega)^2} + \frac{\partial_i \overline{\omega} M \partial_{\bar{j}} \omega}{\overline{\omega} M \omega} . \tag{3.124}$$

This equation can then be numerically evaluated for any values of the moduli. This finishes the mathematical computations and can now be used to test the Swampland conjectures.

Before we come to this we will show the methods developed so far for some more examples. We start by giving the explicit expressions for the partition function for $\mathbb{P}_{11222}[8]$ in the other phases. We will see that the simple diagonal form of M is an artifact of the LG phase and will not persist to other phases.

In the geometric phase, there are two pairs of divisors contributing to the partition function, Z_1Z_2 and Z_2Z_3. Thus in this phase the carefully defined overall signs matter. Carefully performing the algorithm one arrives at

$$M_{LCS} = -8\pi^3 \begin{pmatrix} \frac{168\zeta(3)}{4\pi^3} & 0 & 0 & 0 & 0 & 4i \\ 0 & 0 & 0 & 0 & 4i & 0 \\ 0 & 0 & 0 & 4i & 8i & 0 \\ 0 & 0 & 0 & 4i & 0 & 0 \\ 0 & 0 & 4i & 0 & 0 & 0 \\ 0 & 4i & 8i & 0 & 0 & 0 \\ 4i & 0 & 0 & 0 & 0 & 0 \end{pmatrix} . \tag{3.125}$$

The details of this evaluation can be found in [62]. The I function in this case is given by

$$\begin{aligned} I(z,\epsilon) = & \frac{\Gamma\left(1+\frac{\epsilon_1}{2\pi i}\right)^3 \Gamma\left(1+\frac{\epsilon_2}{2\pi i}\right)^2}{\Gamma\left(1+4\frac{\epsilon_1}{2\pi i}\right)} \sum_{n_1,n_2\geq 0} e^{-z_1 n_1} e^{-z_2 n_2} e^{-z_1 \frac{\epsilon_1}{2\pi i}} e^{-z_2 \frac{\epsilon_2}{2\pi i}} \\ & \cdot \frac{\Gamma\left(1+4n_1+4\frac{\epsilon_1}{2\pi i}\right)}{\Gamma\left(1+n_1+\frac{\epsilon_1}{2\pi i}\right)^3 \Gamma\left(1+n_2+\frac{\epsilon_2}{2\pi i}\right)^2} \begin{cases} \frac{\Gamma\left(1+\frac{\epsilon_1}{2\pi i}-2\frac{\epsilon_2}{2\pi i}\right)}{\Gamma\left(1+n_1-2n_2+\frac{\epsilon_1}{2\pi i}-2\frac{\epsilon_2}{2\pi i}\right)} & n_1 \geq 2n_2 \\ (-1)^{n_1} \frac{\Gamma\left(-n_1+2n_2-\frac{\epsilon_1}{2\pi i}+2\frac{\epsilon_2}{2\pi i}\right)}{\Gamma\left(-\frac{\epsilon_1}{2\pi i}+2\frac{\epsilon_2}{2\pi i}\right)} & n_1 < 2n_2. \end{cases} \end{aligned} \tag{3.126}$$

Finally, the period vectors is given by

$$\omega = (I^{0,0}(z,0), I^{0,1}(z,0), I^{1,0}(z,0), I^{1,1}(z,0), I^{2,0}(z,0), I^{2,1}(z,0) + 2I^{3,0}(z,0)) . \tag{3.127}$$

The pairing matrix is in this case close to being an anti-diagonal matrix. Note that this nice form depends on the chosen basis for the periods. As one can see in the quintic example, even in the LCS regime the matrix can be rather complicated. Next we give the result for the hybrid phase. Again a rather tedious computation gives

$$M = \begin{pmatrix} \gamma_1(0)(\log 2)^3 & -\frac{i\pi}{2}\gamma_1(0) & 0 & 0 & 0 & 0 \\ -\frac{i\pi}{2}\gamma_1(0) & 0 & 0 & 0 & 0 & 0 \\ 0 & 0 & \gamma_2(0)(\log 2)^2 & -\frac{i\pi}{2}\gamma_2(0) & 0 & 0 \\ 0 & 0 & -\frac{i\pi}{2}\gamma_2(0) & 0 & 0 & 0 \\ 0 & 0 & 0 & 0 & \frac{1}{\gamma_1(0)}(\log 2)^3 & -\frac{i\pi}{2}\frac{1}{\gamma_1(0)} \\ 0 & 0 & 0 & 0 & -\frac{i\pi}{2}\frac{1}{\gamma_1(0)} & 0 \end{pmatrix} . \tag{3.128}$$

The entries $\gamma_\delta(\epsilon)$ are again given by the ratio of gamma classes, which in this case take the form

$$\begin{aligned}\widehat{\Gamma}_\delta(\epsilon) &= \Gamma\left(\frac{\delta}{4}+\frac{\epsilon}{\pi i}\right)\Gamma\left(\frac{\delta}{4}\right)^3\Gamma\left(1-\frac{\epsilon}{2\pi i}\right)^2\\ \widehat{\Gamma}^*_\delta(\epsilon) &= \Gamma\left(1-\frac{\delta}{4}-\frac{\epsilon}{\pi i}\right)\Gamma\left(1-\frac{\delta}{4}\right)^3\Gamma\left(1+\frac{\epsilon}{2\pi i}\right)^2 .\end{aligned} \tag{3.129}$$

as well as the I-function

$$I_\delta(z_1,z_2,\epsilon) = \frac{\Gamma\left(1+\frac{\epsilon}{2\pi i}\right)^2}{\Gamma\left(\frac{\delta}{4}+\frac{\epsilon}{\pi i}\right)\Gamma\left(\frac{\delta}{4}\right)^3} e^{-z_2\frac{\epsilon}{2\pi i}} \sum_{a,n\geq 0} \frac{\Gamma\left(a+\frac{\delta}{4}+2n+2\frac{\epsilon}{2\pi i}\right)\Gamma\left(a+\frac{\delta}{4}\right)^3}{\Gamma\left(4a+\delta\right)\Gamma\left(1+n+\frac{\epsilon}{2\pi i}\right)^2} e^{\frac{z_1}{4}(4a+\delta-1)} e^{-z_2 n}.$$

3.4 Numerical CY Metrics

Up to now we have focused on the computation of the periods of the CY. These allow the computation of the effective Kähler- and superpotential. But for some applications the knowledge of the periods is actually not sufficient. For example, the Laplace operator depends on the target space metric directly and cannot be expressed in terms of the periods. Sadly, only few Ricci flat CY metrics are actually known. While the existence of the Ricci flat CY metrics was proven long ago by Yau [69], until recently only the flat metric of the torus was known. In [70,71] explicit constructions of K3 metrics were given using dualities of little string theories. For the phenomenologically relevant CY 3- and 4-folds no analytic expressions are known at all. Thus one has to fall back on numerical methods. Different methods to compute the metric numerically have been developed in [72,73]. More recently neural networks have been used to compute the metrics [74–76].

While the methods used to fix the parameters of the Ansatz differ in the papers mentioned above, the objective functions of the algorithms are all based on the same idea. There are two ways how one can build a top form for a CY three form. First one can use the known unique three-form Ω, second one can use the Kähler form J. As the top-cohomology $H^{3,3}$ contains only a single element, the resulting expressions have to be proportional to each other, i.e.

$$J\wedge J\wedge J = \kappa\, \Omega\wedge\overline{\Omega}\,, \tag{3.130}$$

where κ is constant over the moduli space. Thus computing the ratio of the two expressions gives a measure of the flatness of the metric, as

$$\frac{J\wedge J\wedge J}{\Omega\wedge\overline{\Omega}} = \frac{6i\det g}{\Omega\wedge\overline{\Omega}} = \kappa\,. \tag{3.131}$$

The usual Ansatz for the metric is the so-called algebraic metric. This is motivated by the form of the Fubini-Study metric for a projective space $\mathbb{P}^n$,

$$K = \frac{1}{2\pi}\log(p)\,, \tag{3.132}$$

with

$$p = \sum_{i=0}^{n} z_i \overline{z}_i \ . \tag{3.133}$$

The idea is to replace the polynomial p by more general polynomials. Let s_α be a basis of degree k monomials, then one makes the Ansatz

$$p = \sum_{\alpha=1}^{N_k} s_\alpha h^{\alpha\beta} \overline{s}_\beta \ . \tag{3.134}$$

where N_k is the number of degree k monomials in the coordinates z_i and $h^{\alpha\beta}$ is a coefficient matrix to be fixed by the algorithm, which is interpreted as an inverse metric. Note that this is the metric of a line bundle L=$\mathcal{O}_X(k)$ and not the CY metric itself, which follows in the usual way from the Kähler potential. The monomials s_α then form a basis of the global sections. It was proven by Donaldson [72] that for infinite k this Ansatz does result in the correct Ricci-flat CY metric. The algorithms now have to fix the elements of $h^{\alpha\beta}$. The first algorithm developed for this task was Donaldson's T map introduced in [72]. The T-map is explicitly given by

$$T(h)_{\alpha\beta} = \frac{N_k}{\mathrm{Vol}(X)} \int_X \frac{s_\alpha \overline{s}_\beta}{|s|_h^2} \mathrm{dVol}_X \ . \tag{3.135}$$

The absolute value in the denominator on the right hand side depends on the inverse metric. The T operator thus gives a map from the inverse metric $h^{\alpha\beta}$ to a new metric $T(h)_{\alpha\beta}$. This new metric can then, after inversion, used again as an input for the T operator. Applying the T operator repeatedly converges to a special metric, known as the balanced metric [73]. The precise mathematical statement is that if the automorphism group Aut(X,L) is discrete, for any initial Hermitian metric G_0 and $r \to \infty$ the sequence $T^r(G_0)$ converges to a fixed point. The fixed point has constant scalar curvature proportional to $c_1(X)$ [77], which for a CY implies that it is a Ricci flat metric. In practical applications the convergence is very fast, often a few iterations are enough that the entries of $h_{\alpha\beta}$ do no longer change at double precision.

Another way to find the entries of $h_{\alpha\beta}$ is to reformulate the problem into an optimization problem. In an optimization problem the goal is to extremize, i.e either minimize or maximize an objective function subject to some constraints. There are several possible choices, e.g. the integrated value of the deviation from flatness defined in (3.131). Another possibility are the energy functionals introduced in [78]. These are energies depending indirectly on the Ricci tensor, as for example the Calabi energy

$$\int_X \frac{J^3}{6} R^2 \ . \tag{3.136}$$

Thus minimizing these energies will result in the so-called optimal metric possible with the made Ansatz. Indeed results show that the curvature of these metrics are smaller than the ones of the T-map at a fixed order k. It should be noted that these energy functionals

used are already several years old, due to the increase in computational power it is now possible to directly integrate the Ricci scalar over the CY. [75]. The Ricci scalar depends on the Kähler potential with a fourth derivative. This renders the computation expensive, but the results are obviously better if one uses the Ricci scalar directly. Finally, the most modern approach involves the application of neural networks. This has the advantage that the neural network can directly learn the metric components and no detour to the Kähler potential has to be taken. But for the training the network needs some known results, which have to be obtained by either the T map or optimization. Nevertheless, combining these older methods with neural networks is able to outperform the purely optimization or purely T-map approach in terms of computational time needed [75].

All methods mentioned above need a numerical way to implement the integration operator $\int_X \mathrm{dVol}_X$. This is done by approximating the integral by n points sampled from the geometry. The sampling turns out to be the limiting factor in the computations, as first the maximal possible number of points which can be taken into account is limited by the available memory and second the more advanced sampling algorithms take quite some computation time to generate the sample.

The goal of the sampling is to produce a sample which approximates the integral as close as possible while needing as little computation time as possible. The problem is, that the CY spaces we are interested in are defined only indirectly as hypersurfaces is projective spaces. While homogeneous sampling from a projective space can be realized easily, for hypersurfaces therein some algorithms are required. There are three main ways used in the literature how to perform this:

1. Rejection sampling
2. Solving for a coordinate
3. Intersection Sampling

In the first approach, rejection sampling, one draws random points in the ambient projective space. The distance between the drawn points and the hypersurface is computed by inserting the point in the defining polynomial of the hypersurface. If the point is closer than a given small value of ϵ, the point is added to the sample, otherwise the point is rejected. This leads to a homogeneous sample, but the points to not exactly lie on the hypersurface, leading to errors. Moreover, if one requires the precision ϵ to be smaller than 10^{-4} the algorithm becomes very slowly. As for high precision in the integration of the order of 10^6 to 10^9 points are used, this renders this approach unpractical. It can be improved by projecting the sample points orthogonal onto the hypersurface. This removes the error, but at the same time destroys the homogeneity of the sample, reintroducing the error in the approximation of the integral.

In the second approach the hypersurface constraint is explicitly solved. For this the ambient projective space $\mathbb{P}^n$ with coordinates X_i, $i = 0, \dots n$ is covered by $n+1$ coordinate patches U_i, defined by the coordinate X_i taking the largest value. Without loss of generality

we work in the U_0 coordinate patch. Then homogeneous coordinates are introduced by dividing by X_0, i.e.

$$x_i = \frac{X_i}{X_0} \, . \tag{3.137}$$

As X_0 was the largest coordinate, the x_i have an absolute value $|x_i| \leq 1$, i.e. they take values in the unit disk D. Thus the projective space $\mathbb{P}^n$ is given by $n+1$ copies of D^n. A concrete example for this is $\mathbb{P}^1 = S^2$. This space can be covered by two charts U_0 and U_1, each consisting out of a unit disc parameterized by the coordinates

$$x_1 = \frac{X_1}{X_0} \qquad \text{and} \qquad x_0 = \frac{X_0}{X_1} \, . \tag{3.138}$$

respectively. The two discs represent the two hemispheres centered around the north and south poles. Then the roots of the defining polynomial p can be solved for any of the coordinates, e.g x_n. This requires the solution of a high degree polynomial. For numerical algorithms this does not pose any problems. Analytically this is a surprisingly hard task, but the roots of polynomials of any degree can be expressed in terms of hypergeometric functions [79]. Of course for polynomials of degree ≤ 4 these can be reduced to radicals, for degree 5 to elliptic functions and for degree $d \geq 6$ to genus $d-4$ θ-functions. As an example we take again the quintic defined by the polynomial

$$p = \sum_{n=0}^{4} X_n^5 + 5\psi X_0 X_1 X_2 X_3 X_4 \, . \tag{3.139}$$

This equation is completely symmetric in all 5 coordinates, thus we can simply take 5 copies of the U_0 chart. In this chart the defining equation becomes

$$1 + \sum_{n=1}^{4} x_n^5 + 5\psi x_1 x_2 x_3 x_4 = 0 \, . \tag{3.140}$$

If we want to solve this equation for x_4, we can treat all other coordinates and ψ as fixed coefficients, i.e. we have to solve

$$x_4^5 + \alpha x_4 + \beta = 0 \, , \tag{3.141}$$

where $\alpha = 5\psi x_1 x_2 x_3$ and $\beta = 1 + \sum_{n=1}^{3} x_n^5$. This form of the quintic equation is known as the Bring-Jerrad normal form. The roots of this form can be explicitly stated in terms of the Bring radical BR as

$$x_4 = \sqrt[4]{-\frac{\alpha}{5}} BR\left(-\frac{1}{4}\left(-\frac{5}{\alpha}\right)^{\frac{5}{4}} \beta\right) \, . \tag{3.142}$$

Finally, the Bring radical can be expressed in terms of a hypergeometric ${}_4F_3$ function.

$$BR(a) = -a \, {}_4F_3(\frac{1}{5}, \frac{2}{5}, \frac{3}{5}, \frac{4}{5}; \frac{2}{4}, \frac{3}{4}, \frac{5}{4}, -5^5(\frac{a}{4})^4) \, . \tag{3.143}$$

The hypergeometric function appearing in this solution is rather complicated and does not seem to be in any direct relation with the hypergeometric functions appearing in the periods due to the multiples of 1/4 parameters appearing in the b parameters of the function. This solution allows to write the integration operator on the CY explicitly. The integration is over 3 unit discs parameterized by x_i, i=1,2,3, subject to the constraint that $|x_4| \leq 1$, with x_4 given in (3.142).

Finally, there exists a method to use homogeneous sampling on the sphere to sample homogeneously on a hypersurface. The idea is to draw randomly two points in $\mathbb{P}^n$. These points span a line. This line intersects the hypersurface exactly d times, where d is the degree of the defining polynomial. It can be shown that these points are distributed homogeneously on the hypersurface. Finding the 5 intersection points can be performed numerically with high precision. This allows a fast and precise computation of sample points. Therefore the method is faster than explicitly integrating, but has the disadvantage that localized effects like the conifold can be missed. Indeed, when the scalar Laplace operator is solved using this method, the quintic at $\psi = 1$ does not show any signs of a conifold [80].

3.5 Line Bundle Cohomologies of Toric Varieties

In this section we will give an algorithm to determine analytical formulas for the rank of line bundle cohomologies of toric varieties or hypersurfaces therein. This section is based on the paper [81]. We will be interested in computing the rank of the cohomology group $H^i(\mathcal{O}_X(D))$ of some divisor D of a toric variety X. There exist algorithms which solve this problem , e.g. the CohomCalc algorithm [82]. While these solve the problem for given line bundle charges, they become very slow for more complicated problems and large line bundle charges. In [81] a method was developed to obtain an analytic formula only using the knowledge of a few cohomologies with low line bundle charges. It should be noted that the ranks of the cohomology groups are in principle a hard problem for machine learning techniques as they jump between neighbouring values. This can be seen by the failure of simple neural networks to correctly reproduce the cohomologies, especially in the case of hypersurfaces. The core observation which allows the use of machine learning techniques in form of classification algorithms is that the cohomologies have a phase structure similar to the GLSM of CYs. In each phase the rank of the cohomology group is given by a simple polynomial of the line bundle charges. Thus the problem is reduced to classifying the phase structure and determining the rational coefficients of the polynomials.

The Algorithm

The CohomCalc algorithm [82] allows the determination of the ranks of the cohomology groups for given values of the line bundle charges.[9] In this section an algorithm using

[9] In some of the following examples it is necessary to extend the algorithm by implementing an additional cut in the Koszul sequence, we will not go into details of the CohomCalc algorithm in this thesis and refer

unsupervised learning is presented which allows the identification of analytic expressions.

First a data set S of the cohomologies is calculated for all values of the line bundle charges $\vec{m}$ satisfying $|m_i| \leq a \ \forall i$ for a fixed value of a. Tests have shown that $a = 25$ is sufficient for the algorithm to find the analytic formulas.

The algorithm uses the observation that the h^i have a distinct phase structure. In the interior of one phase the h^i are polynomial functions of the line bundles of maximal degree d, where d is the dimension of the variety. If one can identify the phase structure, it is then easy to perform a polynomial fit. This represents a classification problem. As one a priori does not know the phase structure, unsupervised learning has to be applied.

In unsupervised learning one faces the task to group data points into different sets without specifying any conditions. This leads to a clustering of similar data. The only input is the data to classify and the maximal number of sets to be used. We applied the pre-implemented ClusterClassify function of Mathematica 11.3 with 200 classes and "Quality" as optimization goal as well as "KMeans" as the method to generate the classifiers and the LinearModelFit function for the polynomial fits.

In the interior of one phase, the d-th derivatives of the h^i with respect to $\vec{m}$ are constant and the $(d+1)$-th derivatives vanish. As the h^i are only defined for integer $\vec{m}$, the data forms a lattice. The derivatives are therefore calculated using the central difference scheme with a lattice spacing of one. This leads to a non-vanishing $(d+1)$-th derivative exactly at the phase boundaries. The first step is to remove the boundaries out of the data set S. To do so a cluster classifier with a very large number of classes is trained on the data set

$$\left\{\vec{m}\ ,\ \frac{\partial^{d+1}h^i}{\partial^{d+1}m_1}\ ,\ \frac{\partial^{d+1}h^i}{\partial^d m_1\partial m_2}\ ,\ .....\ ,\ \frac{\partial^{d+1}h^i}{\partial^{d+1}m_R}\right\}\ , \tag{3.144}$$

where $i = 0, \ldots, d$ runs over all cohomology groups. This set takes for a point inside a phase the form

$$\{\vec{m}, 0, 0, 0, ..., 0\} \tag{3.145}$$

and for a point at a phase boundary at least one of the latter entries is non-vanishing. This leads to a classification where all data points which lie in the interior of a phase are classified into one set and various sets of boundary points. For large enough line bundle charges the interior will always be the largest set. The boundaries are simply thrown away. Tests show that the classification works better for a small dimensional space. The number of partial derivatives increases with the degree d and the number of line bundle charges. Therefore this step was divided into several classification steps. First one trains one classifier on a subset of the derivatives of degree $d+1$ and removes the boundary. Then a second classifier is trained on the next subset and so on. As the training of one classifier takes only seconds, this is not a huge performance loss but drastically improves the result. In the examples presented in this paper we used a splitting into two randomly chosen subsets of equal size.

---

to the paper [81] for the details.

With the remaining points forming the interior of the phases the set

$$S_3 = \left\{ \vec{m} \ , \ \frac{\partial^d h^i}{\partial^d m_1} \ , \ \frac{\partial^d h^i}{\partial^d m_1 \partial m_2} \ , \ldots . \ , \ \frac{\partial^d h^i}{\partial^d m_R} \right\} \tag{3.146}$$

is formed and a second classifier trained on this set. The set S_3 is, in contrary to the original data set S, not connected in the $\vec{m}$, which improves the classification and is the reason for the two step procedure. This now classifies the phase structure of the problem. The number of allowed classes is again taken to be very large. While it can happen that one phase is grouped into two classes, this does not pose any problem as in this case the polynomials obtained will agree and the phases can be merged later on.

The final step is to perform the polynomial fit on each set and each h^i. Sets with identical polynomials for all h^i are then merged. This concludes the algorithm. To summarise:

1. Calculate a set of data points using the extended cohomCalg.
2. Determine the $(d+1)$-th derivatives of these points.
3. Classify the data using these derivatives.
4. Determine the d-th derivatives of the remaining data points.
5. Classify the data using these derivatives.
6. Perform a polynomial fit of degree d on each set for each h^i.
7. Merge sets with identical polynomials.

We note that this algorithm requires no input besides the geometric data describing the variety and can therefore be completely automatised. The only thing which has to be done by hand is to extract the boundaries of the phases, as the classifier encodes them not in closed form. This is quite tedious, but for practical purposes one does not need the functions. One can use the classifier to identify in which phase a given $\vec{m}$ lies and apply the polynomial of this phase. For convenience we added the phase boundaries in the tables.

As a non-trivial test of the procedure we calculated the Euler characteristic of the examples by summing up the polynomials and compared them to the Euler characteristic as obtained from the Hirzebruch-Riemann-Roch theorem. The two expressions agree in all examples and phases.

In the following sections this algorithm is applied to some examples.

Line Bundles on Toric Varieties

We start with an example where the analytic expressions are well known, the del Pezzo surface dP_1. This provides on one hand an easy method to cross-check the results and on the other hand is an easy example with only 3 phases.

Using cohomCalg, we generate a data set of the cohomology ranks with the line bundle charges in the range $a = [-25, 25]$. These are shown in figure 3.7. The application of the unsupervised learning on the third derivatives cuts out two phase-boundaries where the underlying function describing the ranks is non-differentiable. The second cluster analysis then classifies the remaining points using the second derivatives into 6 phases, three pairs of which have identical polynomials for h^1. The result is shown in figure 3.8.

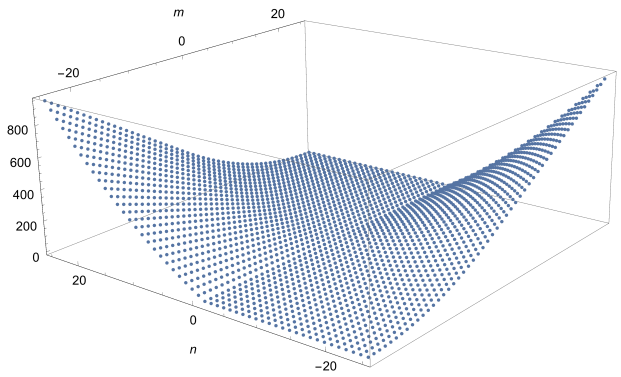

Figure 3.7: $h^1\left(\mathcal{O}(m,n)\right)$ of dP_1.

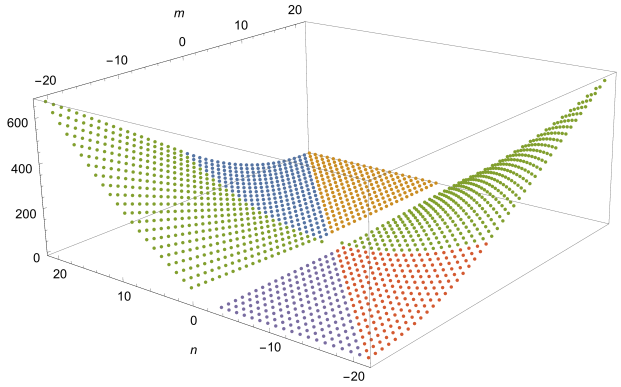

Figure 3.8: Classification result for $h^1\left(\mathcal{O}(m,n)\right)$ of dP_1.

Fitting a polynomial of degree 2 to the ranks in each of these phases results in the polynomials listed in table 3.1. These agree with the known analytic expressions, see e.g. [82].

Phase	Polynomial
$(n \leq -2 \wedge m \geq 0)$ $\vee(n \geq 0 \wedge m \leq -3)$	$-1 - m - \frac{n}{2} - mn + \frac{n^2}{2}$
$(n \leq -2 \wedge n+1 \leq m < 0)$ $\vee(n \geq 0 \wedge -3 < m \leq n-2)$	$\frac{m}{2} + \frac{m^2}{2} - \frac{n}{2} - mn + \frac{n^2}{2}$
else	0

Table 3.1: Polynomials for $h^1(\mathcal{O}(m,n))$ in the case of dP_1.

Line Bundles on Hypersurfaces

We now turn to the more complicated problem of finding analytic expressions for line bundle cohomologies of hypersurfaces in toric varieties. As an example for a hypersurface we take the K3 space $\mathbb{P}^3_{1112}[5]$. This hypersurface has two line bundle charges, so that $\vec{m} = (m,n)$. The expected degree of the polynomials is $d = 2$. Figure 3.9 shows the ranks of the zeroth cohomology for different values of m and n.

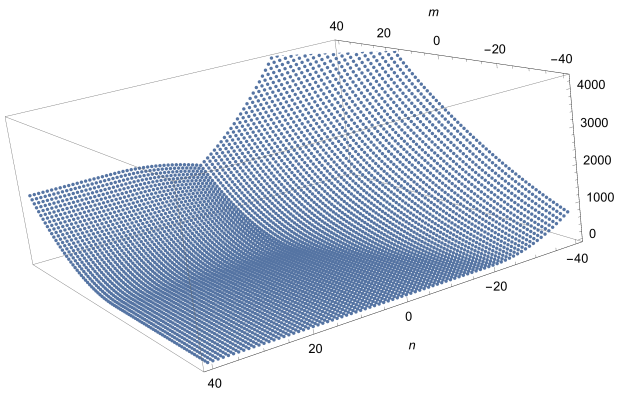

Figure 3.9: $h^0(\mathcal{O}(m,n))$ of $\mathbb{P}^3_{1112}[5]$.

At first glance this seems to consist of 3 phases. But applying the algorithm described in the last section reveals that there are actually 6 phases. Figure 3.10 shows the result of the second classification. The fitted polynomials can be found in table 3.2. One nicely sees the cut boundaries and phases. Also the separation between the orange and brown phase seems redundant from the point of view of h^0, but is necessary because of the higher cohomology groups. Especially interesting is the subdivision in the yellow/purple and red/green phases into even and odd n, which are also described by different polynomials. The phase structure thus is not only defined by some linear functions of m and n. If one tried a polynomial fit in the whole of these phases instead of separating into even/odd one would not obtain rational coefficients. E.g. in the yellow/purple phase the polynomials are $\frac{5m^2}{4} + 2$ for n even and $\frac{5m^2}{4} + \frac{7}{4}$ for n odd. If one mixes these phases, the interpolating polynomial obtained is $1.80407 + 0.0131771\,n + 1.24945\,n^2$, which does obviously not reproduce any of the cohomologies correctly and cannot be extrapolated.

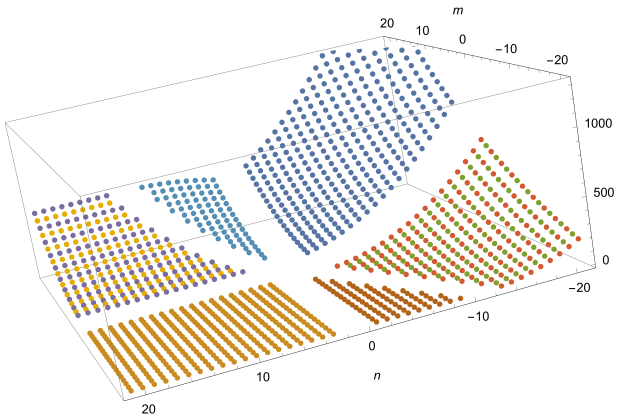

Figure 3.10: $h^0\left(\mathcal{O}(m,n)\right)$ of $\mathbb{P}^3_{1112}[5]$ separated into phases.

Phase	Polynomial
$m<0, n>\frac{m}{2}$	0
$m<0, n<\frac{m}{2}$	$\frac{m^2}{2}-2mn-\frac{3m}{2}+2n^2+3n+1$
$m>0, n>\frac{m}{2}, m$ even	$\frac{5m^2}{4}+2$
$m>0, n>\frac{m}{2}, m$ odd	$\frac{5m^2}{4}+\frac{7}{4}$
$m>0, 0<n<\frac{m}{2}$	m^2+mn-n^2+2
$m>0, n<0$	$m^2-2mn-3m+2n^2+3n+2$

Table 3.2: Polynomials for $h^0\left(\mathcal{O}(m,n)\right)$ in the case of $\mathbb{P}^3_{1112}[5]$.

Another interesting example is the octic $\mathbb{P}^4_{11222}[8]$. Here we expect the polynomials to be of degree $d=3$. Figures 3.11 and 3.12 show again the input data for h^0 and the result after classification. The resulting polynomials for h^0 are listed in table 3.3. We note

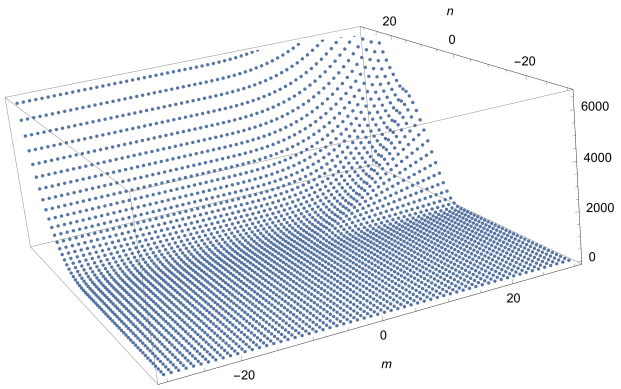

Figure 3.11: $h^0\left(\mathcal{O}(m,n)\right)$ of $\mathbb{P}^4_{11222}[8]$.

that the only disadvantage of this procedure is that the boundaries are cut out and it is not possible to determine the value at the boundaries itself, which is reflected in only $>$

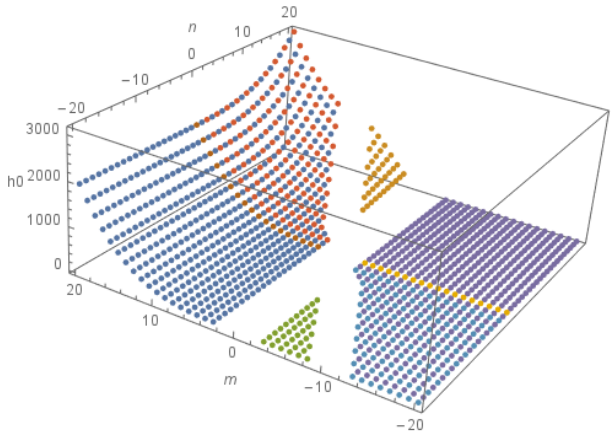

Figure 3.12: Classification result for $h^0\left(\mathcal{O}(m,n)\right)$ of $\mathbb{P}^4_{11222}[8]$.

Phase	Polynomial
$m<0, n\in\mathbb{Z}$	0
$m>0, n<0$	$\frac{m^3}{3}-2m^2+\frac{11m}{3}-1$
$m>0, n>\frac{m}{2}$	$-\frac{8m^3}{3}+2m^2n+\frac{2m}{3}+2n$
$m>0, 0<n<\frac{m}{2}$, m even	$\frac{m^3}{3}-2m^2+\frac{11m}{3}+\frac{n^3}{8}+\frac{3n^2}{8}+\frac{5n}{4}-1$
$m>0, 0<n<\frac{m}{2}$, m odd	$\frac{m^3}{3}-2m^2+\frac{11m}{3}+\frac{n^3}{8}+\frac{3n^2}{8}+\frac{7n}{8}-\frac{11}{8}$

Table 3.3: Polynomials for $h^0\left(\mathcal{O}(m,n)\right)$ in the case of $\mathbb{P}^4_{11222}[8]$.

statements in the table instead of $\geq$. But as these are only a limited number of points one can simply compare these with the results from cohomCalg. The tables for the other cohomology groups can be found in appendix A.6.

While at the time of the paper [81] the appearance of two polynomials in one phase was a surprise, in the meantime a formula for the line bundle charges has been proven in [83]. The formula is based on consecutive projections onto nef divisors. In this procedure ceiling functions appear, explaining the mod 2 structure appearing in some of the examples as well as the fact that polynomials suffice to describe the ranks of the groups.

3.6 Strebel Differentials

In this section we will focus on the computation of a special case of quadratic differentials, the Strebel differentials. Quadratic differentials play an important role in many string theoretic computations, from the definition of a complex structure in terms of Beltrami differentials to the evaluation of string field theory vertices defined in terms of minimal area metrics. In this section we will focus on the latter application, but it should be mentioned

that the developed tools are applicable in other areas too. Especially we will comment at the end of the section on possible applications in the understanding of the moduli space of CY manifolds. The results of this section contain unpublished work.

In string field theory, one of the basic problems is to decompose the diagrams into vertex and propagator contributions. For example, a part of the moduli space of the 4-punctured sphere is already covered by the combination of two 3-vertices combined by a propagator. One solution to this problem is to define the vertices in terms of a minimal area metric [84,85]. This reduces the problem to the computation of minimal area metrics. These in turn can be shown to originate from Strebel differentials.

A Strebel differential is a quadratic differential with second order poles with residues[10] -1 which satisfies the Strebel condition. This means that in a local coordinate z the quadratic differential q can be written as

$$q = \phi(z)\mathrm{d}^2 z \,, \tag{3.147}$$

where $\phi(z)$ is a meromorphic function of z with Laurent expansions around a pole p

$$\phi(z) = \frac{-1}{(z-p)^2} + \frac{b_{-1}}{(z-p)^1} + b_0 + b_1(z-p)\dots \,. \tag{3.148}$$

The coefficients b_i are complex numbers independent of z. The Strebel constraint states that the integral between any two zeroes z_i of the differential is real, i.e.

$$l_{i,j} = \mathrm{Im}\int_{z_i}^{z_j} \sqrt{\phi}\mathrm{d}z = 0\,. \tag{3.149}$$

These integrals are of elliptic type and in general very hard to solve. This in turn renders the explicit computation of Strebel differentials complicated. The general quadratic differential with n second order poles can be written as

$$\phi(z) = \frac{-z^{2n-4} + \sum\limits_{i=0}^{2n-5} a_i z^i}{\prod\limits_{i=1}^{n-1}(z-z_i)^2}\,. \tag{3.150}$$

This form is derived as follows: One puncture is positioned at infinity, which is always possible by using the $SL(2,\mathbb{C})$ symmetry. Then the residue condition at infinity forces the polynomial in the nominator to be of order $2n-4$ and the leading coefficient to be -1. This expression has $2n-4$ undetermined coefficients a_i. $n-1$ of these can be fixed by the remaining residue constraints, leaving $n-3$ unfixed parameters. Thus for the 3-punctured sphere there are no remaining degrees of freedom. Choosing the usual punctures at 0, 1 and infinity, the unique Strebel differential is given by

$$\phi(z) = \frac{-z^2+z-1}{z^2(z-1)^2}\,. \tag{3.151}$$

[10] With residue one means in this context the coefficient of the first term in the Laurent expansion.

For the 4-punctured sphere, there remains one unfixed parameter. Choosing the punctures to be at 0,1, ξ and infinity, the differential takes the form

$$\phi(z) = \frac{a}{(z-1)z(z-\xi)} - \frac{(z^2-\xi)^2}{(z-1)^2 z^2 (z-\xi)^2} \,. \tag{3.152}$$

The undetermined parameter a depends on the position of the fourth puncture ξ. Moreover, the boundaries of the moduli space are a priori unknown and have to be determined by finding the values of ξ for which one of the lengths $l_{i,j} = \pi$. This problem was solved numerically by Möller in [86] and used to compute quartic string field theory vertices. Here we will instead ask the question of how to compute the Strebel differential given the lengths $l_{i,j}$. In the case of 4 punctures there are 3 different lengths which we will denote a,b and c which fulfill due to the residue constraint

$$a + b + c = 2\pi \,. \tag{3.153}$$

Sometimes it is useful to use differently normalized lengths obtained by dividing a,b and c by π

$$\alpha + \beta + \gamma = 2 \,. \tag{3.154}$$

This problem was actually solved by mathematicians for the n-punctured sphere in [87]. For the 4-punctured case some examples have been recently worked out in [88]. The basic idea is the equivalence between the following 3 objects

- Strebel differentials on Riemann surfaces
- Algebraic curves over $\overline{\mathbb{Q}}$
- Ribbon Graphs ("child's drawings" or "dessins d'enfants")

The name child's drawing originates from Groethendieck, who was fascinated by the amount of information stored in such simple figures. These are defined by the inverse image of a Belyi map of the interval [0,1]. A Belyi map is a map from a Riemann surface onto $\mathbb{P}^1$ which is ramified at 0,1, and infinity. This language may be unfamiliar for physicists and is a bit counter intuitive. A function is said to be ramified at a point to a degree d if the *inverse* of its derivative has a branch point of degree d. Effectively this means that a function of the form z^n is ramified at 0 of degree $n-1$. This notion will become more clear in the examples.

Instead of solving the problem of rational lengths and fixed residues, one solves the problem with residues n and integer lengths. The value of n can be chosen as the least common multiple of the denominators of the rational numbers. Rescaling the solution obtained this way by $1/n$ then produces the wanted differential. This approach was also taken in [89], were the Strebel differentials for integer lengths were computed by solving a factorization problem. The authors also show the relation to Belyi maps but do not use it as a computational tool. Our new proposal is to use the property that the Strebel

differential originates from the pull-back of a simple known quadratic differential by a Belyi map, i.e.

$$\phi(z) = f^\star g^\star q \,, \tag{3.155}$$

where the $\star$ denotes the pull-back, q is the known quadratic differential

$$q = \frac{1}{z(1-z)^2}\mathrm{d}^2 z \tag{3.156}$$

and f and g are functions such that $f \circ g$ is a Belyi map. We split the Belyi map into two functions as it was observed in [88] that in the case of a 4-punctured sphere all Belyi maps can be written as $f \circ g$ with

$$g(z) = z^2 \,. \tag{3.157}$$

This Ansatz halves the degree of the unknown function f. The function f has to be ramified only at 0,1 and infinity. It was also worked out in [88] that this restricts the maximal degree the function f can take. We will take a different approach here and simply make different Ansätze for the function f and see how far we can get with each of them. As the first try we take

$$f(z) = -\frac{a_0 + a_1 z + a_2 z^2}{c_0 + c_1 z} \,. \tag{3.158}$$

This is the lowest degree which gives a solution. We now have to determine the 4 complex parameters a_0, a_1, c_0 and c_1. This is done by computing the pullback of q by g and f and comparing the resulting quadratic differential with the known form of a Strebel differential for a 4-punctured sphere given in (3.152). This is most easily done by comparing not the differentials directly but the expansions around the punctures. Around the origin ϕ expands as

$$\phi(z) = \frac{-1}{z^2} + \frac{a-2-2\xi}{z} + \frac{a\xi + a - 3\xi^2 - 2\xi - 3}{\xi^2} + \mathcal{O}(z) \,. \tag{3.159}$$

Requiring the pull back of q to have a residue of -1 has 2 solutions

$$c_0 = -a_0 \qquad \text{and} \qquad c_1 = -a_0 - a_1 \,. \tag{3.160}$$

or

$$c_0 = a_0 \qquad \text{and} \qquad c_1 = 2a_0 + a_1 + a_2 \,. \tag{3.161}$$

Using this and comparing order by order the series expansions gives in the first case the unique solution

$$\phi(z) = -\frac{(\xi + z^2 - 2\xi z)^2}{(z-1)^2 z^2 (\xi - z)^2} \,. \tag{3.162}$$

This is a Strebel differential with only 2 zeroes. It thus corresponds to special symmetric cases at the boundary of the moduli space where one of the lengths shrinks to 0 size. The second case leads only to a solution if $\xi = \frac{1}{2} \pm \frac{i}{\sqrt{3}}$. In this case $a = 2 \pm \frac{2i}{\sqrt{3}}$. This corresponds to the most symmetric configuration of the 4-punctured sphere where the punctures are

positioned on the corners of a tetrahedron. The values found values agree with the values given in [88,89] for this point. This shows that demanding the power expansions to agree is sufficient for a complete solution. But the equations become cumbersome to solve with an increasing degree of the Ansatz for f. Already for a cubic Ansatz the general equation is very hard to solve. But it is possible to find special solutions with fixed ξ as in the second case. The values for these solutions are also in agreement with the table of solutions in [89]. Thus we have shown that it is possible to simplify the computations and reduce them to an algebraic problem by using series expansions.

The unknown function $a(\xi)$ enjoys some modular properties. For example, it is known that [88]

$$a\left(\frac{1}{\xi}\right) = \frac{a(\xi)}{\xi} \qquad a(1-\xi) = 2 - a(\xi)\,. \tag{3.163}$$

This is obtained directly from (3.152) by exchanging two poles and demanding equality. These identities are sufficient to give a solution for all real values of ξ given the values in $[1/2, 1)$ but they do not allow a solution for all complex values. But they are a strong hint that there could be an underlying hypergeometric solution to the general problem. If this is true, the hypergeometric function would reduce at special points to simple rational functions. That this is the often the case is well-known. We leave this interesting possibility for future studies.

Finally we want to comment on the relation to the moduli space of CY manifolds. For 1-parameter models, the moduli space is equivalent to a $\mathbb{P}^1$ with 3 punctures at the LCS, the LG point and the conifold. The inverse mirror map can thus be interpreted as a Belyi map from the Kähler moduli space to the complex structure moduli space. This map defines a unique quadratic differential and thus a metric on the moduli space. This metric is not necessarily the metric following from the periods. It would be interesting to understand its meaning. Moreover, the γ coordinate introduced in [39] is also a Belyi map to the complex structure side, albeit a different one than the mirror map. Thus this interpretation could give a hint on the meaning of this function as well. This finishes the mathematical discussion. We now turn to the application of the developed methods to the swampland conjectures.

Chapter 4

The Swampland Conjectures

In this chapter the swampland conjectures are tested in the context of string theoretic models. First the general idea of the swampland program is introduced. Then the focus is put on two of the conjectures, the swampland distance conjecture as well as the dS conjecture. Finally, explicit string models are constructed and it is shown that all of them satisfy the conjectures.

4.1 The Swampland Program

String theory compactifications give rise to a vast amount of vacua, known as the landscape. While the number of different vacua is huge and ever increasing, famous estimates are ranging between 10^{500} [90] for type II vacua, 10^{1500} in heterotic models [91] and an astonishing 10^{272000} vacua for a single compactification geometry of F-theory [92]. Also, the obtainable gauge groups are huge, including for example the compactification on the fourfold $\mathbb{P}_{1,1,84,516,1204,1806}[3612]$ with gauge group $E_8^{2561} \times F_4^{7576} \times G_2^{20168} \times SU(2)^{30200}$ [93]. Especially embedding the standard model in this huge landscape is rather simple, but the huge amount of possible constructions makes predictions impossible. While it thus may seem that everything can be constructed in string theory, there nonetheless seem to be restrictions. Some low energy theories have no known embedding in string theory or other UV completions. These theories are said to be in the swampland. The swampland program tries to classify the boundary between the swampland and the landscape. This includes the search for criteria which lead to a theory being in the swampland. The first of these conjectures appeared in [9]. The conjecture, now known as the distance conjecture, states that if one formulates an effective theory around one point p_1 in moduli space and deforms the theory away from this point to another point p_2 infinitely far way in moduli space, the effective theory will break down due to an infinite tower of states becoming exponentially light. This conjecture was refined in [94] to include finite distances. I.e. there is a tower of states whose masses scale like

$$m = m_0 \, e^{\lambda \frac{d(p_1,p_2)}{M_{Pl}}} \ , \tag{4.1}$$

for some order one constant λ. This conjecture will be the focus of the next section. Another important conjecture is the weak gravity conjecture (WGC) [95]. This conjecture follows from many different arguments, many of which do not refer to string theory at all but rather to black hole arguments, unitarity or entropy [96–104], all of which are basic assumptions of a general theory of quantum gravity. One of the main arguments is that a charged black hole should always be able to decay to prevent the existence of black hole remnants. For extremal black holes this requires the existence of a particle whose charge is larger than its mass, i.e. for an abelian symmetry[1]

$$m < \sqrt{2} g q M_{Pl} \,, \tag{4.2}$$

where g is the gauge coupling and q the charge of the particle. This is the electric version of the conjecture, there is also a magnetic variant. It limits the allowed gauge coupling depending on the cutoff Λ of the theory,

$$\Lambda < g M_{Pl} \,. \tag{4.3}$$

This already includes another famous conjecture, the no global symmetries conjecture. As a global symmetry can be seen as the limit of a local symmetry where the gauge coupling is sent to 0, (4.3) requires a vanishing cutoff as $g \to 0$. Thus global symmetries would be forbidden. That string compactifications forbid continuous global symmetries has been long known [106]. More recently this was extended to include discrete symmetries [10]. In the same paper it was conjectured that the symmetry groups have to be compact. The breaking of all global symmetries is conjectured to be implemented by Chern-Simons terms [107]. There are several extensions to the weak gravity conjecture. If the WGC is extended to multiple gauge groups, one arrives at the convex hull condition [108]. This requires that the convex hull spanned by the charge vectors of the particles in the theory includes the d-dimensional unit ball, where d is the sum of the ranks of the gauge group.

Another conjecture is the so-called lattice weak gravity conjecture [109]. This conjecture follows from the requirement that if the WGC holds, it should also hold when the theory is compactified. This requires the completeness of the charge lattice, i.e. all particles in the lattice should actually exist in the theory. This is a variant of Polchinski's completeness conjecture [110], which states that all gauge representations allowed by charge quantization have to exist in the theory.

Finally, scalar interactions can be included. This modifies the black hole argument as well as the bound state argument, depending on the sign of the scalar force [111].

Another important conjecture is the non-SUSY AdS conjecture, which forbids stable non-supersymmetric AdS vacua [105]. The reason is the existence of instanton solutions turning the flux stabilising the vacuum into a brane. The charge of the brane will then lead to the decay of the AdS vacuum. The existence of the brane and thus of this decay mechanism is a consequence of the refined WGC.

[1] The originally proposed version states the relation as $\leq$, but as an equality would relate an internal symmetry to the Poincaré symmetry, which is forbidden by the Coleman-Mandula theorem, it was argued in [105] that equality is impossible.

One of the most important conjectures is the dS conjecture [112]. The conjecture relates the scalar potential and its derivative

$$|\nabla V| \geq cV \ , \tag{4.4}$$

for some order one constant c. Especially this forbids dS vacua, as for these the derivatives vanish while $V > 0$. The constant c is not fixed, but cosmology constraints it to be smaller than 0.6 [113]. In fairly general tree-level setups, there exist no-go theorems [114,115] (and extensions in [112]) that explicitly forbid dS vacua. Moreover, in [116] dS was excluded in parametrically controlled regimes. There are several refinements of this conjecture, most importantly there are counter examples to the above conjecture in presence of tachyons (instabilities) of the solution, i.e. dS maxima. To include these, the conjecture is amended as follows [117]:

$$|\nabla V| \geq c\frac{V}{M_{Pl}} \qquad \text{or} \qquad \nabla_i \nabla_j V \leq -c'\frac{V}{M_{Pl}^2} \ . \tag{4.5}$$

This conjecture allows for unstable dS solution as long as the instability is strong enough. The tachyons lead to a decay of the vacuum, with a lifetime of [118]

$$T \propto -\frac{3H}{m_{\text{tachyon}}^2} \ , \tag{4.6}$$

where H is the Hubble constant and m_{tachyon} is the mass of the heaviest, i.e. most negative, tachyon. As the world we live in seems to be approximately a dS space, this conjecture seems to rule out string theory. The conjecture is in sharp contradiction with the explicit constructions of dS in string theory like for example the KKLT construction [119]. This construction has not been carried out in full detail yet despite some recent progress. But it also has not been disproven yet despite many tests and criticism. For some arguments against KKLT see [120–122], and for arguments in favor of the model see [123–125]. We will describe the model itself in more detail in the section focusing on tests of the dS conjecture.

A close cousin to the dS conjecture is the AdS scale separation conjecture. Like dS minima it is surprisingly hard to construct true 4-dimensional AdS minima [126]. The length scale of the 4-dimensional AdS space often turns out to be of the same order than the internal 6-dimensional length scale, invalidating the effective theory and making a 10-dimensional perspective necessary. A string theoretic formulation of the conjecture thus can be stated as follows. The length scale L of an AdS solution of string theory is bounded by the lightest moduli mass m, i.e.

$$m^2 L^2 \leq c'' \ , \tag{4.7}$$

where c'' is another unfixed order one constant. All the different conjectures mentioned above seem to form a tightly interrelated web. It is natural to wonder if there is a common origin to many or all of the conjectures. One possible explanation is the emergence proposal [96, 117, 127–129], stating that the IR couplings as well as gauge dynamics arise from

integrating out an infinite tower of massive states, which is required for the UV theory to be unitary. In this proposal the UV values of the couplings are assumed to be zero, such that the IR effects are emergent in the sense that they originate purely from integrating out UV states. Especially, integrating out a tower of scalar fields results in the distance conjecture [130].

As should be clear from the previous pages, there exists a large net of conjectures, many of which are interconnected. For a recent review of the swampland program see [131]. In the following we will focus on two of the conjectures, the refined swampland distance conjecture as well as the dS conjecture.

4.2 The Refined Swampland Distance Conjecture

In this section we will focus on the refined swampland distance conjecture. The section is mainly based on [2]. The conjecture states, that if one moves for a distance more than M_{Pl}, there is a tower of states which become exponentially light, i.e.

$$m(\phi_0 + \Delta\phi) = m(\phi_0)\, e^{-\lambda \frac{\Delta\phi}{M_{Pl}}} \ . \tag{4.8}$$

The constant λ should be of order 1 but is not fixed in the conjecture. This is a refinement of the original conjecture, which was formulated for infinite distances. It is important to note that $\Delta\phi$ is the proper distance measured along a geodesic curve. When the geodesic is parameterized by a coordinate τ the distance is given by

$$\Delta\phi = \int_{\tau_0}^{\tau} \mathrm{d}\tau \sqrt{g_{\alpha\overline{\beta}} \frac{\mathrm{d}x^{\alpha}}{\mathrm{d}\tau} \frac{\mathrm{d}\overline{x}^{\overline{\beta}}}{\mathrm{d}\tau}} \ , \tag{4.9}$$

where $g_{\alpha\overline{\beta}}$ is the moduli space metric which was computed in chapter 3. The curve has to be a solution to the geodesic equation, i.e. it has to fulfill

$$\frac{\mathrm{d}^2 x^{\mu}}{\mathrm{d}\tau^2} + \Gamma^{\mu}_{\alpha\beta} \frac{\mathrm{d}x^{\alpha}}{\mathrm{d}\tau} \frac{\mathrm{d}x^{\beta}}{\mathrm{d}\tau} = 0 \ , \tag{4.10}$$

where $\Gamma^{\mu}_{\alpha\beta}$ denotes the usual Christoffel symbol.

Recently it was noted in [132] that the addition of a potential can lead to non-geodesic curves. Below a cutoff, heavy directions can be integrated out, restricting the allowed paths. The possible trajectories in this low-energy effective theory are non-geodesics from the point of view of the UV theory. This can lead to larger distances compared to the case without a potential. As the conjecture should also hold in the low energy theory, this produces stronger bounds. The scalar potential depends on both, the Kähler as well as the superpotential, thus full knowledge of the periods is necessary to compute the distances. While this is a doable calculation, here we will focus on the simpler case without fluxes or respectively with vanishing superpotential. In this case one can use the GLSM partition function to compute the metric and the geodesics, simplifying the computations drastically.

But as the partition function is given by multivariate hypergeometric functions, solving the geodesic equation (4.10) analytically is still a hard task. Instead, the equations will be solved numerically.

Examples

The idea how to test the conjecture is most easily explained in a simple one-parameter example, the quintic hypersurface. The model has two phases, a LG phase as well as an LCS or geometric phase. The periods and GLSM partition function of this model have already been computed in chapter 3, see (3.98). The GLSM partition function directly gives the Kähler potential and thus the metric on moduli space. The exact form of the metric is rather long, thus we refrain from writing it down explicitly and instead only present a plot of the metric.

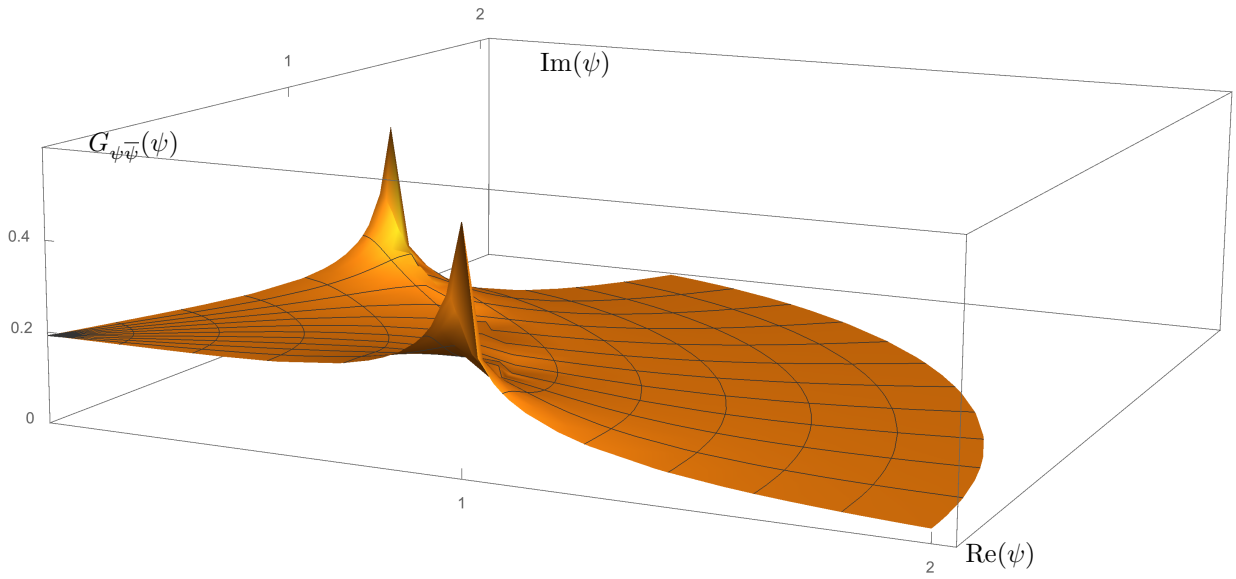

Figure 4.1: The metric on the Kähler moduli space of the quintic.

Figure 4.1 shows the only non-vanishing component of the metric, $G_{\psi\bar{\psi}}$, on the complex structure moduli space. The coordinate ψ is the coordinate appearing in the defining polynomial (3.19). This coordinate is centered around the LG point at $\psi = 0$. The model has a $\mathbb{Z}_5$ symmetry, which causes the physical coordinate to be ψ^5. Thus we restrict our attention to the fundamental domain in the form of a cone. To this end we write $\psi = re^{\phi}$. The phase ϕ is restricted to the interval $[0, \frac{2\pi}{5})$. Moreover, as can be seen from figure 4.1, the metric in the fundamental domain enjoys another $\mathbb{Z}_2$ symmetry corresponding to reflections around the axis $\phi = \frac{\pi}{5}$. The conifold is located at $\psi = 1$ and the pictures of this point under the $\mathbb{Z}_5$ symmetry, which correspond to the points $\psi = e^{\frac{2\pi i n}{5}}$, $n = 1, 2, 3, 4$. Finally, the LCS point is located at $\psi = \infty$. The mirror map relates this to the Kähler

moduli space. The cone in the complex moduli space is mapped to the region shown in figure 4.2.

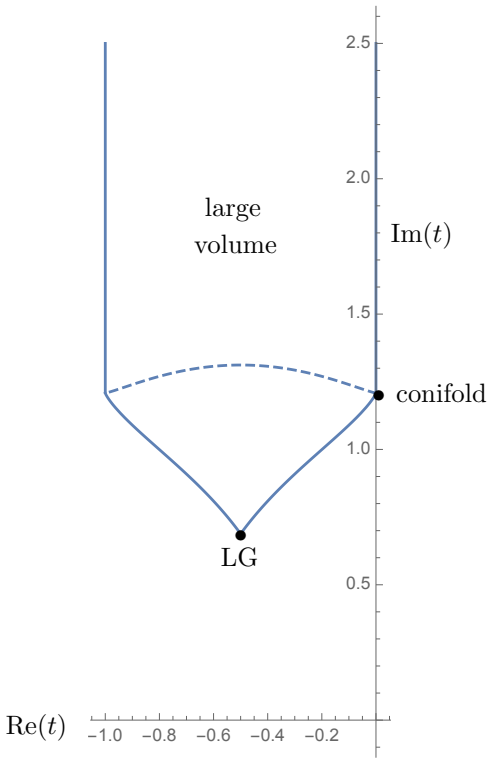

Figure 4.2: Sketch of the Kähler moduli space of the quintic.

In the Kähler coordinate t, the fundamental domain is the Teichmüller space of $SL(2,\mathbb{Z})$. The large volume point lies at $\mathrm{Im}(t) = \infty$. The LG point corresponds to

$$t = -\frac{1}{2} + \sqrt{\frac{1}{4} + \frac{1}{2\sqrt{5}}}i \approx -0.5 + 0.688i.$$

This value has an interesting consequence. As there is only a single Kähler modulus, it's imaginary part is a measure of the volume of the CY. The LG is the point deepest in the non-geometric regime, yet the volume is still non-vanishing. This does hold for all 1-parameter models, but there are known geometries which indeed reach 0 volume [133]. A simple example of this is the two parameter model $\mathbb{P}_{12366}[18]$. There the two Kähler moduli t_x and t_y are only bounded to be positive and follow the further restriction

$$t_x \geq \frac{1}{2\sqrt{3}\Gamma[1/3]^3} e^{-2\pi i t_y} \ . \tag{4.11}$$

This also shows the non-linearity of the Kähler-cone, which due to the exponential function on the right hand side is not really a cone. But as it is commonly denoted cone in the

literature we will continue to denote it as a cone. Also, the Kalb-Ramond field represented by the real part of the Kähler modulus takes the value $-\frac{1}{2}$. This appears to be a general feature of LG points. That the minimal volume can be computed analytically originates from the modular properties of the moduli spaces. The $SL(2,\mathbb{Z})$ does act naturally not on the Kähler modulus t, but on another space γ. There are remarkable similarities to the mirror map if one expresses γ via the complex structure coordinate $x = \frac{1}{\psi}$ [39]:

$$e^{2\pi i(\frac{\gamma}{2\sqrt{5+2\sqrt{5}}}-\frac{1}{2})} = x\frac{\partial_\epsilon\, {}_2F_1(\frac{2}{5}+\epsilon,\frac{3}{5}+\epsilon;1;x^5)|_{\epsilon=0}}{{}_2F_1(\frac{2}{5},\frac{3}{5};1;x^5)} \ . \tag{4.12}$$

We recall the expression for the mirror map of the quintic found in chapter 3:

$$e^{2\pi i t} = x\frac{\partial_\epsilon\, {}_4F_3(\frac{1}{5}+\epsilon,\frac{2}{5}+\epsilon,\frac{2}{5}+\epsilon,\frac{3}{5}+\epsilon;1,1,1;x^5)|_{\epsilon=0}}{{}_4F_3(\frac{1}{5},\frac{2}{5},\frac{3}{5},\frac{4}{5};1,1,1;x^5)} \ . \tag{4.13}$$

While these functions seem very related, the actual map between them is rather complicated. But it explains the omnipresent appearance of the factor $-\frac{1}{2}$ for the Kalb-Ramond field due to the shift of the modular variable γ. This shift is required by the Schwarzian triangle map and thus has to appear in the Kähler modulus at the LG point.

Returning to the distance conjecture, close to the LCS point at $\psi = \infty$ the metric behaves as [39]

$$G_{\psi\bar{\psi}} = \frac{3}{4|\psi|^2\log^2(|\psi|)} \ . \tag{4.14}$$

Applying the asymptotic mirror map, $t = \log(1/\psi)$, to this expression results in

$$G_{t\bar{t}} = \frac{3}{4|\mathrm{Im}(t)|^2} \ . \tag{4.15}$$

This expression is independent of the phase, thus geodesics are straight lines of constant phase. Thus moving a distance r away from the point at infinity corresponds to a distance

$$\Delta = \int_{r_0}^{r_1}\sqrt{G_{t\bar{t}}}dt = \int_{r_0}^{r_1}\sqrt{\frac{3}{4}}\frac{1}{t}dt = \sqrt{\frac{3}{4}}\log\left(\frac{r_1}{r_0}\right) \ . \tag{4.16}$$

This logarithmic behaviour of the proper field distance has the consequence that one can approximate the KK masses as

$$M_{KK} \propto \frac{M_{Pl}}{r^2} = M_{KK,0}e^{-\lambda\Delta} \ , \tag{4.17}$$

with $\lambda = \sqrt{\frac{3}{4}}$. Thus if the proper field distance exceeds $\lambda^{-1} \approx 1.15$ the tower of KK states becomes exponentially light and the effective theory breaks down. Note that this approximation only took the leading order of the mirror map and the prepotential into account. Including the $\zeta(3)$ correction in the prepotential, i.e. taking

$$F = -\frac{\kappa}{6}t^3 + \frac{i\chi\zeta(3)}{(2\pi)^3} \ , \tag{4.18}$$

where $\chi = -200$ is the Euler characteristic and $\kappa = 5$ is the triple intersection number. With this approximation the proper field distance becomes

$$\Delta(t) = \frac{\sqrt{3}}{2}\log(t) + \frac{\sqrt{3}\chi\zeta(3)}{5(2\pi)^3}\frac{1}{t^3} + \mathcal{O}\left(\frac{1}{t^6}\right) . \tag{4.19}$$

A more detailed analysis performed in [2] shows that the first correction in the prepotential becomes relevant roughly at the boundary to the non-geometric phase. Thus the approximation is valid throughout the whole geometric phase. But there are geodesics which do not only traverse the geometric phase, but originate deep in the non-geometric phases. The point in moduli space which is the farthest away from the LCS point is the LG point. While the theory is deformed in the non-geometric phases, there are no modes becoming exponentially light as long as the path remains in a general configuration, i.e. away from the conifold locus. This adds additional field distance without a breakdown of the theory. The requirement that the critical distance where the masses start to become exponentially light is sub-Planckian thus also requires that the distance traversed in the non-geometric phases is smaller than M_{Pl}. In the following the critical distance is split into the contributions in the geometric phase Θ_λ and the contribution from the non-geometric phases, Θ_0. For a 1-parameter model Θ_0 is simply the proper distance between the phase boundary and the LG point, i.e. the value at $|\psi| = 1$. The proper distances are in practice obtained by numerically computing the geodesics starting in the LG point. All possible geodesics starting in this point are parameterized by a single angle at which the geodesic intersects the LG point. We denote this angle by θ. The initial movement in θ is chosen to be 0 to maximize the distance the geodesics span in the fundamental domain. Due to the symmetry we can stop the numerical computation once the geodesics reaches the boundary of the fundamental domain, as there will always be a shorter geodesic to the point outside the fundamental domain. The resulting geodesics are shown in picture 4.3. Obviously they have the same $\mathbb{Z}_2$ symmetry as the metric.

Once the geodesics are computed, the metric can be integrated along them to obtain the proper field distances. From this the parameters need to be extracted. The Θ_0 is obtained by integrating to $|\Psi| = 1$. The value of λ is more difficult. Its asymptotic value is known, but not all geodesics reach very far into the geometric regime. But as the higher order corrections are irrelevant even close to the non-geometric regime, one can fit the Ansatz

$$\Delta(t) = \lambda^{-1}\log(t) + \alpha_0 + \frac{\alpha_1}{t^3} + \mathcal{O}\left(\frac{1}{t^6}\right) . \tag{4.20}$$

The parameters α_0,α_1 and λ^{-1} are determined by the fit, but are asymptotically known by comparing to (4.19). Due to the $\mathbb{Z}_2$ symmetry there are two geodesics in form of a straight line with angles $\theta = 0$ and $\theta = \frac{\pi}{5}$. The first connects the LG point to the conifold, the second is a straight line between the LCS and the LG point. As this geodesic reaches the LCS point, the values of λ^{-1} and α_1 have to be the same as in (4.19), which gives a non-trivial check of the method. The parameters obtained by the fit are listed in table 4.1. The geodesic ending in the LCS point is given by the last entry. The expected value for

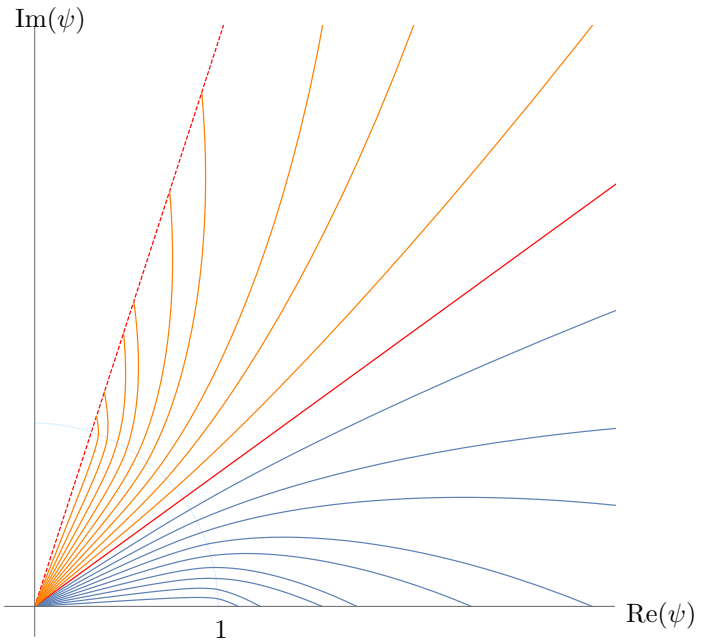

Figure 4.3: Geodesics for the initial data $(r, \dot{r}, \theta, \dot{\theta}) = (0, 1, i \cdot \pi/50, 0)$, for $i = 1, \ldots, 10$. The orange geodesics are the $\mathbb{Z}_2$ images.

λ^{-1} is $\sqrt{\frac{3}{4}} \approx 0.8660$ while the value obtained by the fit is 0.8657, which is accurate with an error of less than 1%. For the α_1 parameter related to the $\zeta(3)$ correction the expected value is 0.168, while the obtained parameter is 0.166, also within an error of 1%.

$\theta_{\text{init}} \cdot \pi/60$	α_0	α_1	λ^{-1}	Θ_0	Θ_c
3	0.1315	0.2043	0.9605	0.4262	1.3866
4	0.1127	0.2099	0.9865	0.4261	1.4125
5	0.0998	0.2213	0.9780	0.4260	1.4040
6	0.0955	0.2294	0.9567	0.4259	1.3827
7	0.0818	0.2475	0.9611	0.4259	1.3869
8	0.0877	0.2592	0.9275	0.4258	1.3533
9	0.0808	0.2825	0.9253	0.4257	1.3510
10	0.0929	0.3093	0.8969	0.4257	1.3226
11	0.0998	0.3497	0.8845	0.4257	1.3102
12	0.1234	0.1662	0.8657	0.4256	1.2914

Table 4.1: Values of the fit-parameters $\alpha_0, \alpha_1, \lambda^{-1}$, critical distance Θ_0 and combined critical distance Θ_c for the family of geodesics with initial angles $\theta_{\text{init}} = i\pi/60$, for $i = 3, \ldots, 12$. We see that Θ_0 is approximately constant for the quintic. The total critical distance varies mostly because of the angular dependence of λ.

The obtained critical values for the proper field distance Θ_c are all smaller than 1.42.

While this value is larger than 1, it is certainly of order 1. This analysis cannot only performed for the quintic, but for all other known 1-parameter models in CICYs. There are in total 14, with 4 of them being hypersurfaces in projective space. The hypersurfaces where treated all in [2], while the more exotic models where discussed in [134]. All results are in agreement with the refined swampland distance conjecture, with the largest values for Θ_c being around 1.8. It should be noted that hybrid phases were seen to have larger values for Θ_0 than the LG phases.

Going beyond 1-parameters the numerical solution to the geodesic equations becomes drastically more difficult. The difficulty lies in the boundary region between phases in multi-parameter models. The convergence close to the boundary is rather bad, thus one needs to take into account many terms in the expressions for the periods. E.g. in the quintic it is necessary to take at least a hundred terms into account to find agreement between the LCS and LG expressions at $|\psi| = 1$. As there is a separate infinite sum for each coordinate, in a n-parameter model one would need 100^n terms to reach the same precision. As this is for a single period and the Kähler metric depends on $2n + 2$ periods, the complexity of the resulting metric soon becomes intractable. Thus instead of numerically computing the metrics, the symmetry of the moduli space is again used to determine straight lines which fulfill the geodesic equations. One class correspond to the boundaries of the moduli space. In the 1-parameter models we have seen that the critical values for the geodesics did not vary much within a phase, but rather strongly between different phases. Thus knowing the boundary values should give a good approximation to the geodesics in the bulk.

Again we will present an example, the two parameter model $\mathbb{P}_{11222}[8]$. This model can be viewed as either a K3 fibration over an elliptic base or as an elliptic fiber over an K3 base. The two Kähler parameters describe the volume of the K3 and of the elliptic curve respectively. The manifold itself is constructed as the hypersurface $P = 0$ for

$$P = x_1^8 + x_2^8 + x_3^4 + x_4^4 + x_5^4 - 8\psi\, x_1x_2x_3x_4x_5 - 2\phi\, x_1^4x_2^4\,, \tag{4.21}$$

where ϕ and ψ represent the complex structure parameters around the LG point. The polynomial fails to be transversal for $\phi = 1$ and for

$$(\phi + 8\psi^4)^2 \;=\; 1\,. \tag{4.22}$$

At these loci the geometry develops conifold singularities. It is useful to introduce the logarithmic coordinates

$$\rho_1 \;=\; \frac{1}{2\pi}\,\log|4\phi^2|\,, \qquad \rho_2 \;=\; \frac{1}{2\pi}\,\log\left|\frac{2^{11}\,\psi^4}{\phi}\right|\,. \tag{4.23}$$

These coordinates are related to the GLSM coordinates and make the "amoeba" structure of the conifold nicely visible. Figure 4.4 shows the moduli space in terms of the ρ_i coordinates. Note that due to the absolute values these coordinates only represent a two dimensional slice of the moduli space. The conifold is still of complex codimension 1 such that it is possible to go around the conifold and traverse several patches.

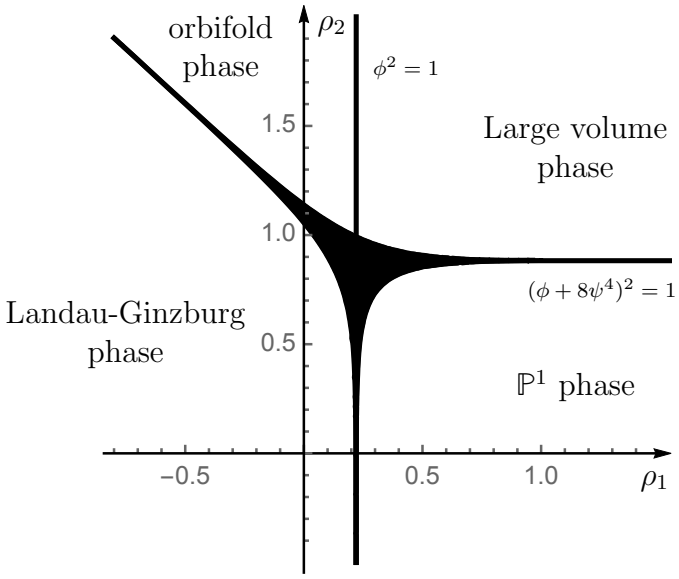

Figure 4.4: The moduli space of $\mathbb{P}_{11222}[8]$. Figure taken from [1].

The model consists of in total 4 phases. The LG and LCS phase as well as 2 hybrid phases. The two hybrid phases consist out of a K3 orbifold, denoted simply orbifold phase in figure 4.4 and a LG theory fibered over a $\mathbb{P}^1$, denoted $\mathbb{P}^1$ phase. The geometric target space is real 6-dimensional in the geometric or large volume phase as well as in the orbifold phase, 2-dimensional in the $\mathbb{P}^1$ phase and 0-dimensional (a point) in the LG phase. But due to quantum fluctuations, the effective dimension is in all cases real 6-dimensional. These contributions are called non-geometric. There are various differing nomenclatures for the phases and their classifications. In this theses all phases which are not a LCS or respectively on the Kähler side a large volume phase will be denoted non-geometric phases. The orbifold and $\mathbb{P}^1$ phase will be denoted hybrid phases, as they correspond to a large value of complex structure for one parameter while the other remains small. Other authors, e.g. the authors of [62] denote orbifold phases as pseudo-hybrid phases and only phases like the $\mathbb{P}^1$ phase as true hybrid phases. There are actual differences appearing in the evaluation of the GLSM partition functions, but from a period point of view there is no difference between a hybrid and a pseudo-hybrid phase.

The methods developed in chapter 3 are fully applicable to this model. As an elliptic curve shrinks to zero size at the $\phi = 1$ conifold, it is possible to analytically determine the transition matrix to this conifold. The symplectic periods obtained this way agree with the periods of $\mathbb{P}^5_{111111}[2\ 4]$, a 1-parameter CICY. This is an example of a conifold transition, where the conifold locus of one CY correspond to the moduli space of another CY.

The Kähler potential is given by the partition function of the corresponding GLSM. The partition function of $\mathbb{P}_{11222}[8]$ is given in equation (3.105) and was evaluated in detail in chapter 3. The GLSM partition functions converges deep in the phases, but the convergence becomes worse at the phase boundaries. For the computation of the distances this does

not pose a problem, but for the computations of the geodesic it is a severe problem, as the resulting metric is not exactly continuous at the boundary where the two phases are glued due to numerical errors. Thus instead of computing the geodesics 9 curves γ_i, $i = 1 \dots 9$, are defined and their lengths computed. The curves along the boundary are actual geodesics, while the curves inside the bulk of the moduli space are not. The curves are shown in figure 4.5, while the exact data is shown in table 4.2.

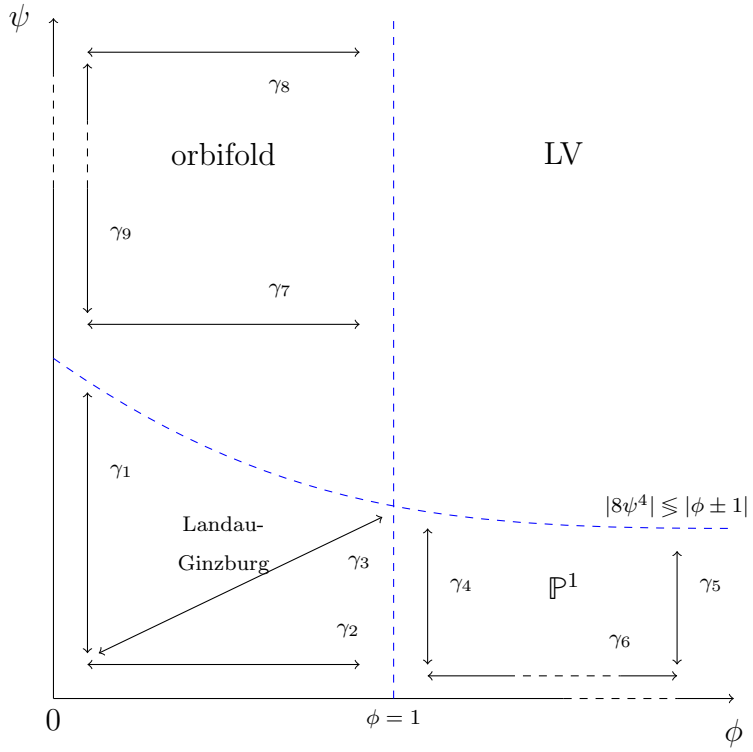

Figure 4.5: Definitions of curves in the moduli space of $\mathbb{P}_{11222}$. The dotted blue lines represent a sketch of the phase boundaries. Adapted from [2].

All finite values of Θ_0 are smaller than 1, in agreement with the refined swampland distance conjecture. There are some interesting observations which can be made form this data. First of, the length of γ_8 is actually 0. This implies that for $\psi = \infty$ the points $\phi = 0$ and $\phi = 1$ are actually the same point. The usually drawn figures of the moduli space are thus misleading when it comes to true distances. Furthermore, there are 2 different infinite distance limits in terms of γ_6 and γ_9. These correspond to large volumes of the elliptic fiber and the K3 respectively. for these the proper distances scale as

$$\Delta\Theta_{\gamma_6} \propto \log\log(\phi) \propto \log(\mathrm{Im}(t_2)) \,, \tag{4.24}$$

$$\Delta\Theta_{\gamma_9} \propto \log\log(\psi) \propto \log(\mathrm{Im}(t_1)) \,. \tag{4.25}$$

Thus these infinite distance limits are exactly as expected from the distance conjecture. The exact proportionality constant depends only on the dimension of the space approaching

i	start	end	Θ_0
1	(0,0)	(0,0.59)	0.40
2	(0,0)	(1,0)	0.24
3	(0,0)	(0.5,0.5)	0.36
4	(1.1,0)	(1.1,0.33)	0.24
5	(0,∞)	(∞,∞)	0.46
6	(0,1)	(0,∞)	∞
7	(0,0.59)	(1,0.59)	0.21
8	(∞,0)	(∞,1)	0
9	(0,0.59)	(0,∞)	∞

Table 4.2: Starting and end points of 9 curves in the moduli space of $\mathbb{P}_{11222}[8]$. The coordinates are given as (ϕ, ψ).

large volume. To see this the asymptotic form of the Kähler potential in the hybrid phases for either $\phi \to \infty$ or $\psi \to \infty$ are computed. These take the form

$$K^{\text{asymp}}_{\mathbb{P}^1} \simeq -\log(t_2 - \bar{t}_2)\,, \tag{4.26}$$

as well as

$$K^{\text{asymp}}_{\text{orbi}} \simeq -3\,\log(t_1 - \bar{t}_1)\,. \tag{4.27}$$

For a d-dimensional space with 1-parameter, one expects an asymptotical Kähler potential of the form

$$K^{\text{asymp}}_{\text{d-dimensional}} \simeq -d\,\log(t - \bar{t})\,. \tag{4.28}$$

This shows nicely that the $\mathbb{P}^1$ phase is a complex 1-dimensional phase, while the orbifold is indeed a 3-dimensional phase. The metric resulting form the d-dimensionl Kähler potential is given by

$$g_{i\bar{j}} = \frac{d}{4\text{Im(t)}^2}\,. \tag{4.29}$$

From this one immediately obtains the constant λ as

$$\lambda = \frac{2}{\sqrt{d}}\,. \tag{4.30}$$

As the critical distance depends on $\Theta_\lambda = \lambda^{-1} = \frac{\sqrt{d}}{2}$, this immediately shows that for all 1-parameter geometric phases the distance conjecture holds. For a CY 4-fold the constant even becomes 1. This also shows an interesting way to violate the distance conjecture: If a supercritical string theory in $d > 12$ dimensions is compactified on a CY $(d\text{-}4)/2$-fold, Θ_λ becomes larger than 1 and is in principle unbounded. Of course such theories include

tachyons and are therefore unstable. What about the multi parameter models? The Kähler potential has the general form

$$K^{\text{asymp}}_{\text{d-dimensional}} \simeq -d \log\left(\frac{\kappa_{ijk}}{6}(t_i-\bar{t}_i)(t_j-\bar{t}_j)(t_k-\bar{t}_k)\right) . \tag{4.31}$$

Interestingly, if one approaches the large volume point at different angles, i.e in a curve

$$t_i(\tau) = a_i \cdot \tau \qquad i = 1 \dots h^{1,1} , \tag{4.32}$$

for constant a_i, the integrand in the proper distance only depends on the dimension, i.e.

$$\sqrt{g_{\alpha\bar{\beta}}\frac{\mathrm{d}x^\alpha}{\mathrm{d}\tau}\frac{\mathrm{d}\overline{x}^{\bar{\beta}}}{\mathrm{d}\tau}} = \frac{\sqrt{d}}{2\,\tau} . \tag{4.33}$$

Especially it is independent of the chosen values of a_i and of the triple intersection numbers. This holds as long as the corrections remain irrelevant, i.e. the $\zeta(3)$ term as wells as the terms linear in t_i can be ignored relative to the cubic terms. While this result can be obtained directly from the form of the asymptotic Kähler potential, it is also possible to apply the nilpotent orbit theorem to arrive at the same conclusion. The theorem states that the period vector can be written as [135]

$$\Pi = e^{tN} A(t) , \tag{4.34}$$

where A is a holomorphic vector and N is the logarithm of the monodromy matrix T which shifts the Kähler moduli by 1, i.e. $Tt_i = t_i + 1$:

$$N = \log T . \tag{4.35}$$

As the vector A is holomorphic it can be expanded in the coordinates, i.e.

$$A = a_0 + \sum_{n=1}^{\infty} a_n z^n . \tag{4.36}$$

For many applications the leading term a_0 independent of the moduli is sufficient. Especially exactly at the LCS point the periods are given by

$$\Pi = e^{tN} a_0 . \tag{4.37}$$

The integer d is now defined as the smallest integer for which

$$N^d a_0 \neq 0 . \tag{4.38}$$

For the point of maximal unipotent monodromy, i.e. the LCS point, d is equal to the dimension of the CY and one directly obtains (4.33). The power of the nilpotent orbit theorem now lies in the fact that it does not only hold at the LCS point but at any boundary of the moduli space. d in these cases is equal to the dimension of the cycle which is still at largest volume. As an example, at the LG point $d = 0$, while for the $\mathbb{P}^1$ phase of $\mathbb{P}_{11222}[8]$ $d = 1$. The resulting critical distances are in agreement with what has been found in the example.

Outlook

This finishes the discussion of the (refined) swampland distance conjecture. While the conjecture still remains unproven, it passed all tests in string theory setups so far. Recently, it was pointed out [132] that the distance conjecture should not only hold in the full theory, but also in effective theories below a certain cutoff. The allowed trajectories in the low energy effective actions are geodesics in the effective theory. But in the full theory they are non-geodesic curves. This allows for further tests of the distance conjecture in these effective theories. In the case of type IIB compactifications on CY manifolds, this implies that the conjecture should also hold in presence of fluxes which stabilize a subset of the moduli. The fluxes induce a superpotential and break the $\mathcal{N} = 2$ supersymmetry, thus for these computations knowledge of the periods is necessary. The methods developed in chapter 3, excluding the GLSM approach, are applicable to such a situation. How the length of the trajectories and the non-geodesity depends on the chosen fluxes will be studied in a forthcoming paper [136].

Chapter 5

KKLT and the dS Conjecture

After discussing the distance conjecture, we will now turn to another swampland conjecture, the dS conjecture. This conjecture forbids the existence of stable dS vacua in quantum gravity. In contrast to the previous conjecture, which is generally expected to be true, the dS conjecture has been discussed controversially. The main reason for this is the existence of explicit constructions of dS spaces in string theory, most famously the construction by Kachru, Kallosh, Linde and Trivedi (KKLT) [119]. The construction is obviously in sharp contradiction to the conjecture. Thus either the conjecture or the construction is wrong. As the construction involves non-perturbative effects, this has not been settled yet. In this chapter we will first describe the construction followed by a detailed look at some of the involved steps, especially the existence of exponentially small superpotentials as well as the consistency of the approximations made in warped throats.

5.1 The KKLT Construction

One of the most famous constructions of dS minima in string theory is the KKLT construction. It consists out of a three step procedure:

1. Stabilize the axio-dilaton and the complex structure moduli using three-form fluxes.
2. Stabilize the Kähler moduli balancing non-perturbative effects against an exponentially small superpotential W_0
3. Uplift the resulting AdS vacuum to dS using an anti D3-brane localized in a warped throat.

In the first step one considers a CY compactification with F and H flux. These do not couple to the Kähler moduli, thus the resulting scalar potential is of the so-called no-scale type, i.e.

$$V = e^K G^{i,\bar{j}} W_i W_{\bar{j}} \,. \tag{5.1}$$

The $-3|W|^2$ term of the general scalar potential was canceled against the Kähler part of the derivatives, i.e. the indices i and j run only over the complex structure and axio-dilaton.

The W_i denote the Kähler covariant derivatives of the superpotential, i.e.

$$W_i = \partial_i W + (\partial_i K) W \ . \tag{5.2}$$

Due to the positive definiteness of the metric there is a Minkowski minimum at $V = 0$. Thus solving $W_i = 0$ results in a supersymmetric Minkowski minimum. The value of the superpotential in this minimum is denoted W_0. In the next step it is assumed that this value is exponentially small, such that it can be balanced against the contribution of Euclidean brane-instantons, such that the superpotential, after integrating out the complex structure moduli and the axio-dilaton, becomes

$$W = W_0 + A\, e^{-aT} \ . \tag{5.3}$$

Here T is a Kähler modulus, A is the Pfaffian and a a constant. The Pfaffian depends on the complex structure moduli. They are rather difficult to compute, in known examples they turn out to be polynomials [137–139] originating from Euclidean D-branes or exponential functions from NS 5-branes [140]. The constant a depends on the origin of the non-perturbative correction. It can be related to the Gromov-Witten invariants of the space in the case of instanton contributions or to the rank of the condensing gauge group in the case of a gaugino condensate.

Note that the existence of such minima with small superpotentials is a priori an assumption. For quite some time there was only a statistical argument that such vacua should exist [141]. More recently, based on an idea of [142, 143], they have been explicitly constructed close to the LCS point [144]. But the existence of a warped throat is required for the uplift in the next step. The geometry develops such throats close to a conifold singularity in moduli space. The algorithm of [144] was generalized to the region close to a conifold in [46, 145].

The minimum obtained after the second step is an AdS minimum with all moduli stabilized. The final third step is to uplift this minimum to dS by adding an anti-D3-brane in a warped throat. This contributes the missing energy to reach dS, but represents a non-perturbative contribution which is not completely understood. Thus this step has received much attention in testing the validity of the construction. Moreover, the existence of the warped throat could lead to light KK modes localized in the throat, invalidating the effective theory as these have been integrated out.

All steps of the above construction have been criticized and tested in many instances with varying conclusions. For example it was questioned whether the 4D AdS minimum is really a solution to the full 10 dimensional string theory [121, 123, 146–153]. Another question is whether the effective action describing the warped regime is valid [154–159]. In the next sections we will take a closer look at two of the assumptions, the existence of small superpotentials and the validity of the effective action in the presence of a warped throat.

5.2 Small Superpotentials in the Quintic

Th first step of the construction requires an AdS vacuum with exponentially small superpotential close to a conifold. We will start the discussion with the method of DKMM [144], which constructs exponentially small superpotentials at the LCS point. Then we will extend this construction to the conifold, following [46, 145].

The authors of [144] propose a two-step procedure to generate exponentially small W_0 terms at weak string coupling and large complex structure. When using mirror variables, the prepotential splits into classical and non-perturbative terms. Initially neglecting the non-perturbative terms, the first step is to find quantized fluxes for which the F-terms and superpotential vanish perturbatively. DKMM formulate a Lemma which gives a sufficient condition to construct such solutions and directly determine the flat direction. In the second step, the previously neglected non-perturbative terms generate a potential along the flat direction which can generically be stabilized to an exponentially small value by a racetrack-like procedure.

The Kähler- and superpotential are as given in (2.130) and (2.127), i.e.

$$\begin{aligned} K &= -\log\left(-i\,\overline{\Pi}\cdot\Sigma\cdot\Pi\right) - \log\left(S+\bar{S}\right)\,, \\ W &= (F+iSH)^T\cdot\Sigma\cdot\Pi\,. \end{aligned} \tag{5.4}$$

When written in terms of the mirror variables, the tree-level prepotential $\mathcal{F}$ can be separated into a classical, perturbative part $\mathcal{F}_{\text{pert}}$ and non-perturbative instanton contributions[1] $\mathcal{F}_{\text{inst}}$, such that $\mathcal{F}(U) = \mathcal{F}_{\text{pert}}(U) + \mathcal{F}_{\text{inst}}(U)$ with

$$\begin{aligned} \mathcal{F}_{\text{pert}}(U) &= -\frac{1}{3!}K_{abc}U^aU^bU^c + \frac{1}{2}a_{ab}U^aU^b + b_aU^a + \xi\,, \\ \mathcal{F}_{\text{inst}}(U) &= \frac{1}{(2\pi i)^3}\sum_{\vec{q}} A_{\vec{q}}\, e^{2\pi i\,\vec{q}\cdot\vec{U}}\,. \end{aligned} \tag{5.5}$$

We denote the moduli here with U, the expressions refer to the mirror CY, so K_{abc} are the triple intersection numbers of the mirror, and the sum runs over effective curves in the mirror. The constants a_{ab}, b_a are rational numbers, and $\xi = -\frac{\zeta(3)\chi}{2(2\pi i)^3}$ with the Euler number χ of the CY. The contributions to the superpotential stemming from $\mathcal{F}_{\text{pert}}$ and $\mathcal{F}_{\text{inst}}$ are respectively denoted W_{pert} and W_{inst}, such that $W = W_{\text{pert}} + W_{\text{inst}}$.

Since the axionic real parts of $\vec{U}$ do not appear in the perturbative Kähler potential, they enjoy a discrete $\mathbb{Z}^n$ shift symmetry which is broken by generic fluxes. The shift symmetry generates a monodromy transformation on the flux vectors, and only if such a monodromy combined with an appropriate $SL(2,\mathbb{Z})$ transformation $(H,F)\to(H,F+rH)$, $r\in\mathbb{Z}$ leaves the flux vectors invariant there can be an unbroken remaining shift symmetry.

The first step in the construction is to find fluxes that do not break the shift symmetry and obey the tadpole cancellation constraint and solve $W_i = 0$ as well as $W_{\text{pert}} = 0$. The

[1] It is important to notice that the "non-perturbative" part in the mirror variables is part of the classical contribution to the type IIB theory.

following is a sufficient condition for the existence of such a perturbatively flat vacuum. If a pair of $\mathbb{Z}^n$ vectors $\vec{M}$, $\vec{K}$ exists such that

- $-\frac{1}{2}\vec{M}\cdot\vec{K} \leq Q_{\mathrm{D3}}$,
- $N_{ab} = \mathcal{K}_{abc}\, M^c$ is invertible,
- $\vec{K}^T N^{-1}\vec{K} = 0$,
- $\vec{p} = N^{-1}\vec{K}$ lies in the Kähler cone of the mirror CY,
- and $a\cdot\vec{M}$ and $\vec{b}\cdot\vec{M}$ are integer-valued,

then the fluxes

$$F = \begin{pmatrix} \vec{b}\cdot\vec{M} \\ a\cdot\vec{M} \\ 0 \\ \vec{M} \end{pmatrix} \qquad \text{and} \qquad H = \begin{pmatrix} 0 \\ \vec{K} \\ 0 \\ 0 \end{pmatrix} . \tag{5.6}$$

are compatible with the Q_{D3} tadpole bound, and the potential is perturbatively flat along $\vec{U} = \vec{p}\,S$ with $W_{\mathrm{pert}}|_{\vec{U}} = 0$. I.e. these combinations stabilize all but one complex structure modulus.

The non-perturbative contributions can now stabilize the remaining flat direction. The effective superpotential along $\vec{U}$ in terms of the axio-dilaton S is given at weak coupling by

$$\frac{W_{\mathrm{eff}}(S)}{\sqrt{2/\pi}} = M^a\partial_a\mathcal{F}_{\mathrm{inst}} = \sum_{\vec{q}} \frac{A_{\vec{q}}\vec{M}\cdot\vec{q}}{(2\pi i)^2} e^{2\pi i\vec{p}\cdot\vec{q}\,S} . \tag{5.7}$$

The final idea is to find flux quanta that stabilize S via a race-track scenario, balancing the two most relevant instantons $\vec{q}_1$, $\vec{q}_2$ against each other. This is achieved when $\vec{p}\cdot\vec{q}_1 \approx \vec{p}\cdot\vec{q}_2$.

The conditions indicate that $h^{2,1} \geq 2$ is necessary in order to apply this mechanism. For a one-parameter model, the vectors and matrices are just numbers and $K^2N^{-1} = 0$ means $K = 0$. But then the perturbative vacuum found by the mechanism is $U = N^{-1}K\,S = 0$ which is both outside the LCS regime of validity and has no flat direction along which the non-perturbative terms could generate a small $|W_0|$.

For a complete stabilization of all moduli, the hope is to continue with a KKLT-like procedure starting with this small W_0. Unfortunately it is not quite so straightforward, as examples show that the perturbatively flat direction produces a mass scale of order $|W_0|$, which coincides with the mass scale of the Kähler moduli in the KKLT scenario. The low energy theory must contain not only the Kähler moduli, but also the axio-dilaton, and the Pfaffian prefactors which appear in the non-perturbative superpotential cannot be treated as a constant. DKMM argue that under some assumptions, the unbroken shift symmetry of the perturbatively flat vacuum would guarantee that the contributions of the axio-dilaton to the Pfaffian factors are exponentially small. Then one could reasonably approximate the Pfaffians by constants. To show this explicitly is however left open, and will also not be treated here.

5.3 Small Superpotentials Close to a Conifold

For really getting the uplifted dS minimum in the last step of KKLT, a strongly warped throat is required. Thus, one needs a similar construction in the region close to a conifold point. This is not straightforward, as the periods take a completely different form when expanded around such a point.

To demonstrate this, we will again take the quintic as our main example. Close to the conifold point the period vector $\Pi^T = (X^0, X^1, F_0, F_1)$ can be expressed as [48, 53, 160–162]

$$\Pi = X^0 \begin{pmatrix} 1 \\ Z \\ A + BZ + O(Z^2) \\ -\frac{1}{2\pi i} Z \log Z + C + DZ + O(Z^2) \end{pmatrix}, \tag{5.8}$$

where $Z = 1 - \psi$ is the conifold modulus and with parameters

$$\begin{aligned} A &= (-0.103412 + 0.090045i)\,, \qquad D = -(0.043170 - 0.039843i)\,, \\ B &= C = (0.074533 + 0.085597i)\,, \end{aligned} \tag{5.9}$$

that are only known numerically[2]. Note that these are in general irrational numbers though featuring certain correlations and rationality properties. The relation $B = C$ is a consequence of the existence of a prepotential for these periods, which reads

$$\mathcal{F} = -\frac{1}{4\pi i} Z^2 \log Z + \frac{A}{2} + BZ + \left(\frac{D}{2} + \frac{1}{8\pi i}\right) Z^2 + O(Z^3)\,. \tag{5.10}$$

Further relations follow from the modularity properties. As the transition matrix is the only source for non-rationalities and the entries of the transition matrix can be expressed in terms of 2 quasi-periods of the quintic, at most 2 of A,B,C and D are independent. The corresponding Kähler potential for the complex structure modulus is given by

$$\begin{aligned} K_{\text{cs}} &= -\log\left[-i\overline{\Pi}\Sigma\,\Pi\right] \\ &= -\log\left[\frac{1}{2\pi}|Z|^2\,\log(|Z|^2) + 2\text{Im}(A) + 2\text{Im}(B)(Z + \overline{Z}) + \cdots\right]. \end{aligned} \tag{5.11}$$

This will be the leading order Kähler potential in the volume-dominated regime, i.e. for $\mathcal{V}|Z|^2 \gg 1$. Including also the overall Kähler modulus $\mathcal{V}$ and the axio-dilaton S, the total unwarped Kähler potential becomes

$$\begin{aligned} K_{\text{unwarp}} = -2\log(\mathcal{V}) - \log(S + \overline{S}) - \log(2\text{Im}(A)) - \frac{\text{Im}(B)}{\text{Im}(A)}(Z + \overline{Z}) \\ - \frac{1}{4\pi\text{Im}(A)}|Z|^2\,\log(|Z|^2) + \cdots\,. \end{aligned} \tag{5.12}$$

[2]There are known expressions for the transition matrix of all hypergeometric 1-parameter models in terms of L-values/quasiperiods of Hecke eigenforms of $\Gamma_0(N)$ [163].

For the strongly warped, throat-dominated regime $\mathcal{V}|Z|^2 \ll 1$, the effective action was derived in [154–156]. Here the warping backreacts non-trivially so that the Kähler potential takes the different form

$$K_{\text{warp}} = -2\log(\mathcal{V}) - \log(S+\overline{S}) + \xi\left(\frac{|Z|}{\mathcal{V}}\right)^{\frac{2}{3}}\,, \tag{5.13}$$

with $\xi = c'M^2$, c' an order one parameter and M denoting the F_3 flux along the conifold A-cycle. This Kähler potential features a warped no-scale structure

$$\sum_{I,\overline{J}} G^{I\overline{J}}\partial_I K \partial_{\overline{J}} K = 3 - (N-1)\frac{\xi|Z|^{\frac{2}{3}}}{\mathcal{V}^{\frac{2N}{3}}} + O(\xi^2)\,, \tag{5.14}$$

where the sum runs over the set $I, J \in \{T, Z\}$. Thus, precisely for the Kähler potential (5.13) the order $O(\xi)$ term vanishes.

Moduli stabilization

A general flux induced superpotential

$$\begin{aligned} W &= \int_{\mathcal{M}} \big(F + iS\,H\big)\wedge\Omega_3 \\ &= (X^\Lambda f_\Lambda - F_\Lambda \tilde{f}^\Lambda) + iS(X^\Lambda h_\Lambda - F_\Lambda \tilde{h}^\Lambda) \end{aligned} \tag{5.15}$$

leading to the stabilization of the conifold modulus at exponentially small values can be expanded as

$$\begin{aligned} W &= -\frac{M}{2\pi i} Z\log Z + \sum_{n=0}^{\infty} M_n Z^n + iS\sum_{n=0}^{\infty} K_n Z^n \\ &= -\frac{M}{2\pi i} Z\log Z + M_0 + M_1 Z + iK_0 S + iK_1 SZ + \mathcal{O}(Z^2)\,, \end{aligned} \tag{5.16}$$

with

$$\begin{aligned} &M = -\tilde{f}^1\,, \quad M_0 = f_0 - A\tilde{f}^0 - C\tilde{f}^1\,, \quad M_1 = f_1 - B\tilde{f}^0 - D\tilde{f}^1\,, \\ &K_0 = h_0 - A\tilde{h}^0\,, \quad K_1 = h_1 - B\tilde{h}^0\,. \end{aligned} \tag{5.17}$$

Here we have chosen $\tilde{h}^1 = 0$ in order to avoid $(SZ\log Z)$-terms. Note that while the quantized fluxes are integers, the coefficients M_n and K_n are in general complex numbers.

Next we have to solve the minimum conditions $D_Z W = D_S W = 0$. Using the Kähler potential (5.12), one finds for the volume-dominated case

$$\begin{aligned} D_Z W &= \partial_Z W + \partial_Z K\, W \\ &= -\frac{M}{2\pi i}\log Z - \frac{M}{2\pi i} + M_1 + iK_1 S - \frac{\mathrm{Im}(B)}{\mathrm{Im}(A)}\big(M_0 + iK_0 S\big) + \cdots\,. \end{aligned} \tag{5.18}$$

As shown in [156], in the warped, throat-dominated case, the warped no-scale structure (5.14) implies that the minimum of the scalar potential is at $\partial_Z W \approx 0$. This gives the same result as in (5.18) once we formally set $\mathrm{Im}(B) = 0$.

Solving (5.18), in both cases at leading order the Z modulus can be written as

$$Z_0 = \zeta_0 \exp\left(-\frac{2\pi \hat{K}_1}{M} S_0\right), \qquad \zeta_0 = \exp\left(2\pi i \frac{\hat{M}_1}{M}\right), \tag{5.19}$$

with parameters

$$\hat{K}_1 = \begin{cases} K_1 - \frac{\mathrm{Im}(B)}{\mathrm{Im}(A)} K_0 & \text{volume-dominated} \\ K_1 & \text{throat-dominated} \end{cases} \tag{5.20}$$

and

$$\hat{M}_1 = \begin{cases} M_1 - \frac{M}{2\pi i} - \frac{\mathrm{Im}(B)}{\mathrm{Im}(A)} M_0 & \text{volume-dominated} \\ M_1 - \frac{M}{2\pi i} & \text{throat-dominated}\,. \end{cases} \tag{5.21}$$

For $\hat{K}_1 > M$ and $\mathrm{Re}(S) > 1$ the value of the conifold modulus can be guaranteed to be exponentially small, hence making our expansion in orders of Z self-consistent.

Looking at the axio-dilaton condition $D_S W = 0$, at leading order we find

$$\begin{aligned} 0 = {} & i K_0 + i K_1 Z \\ & - \frac{1}{S + \overline{S}} \left(M_0 + i K_0 S + \frac{M}{2\pi i} Z + \frac{\mathrm{Im}(B)}{\mathrm{Im}(A)} \big(M_0 + K_0 S\big) Z \right), \end{aligned} \tag{5.22}$$

where $D_Z W = 0$ was invoked. As in [162], for the stabilization of the axio-dilaton we now distinguish the two cases, $K_0 \neq 0$ and $K_0 = 0$.

Case A: $K_0 \neq 0$

In this case, the terms linear in Z in (5.22) can be neglected so that one gets the simple solution

$$\overline{S}_0 = -i \frac{M_0}{K_0}\,. \tag{5.23}$$

For $\mathrm{Re}(S) \gg 1$ we need to require

$$1 \ll \mathrm{Im}(M_0/K_0) = \frac{M_0 \overline{K}_0 - \overline{M}_0 K_0}{2i\,|K_0|^2}. \tag{5.24}$$

For the resulting value of the superpotential in the minimum one obtains

$$W_0 = \underbrace{\frac{M_0 \overline{K}_0 - \overline{M}_0 K_0}{\overline{K}_0}}_{w_0} + O(Z_0)\,. \tag{5.25}$$

Thus, in order to have an exponentially small value of the superpotential in the minimum, the leading order term w_0 in (5.25) must vanish or at least be very tiny. Thinking of M_0 and K_0 as two-dimensional vectors, the superpotential w_0 vanishes if M_0 and K_0 are collinear. Since M_0 and K_0 generically contain model dependent complex valued parameters, solving this condition for the fluxes becomes a number theoretic question.

Let us analyze this in more detail using the concrete values for the (mirror of the) quintic. First one realizes that due to (5.24) $w_0 = 0$ implies $\mathrm{Re}(S) = 0$ which means the string coupling is infinitely large and thus outside the regime of validity. Moreover, using $w_0 = 2i\mathrm{Re}(S)K_0$ and $\mathrm{Re}(S) > 1$ one can derive the lower bound

$$|w_0| > 2|K_0| = 2|h_0 - A\tilde{h}^0| > 2|\mathrm{Im}(A)| = 0.18\,, \tag{5.26}$$

where we used that due to $K_0 \neq 0$ not both h_0 and $\tilde{h}^0$ are allowed to vanish. Thus, at least for the specific case of the quintic, in Case A the superpotential in the minimum is bounded from below by $|w_0| > O(10^{-1})$.

Case B: $K_0 = 0$

This means that we have $h_0 = \tilde{h}^0 = 0$ so that $\hat{K}_1 = K_1 = h_1$ and $M = -\tilde{f}^1$ are both integers. Now, up to order $O(Z)$ the condition (5.22) reads

$$iK_1 Z - \frac{1}{S+\overline{S}}\left(M_0 + \frac{M}{2\pi i}Z\right) = 0\,, \tag{5.27}$$

where Z is related to S as $Z = \zeta_0 \exp(-\frac{2\pi K_1}{M}S)$. We observe that (5.27) is nothing else than the vanishing F-term condition $F_S = 0$ for an effective superpotential

$$W_{\text{eff}} = M_0 + \frac{M}{2\pi i}\zeta_0\, e^{-\frac{2\pi K_1}{M}S}\,. \tag{5.28}$$

This is very reminiscent of the KKLT superpotential, where here we are dealing with a no-scale potential. Writing $S = s + ic$ one obtains for the C_0 axion

$$c = -\frac{M}{2\pi K_1}\arg\left(\frac{M_0}{i\zeta_0}\right) \tag{5.29}$$

and the dilaton is given by the solution of the transcendental equation

$$\left|\frac{M_0}{\zeta_0}\right| = \left(2K_1 s + \tfrac{M}{2\pi}\right)e^{-\frac{2\pi K_1}{M}s}\,. \tag{5.30}$$

As in KKLT this only admits a solution in the controllable regime if the left hand side is very tiny, $M_0 \ll 1$. Whether the flux landscape admits such values is a model dependent number theoretic question. Let us recall the parameters

$$M_0 = f_0 - A\tilde{f}^0 - C\tilde{f}^1\,, \quad M_1 = f_1 - B\tilde{f}^0 - D\tilde{f}^1\,, \quad M = -\tilde{f}^1\,, \tag{5.31}$$

which are in general complex valued. One can easily convince oneself that for the quintic there exist choices of the fluxes that yield $M_0 = O(10^{-4})$, as for instance

$$f_0 = 14\,, \qquad \tilde{f}^0 = 77\,, \qquad \tilde{f}^1 = -81\,. \tag{5.32}$$

This gives $M_0 \approx -(1+i)\cdot 10^{-4}$, $M_1 \approx -3.2 - 3.4i$ and $M = 81$. Moreover, one gets $\zeta_0 \approx 0.46 - 0.12i$. For this choice the solution to (5.29) and (5.30) is

$$c_0 \approx -\frac{33.9}{K_1}\,, \qquad s_0 \approx \frac{180.4}{K_1}\,, \tag{5.33}$$

which for small enough K_1 is in a perturbative regime. For the value of the conifold modulus we find $|Z_0| \sim 4\cdot 10^{-7}$ and the value of the superpotential in the minimum is of the order of M_0 namely

$$|W_0| \sim |M_0| \approx 1.4\cdot 10^{-4}\,. \tag{5.34}$$

Therefore, the Case B provides a controlled KKLT-like stabilization of the complex structure and axio-dilaton moduli giving for the quintic a Minkowski minimum of the no-scale scalar potential with a small value of $|W_0|$. This value was dialed by a suitable choice of flux quantum numbers. In our case these were of the order $O(10^2)$ and so that there is the concern of overshooting in some tadpole cancellation conditions. In the example, there will be a contribution to the D3-brane tadpole $Q_{\rm D3} = h_1\tilde{f}^1 = -K_1 M = O(10^2)$.

Moduli masses

The latter result is encouraging for extending the model à la KKLT by adding a non-perturbative contribution to the superpotential that depends on the Kähler modulus T. Recall that in the DKMM construction the issue arises that the mass of the lightest complex structure modulus is of the same order as the mass of the Kähler modulus, calling for a more detailed analysis. Let us see how the situation is in the conifold regime.

For estimating the masses, we compute the Hessian $V_{ab} = \partial_a\partial_b V$ in the minimum, which for a no-scale model simplifies considerably. Since $F_I = 0$ in the minimum, the only non-vanishing contributions can come from

$$\partial_a\partial_b V = e^K \left(K^{I\overline{J}} (\partial_a D_I W)(\partial_b D_{\overline{J}}\overline{W}) + (a \leftrightarrow b) \right)\,. \tag{5.35}$$

The masses in the canonically normalized field basis are the eigenvalues of the matrix $K^{ac}V_{cb}$, where K^{ac} denotes the inverse Kähler metric.

In the volume-dominated regime, we find for the mass eigenvalues the following scaling[3] with $\mathcal{V}$ and $|Z|$

$$m_Z^2 \sim \frac{M_{\rm pl}^2}{\mathcal{V}^2|Z|^2} \sim \frac{M_{\rm s}^2}{\mathcal{V}|Z|^2}\,, \qquad m_S^2 \sim \frac{M_{\rm pl}^2}{\mathcal{V}^2}\,. \tag{5.36}$$

[3]In the more precise relations also factors of the dilaton and the fluxes appear, but they do not change our conclusion.

In Case B we also have the relation $|Z| \sim M_0/s$. The expression for the mass m_Z makes it evident that the expressions in this regime can only be valid for $\mathcal{V}|Z|^2 \gg 1$, because otherwise the mass of the conifold modulus would come out larger than the string scale. Moreover, one always finds the hierarchy $m_Z \gg m_S$. Extending this model to KKLT by also including a non-perturbative contribution $A\exp(-aT)$ depending on the overall Kähler modulus, the mass of the latter scales as

$$m_\tau^2 \sim \frac{|W_0|^2}{\mathcal{V}^{\frac{2}{3}}} M_{\rm pl}^2 \sim \frac{|M_0|^2}{\mathcal{V}^{\frac{2}{3}}} M_{\rm pl}^2 \sim \frac{|Z|^2}{\mathcal{V}^{\frac{2}{3}}} M_{\rm pl}^2 \,, \tag{5.37}$$

which for small M_0 can be kept much smaller than the complex structure and axio-dilaton moduli.

Next consider the throat-dominated regime, where for Case A we find the mass eigenvalues

$$m_Z^2 \sim \left(\frac{|Z|}{\mathcal{V}}\right)^{\frac{2}{3}} M_{\rm pl}^2 \sim \left(\mathcal{V}|Z|^2\right)^{\frac{1}{3}} M_{\rm s}^2 \,, \qquad m_S^2 \sim \frac{M_{\rm pl}^2}{\mathcal{V}^2} \,. \tag{5.38}$$

The expression for m_Z nicely shows that we need $\mathcal{V}|Z|^2 \ll 1$ in order for the mass to be smaller than the string scale. Moreover, one has the hierarchy $m_S \gg m_Z$. However, at least for the concrete example of the quintic we do not get $|W_0| \ll 1$ in Case A.

For Case B there is an important change in the mass scales

$$m_Z^2 \sim \left(\frac{|Z|}{\mathcal{V}}\right)^{\frac{2}{3}} M_{\rm pl}^2 \,, \qquad m_S^2 \sim \left(\frac{|Z|}{\mathcal{V}}\right)^{\frac{4}{3}} M_{\rm pl}^2 \tag{5.39}$$

so that now we have the inverted hierarchy $m_Z \gg m_S$. In addition, taking into account (5.37) for sufficiently small $|Z|$ the Kähler modulus can be kept lighter than the axio-dilaton, i.e. $m_S \gg m_\tau$.

This looks very promising, so let us summarize our findings: In Case B, by a suitably tuned choice of fluxes one can stabilize the conifold modulus and the axio-dilaton in the controlled regime such that $|W_0| \sim O(10^{-4})$ and their masses are hierarchically larger than the mass of the Kähler modulus. Thus, the AdS KKLT minimum seems to exist. In the throat-dominated regime, there is also a tiny warp factor that in principle could allow to uplift the minimum to dS. However, in this case other issues might appear, like the appearance of light KK modes localized at the tip of the long throat, whose mass has been shown [156] to scale like the mass of the Z modulus. This might spoil the validity of the employed effective action of just the conifold modulus and the axio-dilaton.

While in the simple one-parameter model we could explore the stabilization of the conifold modulus, generalizing the DKMM procedure requires more moduli to work with. That Case B with $h_0 = \tilde{h}^0 = 0$ showed more promise is nice, since these fluxes are also suggested by the procedure of DKMM. In the following we shall propose a general algorithm which extends the work of DKMM to the Coni-LCS regime of a multi-parameter CY.

5.3.1 $|W_0| \ll 1$ in the Coni-LCS Regime

Consider an n-parameter CY with one modulus close to the conifold described in terms of the perturbative prepotential and instanton series

$$\begin{aligned}\mathcal{F}_{\text{pert}} &= -\frac{1}{3!}K_{ijk}X^iX^jX^k + \frac{1}{2}A_{ij}X^iX^j + B_iX^i + C - \frac{Z^2\log Z}{2\pi i}\,,\\ \mathcal{F}_{\text{inst}} &= \frac{1}{(2\pi i)^3}\sum_{\vec{c}} a_{\vec{c}}\prod_{i=1}^{n} {q_i}^{n_i}\,,\end{aligned} \tag{5.40}$$

with q_i the coordinates used to invert the mirror map[4] and $\vec{c}$ running over effective curves. To simplify notation, we use Latin indices to denote all moduli $X^i = (\vec{U}, Z)^T$, $i = 1, \ldots, n$, and Greek indices to denote only the LCS moduli U^α, $\alpha = 1, \ldots, n-1$. If a pair of $\mathbb{Z}^n$ flux vectors $\vec{\tilde{f}}$, $\vec{h}$ exists such that

- $-\frac{1}{2}\vec{\tilde{f}}\cdot\vec{h} \leq Q_{\text{D3}}$,
- $N_{\alpha\beta} = K_{i\alpha\beta}\tilde{f}^i$ is invertible,
- $(N^{-1})^{\alpha\beta}h_\alpha h_\beta = 0$,
- $p^\alpha = (N^{-1})^{\alpha\beta}h_\beta$ lies in the Kähler cone of the mirror CY,
- $A_{i\alpha}\tilde{f}^i$ and $B_i\tilde{f}^i$ are integer-valued,

then the fluxes

$$F = \begin{pmatrix} B_i\tilde{f}^i \\ (A_{i\alpha}\tilde{f}^i,\ f_n)^T \\ 0 \\ \vec{\tilde{f}} \end{pmatrix}\,, \qquad H = \begin{pmatrix} 0 \\ \vec{h} \\ 0 \\ 0 \end{pmatrix} \tag{5.41}$$

are compatible with the Q_{D3} tadpole bound, and there is a perturbatively flat vacuum along

$$U^\alpha = p^\alpha\, S\,, \qquad Z = \zeta_0\, e^{-2\pi\frac{K_1}{M}S}\,, \tag{5.42}$$

with $\zeta_0 = e^{2\pi i\frac{M_1}{M}-1}$ and

$$M = -2\tilde{f}^n\,, \quad M_1 = f_n - A_{ni}\tilde{f}^i + \frac{\tilde{f}^n}{2\pi i}\,, \quad K_1 = h_n - K_{i\alpha n}\tilde{f}^i(N^{-1})^{\alpha\beta}h_\beta \tag{5.43}$$

along which $W_{\text{pert}}|_{\vec{U},Z} \approx \frac{ZM}{2\pi i}$ is exponentially small in $\text{Re}(S)$. As before, the conditions imply that too few moduli break the mechanism. Here , $h^{2,1} \geq 3$ is necessary.

[4]Since we are close to the conifold these coordinates are not simply exponentials of the moduli as in the LCS regime, but rather the conifold modulus enters linearly (3.74).

Following a three-step procedure, let us outline in more detail how this works. The periods are computed from the prepotential as

$$\begin{aligned} &X^0 = 1, \quad X^\alpha = U^\alpha, \quad X^n = Z, \\ &F_0 = 2C + B_i X^i + \frac{1}{3!} K_{ijk} X^i X^j X^k + \frac{Z^2}{2\pi i}, \\ &F_i = -\frac{1}{2} K_{ijk} X^j X^k + A_{ij} X^j + B_i - \delta_{in} \left(\frac{Z}{2\pi i} + \frac{Z \log(Z)}{\pi i} \right) . \end{aligned} \tag{5.44}$$

By restricting our choice of fluxes to

$$\tilde{h}^\Lambda = (0,0), \quad h_\Lambda = (0, h_i), \quad \tilde{f}^\Lambda = (0, \tilde{f}^i), \quad f_\Lambda = (B_i \tilde{f}^i, A_{\alpha i} \tilde{f}^i, f_n) \tag{5.45}$$

we obtain a superpotential which, similar to the DKMM case, is homogeneous of order two at $Z = 0$. Note that for this to work, $B_i \tilde{f}^i$, $A_{\alpha i} \tilde{f}^i$ must be *integer* valued, which calls for the parameters A_{ij} and B_i in the prepotential (5.40) to be *rational* numbers. The resulting superpotential can be expanded as

$$\begin{aligned} W &= (F + iSH)^T \cdot \Sigma \cdot \Pi = (X^\Lambda f_\Lambda - F_\Lambda \tilde{f}^\Lambda) + iS(X^\Lambda h_\Lambda - F_\Lambda \tilde{h}^\Lambda) \\ &= \frac{1}{2} K_{ijk} \tilde{f}^i X^j X^k + \frac{\tilde{f}^n Z}{2\pi i} + \frac{\tilde{f}^n Z \log(Z)}{\pi i} + i h_i X^i S + (f_n - A_{ni} \tilde{f}^i) Z \, . \end{aligned} \tag{5.46}$$

To proceed, at zeroth order in Z we first stabilize the U^α moduli in a supersymmetric minimum with vanishing superpotential

$$\begin{aligned} W = \frac{1}{2} N_{\alpha\beta} U^\alpha U^\beta + i S h_\alpha U^\alpha = 0 \, , \\ \partial_\alpha W = 0 \, , \end{aligned} \tag{5.47}$$

with $N_{\alpha\beta} = K_{i\alpha\beta} \tilde{f}^i$. Provided $N_{\alpha\beta}$ is invertible, the minimum is located at

$$U^\alpha = p^\alpha S = -iS (N^{-1})^{\alpha\beta} h_\beta \, . \tag{5.48}$$

Demanding that $W = 0$ results in a condition on the fluxes, $(N^{-1})^{\alpha\beta} h_\alpha h_\beta = 0$.

Integrating out the moduli U^α, since we invoked a vanishing superpotential at zeroth order in Z, the remaining terms of the superpotential are at least of order Z

$$W_{\text{pert}}(S, Z) = -\frac{M Z \log(Z)}{2\pi i} + M_1 Z + i K_1 S Z + O(Z^2) \, , \tag{5.49}$$

with the parameters given in (5.43). For the F-term we find

$$\begin{aligned} D_Z W &= \partial_Z W + \partial_Z K \cdot O(Z) \\ &= -\frac{M}{2\pi i} \log(Z) - \frac{M}{2\pi i} + M_1 + i K_1 S + O(Z) \, , \end{aligned} \tag{5.50}$$

showing that the Kähler potential contribution to $D_Z W$ is of subleading order. Thus, the conifold modulus is stabilized at

$$Z_0 = \zeta_0 \, e^{-2\pi \frac{K_1}{M} S} \,, \qquad \text{with } \zeta_0 = e^{2\pi i \frac{M_1}{M} - 1} \,. \tag{5.51}$$

What we have found is a perturbatively flat vacuum extending the Lemma of DKMM, where the complex structure moduli are stabilized in terms of the axio-dilaton as $\log(Z) \sim U^\alpha \sim S$.

The final step is to integrate out Z, resulting in an effective superpotential composed of the instanton superpotential $W_{\text{inst}} = -\tilde{f}^i \partial_i \mathcal{F}_{\text{inst}}$ as well as the linear corrections in Z resulting from $W_Z = W_{\text{pert}}|_{Z=Z_0} = \frac{ZM}{2\pi i}$,

$$W_{\text{eff}} = -\tilde{f}^i \partial_i \mathcal{F}_{\text{inst}} + \frac{ZM}{2\pi i} \sim \sum a_n \, e^{c_n S} \,. \tag{5.52}$$

Similar to DKMM, such an effective non-perturbative superpotential has the potential to stabilize the axio-dilaton by choosing fluxes that balance the leading terms against each other in a racetrack-like way. As long as the approximations we did along the way hold true in the minimum, the resulting W_0 can be stabilized at exponentially small values. Here it is important to keep the instanton series under control, as the conditions $|q_i| < 1$ will result in non-trivial constraints on the fluxes we may choose.

5.3.2 Example: $\mathbb{P}_{1,1,2,8,12}[24]$

Now let us apply this generic algorithm to the example $\mathbb{P}_{1,1,2,8,12}[24]$ worked out in detail in section 3.2.3. Recall the form of the prepotential (3.78), from which one can read off the data for the perturbative part

$$\begin{aligned} &K_{111} = 8,\, K_{112} = 2,\, K_{113} = 4,\, K_{123} = 1,\, K_{133} = 2 \,, \\ &A_{33} = \left(\frac{1}{2} + \frac{3 - 2\log(2\pi)}{2\pi i} \right) \,, \qquad B = \left(\frac{23}{6}, \, 1, \, \frac{23}{12} \right)^T \,. \end{aligned} \tag{5.53}$$

Moreover, the leading instanton contributions are

$$\begin{aligned} \mathcal{F}_{\text{inst}} &= -\frac{5i \, q_{U1}}{36\pi^3} - \frac{493 \, q_{U^1}^2}{10368\pi^3} + \frac{5i \, q_{U^1} q_Z}{36\pi^3} + \dots \\ &= -\frac{120i}{\pi^3} e^{2\pi i U^1} - \frac{35496i}{\pi^3} e^{4\pi i U^1} + \frac{120}{\pi^2} e^{2\pi i U^1} Z + \cdots \,. \end{aligned} \tag{5.54}$$

The generic relation (5.48) provides a minimum at $U^\alpha \sim S$ which is flat along S as long as the following condition on the fluxes is satisfied

$$\begin{aligned} \vec{U} &= S \begin{pmatrix} p_1 \\ p_2 \end{pmatrix} = S \frac{i h_2}{2\tilde{f}^1 + \tilde{f}^3} \begin{pmatrix} -1 \\ \frac{4\tilde{f}^1 + \tilde{f}^2 + 2\tilde{f}^3}{2\tilde{f}^1 + \tilde{f}^3} \end{pmatrix} \,, \\ h_1 &= \left(2 + \frac{\tilde{f}^2}{2\tilde{f}^1 + \tilde{f}^3} \right) h_2 \,. \end{aligned} \tag{5.55}$$

Additionally the conifold modulus is stabilized by (5.51) with

$$\begin{aligned} M &= -2\tilde{f}^3\,, \\ M_1 &= f_3 - \tilde{f}^3\left(\frac{1}{2} + \frac{1-\log(2\pi)}{\pi i}\right)\,, \\ K_1 &= h_3 - \frac{(\tilde{f}^1+\tilde{f}^3)(4\tilde{f}^1+\tilde{f}^2+2\tilde{f}^3)}{(2\tilde{f}^1+\tilde{f}^3)^2}h_2\,. \end{aligned} \tag{5.56}$$

Note that with the exception of M_1, the parameters are real and $|\zeta_0| = \frac{1}{2\pi}$ is independent of the fluxes. Hence, the conifold modulus is guaranteed to be small for $\mathrm{Re}(S) \gg 1$ and our trusted regimes overlap.

So to first order in Z, which we can trust if we can stabilize at $\mathrm{Re}(S) \gg 1$, we have a "perturbatively flat vacuum". The final step is to realize a racetrack-like vacuum for S with $\mathrm{Re}(S) \gg 1$ and resulting in $|W_0| \ll 1$. The effective superpotential (5.52) evaluates to

$$W_{\text{eff}} = -\frac{5}{36\pi^2}(2\tilde{f}^1+\tilde{f}^3)q_{U^1} - \frac{\tilde{f}^3}{\pi^2}q_Z + O({q_i}^2)\,. \tag{5.57}$$

By now we have several constraints on the fluxes. Besides the original choices and the condition we get from the U^α minimization, we need $\mathrm{Re}(S) \gg 1$. The instanton expansion is under control if $|q_i| < 1$ with q_i given in (3.74). Altogether we have

$$\begin{aligned} f_0 = \tilde{f}^i B_i \quad &\Rightarrow\ \frac{2\tilde{f}^1+\tilde{f}^3}{12} \in \mathbb{Z}\,, \\ h_1 = \left(2 + \frac{\tilde{f}^2}{2\tilde{f}^1+\tilde{f}^3}\right)h_2 \quad &\Rightarrow\ \frac{h_2\tilde{f}^2}{2\tilde{f}^1+\tilde{f}^3} \in \mathbb{Z} \end{aligned} \tag{5.58}$$

and from the instanton series

$$\begin{aligned} 1 > |q_{U^1}| &= \left|864\,\exp\left(2\pi\frac{h_2}{2\tilde{f}^1+\tilde{f}^3}S\right)\right|\,, \\ 1 > |q_{U^2}| &= \left|64\,\exp\left(2\pi\Big(\frac{4\tilde{f}^1+\tilde{f}^2+2\tilde{f}^3}{(2\tilde{f}^1+\tilde{f}^3)\tilde{f}^3}h_2 - \frac{2}{\tilde{f}^3}h_3\Big)S\right)\right|\,, \\ 1 > |q_Z| &= \left|\frac{1}{2}\,\exp\left(\pi\Big(-\frac{(\tilde{f}^1+\tilde{f}^3)(4\tilde{f}^1+\tilde{f}^2+2\tilde{f}^3)}{(2\tilde{f}^1+\tilde{f}^3)^2\tilde{f}^3}h_2 + \frac{1}{\tilde{f}^3}h_3\Big)S\right)\right|\,. \end{aligned} \tag{5.59}$$

Also, it is assumed that $\tilde{f}^3 \neq 0$ and $2\tilde{f}^1+\tilde{f}^3 \neq 0$ in order to be able to invert the relations of steps 1 and 2. It is straightforward to find flux combinations that fulfill these requirements

without going to very large flux numbers, e.g.

$$F = \begin{pmatrix} 74 \\ 0 \\ 0 \\ 0 \\ 0 \\ -24 \\ 120 \\ 24 \end{pmatrix} \qquad H = \begin{pmatrix} 0 \\ -9 \\ 3 \\ -4 \\ 0 \\ 0 \\ 0 \\ 0 \end{pmatrix} . \tag{5.60}$$

The final step is to search for a racetrack type Minkowski minimum close to the perturbatively flat minimum. Semi-analytically minimizing the effective scalar potential for S, with superpotential (5.57) evaluated along the perturbatively flat valley, we find approximate positions for the axio-dilaton (see figure 5.1) that lie close to the minimum of the full scalar potential depending on all eight real scalar fields. This true Minkowski vacuum can then be found by a numerical search using those starting points.

We have checked that in this example for the specific choice of fluxes (5.60) such a numerical minimum indeed exists at

$$\langle U^1 \rangle = 2.79\, i, \quad \langle U^2 \rangle = 8.36\, i, \quad \langle Z \rangle = 1.36 \cdot 10^{-6} i, \quad \langle S \rangle = 22.3\,. \tag{5.61}$$

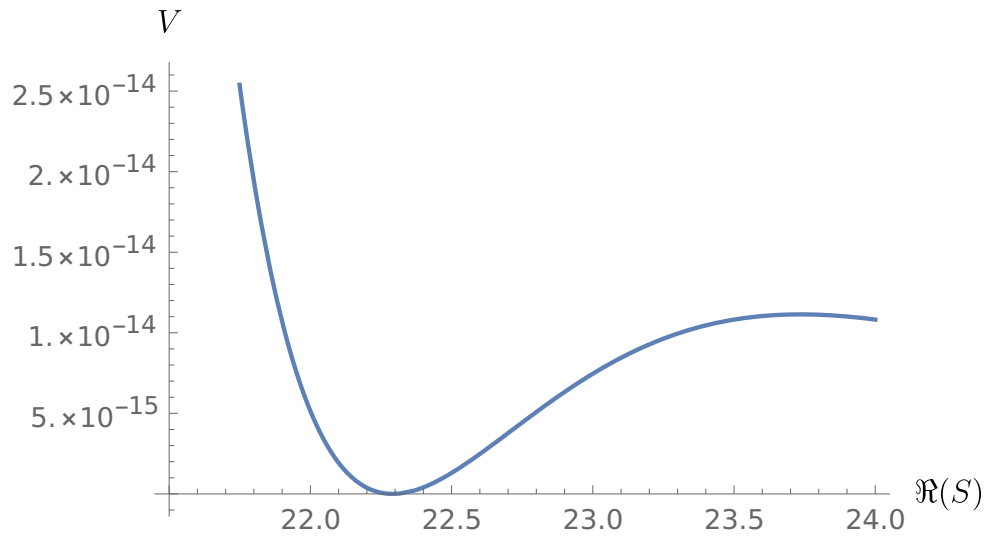

Figure 5.1: The effective scalar potential for the real part of S shows the existence of a Minkowski minimum.

With these values we observe that the instanton series is nicely under control with $|q_i| \approx (2 \cdot 10^{-5}, 0.2, 4 \cdot 10^{-6})$. The superpotential in this minimum is very well approximated by (5.57) and evaluates to

$$W_0 = -3.10 \cdot 10^{-6}\,. \tag{5.62}$$

Sections through the full potential are shown in figure 5.2.

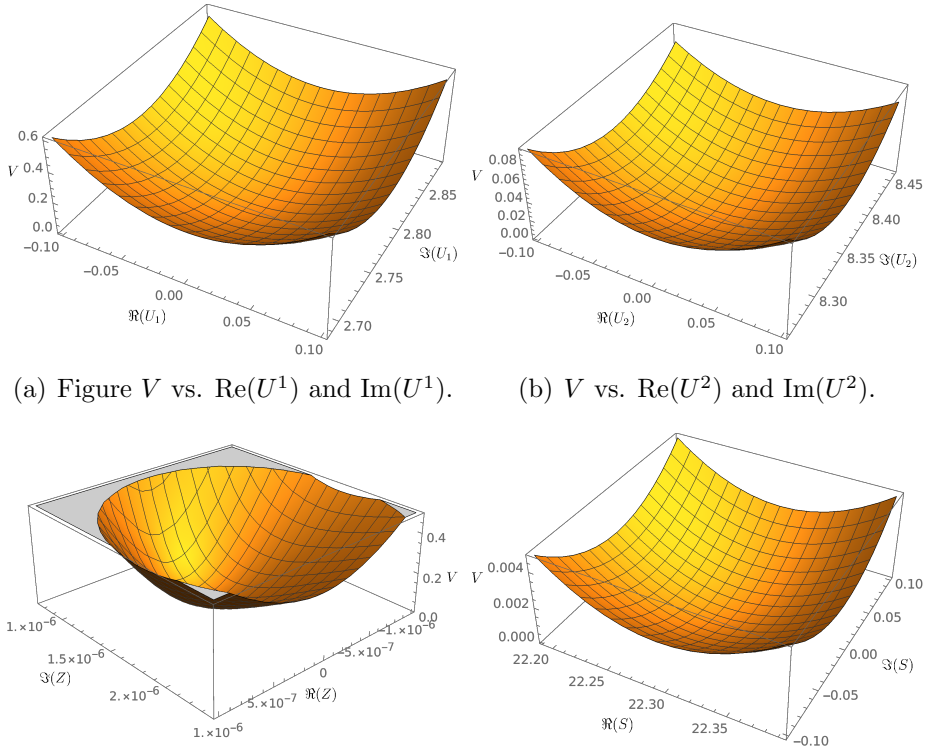

(a) Figure V vs. $\mathrm{Re}(U^1)$ and $\mathrm{Im}(U^1)$.

(b) V vs. $\mathrm{Re}(U^2)$ and $\mathrm{Im}(U^2)$.

(c) V vs. $\mathrm{Re}(Z)$ and $\mathrm{Im}(Z)$.

(d) V vs. $\mathrm{Re}(S)$ and $\mathrm{Im}(S)$.

Figure 5.2: Full scalar potential around the minimum.

Computing the mass eigenvalues for our example, we find a very heavy eigenvalue corresponding to the conifold modulus, two less heavy directions which mix the complex structure moduli U^i with the axio-dilaton, and a very light direction along the perturbatively flat vacuum

$$\{m^2\} = \{6 \cdot 10^{14},\, 1 \cdot 10^3,\, 3 \cdot 10^2,\, 2 \cdot 10^{-11}\} M_{\mathrm{pl}}^2 \,. \tag{5.63}$$

The smallest value is approximately $|W_0|^2$, which also corresponds to the mass scale of the Kähler modulus in the KKLT scenario. The challenge of further stabilizing the remaining moduli thus persists from the LCS point.

In an inexhaustive search over fluxes and performing the semi-analytic minimization of the effective potential for S to keep the computation tractable, we find more than 10^4 (approximate) vacua for which $|W_0| \leq 10^{-6}$, with values like $|W_0| \approx 10^{-12}$ being commonplace. Indeed it seems that arbitrarily small values of W_0 can be reached with reasonably small fluxes, however it is not clear if those minima are true vacua or if the approximations and numerics break down around those small values. This has to be tested case by case using the full potential without approximations, as has been done in the example above. The search suggests that examples with reasonably small W_0 as the one discussed are nonetheless plentiful.

Thus the assumption of exponentially small superpotentials close to a conifold can be explicitly realized in a string theory setup. Of course this analysis focused purely on the complex structure side, it remains to be seen if the additional steps, especially the stabilization of the Kähler moduli as well as the uplift can be realized as well. Instead of pursuing this direction, the next section will discuss the validity of warped throats.

5.4 Warped Throats

One possible issue of the KKLT construction is the existence of a warped throat. In an effective field theory the geometry is usually assumed to be fixed and the KK modes as well as winding modes are integrated out. If some of these become light, they could spoil the validity of the effective theory. In this section we will study the effect of KK modes localized in a warped throat. It will turn out the corrections due to the KK modes are of the same form as the tree-level results. This precise agreement renders the effect of the KK-modes harmless, such that the effective theory can still be applied, yet with some different numerical values.

As analytic CY metrics are unknown, global descriptions of warped throats are not available. Instead, one refers to local descriptions, which are then glued into a global picture. This has the disadvantage that on the one hand one has to ensure to stay in the regime where the approximation is valid and on the other hand modes originating from the bulk of the CY cannot be taken into account. Even the numerical methods reviewed in section 3.4 are not applicable. While these allow to compute the spectrum of the theory to arbitrary precision at general points in moduli space, they fail close to the conifold, where a warped throat develops. While it would certainly be interesting to obtain a global picture, we will thus in the following restrict to the local description and ensure that the modes are completely localized inside the throat. This section strongly follows [156]. In the case of a flux compactification, the fluxes will backreact on the geometry. Thus in the presence of fluxes, a CY is no longer a solution to the equations of motion of string theory. This is usually remedied by assuming the dilute flux limit, where the flux is small compared to the volume of the CY, rendering the corrections to the CY geometry negligible and thus allowing one to work with a CY approximation. This method works well for moduli stabilization close to the LCS point. But close to a warped throat the warping becomes strong and thus also the backreaction. Indeed, it is well known that the backreaction of such a three-form flux and of localized D3-branes on the geometry leads to a warped CY metric [164]

$$ds^2 = e^{2A(y)} g_{\mu\nu} dx^\mu dx^\nu + e^{-2A(y)} \tilde{g}_{mn} dy^m dy^n \,. \tag{5.64}$$

Here $g_{\mu\nu}$ is the 4-dimensional space time metric, while $\tilde{g}_{mn}$ is the metric of the 6-dimensional internal space, which is paramterized by 6 coordinates y^m. The so called warp factor $A(y)$ depends only on the internal coordinates.

The prime example of a warped throat solution of SUGRA theories is the Klebanov-Strassler(KS) throat [165]. For this geometry the metric is explicitly known, it is given

by

$$\widetilde{ds}^2 = \frac{1}{2}|S|^{\frac{2}{3}}K(y)\left[\frac{dy^2+(g^5)^2}{3K^3(y)} + \cosh^2\left(\frac{y}{2}\right)\left((g^3)^2+(g^4)^2\right) + \sinh^2\left(\frac{y}{2}\right)\left((g^1)^2+(g^2)^2\right)\right] . \tag{5.65}$$

This metric is describing a 6-dimensional warped throat. Topologically, it is an infinite cone over $S^2 \times S^3$. The coordinate y is parameterizing the cone. At $y = 0$ the S^2 shrinks to zero size while the S^3 retains a finite volume. Note that exactly at the conifold singularity also the S^3 shrinks to zero size. The KS throat thus describes a so-called deformed conifold and only at $S = 0$ the real conifold. We will in the following simply write conifold, not distinguishing the cases. All compactifications will assume a non-zero value of S. The base $S^2 \times S^3$ is described by the einbeins g^i, $i = 1 \ldots 5$. The overall scale parameter S is related to the conifold modulus, i.e. the distance in moduli space one is away from the conifold singularity. The function $K(y)$ is explicitly given by

$$K(y) = \frac{(\sinh(2y) - 2y)^{\frac{1}{3}}}{2^{\frac{1}{3}}\ \sinh(y)} . \tag{5.66}$$

The warp factor corresponding to the KS solution is given by

$$e^{-4A(y)} = 2^{\frac{2}{3}}\frac{(\alpha' g_s M)^2}{|S|^{\frac{4}{3}}}\mathcal{I}(y) , \tag{5.67}$$

where M is a flux parameter and

$$\mathcal{I}(y) = \int_y^\infty dx \frac{x\coth x - 1}{\sinh^2 x}(\sinh(2x) - 2x)^{\frac{1}{3}} . \tag{5.68}$$

The exact relation between the SUGRA parameter S and the conifold modulus Z can be worked out by a dimensional analysis. Z is dimensionless, while from the warp factor 5.67 one can see that S is of dimension [length^3]. Moreover, scaling the internal metric via $\tilde{g} \to \lambda^2\tilde{g}$ describes the breathing mode of the CY, i.e. the Kähler modulus for the overall volume. As the fluxes do not stabilize the Kähler moduli, this should better be an unconstrained deformation. There exists the relation $\lambda \sim \mathcal{V}_w^{1/6}$ where[5]

$$\mathcal{V}_w = \frac{1}{g_s^{3/2}(\alpha')^3}\int d^6y\, e^{-4A}\sqrt{\tilde{g}} \sim \tau^{\frac{3}{2}} \tag{5.69}$$

[5]Our notation is related to the one used in [154,155] by a rescaling of the moduli fields τ and Z (called ρ and S in [154, 155]) by suitable powers of $||\Omega||^2$ and V_w. Note that the latter two quantities are not considered to be moduli dependent but just values around which one expands.

denotes the warped volume of the CY in units of α'. In [166] it was shown that the 10D string equations of motion admit an unconstrained deformation λ only if the warp factor scales non-trivially

$$e^{-4A} = 1 + \frac{e^{-4A_{\rm con}}}{\lambda^4} \sim 1 + \frac{c}{(\mathcal{V}_w |Z|^2)^{\frac{2}{3}}} + \dots \,, \tag{5.70}$$

where we have chosen the warp factor to be one in the large volume, unwarped regime. Putting the last two observations together, the coordinate S in the KS solution (5.65), (5.67) and the conifold coordinate Z are related via the rescaling

$$S \to (\alpha')^{3/2} \sqrt{g_s^{3/2}\, \mathcal{V}_w} Z \,. \tag{5.71}$$

Thus the warp factor close to the conifold locus can be written as

$$e^{-4A(y)} \approx 2^{\frac{2}{3}} \frac{g_s M^2}{(\mathcal{V}_w |Z|^2)^{\frac{2}{3}}} \mathcal{I}(y) \,. \tag{5.72}$$

The KS throat is non-compact due to the infinite y direction. Thus for string theory applications one assumes that the geometry ends at some fixed finite value of y, denoted y_{UV}, where the geometry is glued into the bulk of the CY. The resulting geometry is shown in picture 5.3. This requires that all modes one takes into account are localized inside the throat.

KK modes in the warped throat

It is now possible to examine the KK modes arising inside the KS throat. We will employ two methods, the first will be a leading order approximation and the second a numerical analysis. Let us do the dimensional reduction of a ten-dimensional scalar field Φ with mass m to four dimensions. Starting with the action

$$S \sim \int d^{10}x \sqrt{-G} \Big(G^{MN} \partial_M \Phi \partial_N \Phi + m^2 \Phi^2 \Big) \tag{5.73}$$

and making the usual warped Ansatz for the ten-dimensional metric

$$G = \begin{pmatrix} e^{2A(y)} g_4 & 0 \\ 0 & e^{-2A(y)} \tilde{g}_{\rm CY} \end{pmatrix} \,, \tag{5.74}$$

the action can be written as

$$\begin{aligned} S \sim \int d^4x \sqrt{-g_4} \int d^6y \sqrt{\tilde{g}_{\rm CY}} \Big[& e^{-4A} g_4^{\mu\nu} \partial_\mu \Phi \partial_\nu \Phi + \\ & \tilde{g}_{\rm CY}^{mn} \partial_m \Phi \partial_n \Phi + e^{-2A} m^2 \Phi^2 \Big] \,. \end{aligned} \tag{5.75}$$

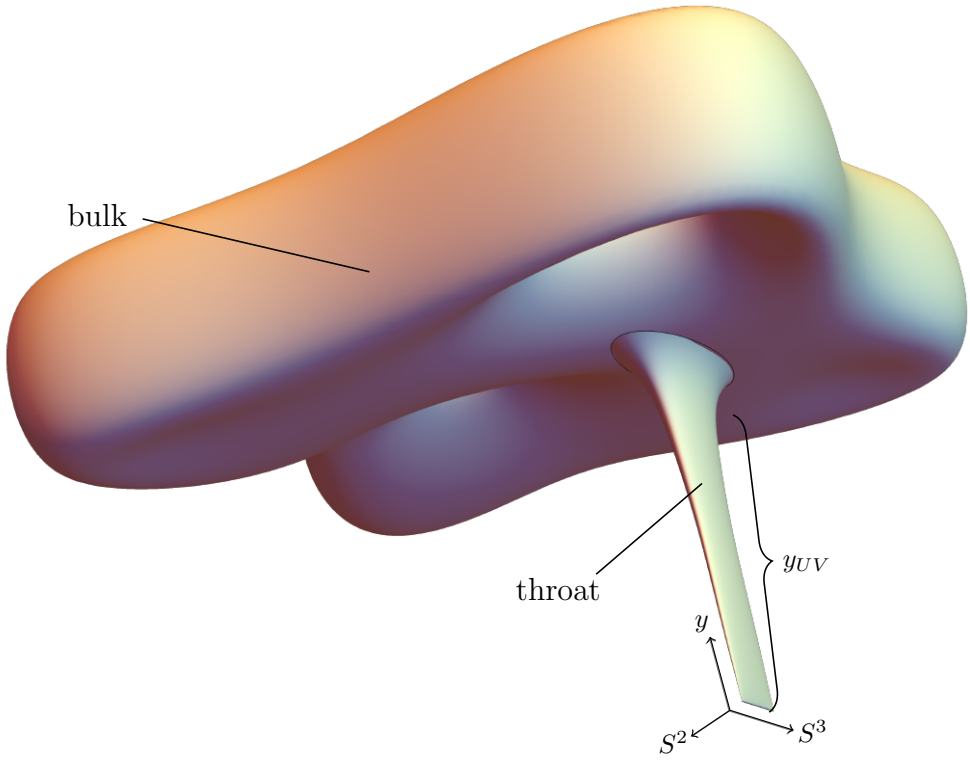

Figure 5.3: A sketch of a Calabi-Yau with a KS-throat. At the tip of the throat the S^2 shrinks to zero size while the S^3 remains finite. y_{UV} marks the cutoff where the throat meets the bulk.

The resulting equation of motion for the field $\Phi(x, y)$ becomes

$$\Box_4 \Phi + e^{4A} \tilde{\nabla}^m \tilde{\nabla}_m \Phi - e^{2A} m^2 \Phi = 0 \,. \tag{5.76}$$

Doing a product Ansatz $\Phi(x, y) = \varphi(x)\chi(y)$ the four-dimensional KK masses m^2_{KK} are given by the eigenvalues of the six-dimensional warped Laplace equation

$$e^{4A(y)} \tilde{\nabla}^m \tilde{\nabla}_m \chi(y) - m^2 \, e^{2A(y)} \chi(y) = -m^2_{\text{KK}} \, \chi(y) \,. \tag{5.77}$$

We are heading for the lightest modes, which are expected to arise from the KK modes of the four-dimensional components of the metric $g_{4\,\mu\nu}(x, y)$. The zero mode is the 4D graviton that is the lowest excitation of the closed string. Placing such a closed string deep into the throat region, we expect to find highly red-shifted KK masses. Therefore, we set $m = 0$ and note that at linear order KK modes of the 4D metric are also governed by the same Laplace equation (see [167])

$$e^{4A(y)} \, \widetilde{\nabla}^2_{\text{CY}} \, \chi(y) = -m^2_{\text{KK}} \, \chi(y) \,. \tag{5.78}$$

Actually, one now has to solve this equation on the entire Calabi-Yau manifold for a point in complex structure moduli space that is very close to a conifold singularity. This is a horrendous task that is beyond the scope of this paper.

Here, we take a simpler approach and first look for local solutions that are supported close to the tip of the cone of the KS solution (5.65). These are the ones which are expected to yield small red-shifted masses. For this purpose, we take the local CY metric of the KS throat and evaluate the Laplacian $\widetilde{\nabla}^2_{\rm CY}$ for solutions that do only depend on the radial direction y and are constant on the $S^2 \times S^3$ base of the cone. These are expected to be the ones that have minimal mass. We compute the relevant Laplace equation from the KS metric (5.65) and warp factor (5.67)

$$2^{1/3}\frac{(\mathcal{V}|Z|^2)^{\frac{1}{3}}}{g_s^{3/2}M^2}\frac{1}{\mathcal{I}(y)}\Big[3K^2(y)\,\partial_y^2\chi(y)+4\frac{\partial_y\chi(y)}{\sinh(y)\,K(y)}\Big]=-\alpha' m_{\rm KK}^2\,\chi(y)\,. \tag{5.79}$$

Leading order approximation

Before we solve this differential equation numerically, to get an idea what the solutions might look like, we expand all quantities up to leading order around $y=0$. Using

$$\begin{aligned} K(y) &= \left(\frac{2}{3}\right)^{\frac{1}{3}}+O(y^2),\\ \sinh(y)\,K(y) &= \left(\frac{2}{3}\right)^{\frac{1}{3}}y+O(y^3),\\ \mathcal{I}(y) &= \kappa+O(y^2), \end{aligned} \tag{5.80}$$

with $\kappa\approx 0.72$, we arrive at

$$\frac{2\cdot 3^{1/3}}{\kappa}\frac{(\mathcal{V}|Z|^2)^{\frac{1}{3}}}{g_s^{3/2}M^2}\Big[\partial_y^2\chi+\frac{2}{y}\partial_y\chi\Big]=-\alpha' m_{\rm KK}^2\,\chi\,. \tag{5.81}$$

Up to some scaling factors, this is the spherical Bessel differential equation

$$\Big[\partial_y^2\chi+\frac{2}{y}\partial_y\chi+k^2\chi\Big]=0\,, \tag{5.82}$$

whose solution with Neumann boundary conditions at $y=0$ is

$$\chi(y)=\frac{\sin(ky)}{ky}\,, \tag{5.83}$$

where $k_n=f_n/y_{\rm UV}$ is expected to be quantized by imposing (Neumann) boundary conditions at the UV end $y_{\rm UV}$ of the throat. Here f_n denotes the solutions of the equation $\tan f=f$ that are approximately $f_n\approx(2n+1)\pi/2$ with $n\geq 1$.

Therefore, the KK masses of these localized solution scale

$$m_{\rm KK}^2=\frac{2\cdot 3^{1/3}}{\kappa}\frac{f_n^2\,(\mathcal{V}_w|Z|^2)^{\frac{1}{3}}}{g_s^{3/2}(My_{\rm UV})^2}\,M_{\rm s}^2\,. \tag{5.84}$$

Note that, with respect to M_s, g_s, M and $(\mathcal{V}_w|Z|^2)$ this scales precisely in the same way as the mass (5.38) of the conifold modulus, so that

$$\frac{m_{\rm KK}^2}{m_Z^2} = c\,\frac{f_n^2}{y_{\rm UV}^2}\,, \tag{5.85}$$

where c is an order one coefficient. Note that $y_{\rm UV}$ is bounded from below by

$$1 \ll g_s|M|\,y_{\rm UV}^2\,. \tag{5.86}$$

This constraint is obtained by demanding that the length of the throat is larger than the string length. This constraint is weaker than imposing $y_{\rm UV} > 1$. In the latter regime there are finitely many KK modes that have a mass lighter than the conifold modulus. This indicates that the employed effective action might be at the edge of reliability. We will further analyze this important question in the upcoming sections.

In Einstein frame, massive bulk string excitations have a mass $m_{\rm str}^2 \sim g_s^{1/2} M_s^2$. If placed into the warped throat we have checked that there exist localized solutions of (5.77) leading to KK masses that are shifted up by

$$m_{\rm str,throat}^2 \sim \frac{1}{M}(\mathcal{V}_w|Z|^2)^{\frac{1}{3}} M_s^2\,. \tag{5.87}$$

With respect to $\mathcal{V}_w$ and Z this scales in the same way as the mass of the conifold modulus and the KK modes. Note, that in this way each of the string modes comes with a whole tower of KK excitations with spacing of the order (5.84).

Numerical solution of warped Laplace equation

For $y > 1$ we do not expect our leading order approximation to be valid so that a full numerical analysis of the solution of (5.79) is necessary. Except for the radial dependence of $\mathcal{I}(y)$, this is a one dimensional differential equation with Neumann boundary conditions. This function could only be evaluated numerically. To obtain an expression which can be inserted into the numerical procedure, the function was sampled at 5000 points in the interval $[0, 50]$ and interpolated using a degree three polynomial. Figure 5.4 shows the first and second eigenfunctions of the approximate analytical solution as well as the numerical solution.
The functions are normalized such that the integral over the absolute values squared is equal to one. Only the radial contribution is shown, i.e. all prefactors are set to one:

$$\frac{(\mathcal{V}_w|Z|^2)^{\frac{1}{3}}}{g_s M^2 \alpha'} = 1\,. \tag{5.88}$$

To estimate the numerical errors made in solving the differential equations, the same methods were used to solve the spherical Bessel equation numerically, the results are shown in all figures in black. The functions as well as eigenvalues agree with the analytical result,

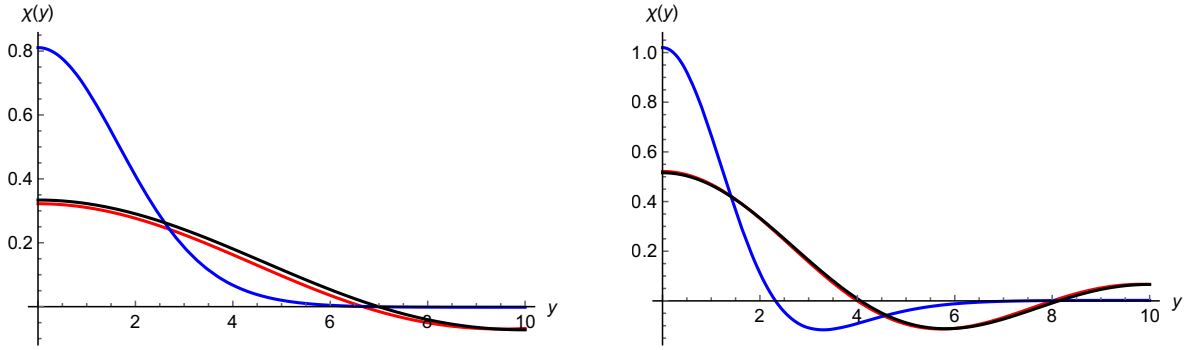

Figure 5.4: Eigenfunction of the numerical solution (blue) and analytical approximation (red) of the first (left) and second (right) radial mode.

showing that the numerical errors are small. We notice that the numerical functions are shifted towards small y relative to the analytical spherical Bessel functions, improving the localization in the warped throat.

The eigenvalues of the numerical solution scale approximately like $1/y_{UV}$ for small values of y_{UV} and approach an asymptotic value for $y_{UV} \gtrapprox 10$ due to the localization of the functions at small y. The left hand side of figure 5.5 shows this behavior exemplary for the case of the first eigenmode. The right figure shows the mass eigenvalues obtained via the analytical and the numerical method.

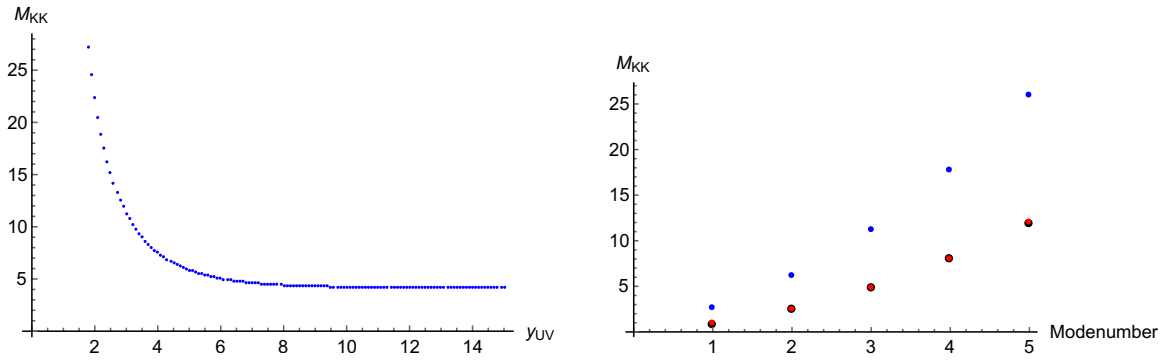

Figure 5.5: Left: The first eigenvalue of the numerical solution for different y_{UV}. Right: Eigenvalues of the numerical solution (blue) and analytical approximation (red) of the first five radial modes. The numerical evaluation of the spherical Bessel equation is shown in black.

Validity of the effective action

Now that the mass scaling has been determined, the KK modes can be integrated out to study their effect on the effective theory. In the regime $g_s M^2 \gg 1$ the tower of KK modes

with spacing

$$\Delta m \approx \frac{1}{\sqrt{g_s M^2}\, y_{\rm UV}} \left(\frac{|Z|}{\mathcal{V}_w}\right)^{\frac{1}{3}} M_{\rm pl} \,, \tag{5.89}$$

is supposed to be lighter than the cut-off. Integrating out these light gravitationally coupled KK modes leads to a one-loop correction to the field space metric of the conifold modulus

$$\begin{aligned} g_{Z\overline{Z}}^{1-\text{loop}} &\sim M_{\rm pl}^{-2} \sum_{n=1}^{N_{\rm sp}} \Big(\partial_Z m_n(Z)\Big)^2 \sim \sum_{n=1}^{N_{\rm sp}} n^2 \left(\frac{1}{\sqrt{g_s M^2} y_{\rm UV}} \frac{1}{(\mathcal{V}_w |Z|)^{1/3}}\right)^2 \\ &\sim N_{\rm sp}^3 \frac{1}{g_s M^2 y_{\rm UV}^2} \frac{1}{(\mathcal{V}_w |Z|)^{2/3}} \,. \end{aligned} \tag{5.90}$$

Consistency with the picture of kinetic terms arising from integrating out fields in the UV as assumed by the emergence proposal demands that the parametric scaling of this contribution matches the tree level result

$$g_{Z\overline{Z}}^{1-\text{loop}} \sim \frac{g_s M^2}{(\mathcal{V}_w |Z|^2)^{2/3}} \,. \tag{5.91}$$

Enforcing this scaling in (5.90) constrains the number of light KK species in the effective description to scale as

$$N_{\rm sp} \sim \left(g_s M^2 y_{\rm UV}\right)^{2/3} \,. \tag{5.92}$$

Note that due to the lower bound (5.86), this number is guaranteed to satisfy $N_{\rm sp} \gtrsim |M|^{2/3}$. Thus, there is a finite number of KK modes whose mass is lighter than the species scale.

Using this scaling, analogously one finds that the corrections $g_{Z\overline{T}}^{1-\text{loop}}$ and $g_{T\overline{T}}^{1-\text{loop}}$ are proportional to the tree-level expressions following from the Kähler potential $K \sim g_s M^2 |Z|^{\frac{2}{3}}/(T+\overline{T})$. As a result, a consistent effective description of the warped throat should accommodate at most $N_{\rm sp}$ light KK modes and thus should have a cutoff of at most

$$\tilde{\Lambda}_{\rm sp} \sim N_{\rm sp} \Delta m \sim \left(\frac{g_s M^2}{y_{\rm UV}^2}\right)^{\frac{1}{6}} \left(\frac{|Z|}{\mathcal{V}_w}\right)^{\frac{1}{3}} M_{\rm pl} \,. \tag{5.93}$$

In analogy to the "gravitational" species scale $\Lambda_{\rm sp} = M_{\rm pl}/\sqrt{N_{\rm sp}}$ this scale can be interpreted as a generalized species scale[6]

$$\tilde{\Lambda}_{\rm sp} = \frac{\Lambda}{\sqrt{N_{\rm sp}}} \,, \tag{5.94}$$

for an effective gravity theory with a cut-off

$$\Lambda \sim \sqrt{g_s M^2} \left(\frac{|Z|}{\mathcal{V}_w}\right)^{\frac{1}{3}} M_{\rm pl} \,. \tag{5.95}$$

[6]At this scale the one-loop correction to the Planck-scale $M_{\rm pl}^2(\mu) = M_{\rm pl}^2(0) - \frac{\mu^2}{12\pi} N_{\rm sp}$ becomes of the order of the cut-off scale Λ.

In contrast to the emergence of the SDC at large volume, here the ultimate cut-off Λ is also field dependent. This implies a finite distance of the conifold point in complex structure moduli space

$$\Phi = d(0,|Z_0|) \sim \int_0^{|Z_0|} \sqrt{g_{Z\overline{Z}}} \sim \sqrt{g_s M^2} \left(\frac{|Z_0|}{\mathcal{V}_w}\right)^{\frac{1}{3}} \sim \frac{\Lambda}{M_{\rm pl}}\,, \tag{5.96}$$

where $\Phi < 1$ is the canonically normalized field corresponding to Z. In terms of Φ the relevant quantities become

$$\Lambda \sim \Phi\, M_{\rm pl}\,, \qquad \Delta m \sim \frac{\Phi}{g_s M^2\, y_{\rm UV}}\, M_{\rm pl}\,, \qquad \tilde{\Lambda} \sim \frac{\Phi}{(g_s M^2\, y_{\rm UV})^{\frac{1}{3}}}\, M_{\rm pl}\,, \tag{5.97}$$

with still $N_{\rm sp} \sim (g_s M^2\, y_{\rm UV})^{2/3}$. The mass of the conifold modulus Z scales as $m_Z \sim \Phi/(g_s M^2)$ and the coupling constant in the three-point vertex $\gamma\phi h_n^2$ reads

$$\gamma \sim m(\Phi)\partial_\Phi m(\Phi) \sim \frac{\Phi}{(g_s M^2\, y_{\rm UV})^2} \ll 1 \tag{5.98}$$

so that perturbation theory makes sense. We notice that, in contrast to the SDC for infinite field distances, at the conifold point Δm does not scale exponentially with the proper field distance but only linearly. In addition, the number of light species does not increase exponentially but stays constant.

How can these results be interpreted? The cutoff obtained in (5.95) turns out to scale exactly like the mass of a D3 brane. The action of a D3 brane is given by

$$S_{\rm D3} \sim \frac{M_s^4}{g_s} \int dt \int_{S^3} d^3y \sqrt{-G} \sim \frac{M_s^4}{g_s} \int dt \int_{S^3} d^3y\, e^{-2A} \sqrt{\tilde{g}_{\rm CY}}\,. \tag{5.99}$$

Using the scaling of the metric (5.65) and the warp factor (5.72), the mass of the dimensionally reduced brane turns out to be

$$m_{\rm D3}^2 \sim g_s^{\frac{1}{2}} M^2 (\mathcal{V}_w |Z|^2)^{\frac{1}{3}} M_s^2 \sim g_s M^2 \left(\frac{|Z|}{\mathcal{V}_w}\right)^{\frac{2}{3}} M_{\rm pl}^2\,, \tag{5.100}$$

which scales exactly like the cutoff. As this is a non-perturbative state not taken into account in the original formulation of the effective theory, it's mass is a natural cutoff.

As the 1-loop corrections arising from integrating out a finite number of KK modes below this cutoff are proportional to the tree level metric, the corrections are effectively harmless, only modifying the numerical prefactors.

This is of course an optimistic interpretation of the results. One could also interpret the result negatively, stating that the Wilsonian action cannot be trusted as there are light modes which have been integrated out. Depending on which interpretation one chooses, the consequences for the KKLT construction differ drastically. We will here simply state that there are indeed corrections to to light KK modes, but that these are not necessarily dangerous for the construction.

Chapter 6

Other Ways to dS

In this chapter we will discuss more exotic ways to obtain dS in string theory. These methods are much less established than the KKLT scenario discussed in the previous chapter. We will focus on two main approaches. First the idea of spontaneous compactification mediated via tachyon condensation, which leads to theories on dS space in fewer dimensions. This kills two birds with one stone, as the construction results in dS spaces as well as avoiding the no-gos following from the cobordism conjectures as it does not include any compactified dimensions. The second idea is to modify the signature of space-time, by either including additional time dimensions or changing the signature of the world-sheet. This allows for a rather easy construction of dS spaces, but of course introduces many problems like non-unitarities, closed timelike curves and ghosts.

6.1 dS Spaces from Tachyons

One of the conjectured reasons for the non-existence of dS lies in another conjecture, the cobordism conjecture [3]. This conjecture states that the cobordism group of quantum gravity should be trivial,

$$\Omega_d^{QG} = 0\,. \tag{6.1}$$

Two d-dimensional manifolds are said to be in the same cobordism class if they form the boundary of a $(d+1)$-dimensional manifold. Thus the cobordism group is given by the set

$$\Omega_d = \{\text{compact, closed d} - \text{dimensional manifolds}\}/\sim\,, \tag{6.2}$$

where $\sim$ denotes the equivalence of manifolds under bordisms as described above. For geometric compactifications the physical equivalence relation is exactly the mathematical definition of a cobordism group. But quantum gravity, especially in the string theoretic examples, allows for dynamical changes of the topology, e.g. flop or conifold transitions of the compactification geometry. In these cases the equivalence relation $\sim$ has to be modified. Also, if additional structures exist these have to be taken into account. The most important example is the spin structure, playing an important role for the existence of supersymmetry.

The cobordism equivalence then asks for the boundary of a spin-manifold. Some cobordism groups have already been computed, table 6.1 lists the known groups which are important for string theory.

k	0	1	2	3	4	5	6	7	8	9	10
Ω_k^{Spin}	$\mathbb{Z}$	$\mathbb{Z}_2$	$\mathbb{Z}_2$	0	$\mathbb{Z}$	0	0	0	$\mathbb{Z}^2$	$\mathbb{Z}_2^2$	$\mathbb{Z}_2^3$
$\Omega_k^{\text{Pin}^+}$	$\mathbb{Z}_2$	0	$\mathbb{Z}_2$	$\mathbb{Z}_2$	$\mathbb{Z}_{16}$	0	0	0	$\mathbb{Z}_2 \times \mathbb{Z}_{32}$	0	$\mathbb{Z}_2^3$
$\Omega_k^{\text{Spin}^c}$	$\mathbb{Z}$	0	$\mathbb{Z}$	0	$\mathbb{Z}^2$	0	$\mathbb{Z}^2$	0	$\mathbb{Z}^4$	0	$\mathbb{Z}^4$
Ω_k^{String}	$\mathbb{Z}$	$\mathbb{Z}_2$	$\mathbb{Z}_2$	$\mathbb{Z}_{24}$	0	0	$\mathbb{Z}^2$	0	$\mathbb{Z}_2 \times \mathbb{Z}$	$\mathbb{Z}_2^2$	$\mathbb{Z}_6$

Figure 6.1: Cobordism groups appearing in string theory. Table taken from the appendix of [3].

The triviality of cobordism groups has dramatic consequences. One possible problem for a compactification is the existence of so-called bubbles of nothing. These were first found to destabilize non-supersymmetric Kaluza-Klein theories [168], but were expected to be absent in supersymmetric theories. Recently, in [169] the authors showed that the existence of a bubble of nothing is related to the spin structure of the compactification manifold. If the spin-cobordism group Ω_d^{Spin} is trivial, the construction of a bubble of nothing is always possible. In these cases the vacuum has no topological protection against its decay. Of course there are also dynamical obstructions, but these are often absent if supersymmetry is broken. This is closely related to the conjectures that non-supersymmetric stable vacua of quantum gravity do not exist [170, 171]. The known constructions of dS vacua break supersymmetry, thus the conjectures would rule these out. It is important to note that these arguments only forbid eternally stable dS vacua, meta stable vacua with a finite lifetime are not forbidden. To reach a phenomenologically interesting theory from the 10-dimensional superstrings or the 11-dimensional M-theory, they have to be compactified on a 6- or 7-dimensional internal manifold. The spin-cobordism groups of these manifolds are $\Omega_6^{\text{Spin}} = \Omega_7^{\text{Spin}} = 0$. This implies that the usual non-supersymmetric compactifications would be unstable to a decay into nothing.

The arguments above have two loop-holes. First, string theory includes additional degrees of freedom, which require modified cobordism groups. Especially in non-geometric compactification it is unclear how to compute the groups or how to define them, as they are an intrinsically geometric statement and thus it is unclear if the logic above applies. Second, even if the cobordism conjecture holds and the quantum gravity cobordism group is trivial if all degrees of freedom are taken into account independent of the dimension, the existence of the bubble of nothing has a second requirement, which is that the theory includes an internal manifold or equivalently that there exist additional dimensions. There are known consistent string theories formulated in 4 dimensions, most prominently the $\mathcal{N} = 2$ superstring or the bosonic string in a linear dilaton background. As these do

not include extra dimensions there is no bubble of nothing instability. But of course these theories have other problems, especially the existence of tachyons or a broken 4-dimensional Lorentz-symmetry. But nothing forbids in principle the existence of a stable 4-dimensional string theory. One way to construct lower dimensional string theories is to actually use the bubbles of nothing. The endpoint of a closed string bulk tachyon condensation is in general a lower dimensional theory. In the next sections the tachyon condensations will be described in detail and how they give rise to eternal dS spaces in string theory. Interestingly it will turn out that the constructed theories exist exactly in the dimensions which are allowed by the non-trivial spin cobordism groups.

6.1.1 Tachyon Condensation

Before we go into the details of tachyon condensation in string theory we give a short review of tachyon dynamics. We start with the usual Lagrangian for a real interacting massive scalar field.

$$L = \partial_\mu \Phi \partial^\mu \Phi + m^2 \Phi^2 + \lambda \Phi^4 \ . \tag{6.3}$$

For negative $m^2 < 0$ the potential has 3 extremal points, a maximum at the origin $\Phi = 0$ as well as two minima at $\Phi = \pm\sqrt{\frac{-m^2}{2\lambda}}$.[1] The mass squared at the origin is negative, while the mass at the minima is positive. Explicitly for the Lagrangian (6.3) the masses are

$$m(\Phi = 0) = 2m^2 \qquad m(\Phi = \pm\sqrt{\frac{-m^2}{2\lambda}}) = -4m^2 \ . \tag{6.4}$$

Thus if the theory is expressed in fields expanded around the minimum it is free of tachyons and well defined. There is nothing pathological about tachyons if the potential is bounded from below. If the latter is not the case the theory is inconsistent even in the absence of tachyons due to tunneling effects induced by instantons. As the instanton action depends on the energy difference between two extremal points, an unbounded potential has an infinite instanton action. Thus, in a consistent theory a tachyon always assumes the value in its minimum, where its mass is no longer tachyonic. Note that the theory in the minimum can look drastically different compared to the theory formulated around the maximum. The most famous theory including a tachyonic field is the standard model, where the Higgs field is tachyonic. The process of tachyon condensation corresponds in this case to the electro-weak symmetry breaking.

String theoretic tachyons do not behave much differently from their field theoretic counterparts. Their potential can be computed in a string field theory approach. It was conjectured by Ashoke Sen [172] that the open string tachyon condensation represents the decay of the D-branes where the strings end on. Thus in the real minimum of bosonic open string theory there are no branes left and the perturbative cohomology is empty. These

[1] This holds for a real field, in the case of a complex field there is a whole circle of degenerate minima with radius $\sqrt{\frac{-m^2}{2\lambda}}$.

conjectures are now proven, the analytic solution of Schnabl [173] correctly reproduces the mass of the brane as the energy difference between the vacua. The theory formulated around the true stable vacuum is known as vacuum string field theory [174]. As there are no perturbative states left due to the absence of branes, the only degrees of freedom are non-perturbative instantons, corresponding to the creation of a brane out of the vacuum. Thus by now it is well understood how open string tachyons describe brane decays. The same mechanisms apply for superstrings. While there is no analytic solution known, level truncation approaches in open superstring field theory have confirmed Sen's conjecture also in this case. In the superstring case some open tachyons get removed by the GSO projection. These correspond to the stable BPS branes which have no tachyons in their spectra. But in the spectrum of a brane-anti-brane pair a tachyon appears whose condensation describes the annihilation of the two branes.

In the closed string sector much less is understood. Localized tachyons are known to describe the decay of the defect or space they are localized at, e.g. the decay of $\mathbb{C}/\mathbb{Z}_n$ orbifolds to flat space [175] or the decay of tori into nothing. Bulk tachyons can either change the dimension of the theory or even change the type of theory. Examples of such processes have been worked out exactly by Hellerman et al. in a series of papers [18, 176–178]. Figure 2.2 in chapter 2 shows a simplified summary of the known tachyon condensations. There is a tower of bosonic theories decaying into each other which ends in a two-dimensional theory. Moreover, there are several tachyonic variants of the heterotic string. These will be discussed in the next section.

6.1.2 Heterotic String Tachyon Condensation

That the heterotic strings condense to lower dimensional theories was first worked out in [179], where it was shown that the heterotic E8 string decays to a 9-dimensional string theory. More recently the same methods were applied to the other heterotic theories [5], resulting in even lower dimensional theories.

We follow [5] and start with a partition function of a heterotic superstring theory in ten dimensions

$$Z = Z_{\mathrm{NS}} - Z_{\mathrm{R}}\,, \tag{6.5}$$

$$Z_{\mathrm{NS}} = |\eta|^{-16}\left[(Z_0^0)^8(\overline{Z_0^0})^{32} - (Z_1^0)^8(\overline{Z_1^0})^{32}\right]\,, \tag{6.6}$$

$$Z_{\mathrm{R}} = |\eta|^{-16}(Z_0^1)^8(\overline{Z_0^1})^{32}\,, \tag{6.7}$$

where η is the Dedekind eta-function and

$$Z_\beta^\alpha = \sqrt{\frac{\theta_{\alpha\beta}}{\eta}}\,. \tag{6.8}$$

The θ-functions are defined in appendix A.4.1. This partition function is modular invariant.

Expanding the partition functions to low order in q one obtains

$$Z_{\mathrm{NS}} = 32q^{-1/2} + 4032 + 188928(q\overline{q})^{1/2} + \dots \,, \tag{6.9}$$
$$Z_{\mathrm{R}} = 8388608q\overline{q} + \dots \,. \tag{6.10}$$

From this one can see that there are 32 tachyons. Moreover, the theory is non-supersymmetric as there are at each level a different amount of states in the NS and R sector. Finally, it is possible to read of the gauge group. In a heterotic string theory there are at the massless level the Kalb-Ramond field, the dilaton, the metric and a gauge field. In 8 transverse dimensions this corresponds to 64 degrees of freedom excluding the gauge field. Thus the 4032 minus the 64 other degrees of freedom should decompose into the gauge representation. A gauge field in d dimensions has $(d-2)\cdot\dim(G)$ degrees of freedom. Thus it follows that the dimension of the gauge representation is

$$\dim(G) = \frac{4032 - 64}{8} = 496 \,. \tag{6.11}$$

This is exactly the dimension of the adjoint of SO(32).[2] The free fermion formulation of the theory shows a $\mathbb{Z}_2^5$ symmetry which can be used to generate twisted versions of this partition function. These twists correspond to n of these symmetries being gauged. The partition functions are explicitly given by

$$Z_{\mathrm{NS}} = |\eta|^{-16}\left[(Z_0^0)^8 L_0^0 - (Z_1^0)^8 L_1^0\right] \,, \tag{6.12}$$
$$Z_{\mathrm{R}} = |\eta|^{-16}(Z_0^1)^8 L_0^1 \,, \tag{6.13}$$

where the L_α^β are given by [5]

$$L_0^0 = \frac{1}{2^n}(\overline{Z_0^0})^{16}\left[(\overline{Z_0^0})^{16} + (2^n-1)(\overline{Z_1^0})^{16} + (2^n-1)(\overline{Z_0^1})^{16}\right] \,, \tag{6.14}$$
$$L_1^0 = \frac{1}{2^n}(\overline{Z_1^0})^{16}\left[(\overline{Z_1^0})^{16} + (2^n-1)(\overline{Z_0^0})^{16} + (2^n-1)(\overline{Z_0^1})^{16}\right] \,, \tag{6.15}$$
$$L_0^1 = \frac{1}{2^n}(\overline{Z_0^1})^{16}\left[(\overline{Z_0^1})^{16} + (2^n-1)(\overline{Z_0^0})^{16} + (2^n-1)(\overline{Z_1^0})^{16}\right] \,. \tag{6.16}$$

These theories can be formulated for $n = 0, \dots, 5$. For $n = 0$ the theory reduces to the original SO(32) theory. From these partition functions one can read of the data listed in table 2.1, especially the theories have $t = 2^{5-n}$ tachyons. When closed string tachyons condense, they need to break the Lorentz symmetry in the dimensions which are removed from the theory. Each tachyon can thus only remove one dimension. After all tachyons condensed, there are two possibilities. First, the resulting theory is stable, then the endpoint is a $d-t$ dimensional theory. But during the condensation other fields can become tachyonic. In this case a secondary condensation appears. In all heterotic theories the endpoints are stable. In type 0 theories, there is only a single tachyon. But the resulting theories are still

[2] This does not rule out $E8 \times E8$ or even $U(1)^{496}$ yet, but the massive representations ensure that it is indeed a SO(32) theory.

tachyonic, leading to a cascade of theories ending only in a stable 2 dimensional theory. This implies that theories with at least 8 tachyons condense to 2-dimensional theories. The remaining tachyons become massless in two dimensions, such that these theories are always an endpoint of tachyon condensation. But if a theory has less than 8 tachyons, it cannot condense to a 2-dimensional theory. In these cases the theory ends up in a $10-t$ dimensional vacuum, where t is the number of tachyons in the 10-dimensional theory. Therefore the non-supersymmetric string theories with $n = 3, 4, 5$ end up in a $d = 6, 8, 9$ dimensional theory. These theories do no longer include any tachyons and are thus interesting theories to study. Their partition functions are obtained by integrating out t dimensions. This leads to

$$Z_{\rm NS} = |\eta|^{-16+2^{6-n}} \left[(Z_0^0)^{8-2^{5-n}} L_0^0 - (Z_1^0)^{8-2^{5-n}} L_1^0 \right] , \tag{6.17}$$

$$Z_{\rm R} = |\eta|^{-16+2^{6-n}} (Z_0^1)^{8-2^{5-n}} L_0^1 . \tag{6.18}$$

where L_b^a are now given by

$$L_0^0 = \frac{1}{2^n} (\overline{Z_0^0})^{16-2^{5-n}} \left[(\overline{Z_0^0})^{16} + (2^n-1)(\overline{Z_1^0})^{16} + (2^n-1)(\overline{Z_0^1})^{16} \right] , \tag{6.19}$$

$$L_1^0 = \frac{1}{2^n} (\overline{Z_1^0})^{16-2^{5-n}} \left[(\overline{Z_1^0})^{16} + (2^n-1)(\overline{Z_0^0})^{16} + (2^n-1)(\overline{Z_0^1})^{16} \right] , \tag{6.20}$$

$$L_0^1 = \frac{1}{2^n} (\overline{Z_0^1})^{16-2^{5-n}} \left[(\overline{Z_0^1})^{16} + (2^n-1)(\overline{Z_0^0})^{16} + (2^n-1)(\overline{Z_1^0})^{16} \right] , \tag{6.21}$$

Note that these are effectively the same partition functions as before, only the exponents of the untwisted Z_β^α are reduced to match the dimension. These partition functions can be integrated over the fundamental domain to obtain the cosmological constant of the theories. As usual the integration over τ_1 eliminates all states which are not level-matched. In all cases one obtains a small positive cosmological constant. How is this to be interpreted? The theories are free of anomalies and tachyons, thus they represent consistent theories. But this comes at the cost of a linear dilaton. Moreover, they are obtained by a light-like tachyon profile

$$T^i = e^{\beta X_+} X_i . \tag{6.22}$$

This has the effect of suppressing the i-th dimension in the $X_+ \to \infty$ limit. But the linear dilaton profile is along the X_1 direction. Thus only in the double limit $X_+ \to \infty$, $X_1 \to -\infty$ the theory is in a weak coupling regime and true lower dimensional. For larger X_1 one has to use a dual description. Also there is no domain wall separating these regions. All of this is phenomenologically problematic, but from a purely theoretic point of view these are still valid theories in conflict with the dS conjecture. But there is a way out of this dilemma.

The heterotic theories have 2^{n-5} tachyons. Thus the only endpoints of the condensation of heterotic theories are $d = 2, 6, 8, 9$. It appears to be impossible to construct a 4-dimensional tachyon free theory using this mechanism. It is interesting to note that

the obtained theories are in complete agreement with the cobordism conjecture. Comparing with table 6.1, one can see that the only allowed stable compactifications of a 10-dimensional theory by the cobordism conjecture are $d = 0, 1, 2, 6, 8, 9$. Tachyon condensation always stops at $d = 2$ as there are no longer any tachyons, but otherwise the obtainable theories agree exactly. Turning this argument around, the cobordism conjecture would forbid a 10-dimensional theory with $t = 3, 5, 6, 7$ tachyons in the spectrum. To test this conjecture one thus could try to classify all possible heterotic partition functions in ten dimensions. In [5] it was commented that further 10 dimensional modular invariant partition functions can be obtained by allowing for torsion in the gauged $\mathbb{Z}_2^5$ group, which corresponds to additional phases in the partition functions. If all partition functions can be classified like the GSO projections in the type 0/II theories, this would allow to reject this mechanism as a way to obtain dS, or, if a theory with 6 tachyons exists, to construct a 4-dimensional dS theory.

Without knowing if such a 10-dimensional theory exists, we can still say something about the would be 4-dimensional theory. The gauge algebras arising from possible twists are of the form $\mathfrak{so}(t)\mathfrak{so}(32-t)$, where t is again the number of tachyons. The $\mathfrak{so}(32-t)$ factor can be enhanced to a larger gauge algebra of the same rank. When the tachyons condense, the $\mathfrak{so}(t)$ factor gets broken, while the $\mathfrak{so}(32-t)$ factor remains intact. Thus if there would exist a twist to 6 tachyons, the resulting 4-dimensional theory would include a $\mathfrak{so}(26)$ gauge algebra or an enhanced version of it, i.e. a algebra of rank 13. This algebra is large enough to embed any GUT gauge group usually used. It would be interesting to see if these theories exist and to study them, but we leave this for future work.

6.1.3 Closed Bosonic String Tachyon

After having discussed the 10-dimensional tachyon condensations, we will now turn to the 26-dimensional closed string tachyon. This was one of the first tachyons to appear in string theory, yet it is still unclear what it condenses to. In the usual approaches to study string theory it mainly gets ignored, stating that in a supersymmetric construction the bulk tachyon gets projected out by a GSO projection. As we have seen in the last section, non-supersymmetric tachyons can lead to interesting lower dimensional theories, thus the endpoint of the bosonic bulk tachyon could be an interesting theory. In view of the c-theorem, stating that different UV conformal field theories flow to the same IR CFT, the bosonic tachyon is especially interesting as bosonic string theory with $c = 26$ is one of the best studied CFTs with a large central charge.

The potential of the closed string bulk tachyon has been studied in detail in bosonic string field theory [86, 180–184]. A high level computation to quintic order shows the existence of a stable non-perturbative vacuum with a non-zero tachyon vev. Unlike the case of open tachyon condensation it is unknown if the cohomology of the theory formulated around this vacuum is empty. As the energy of the potential at the minimum seems to converge to a non-zero value it is also unclear how to interpret this value. In the open string case the value of the potential corresponds to the tension of the brane. An analogous interpretation in the case of closed strings would correspond to an energy of space-time.

But as the process changes the number of dimensions in the theory it is unclear how to even define an energy.

The meaning of the non-perturbative minimum is still unclear. One conjecture is that it resembles one of the supersymmetric 10 dimensional theories and the tachyon thus describes the decay of 16 dimensions [185]. As the left-moving sector of the heterotic string theories can be describes by the bosonic string compactified on a 16-dimensional lattice, a mechanism could exist which freezes out the remaining d.o.f. of the 16 dimensions by condensing the bulk tachyon [186].

More recently in [187] the bosonic bulk tachyon potential was studied in a superstring field theory setup. Due to the complexity of the computation it was performed only at massless level and cubic order, but already at this level the result deviates from the bosonic string field theory result. Additional tachyonic states originate from the supersymmetric ghosts, destabilizing the bosonic solutions. At the low orders studied in [187] the potential appears to be unbounded from below. Of course the same appears to be the case for the potential in the bosonic SFT at quartic order and only gets resolved at higher orders. As these seem to be out of reach at this time it is unclear how to interpret the results of [187]. Nevertheless it is interesting that even 40 years after the discovery of the closed bulk tachyon, it is still unclear what its true meaning is.

This finishes the discussion of tachyon condensation. As we have seen, tachyons can result in a loophole for the usual conjectures. But they also seem to respect the cobordism conjecture and do not result in 4-dimensional dS theories. In the next section another possible loophole will be investigated, a change of the signature of spacetime, either of the world-sheet or of the target space.

6.2 Exotic String Theories

As we have seen in the previous sections, 4-dimensional dS seems to not be obtainable from the usual 10 dimensional string theories. Non-supersymmetric compactifications on CY 3-folds suffer from bubbles of nothing, while the tachyon condensations which remove the extra dimensions are constraint in such a way that they never lead to a 4-dimensional theory. In this section we will try to think about another way around the no-go conjecture, by modifying the signature of spacetime. The usual constraints on the allowed dimensions in string theory, like the vanishing of the conformal anomaly, the nilpotence of the BRST operator or the little group of the graviton, only restrict the allowed number of dimensions, not the metric signature. The usual choice is the signature $(d-1,1)$. For this choice no-ghost theorems can be proven [188].[3] Note that with ghosts in the following we mean Pauli-Villar ghosts, i.e. states of negative norm which violate unitarity. A ghost field has the wrong sign of the kinetic term in the Lagrangian. Note that this is not in one-to-one correspondence with tachyons, which have negative mass squared or equivalently imaginary mass, but the correct sign of the kinetic term. For other signatures no analogous theorems

[3]The same theorem holds in 2 time dimensions for the $\mathcal{N}=2$ string, i.e. signature (2,2) corresponding to one complex time boson.

are known. But nevertheless there exists a whole net of exotic string theories in different signatures. The aim of this section is a study of the phenomenology of these theories. The section closely follows [12]. We will start with a short motivation why additional times allow the construction of dS spaces by Wick-rotating the well known $AdS \times S^5$ solution of the type II string. After reviewing the net of theories, the quantization of closed and open strings in arbitrary dimensions is worked out, including the boundary states required for D-branes and O-planes. This will then be used to identify ghost-free gauge-subsectors of the theories.

6.2.1 Fluxed $AdS \times dS$ Solutions

In this section we first recall that in theories with more time-like directions the $AdS_5 \times S^5$ solution of type IIB supergravity generalizes to solutions containing de Sitter spaces (cf. [189]). The natural habitat of these solutions are Hull's exotic string theories that we review in the second part of this section. The prototype solution of the type IIB superstring theory with flux is $AdS_5 \times S^5$ with self-dual five-form flux supported on AdS_5 and S^5, respectively. Of course this theory has just a single time-like coordinate which is part of the AdS_5 background. The question that we would like to approach in this section is what happens if more than one of the ten directions of type IIB were time-like, i.e. on a space with signature $(10-p, p)$. For the five-form to still satisfy a self-duality relation, one must have p odd.

The 10D effective (quasi-)action governing the dynamics of the metric and a form field C_{n-1} reads

$$S \sim M_s^8 \int d^{10}x \sqrt{|G|} \left(e^{-2\phi} R - \frac{\kappa}{2} |F_n|^2 \right) , \tag{6.23}$$

where in the following we will set the dilaton to a constant. This is justified for the actual case of interest, namely the R-R four-form, for which in addition one has to impose the self-duality relation $F_5 = \pm \star F_5$ by hand and change the prefactor of $|F_n|^2$ to $\kappa/4$. Here we have left the sign $\kappa = \pm 1$ of its kinetic term open, where $\kappa = 1$ is the usual case. The kinetic term of the n-form F_n is defined as

$$|F_n|^2 = \frac{1}{n!} G^{i_1 j_1} \dots G^{i_n j_n} F_{i_1 \dots i_n} F_{j_1 \dots j_n} . \tag{6.24}$$

The resulting equation of motion for the metric reads

$$R_{ij} - \frac{1}{2} g_{ij} R \;=\; \frac{\kappa}{2(n-1)!} \left(F_{i\, k_2 \dots k_n} F_j^{k_2 \dots k_n} - \frac{1}{2n} g_{ij} F_{k_1 \dots k_n} F^{k_1 \dots k_n} \right) \tag{6.25}$$

and for C_{n-1}

$$\partial_i \left(\sqrt{|G|}\, F^{i\, k_2 \dots k_n} \right) = 0 . \tag{6.26}$$

We can write the first relation (6.25) as a matrix equation $\mathbf{R} = \kappa \mathbf{T}$.

Now, we want to consider these equations in a theory with more time-like directions. Generalizing the $AdS_5 \times S^5$ solutions, we make the Ansatz

$$AdS_{5-m,m} \times dS_{5-n,n}\,, \qquad \text{with} \quad m+n=p=\text{odd}\,. \tag{6.27}$$

The description of such multiple times AdS and dS spaces is reviewed in appendix A.1. For a self-dual five-form flux we can then solve (6.26) simply by choosing F_5 to satisfy the Bianchi identity $dF_5 = 0$. This is the case for

$$F_5 = fE^1 \wedge \ldots \wedge E^5 - f\mathcal{E}^1 \wedge \ldots \wedge \mathcal{E}^5 \tag{6.28}$$

with constant f and with the 5-beins of $AdS_{5-m,m}$ and $dS_{5-n,n}$ as reviewed in appendix A.1. Choosing the same curvature radius α for the AdS and dS factors, the Ricci scalar vanishes and the left hand side of (6.25) becomes

$$\mathbf{R} = \begin{pmatrix} -\frac{4}{\alpha^2}\eta^{(m,5-m)} & 0 \\ 0 & \frac{4}{\alpha^2}\eta^{(n,5-n)} \end{pmatrix}. \tag{6.29}$$

The right hand side then is

$$\kappa\mathbf{T} = \kappa\,(-1)^n \begin{pmatrix} -\frac{f^2}{4}\eta^{(m,5-m)} & 0 \\ 0 & \frac{f^2}{4}\eta^{(n,5-n)} \end{pmatrix}. \tag{6.30}$$

Therefore, for $\alpha = 4/f$ the equations of motion are satisfied if we choose $\kappa = 1$ for n even and $\kappa = -1$ for n odd.

Let us mention a few special cases: For $m = 1$, $n = 0$ one gets the original $AdS_5 \times S^5$ solution and for $m = 0$, $n = 1$ one finds $\mathcal{H}_5 \times dS_{4,1}$, where $\mathcal{H}_5$ denotes the hyperbolic 5-space. However, the price one has to pay to get this simple solution is that the R-R five-form has the wrong sign of the kinetic term.

We note that all these solutions can also be understood by applying $(m-1, n)$ Wick-rotations to the respective coordinates of the original type IIB $AdS_5 \times S^5$ background. From this perspective, in order to keep F_5 purely real or imaginary, one has to apply either an $(\text{even}, \text{even})$ or an (odd, odd) number of Wick-rotations. In the first case, F_5 remains real, giving the solutions with n even and $\kappa = 1$. In the second case however, F_5 becomes purely imaginary, so the sign of the kinetic term indeed changes and one finds the n odd, $\kappa = -1$ solutions. If for the original type IIB the 5-form is chosen to be self-dual $\star F_5 = F_5$, the Wick rotation changes this to $\star F_5 = \kappa F_5$. Thus, the sign of the kinetic term of F_5 and the one in the self-duality relation are related.

We have seen that in type IIB-like supergravities with multiple time directions and possibly wrong signs of the kinetic term for the 5-five form, dS solutions do exist. Of course, our analysis was only applied to a subsector of the full initial type IIB supergravity action so that one might wonder whether fully consistent supergravity or string theories exist that exhibit precisely those two features.

6.2.2 Exotic Superstring Theories

Since the early work of Hull [190,191] it is known that string theories with exotic signatures arise from the usual type II theories with $(9,1)$ signature by applying successive T-duality also along time-like directions. This leads to an intricate web of dual theories in ten dimensions of more general signature $(10-p,p)$, whose supergravity actions (quadratic in derivatives) are similar to the type II actions but contain kinetic terms of opposite sign. Despite these apparent ghosts, it was argued that each theory of this duality web represents a different limit of ordinary type II theories, and as a full non-perturbative theory should therefore be intrinsically well-behaved.

However, since these theories are reached via a circle compactification of a time-like direction, they could also all be severely pathological, as at an intermediate step closed time-like curves are encountered that are generally thought to be highly problematic. In the course of this paper we assume that this is not the case and that Hull's exotic theories can make sense.

The de Sitter solutions from the previous subsection will find their natural home in these exotic supergravity theories, meaning that they arise as solutions to the effective theories at leading order in derivatives and at weak string coupling. Therefore, it is this limit that we are most interested in. The perturbative spectrum of the exotic closed string theories which arises via quantization of the corresponding fundamental string was recently worked out in [4]. As expected, the perturbative description of exotic theories carries many pathologies, most prominently ghosts. In this section we review the bouquet of exotic string theories, for more details we refer to the original literature.

The zoo of type II$^{\alpha\beta}$ theories

T-duality along a space-like direction exchanges type IIA and IIB string theory. Along a time-like direction, this cannot be the case. For instance, Dirichlet and Neumann boundary conditions of a D-brane are interchanged in the direction that T-duality is applied to. Since regular type II theories only contain Lorentzian D-branes, this means that the T-dual theory can only have Euclidean branes.

Adopting the notation introduced in [4], we label the theories as $\text{IIA}^{\alpha\beta}_{(10-p,p)}$ and $\text{IIB}^{\alpha\beta}_{(10-p,p)}$ with two signs $\alpha,\beta\in\{+,-\}$ and the space-time signature $(10-p,p)$. The first sign indicates whether the theory contains Lorentzian $(+)$ or Euclidean $(-)$ fundamental strings, while the second indicates the same for D1/D2 branes. Here, we will call any even (odd) number of time-like directions Euclidean (Lorentzian). If the signature is omitted we assume $(9,1)$. The usual string theories in this notation are IIA^{++}, IIB^{++}. We will also use the notation IIA^{L} and IIB^{L} collectively for all theories with Lorentzian fundamental strings and IIA^{E} and IIB^{E} for the ones with Euclidean strings.

Starting from the usual string theories, time-like T-duality as discussed above leads to Euclidean branes of one dimension less. This means that $(\text{IIA}^{++}\leftrightarrow\text{IIB}^{+-})$ and $(\text{IIB}^{++}\leftrightarrow\text{IIA}^{+-})$ are related by time-like T-duality, just as $(\text{IIA}^{++}\leftrightarrow\text{IIB}^{++})$ and $(\text{IIB}^{+-}\leftrightarrow\text{IIA}^{+-})$ are space-like T-duals.

Now taking the strong coupling limit of the type IIB theories, S-duality acts by exchanging F1↔D1 and NS5↔D5, while D3 is self-dual. Then while IIB^{++} is self-dual, IIB^{+-} has Euclidean D-branes that now get exchanged with the fundamental string and NS5-brane. The resulting theory must be of type IIB^{-+} with Lorentzian D1 and D5 and Euclidean F1, NS5 and D3-branes.

One can now complete the type II picture by considering the T-duals of this exotic IIB^{E} theory. However since the D-branes of type IIB^{-+} are not homogeneously Lorentzian, one can see that type IIB^{-+} compactified along a space-like circle must be dual to a theory compactified along a time-like direction! This theory has Euclidean D2-branes and is thus of type $\text{IIA}^{--}_{(8,2)}$.

All theories with Euclidean F1 have the property that T-duals are with respect to different signature directions. Their respective D-brane spectrum is alternating between Euclidean and Lorentzian as was the case for type IIB^{-+}, and each T-dualization changes the signature. The list of T-dual theories with Euclidean fundamental strings is schematically given by

$$\text{IIA}^{-+}_{(10,0)} \leftrightarrow \text{IIB}^{-+}_{(9,1)} \leftrightarrow \text{IIA}^{--}_{(8,2)} \leftrightarrow \text{IIB}^{--}_{(7,3)} \leftrightarrow \text{IIA}^{-+}_{(6,4)} \leftrightarrow ... \leftrightarrow \text{IIB}^{-+}_{(1,9)} \leftrightarrow \text{IIA}^{--}_{(0,10)} \tag{6.31}$$

where going to the right (left) means T-dualizing along a space-like (time-like) direction.

Now that we have found more signatures of type IIB^{-+}, we can S-dualize back to the theories with Lorentzian fundamental strings, where we find that they correspond to type IIB^{+-} with the same signatures. The full bouquet of dual theories and their relations is shown in figure 6.2.

For completeness let us mention that the strong coupling limit of the type IIA theories are two M-theory variants. In other words, the type IIA theories arise from M theories with Lorentzian or Euclidean M2-branes on various signatures, compactified on space- or time-like circles. For more on the exotic M-theories see [4, 191].

Type $\text{II}^{\alpha\beta}$ supergravities

The bosonic parts of the low-energy SUGRA actions for the exotic theories have been worked out in [190, 191]. Here we provide the compact presentation given in [4]. As usual the 10D actions are given by a sum over NS-NS, R-R and Chern-Simons contributions

$$S[\text{IIA/B}^{\alpha\beta}] = S^{\alpha\beta}_{\text{NS}} + S_{\text{R}}[\text{A/B}]^{\alpha\beta} + S_{\text{CS}}[\text{A/B}]\,, \tag{6.32}$$

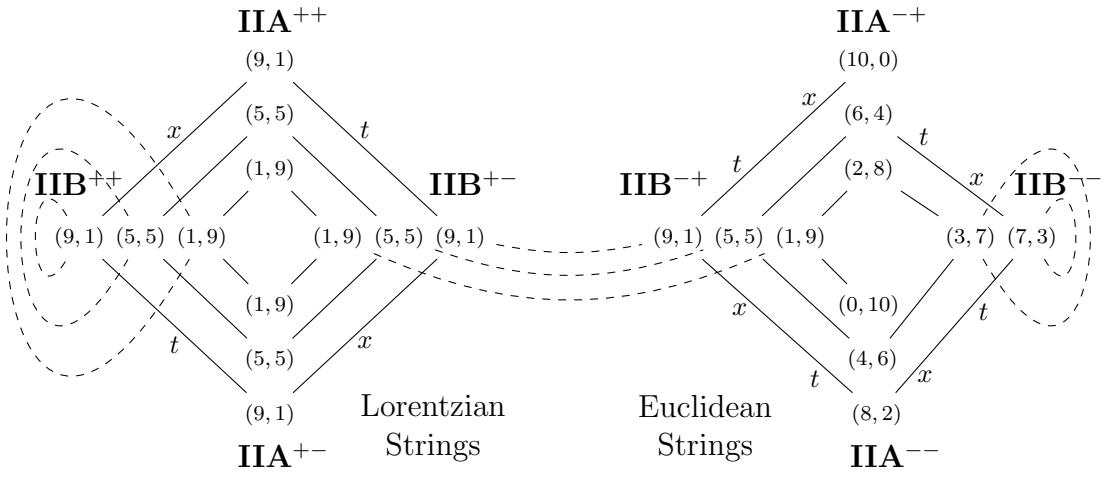

Figure 6.2: T-dualities (solid lines) and S-dualities (dashed lines) relating type II string theories. The label x (t) indicates dualities arising from compactification on a spatial (time-like) circle. The left side consists of the type $\mathrm{IIA}^{\mathrm{L}}/\mathrm{IIB}^{\mathrm{L}}$ theories with Lorentzian fundamental strings, the theories with Euclidean fundamental strings ($\mathrm{IIA}^{\mathrm{E}}/\mathrm{IIB}^{\mathrm{E}}$) are on the right. (Diagram adopted from [4])

where the NS-NS part is the same for type IIA and IIB and the CS part is independent of α, β. The respective terms in the action are given by

$$\begin{aligned}
S_{\mathrm{NS}}^{\alpha\beta} &= \frac{1}{2\kappa_{10}^2}\int \mathrm{d}^{10}x\sqrt{|\det G|}\; e^{-2\Phi}\Big[\mathcal{R} + 4(\nabla\Phi)^2 - \frac{\alpha}{2}|H_3|^2\Big]\,,\\
S_{\mathrm{R}}[\mathrm{A}]^{\alpha\beta} &= -\frac{1}{2\kappa_{10}^2}\int \mathrm{d}^{10}x\sqrt{|\det G|}\left[\frac{\alpha\beta}{2}|F_2|^2 + \frac{\beta}{2}|\tilde{F}_4|^2\right]\,,\\
S_{\mathrm{R}}[\mathrm{B}]^{\alpha\beta} &= -\frac{1}{2\kappa_{10}^2}\int \mathrm{d}^{10}x\sqrt{|\det G|}\left[\frac{\alpha\beta}{2}|F_1|^2 + \frac{\beta}{2}|\tilde{F}_3|^2 + \frac{\alpha\beta}{4}|\tilde{F}_5|^2\right]\,,\\
S_{\mathrm{CS}}[\mathrm{A}] &= -\frac{1}{4\kappa_{10}^2}\int B_2\wedge F_4\wedge F_4\,,\\
S_{\mathrm{CS}}[\mathrm{B}] &= -\frac{1}{4\kappa_{10}^2}\int B_2\wedge F_3\wedge F_5\,,
\end{aligned} \tag{6.33}$$

where $H_3 = dB_2$, $F_p = dC_{p-1}$, and $\tilde{F}_p = F_p - H_3\wedge C_{p-3}$. These actions are very reminiscent of the usual SUGRA actions (2.77), only modified by some signs α and β .The actions are all independent of the respective signature (p,q), and as usual one has to additionally require (anti-)self-duality $\tilde{F}_5 = (\alpha\beta)\star\tilde{F}_5$ in the type IIB variants. Note that as in the previous subsection the sign of the kinetic term of the 5-form flux is correlated with the sign in the self-duality relation. Moreover, we have set the Romans mass of type IIA

variants to zero for simplicity.

It is clear that in general these actions feature the appearance of ghost states, i.e. states whose kinetic term has the wrong sign. This sign is the result of two effects. First, there is the overall sign of the kinetic terms in (6.33) and second the combination of signs of the inverse metric factors in

$$\mathcal{L}_{\text{kin}} \sim -\kappa \sqrt{|G|}\, |F_n|^2 = -\frac{\kappa}{n!} \sqrt{|G|}\, G^{i_1 j_1} \dots G^{i_n j_n}\, F_{i_1 \dots i_n}\, F_{j_1 \dots j_n} \,. \tag{6.34}$$

If $\kappa = +/-1$, an odd/even number of time-like indices indicates a ghost. The presence of ghosts is of course strongly related to the existence of dS solutions. Recall that in section 6.2.1 we have seen that theories with ghosts can admit solutions to the SUGRA equations of motion that contain dS factors. These ghosts could arise either due to wrong overall signs of the kinetic terms or due to extra time-like directions. These are precisely the two issues that also appear for the exotic superstring theories, making them the natural framework for a string theory embedding of the dS solutions of section 6.2.1. While dS is conjectured to be forbidden in string theory and there exist no-go theorems in certain setups, compare section 4.1, the derivation of most of the arguments implicitly assumes that all fields have the usual kinetic terms. The explicit dS solutions show that violations of the dS no-go theorems can potentially arise from the presence of ghost fields. For a concrete set-up, an effective 4D potential is generated via dimensional reduction of an exotic string theory on some internal space with non-trivial fluxes turned on. Whether this effective potential indeed admits dS minima requires a more detailed investigation, but as long as there are ghosts present we expect that the no-go theorems will not hold. But there could be ways around this problem. In the next section we will examine the ghosts more closely, as well as the possibility to remove them by applying an orbifold construction.

6.2.3 Ghosts in Exotic String Theories

In this section we continue the discussion of ghosts in the exotic string theories. Ghosts are states of negative norm in the Hilbert space, preventing a probabilistic interpretation and, even when removed by hand from the set of physical states, leading to a violation of unitarity. While they might be an important ingredient to find dS solutions, massless or light ghosts are phenomenologically excluded.

A standard procedure to get rid of such states is to gauge more symmetries on the world-sheet, hence introducing new (b, c) ghost systems that change the critical central charge of the theory and cancel the contributions of the problematic ghosts. A famous example is the $N = 2$ superstring with a critical central charge of $c = 6$ and a four-dimensional target-space of signature $(2, 2)$ or $(0, 4)$ [20]. Due to the extra gauge symmetry, more target-space directions can be gauged away.

However, since we do not want to change the critical dimension, there will only be the usual gauge invariances leading to a critical central charge of 26 (15) for the bosonic (super) string theory. This means there will be a single distinctive time direction and the corresponding bc (and $\beta\gamma$) ghost system. Let us analyze the appearance of ghosts for the

Lorentzian IIA$^{\mathrm{L}}$/IIB$^{\mathrm{L}}$ theories and the Euclidean IIA$^{\mathrm{E}}$/IIB$^{\mathrm{E}}$ theories in more detail. For simplicity, we present the string world-sheet arguments only for the bosonic string, while they analogously hold for the superstring theories.

Ghosts for the Lorentzian string

The Lorentzian fundamental strings in the IIA$^{\mathrm{L}}$/IIB$^{\mathrm{L}}$ theories can be quantized in complete analogy to the usual IIA and IIB (super-) strings with signature $(9,1)$. This means that the mode algebra for the bosonic fields X^μ reads

$$[\alpha_m^\mu, \alpha_n^\nu] = m\, \eta^{\mu\nu}_{(10-p,p)}\, \delta_{m,-n}\ , \tag{6.35}$$

where $\eta^{\mu\nu}_{(10-p,p)}$ denotes the flat metric of signature $(10-p,p) \in \{(9,1),(5,5),(1,9)\}$. In the following let us denote the space-like directions and the single universal time direction with indices $m, n, \ldots$ and the additional new time-like directions by $a, b, \ldots$. Note that the universal time and one space direction can be gauged away as usual. Then for instance the off-diagonal graviton states

$$|V_G^{st}(0)\rangle = \epsilon_{\mu a}\alpha_{-1}^m \tilde{\alpha}_{-1}^a |0\rangle \tag{6.36}$$

have negative norm (for $\langle 0|0\rangle = 1$) and give physical ghosts that cannot be gauged away. Note that the graviton modes $|V_G^{ss}(0)\rangle = \epsilon_{\mu\nu}\alpha_{-1}^m\tilde{\alpha}_{-1}^n|0\rangle$ and $|V_G^{tt}(0)\rangle = \epsilon_{ab}\alpha_{-1}^a\tilde{\alpha}_{-1}^b|0\rangle$ have positive norm.

In the NS-NS sector of the superstring, one only has to replace the X^μ by their fermionic superpartners ψ^μ and the logic goes through analogously. In the R-R sector, there is the distinction between the IIA/B^{++} and the IIA/B^{+-} theories, where the latter carry a wrong overall sign for the kinetic terms of the massless R-R fields. This can be taken care of in the world-sheet theory by flipping by hand the overlap between the R-R ground states

$$\langle 0|0\rangle_{\mathrm{RR}}^{+-} = -\langle 0|0\rangle_{\mathrm{RR}}^{++}\,. \tag{6.37}$$

Light cone gauge and Lorentz symmetry

The (time-like) T-duality arguments suggest that a change of the target-space signature does not affect the critical dimension of the string theory. Let us check this explicitly on the world-sheet. This can be readily seen for the bosonic string in light cone gauge by checking for anomalies of the $SO(p,q)$ Lorentz symmetry. The world-sheet metric is fixed as $h_{\alpha\beta} = \eta_{\alpha\beta}$ and we introduce light cone coordinates in space time $X^+ = 1/\sqrt{2}\,(X^0 + X^1)$, $X^- = 1/\sqrt{2}\,(X^0 - X^1)$, where we singled out one time and spatial direction X^0, X^1. The target-space metric becomes $\eta_{+-} = \eta_{-+} = -1$ for the light cone, $\eta_{ab} = -\delta_{ab}$ for $a, b = 1, \ldots, p-1$ remaining time directions and $\eta_{mn} = \delta_{mn}$ for the $m, n = 1, \ldots, q-1$ spatial directions.

We follow the standard procedure and look at the open string with (NN) boundary conditions. The remaining gauge freedom is fixed by setting $X^+(\sigma,\tau) = x^+ + p^+\tau$. Using

the Virasoro constraint equation $\eta_{\mu\nu}(\dot{X}^\mu \pm X'^\mu)(\dot{X}^\nu \pm X'^\nu) = 0$ to express the oscillator modes of X^- in terms of the transverse modes yields

$$\alpha_n^- = \frac{1}{p^+}\left(\frac{1}{2}\sum_{k=-\infty}^{\infty} :\eta_{ij}\,\alpha_{n-k}^i\alpha_k^j: - a\,\delta_{n,0}\right) \tag{6.38}$$

with i, j running over the transverse directions and for simplicity setting $\alpha' = 1/2$. The modes still satisfy a "transverse" Virasoro algebra

$$\begin{aligned}\left[p^+\alpha_m^-, p^+\alpha_n^-\right] =& (m-n)\,p^+\alpha_{m+n}^- + \\ & \left(\frac{D-2}{12}(m^3-m) + 2am\right)\delta_{m+n}\end{aligned} \tag{6.39}$$

and have commutation relations with the transverse oscillator modes

$$\left[\alpha_n^i, p^+\alpha_k^-\right] = n\,\alpha_{n+k}^i\,. \tag{6.40}$$

The only relevant appearance of the space-time metric is in commutation relations $[\alpha_m^\mu, \alpha_n^\nu] = k\,\eta^{\mu\nu}\delta_{m+n,0}$. We can use these commutation relations and follow the standard computation for the potentially anomalous commutator $[J^{i-}, J^{j-}]$ of Lorentz generators $J^{\mu\nu}$. Doing so we find

$$\left[J^{i-}, J^{j-}\right] = 0 \quad \Leftrightarrow \quad D = 26,\, a = 1\,, \tag{6.41}$$

but no additional constraints on the number of time respectively spatial dimensions. Hence Lorentz symmetry $SO(p, q)$ is preserved for a total of $p + q = 26$ space-time dimensions.

Orbifolding ghosts

Generally, having a theory that has too many degrees of freedom one can proceed in two ways. Either one gauges extra symmetries or one projects out the unwanted states. Since gauging symmetries completely removes the time-like directions, we want to take the second route. Can one remove the massless ghosts by performing an appropriate orbifold projection? In contrast to the gauging procedure an orbifold will not change the critical central charge, but will potentially break the 10D diffeomorphism symmetry to a subgroup.

Following the usual recipe for performing an orbifold in string theory, the untwisted sector is projected to invariant states and a twisted sector must be introduced. Let us discuss appropriate orbifold projections to remove light ghosts from the Lorentzian theories. In the IIA/$\mathrm{B}^{+-}_{(9,1)}$ theory, the ghost R-R fields can be projected out by performing an orbifold by $(-1)^{F_L}$. To avoid the appearance of new massless ghosts in the $\mathbb{Z}_2$ twisted sector, one can combine this action with a half-shift $S : X \to X + \pi R$ along a compactified spatial direction. For the IIA/$\mathrm{B}^{++}_{(5,5)}$ theories physical ghosts are related to four extra time-like directions. These ghosts can be removed by taking the quotient by a $\mathbb{Z}_2$ reflection $I_4 : x^a \to -x^a$ along these four directions. Similarly, the ghosts in IIA/$\mathrm{B}^{++}_{(1,9)}$ are removed by I_8, reflecting the eight extra time-like coordinates. Finally, the massless ghosts of IIA/$\mathrm{B}^{+-}_{(5,5)}$ and IIA/$\mathrm{B}^{+-}_{(1,9)}$ are projected out by $I_4(-1)^{F_L}$ and $I_8(-1)^{F_L}$, combining the previous reasoning. These results are summarized in figure 6.3.

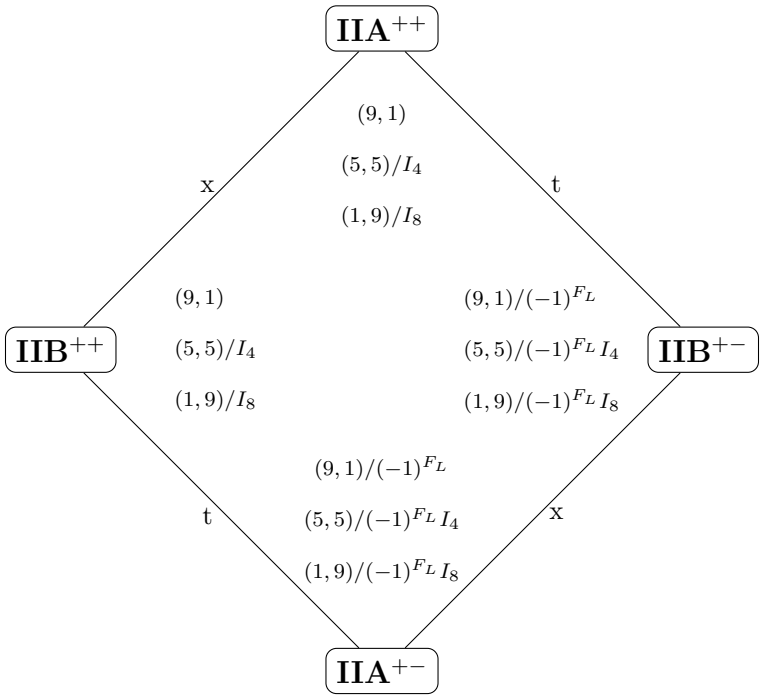

Figure 6.3: Orbifold projections that remove the massless ghosts for Lorentzian theories. New ghosts in twisted sectors can be avoided by combining these actions with a shift along a spatial direction.

Compact time-like dimensions

Eventually, we are interested in compactifications of the exotic string theories to 4 dimensions with signature $(3, 1)$, so in theories with multiple time-like directions some of them will need to be compactified. The standard problem of compact time-like dimensions are closed time-like curves which violate causality. Since the orbifolds project out massless excitations in these directions, one might naively think that the quotient theories are safe. However, we will see that compact time dimensions in exotic string theories lead to further complications.

For the $\mathrm{IIA}/\mathrm{B}^{+-}_{(9,1)}$ theory the orbifold by $(-1)^{F_L}$ removes all ghost fields from the untwisted sector. In case of the $\mathrm{IIA}/\mathrm{B}^{++}_{(5,5)}$ theories however, even though the massless mixed graviton modes $|V_G^{(ev,odd)}(0)\rangle = \epsilon_{ma}\alpha^m_{-1}\tilde{\alpha}^a_{-1}|0\rangle$ are projected out, for non-vanishing momentum/energy the linear combination

$$|V_G^{(ev,odd)}(p^n, e^b)\rangle = \epsilon_{ma}\alpha^m_{-1}\tilde{\alpha}^a_{-1}|p^n, e^b\rangle - \epsilon_{ma}\alpha^m_{-1}\tilde{\alpha}^a_{-1}|p^n, -e^b\rangle \tag{6.42}$$

remains in the spectrum. Here the upper index pair indicates the behavior of the left and right moving part under the $\mathbb{Z}_2$ operation. Here p^n, $m, n \in \{0, 1, \ldots, 5\}$ denote the usual energy $p^0 = E$ and space-like momenta, and e^b, $a, b \in \{6, \ldots, 9\}$ denote the extra time-like

energies. Therefore, there are still massive ghosts in the string spectrum, a $\mathbb{Z}_2$ projection does not allow to remove all of them.

The on-shell condition for such a state is

$$E^2 + \sum_a (e^a)^2 = \sum_i (p^i)^2 + m^2 \,, \tag{6.43}$$

where m is the mass of the state. We interpret this condition such that for a state of mass m with momenta p^i the total energy can be distributed among all the time-like energies such that this quadratic relation is satisfied [192]. Only E is the energy that we have access to. Note that while for negative E we have an interpretation in terms of anti-particles with positive E, the additional energies e^a can be both positive and negative.

Let us now consider a Lorentzian string on a time-like torus of radius R . As for a space-like compactification, the time-like momentum (i.e. energy) gets quantized along the compact direction and leads to a mass contribution, resulting in a KK tower of massive states. Similarly, the winding modes contribute to the mass so that in total we find the on-shell condition

$$E^2 + \sum_b \left[\left(\frac{m_b}{R}\right)^2 + \left(\frac{n_b R}{\alpha'}\right)^2 \right] = \sum_i (p^i)^2 + \frac{2}{\alpha'}(N + \overline{N} - 2a) \tag{6.44}$$

with $a = 1/2$ for the superstring and the level-matching condition $\sum_a m_a n_a = -(N - \overline{N})$. For $R > \sqrt{\alpha'}$ it is tempting to identify a UV cutoff with the Kaluza-Klein scale $\Lambda_{\rm UV} = 1/R$ that we assume to be only a few orders of magnitude below the string scale. Let us analyze this on-shell condition in the IR regime $|p| < \Lambda_{\rm UV}$.

In the massless sector $N = \overline{N} = 1/2$, a non-vanishing time-like KK/winding mode $(m_a, n_a) \neq (0, 0)$ already lies outside the IR regime. Thus all the light on-shell states that we have access to are frozen in the extra time directions and feature $e^a = 0$. Then together with the $\mathbb{Z}_2$ projections there are no light ghosts left, so it seems that we are safe. However, for the tower of massive string excitations $N = \overline{N} > 1/2$ their contribution to the right hand side of (6.44) can be balanced against KK/winding contributions. Therefore, these massive excitations combine with time-like KK/winding modes to appear as extremely light particles from a 4D perspective. As already observed in [4], even for irrational values of the radius there will always be integers $N, \overline{N}, m_a, n_a$ such that their 4D mass lies below any cut-off. Related, there exist kinematically allowed scattering processes like

$$\begin{aligned} |V_{m_1=0}(p_1^m, e_1^a = 0)\rangle + |V_{m_2=0}(p_2^m, e_2^a = 0)\rangle \\ \longrightarrow |V_{m_3>0}(p_3^m, e_f^a)\rangle + |V_{m_4>0}(p_4^m, -e_f^a)\rangle \end{aligned} \tag{6.45}$$

with the extra energies in the final state $e_f^a \neq 0$. Thus, the ultralight states with $N = \overline{N} > 1/2$ do not decouple in the scattering amplitudes of massless states with $N = \overline{N} = 1/2$. We can summarize these findings by saying that the dimensionally reduced 10D Lorentzian supergravity actions cannot be considered as Wilsonian effective actions of a 4D theory.

Ghosts for the Euclidean string

The quantization of the Euclidean fundamental string has been investigated in [4] and features a couple of new aspects and pathologies. Note that this theory is different from the Wick rotated Lorentzian string. In section 6.2.4 we will review and continue this analysis, where our special focus will be on the construction of boundary states, providing the CFT description of D-branes for these exotic string theories.

One new aspect of the quantization is that factors of $i = \sqrt{-1}$ appear at various places. For instance, the mode algebra for the bosonic fields X^μ now reads

$$[\hat{\alpha}^\mu_m, \hat{\alpha}^\nu_n] = -i\, m\, \eta^{\mu\nu}_{(10-p,p)}\, \delta_{m,-n} \ . \tag{6.46}$$

As a consequence, the diagonal graviton/B-field states $|V_G^{ss}(0)\rangle$ and $|V_G^{tt}(0)\rangle$ have negative norm and the off-diagonal ones $|V_G^{st}(0)\rangle$ positive norm (for $\langle 0|0\rangle = 1$). However, this is not consistent with the normalization of the Einstein-Hilbert term for the Euclidean string SUGRA actions (6.33). This can be remedied by choosing the correct normalization of the vertex operators. These have been worked out in [4]. The graviton gets an extra factor of $-i$, rendering its norm positive, while the B-field remains a ghost. Of course the time-like ghosts from the previous section also remain in the spectrum.

Orientifolding ghosts

Now we investigate whether there also exist $\mathbb{Z}_2$ operations that can mod out all the massless ghost fields for the Euclidean exotic string theories $\text{IIA}^E/\text{IIB}^E$. Let us start with the $\text{IIB}^{-+}_{(9,1)}$ theory, which is the S-dual of the $\text{IIB}^{+-}_{(9,1)}$ theory. By looking at its SUGRA action (6.33) we see that H_3, F_1, F_5 have the wrong sign of the kinetic terms and F_3 the usual sign. These are precisely the p-form fields that are odd and even under the world-sheet parity transformation Ω, and indeed the S-dual of $(-1)^{F_L}$ is known to be Ω. Therefore, the orientifold $\text{IIB}^{-+}_{(9,1)}/\Omega$ has no ghost fields in the closed string sector. Depending on whether the orientifold projection has fixed loci or acts freely (after combining it again with a shift symmetry), there will be a twisted sector in the form of appropriate D-branes that need to be introduced to cancel the R-R tadpole of the O-plane. This open string sector can host additional ghosts. We will come to this point in section 6.2.6.

Now by successively applying spatial T-dualities we can find the orientifold projections for all the $\text{IIA/B}^{-,\beta}_{(10-p,p)}$ theories. After one T-duality one gets $\text{IIA}^{--}_{(8,2)}$ with the projection ΩI_1, where I_1 reflects the new additional time-like coordinate. The corresponding branes are D8-branes localized at a point in the new time-like direction. Another T-duality leads to the $\text{IIB}^{--}_{(7,3)}/\Omega I_2(-1)^{F_L}$ orientifold, etc. All the resulting quotients are shown in the right hand part of figure 6.4. T-dualizing instead along the time-like direction, we find the appropriate orientifold quotient to be $\text{IIA}^{-+}_{(10,0)}/\Omega\tilde{I}_1(-1)^{F_L}$, where $\tilde{I}_1$ is a reflection along the space-like direction that was created by T-dualizing.

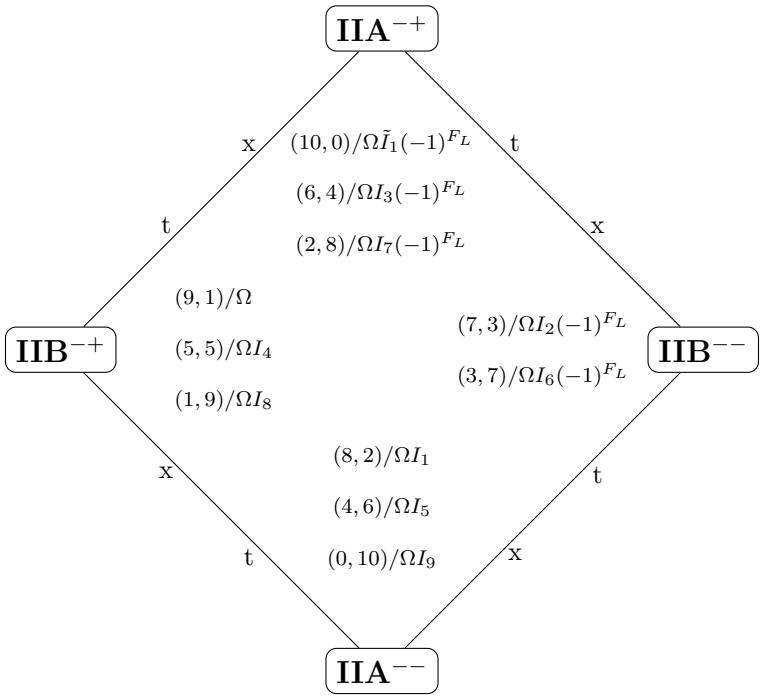

Figure 6.4: Orientifold projections removing the massless ghosts for Euclidean theories.

Compact dimensions

Another new aspect of the Euclidean theories is that the tower of string excitations has imaginary squared mass m^2. Moreover, since under T-duality a space-like circle maps to a time-like one and vice versa, the winding modes contribute with the opposite sign as the KK modes. Thus, the on-shell relation for a compactification on a torus T^D of radii R_k with metric $\eta_k = \pm 1$ now reads

$$E^2 - \sum_{k=1}^{D} \eta_k \left[\left(\frac{m_k}{R_k} \right)^2 - \left(\frac{n_k R_k}{\alpha'} \right)^2 \right] = \sum_i (p^i)^2 - i \, \frac{2}{\alpha'} (N + \overline{N} - 2a) \, . \tag{6.47}$$

with the level-matching condition $\sum_k \eta_k m_k n_k = N - \overline{N}$. In contrast to the Lorentzian string, here the KK/winding modes can never cancel against the string oscillations. However, for both space-like and time-like compactifications the KK mode contribution can cancel up to arbitrary precision against the winding mode contribution, leading again to the conceptual problem of interpreting the dimensional reduction of the 10D Euclidean supergravity actions as Wilson effective theories. As for the Lorentzian string, these ultralight modes do not decouple in string scattering amplitudes.

The CFT perspective is rather robust against signature changes as the signature at the level of the CFT is merely a sign change in the commutation relations. Thus we will now focus on developing the required tools to compute the brane spectrum of the Euclidean theories and especially the tensions of the branes from the CFT.

6.2.4 CFT Description of Euclidean Exotic Strings

In this rather technical section we will take a closer look on the Euclidean world-sheet CFTs. After a short review of the closed string construction of [4] we construct the purely Euclidean open string theories including the fermionic sector. We use this to identify the allowed D-branes of the different theories as well as the tension of the branes. In section 6.2.6 these results will be confirmed using the map (6.136) inspired by horizon crossing in the presence of negative branes.

Let us first present a couple of basic results for the structure of CFTs on purely Euclidean world-sheets. We will see that in this case some extra factors of i appear.

Lorentzian vs. Euclidean world-sheets

When considering purely Euclidean bosonic closed strings we have to thoroughly disentangle the differences between a Lorentzian, a Wick-rotated Euclidean and a purely Euclidean field theory. We could take several approaches to quantize the theory, but the differences in the mode algebra of the field become most apparent when using the path integral formalism. Consider the path integral

$$Z = \int [D\gamma]\,[DX]\, e^{KS_\varepsilon}\,, \tag{6.48}$$

where we introduced $K = \{i, -1\}$ with $K = -1$ only in the Wick-rotated case, and $\varepsilon = \{1, -1\}$ labels the Euclidean or Lorentzian world-sheet action. Thus $K = i$, $\varepsilon = -1$ is the Lorentzian string, $K = -1$, $\varepsilon = 1$ is the Wick-rotated Euclidean string and finally $K = i$, $\varepsilon = 1$ is the purely Euclidean string. Before applying path integral methods we have to bring the action into a quadratic form

$$S = -\frac{\varepsilon}{2\pi\alpha'} \int \mathrm{d}^2\sigma \sqrt{\varepsilon \det\gamma}\, \eta_{\mu\nu}\, X^\mu \partial^a \partial_a X^\nu\,. \tag{6.49}$$

The kinetic operator depends on the world-sheet metric and thus differs for Lorentzian and Euclidean field theories. The two point function has to satisfy the identity

$$\frac{2\pi\alpha'}{K\varepsilon}\, \delta^{\mu_2}_{\mu_1}\, \delta^2(\sigma - \sigma') = \sqrt{\varepsilon \det\gamma}\, \eta_{\mu_1\nu}\, \partial^a \partial_a \left\langle X^{\mu_2}(\sigma) X^\nu(\sigma') \right\rangle\,, \tag{6.50}$$

where σ, σ' are coordinates on the world-sheet. The kinetic operator on the rhs is in the $\sigma = (\sigma_1, \sigma_2)$ coordinates. Let us concentrate for a moment on the two Euclidean field theories. Introducing the usual cylinder world-sheet coordinate

$$z = e^{\sigma_1 + i\sigma_2}\,, \tag{6.51}$$

the equation for the two point function becomes

$$\frac{2\pi\alpha'}{K}\, \delta^{\mu_2}_{\mu_1}\, \delta^2(z - w) = \eta_{\mu_1\nu}\, \partial_z \partial_{\overline{z}} \left\langle X^{\mu_2}(z, \overline{z}) X^\nu(w, \overline{w}) \right\rangle\,. \tag{6.52}$$

The solution to this is given by

$$\langle X^\mu(z,\overline{z})X^\nu(w,\overline{w})\rangle = \eta^{\mu\nu}\frac{\alpha'}{K}\log|z-w|^2\,. \tag{6.53}$$

We want to derive the mode algebra for the CFT. The action in the above coordinates reads

$$S = \frac{1}{2\pi\alpha'}\int \mathrm{d}^2z\,\partial X(z,\overline{z})\cdot\overline{\partial}X(z,\overline{z})\,, \tag{6.54}$$

where the target-space metric is hidden in the multiplication dot. Going through the usual steps for the above action we find holomorphic and anti-holomorphic currents $\partial X^\mu(z)$, $\overline{\partial}X^\mu(\overline{z})$. Using (6.52) we find for their two-point functions

$$\langle \partial X^\mu(z)\partial X^\nu(w)\rangle = \eta^{\mu\nu}\frac{\alpha'}{K}\frac{1}{(z-w)^2}\,. \tag{6.55}$$

Expanding the current fields $\partial X^\mu(z) = -\sqrt{\frac{\alpha'}{2\varepsilon}}\sum \hat{\alpha}^\mu_m\, z^{-m-1}$, the mode algebra reads

$$[\hat{\alpha}^\mu_m,\hat{\alpha}^\nu_n] = \varepsilon\,\eta^{\mu\nu}\frac{\alpha'}{K}\,m\,\delta_{m+n,0}\,. \tag{6.56}$$

Thus we see that for the Wick-rotated Euclidean string ($K=-1$) the procedure gives the usual commutation relations, whereas in the purely Euclidean field theory ($K=i$) the commutation relations get an extra factor of $-i$.

Closed and open Euclidean strings

From now on we will only be concerned with the purely Euclidean theories, i.e. the world-sheet theories of the IIA^E and IIB^E exotic string theories. To construct the world-sheet theory we follow [4] closely. This section follows the same line of arguments already presented in chapter 2, now allowing for a general signature. This introduces additional phase factors, which have to be treated carefully, which especially includes correct treatment of branches. The action for a free boson is given by

$$S_b = \frac{1}{2\pi\alpha'}\int \mathrm{d}^2\sigma\sqrt{\mathrm{det}g}\,g^{ab}\,\eta_{\mu\nu}\,\partial_a X^\mu\partial_b X^\nu\,. \tag{6.57}$$

The world-sheet metric g is gauge fixed to the flat metric $g_{\sigma_1\sigma_1} = g_{\sigma_2\sigma_2} = 1$ and light cone coordinates are chosen as

$$\sigma_\pm = \sigma_1 \pm i\sigma_2\,, \tag{6.58}$$

such that the derivatives become

$$\partial_\pm = \frac{1}{2}(\partial_{\sigma_1}\mp i\partial_{\sigma_2})\,. \tag{6.59}$$

We now choose a convenient mode expansion, simplifying the mode algebra as much as possible. In this framework the oscillators will behave as in the usual string theories. The zero modes will be solely responsible for the changes in the physics. The mode expansion of the closed string sector is given by

$$\begin{aligned} X^\mu(\sigma_1,\sigma_2) &= x^\mu + \alpha' p^\mu \sigma_1 + \sqrt{\frac{\alpha'}{2i}} \sum_{n\neq 0} \left(\frac{\alpha_n^\mu}{n} e^{-n\sigma^+} + \frac{\overline{\alpha}_n^\mu}{n} e^{-n\sigma^-} \right) \\ &= x^\mu + \frac{\alpha'}{2} p^\mu \log(|z|^2) + \sqrt{\frac{\alpha'}{2i}} \sum_{n\neq 0} \left(\frac{\alpha_n^\mu}{n} z^{-n} + \frac{\overline{\alpha}_n^\mu}{n} \bar{z}^{-n} \right) , \end{aligned} \tag{6.60}$$

so that the mode algebra becomes

$$[x^\mu, p^\nu] = i\eta^{\mu\nu} , \qquad [\alpha_m^\mu, \alpha_n^\nu] = [\overline{\alpha}_m^\mu, \overline{\alpha}_n^\nu] = m\, \delta_{m,-n}\, \eta^{\mu\nu} \tag{6.61}$$

for $m, n \neq 0$. Moreover, one has as usual $[\alpha_m^\mu, \overline{\alpha}_n^\nu] = 0$, and the oscillators α_m^μ, $\overline{\alpha}_m^\mu$ commute with the zero modes x^μ and p^μ.

Let us make a couple of remarks. To arrive at this standard mode algebra, we have effectively rescaled the standard oscillator modes $\hat{\alpha}$ by a factor of $\sqrt{i}$. As a consequence, one needs to be very careful when computing overlaps of states $\langle \phi^1 | \phi^2 \rangle$. Indeed, taking the general definition of the conjugate $(\phi_n)^\dagger = (\phi^\dagger)_{-n}$ for a field ϕ in Euclidean CFT into account, the rescaling leads to phase factors, as some of the fields won't be purely real anymore. On the one hand, in this paper we are mostly concerned with partition functions where these phases do not matter as one simply counts the number of states at each level. On the other hand, in the boundary state overlaps (to be introduced later in (6.79)), due to loop-channel tree-channel equivalence the (suitably generalized) CPT operator Θ has to remove these factors. These two facts make this basis very useful for our computations.

If one wants to calculate the low energy effective action and determine for instance the sign of the kinetic terms, one also needs to know the normalization of the corresponding vertex operators. In fact in [4] the normalizations for the metric and the B-field vertex operators have been determined. The graviton state turned out to be

$$|V_G(p)\rangle = i\epsilon_{\mu\nu}\, \hat{\alpha}_{-1}^\mu \hat{\overline{\alpha}}_{-1}^\nu |p\rangle = \epsilon_{\mu\nu}\, \alpha_{-1}^\mu \overline{\alpha}_{-1}^\nu |p\rangle , \tag{6.62}$$

whereas the Kalb-Ramond state has a different normalization

$$|V_B(p)\rangle = -b_{\mu\nu}\, \hat{\alpha}_{-1}^\mu \hat{\overline{\alpha}}_{-1}^\nu |p\rangle = -ib_{\mu\nu}\, \alpha_{-1}^\mu \overline{\alpha}_{-1}^\nu |p\rangle . \tag{6.63}$$

Thus, working with the modes $\alpha^\mu, \overline{\alpha}^\mu$ and treating them in the same way as the usual oscillators in string theory makes it evident that the B-field is a ghost.

In a similar fashion one can expand the open string into modes. For Neumann-Neumann (NN) and Dirichlet-Dirichlet (DD) boundary conditions the mode expansion reads

$$\begin{aligned} X^\mu_{\text{NN}} &= x^\mu + 2\alpha' p^\mu \sigma_1 + \sqrt{-2i\alpha'} \sum_{n\neq 0} \frac{\alpha_n^\mu}{2n} \Big(e^{-n\sigma_-} + e^{-n\sigma_+} \Big), \\ X^\mu_{\text{DD}} &= x^\mu + \frac{\Delta x^\mu}{\pi} \sigma_2 + \sqrt{-2i\alpha'} \sum_{n\neq 0} \frac{\alpha_n^\mu}{2n} \Big(e^{-n\sigma_-} - e^{-n\sigma_+} \Big), \end{aligned} \tag{6.64}$$

with the distance between the branes $\Delta x^\mu = x_a^\mu - x_b^\mu$. Taking the derivatives one gets

$$\begin{aligned}\partial_\pm X^\mu_{\rm NN} &= \alpha' p^\mu - \sqrt{\frac{\alpha'}{2i}} \sum_{n\neq 0} \alpha_n^\mu \, e^{-n\sigma_\pm} = -\sqrt{\frac{\alpha'}{2i}} \sum_{n\in\mathbb{Z}} \alpha_n^\mu \, e^{-n\sigma_\pm} \,, \\ \partial_\pm X^\mu_{\rm DD} &= \mp i \frac{\Delta x^\mu}{2\pi} \pm \sqrt{\frac{\alpha'}{2i}} \sum_{n\neq 0} \alpha_n^\mu \, e^{-n\sigma_\pm} = \pm \sqrt{\frac{\alpha'}{2i}} \sum_{n\in\mathbb{Z}} \alpha_n^\mu \, e^{-n\sigma_\pm} \,,\end{aligned} \tag{6.65}$$

where we have defined the zero modes as

$$\alpha_0^{\mu,\rm NN} = -p^\mu \sqrt{2i\alpha'} \,, \qquad \alpha_0^{\mu,\rm DD} = -\frac{\sqrt{-i}}{\sqrt{2\alpha'\pi}} \Delta x^\mu \,. \tag{6.66}$$

For completeness we also present the mode expansion for mixed boundary conditions

$$\begin{aligned}X^\mu_{\rm ND} &= x^\mu + \sqrt{-2i\alpha'} \sum_{n\in\mathbb{Z}+1/2} \frac{\alpha_n^\mu}{2n} \Big(e^{-n\sigma_-} + e^{-n\sigma_+} \Big) \,, \\ X^\mu_{\rm DN} &= x^\mu + \sqrt{-2i\alpha'} \sum_{n\in\mathbb{Z}+1/2} \frac{\alpha_n^\mu}{2n} \Big(e^{-n\sigma_-} - e^{-n\sigma_+} \Big) \,.\end{aligned} \tag{6.67}$$

Next we want to define the closed and open string partition functions. For that purpose we first focus just on a single direction $X(\sigma_1, \sigma_2)$ and recall that in the Sugawara construction the energy momentum tensor reads

$$T(z) = \frac{i}{\alpha'} \eta_{\mu\nu} : \partial X^\mu(z) \partial X^\nu(z) : \,. \tag{6.68}$$

With this, the normal ordered Hamiltonian becomes

$$H = \int_0^{2\pi} \frac{\mathrm{d}\sigma}{2\pi\alpha'} \Big((\partial_+ X)^2 + (\partial_- X)^2 \Big) = -i \left(L_0 + \overline{L}_0 - \tfrac{c}{12} \right) , \tag{6.69}$$

where the factor of i originates in the mode expansion. The explicit form of the energy momentum tensor's zero mode L_0 is

$$L_0 = i \frac{\alpha' p^2}{4} + \sum_{n>0} \eta_{\mu\nu} \, \alpha_{-n}^\mu \alpha_n^\nu \tag{6.70}$$

and similarly for $\overline{L}_0$. The second term is just the number operator which has non-negative integer eigenvalues. In contrast to the usual case, the zero mode contribution is purely imaginary.

The momentum P which generates σ_2 translations is now given by

$$P = -i \int_0^{2\pi} \frac{\mathrm{d}\sigma}{2\pi\alpha'} \Big((\partial_+ X)^2 - (\partial_- X)^2 \Big) = -(L_0 - \overline{L}_0) \,. \tag{6.71}$$

In this case the normal ordering constant cancels out. As a consequence the torus and cylinder amplitudes receive additional factors of i. The torus amplitude with complex structure $\tau = \tau_1 + i\tau_2$ is constructed by taking a field theory on a circle, translating in σ_1 direction by τ_2, in σ_2 direction by τ_1 and identifying the ends, producing the trace. With

$$q = e^{2\pi i(\tau_1 + i\tau_2)}\,, \tag{6.72}$$

the torus partition function can be written as

$$Z^{\text{torus}} = \text{Tr}(e^{-2\pi i\tau_2 H - 2\pi i\tau_1 P}) = \text{Tr}\left(q^{L_0 - \frac{c}{24}}\,\overline{q}^{\overline{L}_0 - \frac{c}{24}}\right)\,. \tag{6.73}$$

Note that due to the missing Wick rotation for the Euclidean CFT, the coefficient in front of the Hamiltonian is $-2\pi i$ instead of the usual -2π. But this factor gets multiplied by the additional factor of $-i$ in the Hamiltonian (6.69), such that the expression for the partition function is still the usual one. Evaluating the amplitude for a single direction one obtains

$$Z^{\text{torus}} = \frac{e^{i\pi/4}}{\sqrt{4\pi\alpha'\tau_2}\,|\eta(\tau)|^2}\,, \tag{6.74}$$

reproducing the result of [4].

Now we turn to the open string cylinder amplitude which is defined as

$$Z^{\mathcal{C}}(t) = \text{Tr}\left(e^{-2\pi i t H_{\text{open}}}\right) = \text{Tr}\left(e^{-2\pi t(L_0 - \frac{c}{24})}\right)\,, \tag{6.75}$$

with t the circumference of the cylinder. The explicit form of L_0 for NN and DD boundary conditions is

$$L_0^{\text{NN}} = i\alpha' p^2 + \sum_{n>0}\eta_{\mu\nu}\,\alpha_{-n}^{\mu}\alpha_n^{\nu}\,, \qquad L_0^{\text{DD}} = \frac{i}{4\pi^2\alpha'}Y^2 + \sum_{n>0}\eta_{\mu\nu}\,\alpha_{-n}^{\mu}\alpha_n^{\nu}\,. \tag{6.76}$$

The total distance between the Dirichlet loci is defined as $Y^2 = \eta_{\mu\nu}\Delta x^\mu \Delta x^\nu$. Now, considering only a single direction of either NN or DD type, the open string partition functions can be evaluated straightforwardly with the result

$$Z^{\mathcal{C}(\text{NN})}(t) = \frac{e^{-i\pi/4}}{\sqrt{2\alpha' t}\,\eta(it)}\,, \qquad Z^{\mathcal{C}(\text{DD})}(t) = e^{-\frac{it}{2\pi\alpha'}Y^2}\frac{1}{\eta(it)}\,. \tag{6.77}$$

The additional factor of $e^{-i\pi/4}$ in the Neumann-Neumann case arises from the analytic continuation of the Gaussian integral for the zero mode[4]. For mixed boundary conditions one finds

$$Z^{\mathcal{C}(\text{ND})}(t) = \sqrt{\frac{2\eta(it)}{\theta_4(it)}}\,. \tag{6.78}$$

[4]We often employed the Gaussian integral $\int_{-\infty}^{\infty}\mathrm{d}x\,e^{-ax^2+bx} = \sqrt{\frac{\pi}{a}}\cdot e^{\frac{b^2}{4a}}$ and its analytic continuation. This is where most of the phases arise.

As usual, the open string (loop-channel) cylinder amplitude is closely related to the (tree-channel) overlap of boundary states

$$\tilde{Z}(l) = \langle \Theta B | \, e^{2\pi i l H_{\text{closed}}} \, |B\rangle = \langle \Theta B | \, e^{-2\pi l (L_0 + \overline{L}_0 - \frac{c}{12})} \, |B\rangle \ , \tag{6.79}$$

with l the length of the cylinder formed by the closed strings exchanged between the boundaries. We will construct the appropriate boundary states in the next section.

Boundary states

Next we analyze the construction of boundary states in a Euclidean world-sheet CFT[5]. For the moment we assume also a purely Euclidean space-time and postpone the treatment of the effects of the target-space metric signature to the next section. The boundary conditions are unaffected by the signature of the world-sheet. Despite the now Euclidean signature we will think of the coordinate $\sigma_1 \in (0, l)$ as the time coordinate and $\sigma_2 \in (0, \pi)$ as the space component. The conformal map exchanging the open and closed channels acting on the complexified coordinate $\xi = \sigma_2 + i\sigma_1$ is then given by

$$f(\xi) = -i\frac{\pi}{l}\xi \, , \tag{6.80}$$

which is the same as in the Lorentzian case exchanging world-sheet time τ and space σ. The Neumann and Dirichlet gluing conditions are given by

$$\partial_{\sigma_1} X^\mu|_{\sigma_1=0} \, |B_N\rangle = 0 \, , \qquad \partial_{\sigma_2} X^\mu|_{\sigma_1=0} \, |B_D\rangle = 0 \, . \tag{6.81}$$

Inserting the mode expansion (6.60) results in

$$p^\mu \, |B_N\rangle = 0 \, , \qquad (\alpha^\mu_n + \overline{\alpha}^\mu_{-n}) \, |B_N\rangle = 0 \tag{6.82}$$

as well as

$$x^\mu \, |B_D\rangle = y^\mu \, , \qquad (\alpha^\mu_n - \overline{\alpha}^\mu_{-n}) \, |B_D\rangle = 0 \, , \tag{6.83}$$

where y^μ is the position of the brane. These are exactly the same conditions as in the Lorentzian case. Defining a matrix $S_{\mu\nu} = \pm\eta_{\mu\nu}$, with the + sign for Neumann directions and the − sign for Dirichlet directions, the non-zero mode conditions are given by

$$\left(\alpha^\mu_n + S^\mu{}_\nu \, \overline{\alpha}^\nu_{-n}\right) |B\rangle = 0 \, . \tag{6.84}$$

As usual the solution to these gluing conditions is

$$|B\rangle = \frac{1}{\mathcal{N}} \exp\left(- \sum_{n=1}^{\infty} \frac{1}{n} \alpha^\mu_{-n} \, S_{\mu\nu} \, \overline{\alpha}^\nu_{-n} \right) |0\rangle \, . \tag{6.85}$$

[5]Our analysis follows that of [193–196] for Lorentzian strings.

Using the explicit form of the boundary states (6.85), the overlap (6.79) becomes

$$\tilde{Z}^{\mathcal{C}(\mathrm{NN})}(l) = \frac{1}{\mathcal{N}_N^2}\frac{1}{\eta(2il)}\,. \tag{6.86}$$

Mapping the open string loop-channel result with $t = 1/2l$ and a modular S transformation to the closed string tree-channel, the normalization constant can be determined via

$$Z^{\mathcal{C}(\mathrm{NN})}(t) = \frac{e^{-i\pi/4}}{\sqrt{2\alpha' t}\,\eta(it)} = \frac{e^{-i\pi/4}}{\sqrt{\alpha'}\,\eta(2il)} \stackrel{!}{=} \frac{1}{\mathcal{N}_N^2\eta(2il)} \;\Rightarrow\; \mathcal{N}_N = (\alpha')^{1/4}e^{i\pi/8}\,. \tag{6.87}$$

Turning to the DD case, the only thing that changes is the α_0 zero-mode contribution which is now given by

$$\begin{aligned}
&\int_{-\infty}^{\infty}\frac{dk_a dk_b}{2\pi}e^{ik_a x_a}\,e^{ik_b x_b}\,\langle k_a|\,e^{-2\pi l(\alpha_0)^2}\,|k_b\rangle \\
&= \int_{-\infty}^{\infty} dk_a dk_b\, e^{ik_a x_a}\,e^{ik_b x_b}\,e^{-\pi i l\alpha' k_b^2}\,\delta(k_a+k_b) \\
&= \int_{-\infty}^{\infty} dk_a\, e^{ik_a(x_a-x_b)}\,e^{-\pi i l\alpha' k_a^2} = \frac{e^{i\pi/4}}{\sqrt{\alpha' l}}\,e^{-i\frac{Y^2}{4\pi\alpha' l}}\,,
\end{aligned} \tag{6.88}$$

where we used $\langle 0|0\rangle = 2\pi\delta(0)$ and that the CPT operator Θ in (6.79) involves a complex conjugation. Therefore the total DD overlap is

$$\tilde{Z}^{\mathcal{C}(\mathrm{DD})}(l) = \frac{e^{-i\pi/4}}{\mathcal{N}_D^2}\frac{1}{\sqrt{4\pi^2\alpha' l}\,\eta(2il)}\,e^{-i\frac{Y^2}{4\pi\alpha' l}}\,. \tag{6.89}$$

Comparing this to the open string amplitude we obtain

$$\mathcal{N}_D = (\alpha')^{-1/4}\,e^{-i\pi/8}\,. \tag{6.90}$$

Finally, as a cross-check for the normalization factors, we evaluate the mixed case as

$$\tilde{Z}^{\mathcal{C}(\mathrm{ND})}(l) = \frac{1}{\mathcal{N}_N\mathcal{N}_D}\sqrt{\frac{2\eta(2il)}{\theta_2(2il)}} = \sqrt{\frac{2\eta(it)}{\theta_4(it)}} = Z^{\mathcal{C}(\mathrm{ND})}(t)\,, \tag{6.91}$$

featuring that the normalizations of the boundary states are indeed consistent.

The total cylinder amplitudes

After having studied the open string amplitude for just a single direction, we now combine the separate contributions into a total cylinder amplitude of two parallel d-dimensional branes in D space-time dimensions[6]. For the open string loop-channel amplitude one obtains

$$\mathcal{A} = V_d\int_0^{\infty}\frac{dt}{2t}\left(\frac{e^{-i\pi/4}}{\sqrt{8\pi^2\alpha' t}}\right)^d\frac{1}{\eta^{D-2}(it)}e^{-\frac{it}{2\pi\alpha'}Y^2}\,, \tag{6.92}$$

[6]Note that in this convention a Dp-brane has $d = p+1$.

where the additional $\eta^2(it)$ factor originates from the ghost contribution. The total closed string tree-channel amplitude is

$$\tilde{\mathcal{A}} = \frac{V_d}{\mathcal{N}^2} \int_0^\infty dl\, e^{i\pi(D-d)/4} \left(\frac{1}{4\pi^2\alpha' l}\right)^{(D-d)/2} \frac{1}{\eta^{D-2}(2il)}\, e^{-\frac{i}{4\pi\alpha' l}Y^2} \,. \tag{6.93}$$

Applying a modular S-transformation, this amplitude is mapped to the loop-channel and comparing it to (6.92) one can read off the normalization

$$\mathcal{N}^{-1} = 2^{\frac{D-2}{4}} e^{\frac{i\pi}{8}(D-2d)} (4\pi^2\alpha')^{\frac{1}{4}(D-2d-2)} \,. \tag{6.94}$$

Finally, the tension of the branes is determined by the coupling of the boundary state to a graviton with polarization $\epsilon_{\mu\nu}$

$$\langle V_g|B\rangle = -\frac{1}{\mathcal{N}} \langle 0|\, \epsilon_{\mu\nu} S^{\mu\nu}\, |0\rangle = -\frac{1}{\mathcal{N}}\, \epsilon_{\mu\nu} S^{\mu\nu}\, V_{d+1} \stackrel{!}{=} -T_d\, \epsilon_{\mu\nu} S^{\mu\nu}\, V_{d+1} \,, \tag{6.95}$$

so that the tension is given by the normalization of the boundary state as $T_d = \mathcal{N}^{-1}$. For connecting a D-brane theory to phenomenology, we require the tension to be real, so that the normalization of the boundary state also has to be real. Inserting $D = 10$ into (6.94), we see that there are exactly three cases fulfilling this condition, $d \in \{1, 5, 9\}$ with tension

$$T_d = \pm 2^2 (4\pi^2\alpha')^{(4-d)/2} \,, \tag{6.96}$$

with the minus sign for $d \in \{1, 9\}$ and the plus sign for $d = 5$.

Fermionic boundary states

So far we have only discussed the contribution of the world-sheet bosons to the boundary states. Let us now also discuss the inclusion of the world-sheet fermions. The action for a free fermion is

$$S_f = \frac{i\epsilon}{4\pi} \int \mathrm{d}^2\sigma \sqrt{\epsilon \det g}\ \eta_{\mu\nu}\, \overline{\Psi}^\mu\, \gamma^\alpha \partial_\alpha \Psi^\nu \,, \tag{6.97}$$

where the 2×2 matrices γ^α satisfy the Clifford algebra with respect to the world-sheet metric $g_{\alpha\beta}$

$$\{\gamma^\alpha, \gamma^\beta\} = 2g^{\alpha\beta}\, \mathbb{1}_2 \,. \tag{6.98}$$

Moreover, one defines

$$\begin{aligned} \overline{\Psi}^\mu &= \Psi^\mu \gamma^0 \qquad \text{in the Lorentzian case and} \\ \overline{\Psi}^\mu &= \Psi^\mu C \qquad \text{in the Euclidean case,} \end{aligned} \tag{6.99}$$

with C the charge conjugation matrix

$$(\gamma^\alpha)^{\mathsf{T}} = C\gamma^\alpha C^{-1} \,, \quad C^{\mathsf{T}} = C^\dagger = C^{-1} = C \,. \tag{6.100}$$

For Lorentzian signature we choose the representation

$$\gamma^0 = \begin{pmatrix} 0 & 1 \\ 1 & 0 \end{pmatrix} = \hat{\sigma}_1 \,, \qquad \gamma^1 = \begin{pmatrix} 0 & 1 \\ -1 & 0 \end{pmatrix} . \tag{6.101}$$

Under Wick rotation $\tau = i\sigma_1$ one has $\partial_\tau \to -i\partial_{\sigma_1}$, so effectively γ^1 is replaced with

$$\gamma^1 = \begin{pmatrix} 0 & -i \\ i & 0 \end{pmatrix} = \hat{\sigma}_2 \,. \tag{6.102}$$

Therefore, the Wick rotation has the effect of replacing the Lorentzian gamma matrices with the Euclidean gamma matrices. Then, the kinetic term of the Wick rotated theory is the same as in the purely Euclidean theory up to an overall sign. Choosing the same Pauli matrices $\hat{\sigma}_1, \hat{\sigma}_2$ also as a representation for the Euclidean Clifford algebra, the conditions (6.100) uniquely determine C to be

$$C = \begin{pmatrix} 0 & -1 \\ -1 & 0 \end{pmatrix} = -\gamma^0 \,. \tag{6.103}$$

Denoting the components of a 2D spinor as $\Psi^\mu = (\Psi^\mu_+, \Psi^\mu_-)^\mathsf{T}$, the action reduces to

$$S_f = -\frac{K}{2\pi} \int \mathrm{d}^2\sigma \; \eta_{\mu\nu} \Big(\Psi^\mu_+ \partial_- \Psi^\nu_+ + \Psi^\mu_- \partial_+ \Psi^\nu_- \Big) \,, \tag{6.104}$$

where $K = -1$ for the (Wick-rotated) Lorentzian world-sheet and $K = i$ for the Euclidean case. Here we have used again the coordinates $\sigma^\pm = \sigma_1 \pm i\sigma_2$. The equations of motion are

$$\partial_- \Psi^\mu_+ = \partial_+ \Psi^\mu_- = 0 \tag{6.105}$$

with the usual (anti-)holomorphic solutions $\Psi^\mu_+ = \Psi^\mu_+(\sigma^+)$ and $\Psi^\mu_- = \Psi^\mu_-(\sigma^-)$, which can be expanded as

$$\Psi^\mu_+ = \sqrt{-K} \sum_r b^\mu_r \, e^{-2\pi i r \sigma^+} \,, \qquad \Psi^\mu_- = \sqrt{-K} \sum_r \overline{b}^\mu_r \, e^{-2\pi i r \sigma^-} \,. \tag{6.106}$$

As in the bosonic case, the factor $\sqrt{-K}$ ensures that the mode algebra takes the usual form

$$\{b^\mu_r, b^\nu_s\} = \delta_{r,-s} \, \eta^{\mu\nu} \,, \qquad \{\overline{b}^\mu_r, \overline{b}^\nu_s\} = \delta_{r,-s} \, \eta^{\mu\nu} \qquad \{b^\mu_r, \overline{b}^\nu_s\} = 0 \,. \tag{6.107}$$

The energy momentum tensor is obtained by the Sugawara construction, resulting in the explicit expression for the zero mode

$$L_0 = \sum_{r \geq 1/2} \big(r + \tfrac{1}{2}\big) \, \eta_{\mu\nu} \, b^\mu_{-r} \, b^\nu_r \,. \tag{6.108}$$

Now that we have the algebra of the fermions we turn to the construction of the boundary state. We will work again in the Euclidean formalism. The exchange of σ_1 and σ_2 acts on the Euclidean light cone variables as

$$\sigma^\pm \to \sigma'^\pm = \mp i \sigma^\pm \,. \tag{6.109}$$

The fermions transform under this conformal transformation as

$$\Psi'_{\pm}(\sigma'^{\pm}) = \left(\frac{\partial\sigma'^{\pm}}{\partial\sigma^{\pm}}\right)^{-1/2} \Psi_{\pm}(\sigma^{\pm}) \,. \tag{6.110}$$

Imposing the open string boundary conditions on the boundary state, and taking the transformation behavior into account one obtains conditions on the boundary states

$$\left(\Psi^{\mu}_{+}(\sigma^{+}) + i\eta S^{\mu}{}_{\nu}\, \Psi^{\nu}_{-}(\sigma^{-})\right) |B,\eta\rangle = 0\,, \tag{6.111}$$

where $\eta = \pm 1$ labels periodic/antiperiodic boundary conditions. Expanding into modes results in the fermionic gluing conditions

$$\left(b^{\mu}_{r} + i\eta S^{\mu}{}_{\nu}\, \overline{b}^{\nu}_{-r}\right) |B,\eta\rangle = 0\,. \tag{6.112}$$

As usual, these gluing conditions are solved by the state

$$|B,\eta\rangle_{\mathrm{NS}} = \frac{1}{\mathcal{N}} \exp\left(-i\eta \sum_{r=1/2}^{\infty} b^{\mu}_{-r}\, S_{\mu\nu}\, \overline{b}^{\nu}_{-r}\right) |0\rangle \tag{6.113}$$

in the NS sector and by

$$|B,\eta\rangle_{\mathrm{R}} = \frac{1}{\mathcal{N}} \exp\left(-i\eta \sum_{n=1}^{\infty} b^{\mu}_{-n}\, S_{\mu\nu}\, \overline{b}^{\nu}_{-n}\right) |0\rangle_{\mathrm{R}} \tag{6.114}$$

in the R sector, where $|0\rangle_R$ is the Ramond ground state which satisfies the gluing conditions for the zero modes. The resulting tree-channel annulus amplitudes for a single fermion read

$$\begin{aligned}
\langle B,\eta|\, e^{-2\pi l(L_0+\overline{L}_0-\frac{c}{12})}\, |B,\eta\rangle_{\mathrm{NS}} &= \sqrt{\frac{\theta_3(2il)}{\eta(2il)}}\,, \\
\langle B,\eta|\, e^{-2\pi l(L_0+\overline{L}_0-\frac{c}{12})}\, |B,-\eta\rangle_{\mathrm{NS}} &= \sqrt{\frac{\theta_4(2il)}{\eta(2il)}}\,, \\
\langle B,\eta|\, e^{-2\pi l(L_0+\overline{L}_0-\frac{c}{12})}\, |B,\eta\rangle_{\mathrm{R}} &= \sqrt{\frac{\theta_2(2il)}{\eta(2il)}}\,, \\
\langle B,\eta|\, e^{-2\pi l(L_0+\overline{L}_0-\frac{c}{12})}\, |B,-\eta\rangle_{\mathrm{R}} &= 0\,.
\end{aligned} \tag{6.115}$$

Applying a modular S-transformation leads to the open channel amplitudes

$$\begin{aligned}
\mathrm{Tr}_{\mathrm{NS}}\Big(e^{-2\pi t(L_0-\frac{c}{24})}\Big) &= \sqrt{\frac{\theta_3(it)}{\eta(it)}}\,,\\
\mathrm{Tr}_{\mathrm{NS}}\Big((-1)^F e^{-2\pi t(L_0-\frac{c}{24})}\Big) &= \sqrt{\frac{\theta_4(it)}{\eta(it)}}\,,\\
\mathrm{Tr}_{\mathrm{R}}\Big(e^{-2\pi t(L_0-\frac{c}{24})}\Big) &= \sqrt{\frac{\theta_2(it)}{\eta(it)}}\,,\\
\mathrm{Tr}_{\mathrm{R}}\Big((-1)^F e^{-2\pi t(L_0-\frac{c}{24})}\Big) &= 0\,,
\end{aligned} \tag{6.116}$$

which are the same as for Lorentzian superstrings.

Now let us construct the boundary state for a full d-dimensional D-brane in 10D. As usual, invariance of the boundary states under the left and right GSO projections and stability requires the presence of all sectors. Then the total loop-channel annulus amplitude for two parallel d-dimensional branes becomes

$$A = V_d \int_0^\infty \frac{dt}{2t} \left(\frac{1}{\sqrt{8\pi^2\alpha' t}}\right)^d e^{i\pi d/4}\, \frac{\theta_3^4(it)-\theta_4^4(it)-\theta_2^4(it)}{\eta^{12}(it)}\, e^{-\frac{it}{2\pi\alpha'}Y^2}\,. \tag{6.117}$$

Transforming this amplitude to the closed tree-channel amplitude

$$\tilde{A} = V_d \int_0^\infty dl \left(\frac{\sqrt{l}}{\sqrt{4\pi^2\alpha'}}\right)^d e^{i\pi d/4}\, \frac{\theta_3^4(2il)-\theta_2^4(2il)-\theta_4^4(2il)}{\eta^{12}(2il)\cdot(\sqrt{2l})^8}\, e^{-\frac{i}{4\pi\alpha' l}Y^2}\,, \tag{6.118}$$

allows us to fix the relative contribution from the boundary states as

$$|D\rangle = \frac{1}{2\mathcal{N}}\Big(\,|B,-\rangle_{\mathrm{NS}} - |B,+\rangle_{\mathrm{NS}} + i\,|B,+\rangle_{\mathrm{R}} + i\,|B,-\rangle_{\mathrm{R}}\Big)\,, \tag{6.119}$$

where the normalization $\mathcal{N}$ is the same as in the bosonic case.

6.2.5 The Influence of Space-time Signature

In the CFT approach the signature of the space-time merely appears as a sign change in the commutation relations. This is hidden in most formulas we have written down so far. In this section we will take a closer look how the signature influences the amplitudes and boundary states.

We have seen that after absorbing the factor $K = i$ in a redefinition of the modes, we essentially get back the results for the Lorentzian string. The only difference resides in the zero mode contribution. As we will be concerned with branes wrapping various amounts of time dimension, in the following a $\mathrm{D}^{(s,t)}_{(10-p,p)}$-brane will fill t time and s space dimensions in a $\mathbb{R}^{10-p,p}$ target-space with p time and $10-p$ space dimensions. Thus the system we are concerned with consists of

- $N_t = t$ time dimensions with Neumann boundary conditions,
- $D_t = p - t$ time dimensions with Dirichlet boundary conditions,
- $N_s = s$ space dimensions with Neumann boundary conditions,
- $D_s = 10 - p - s$ space dimensions with Dirichlet boundary conditions.

In the analysis so far all directions were assumed to be space-like. Let us now analyze what changes in case some of the directions become time-like. First, recall that the oscillator part of the boundary state (6.85) involves the matrix $S_{\mu\nu}$. For a $\mathrm{D}^{(s,t)}_{(10-p,p)}$-brane this takes the form

$$S = \begin{pmatrix} \mathbb{1}_{N_s} & & & \\ & -\mathbb{1}_{N_t} & & \\ & & -\mathbb{1}_{D_s} & \\ & & & \mathbb{1}_{D_t} \end{pmatrix} . \tag{6.120}$$

Thus, we see that the oscillators of a space-like N/D direction contribute to the boundary state like a D/N time-like direction. However, these signs in $S_{\mu\nu}$ cancel anyway when computing the overlap.

Now, let us consider the zero mode contribution, where some phase factors appeared from the zero mode integrals. For a Neumann boundary condition in a space-like direction this phase is

$$\mathcal{N}^{-2}_{N,\text{space}} \propto \int_0^\infty \mathrm{d}p \; e^{-\pi i p^2} = e^{-i\pi/4} . \tag{6.121}$$

Changing the signature replaces p^2 by $-p^2$, so that

$$\mathcal{N}^{-2}_{N,\text{time}} \propto \int_0^\infty \mathrm{d}p \; e^{\pi i p^2} = e^{i\pi/4} . \tag{6.122}$$

Similarly, for a Dirichlet direction the exact same integrals appear in the overlap of the zero modes of the boundary states, i.e. for a space-like direction the phase

$$\begin{aligned} \mathcal{N}^{2}_{D,\text{space}} &\propto \int_0^\infty \mathrm{d}p \; e^{-\pi i p^2} = e^{-i\pi/4} \\ \Rightarrow \mathcal{N}^{2}_{D,\text{time}} &\propto \int_0^\infty \mathrm{d}p \; e^{\pi i p^2} \;\; = e^{i\pi/4} \end{aligned} \tag{6.123}$$

appears. This implies that changing the signature, the only effect on the normalization of the boundary state is a change of the phase factor such that

$$\begin{aligned} \arg\left(\mathcal{N}_{N,\text{space}}\right) &= \arg\left(\mathcal{N}_{D,\text{time}}\right) , \\ \arg\left(\mathcal{N}_{N,\text{time}}\right) &= \arg\left(\mathcal{N}_{D,\text{space}}\right) . \end{aligned} \tag{6.124}$$

Effectively this means that the formula for the normalization (6.94) holds in all signatures, one just has to adjust the phase factor as

$$T^{(s,t)}_{(10-p,p)} = 2^2 e^{\frac{i\pi}{4}(5+t-p-s)}(4\pi^2\alpha')^{\frac{1}{2}(4-s-t)}\,. \tag{6.125}$$

Note that we have simply replaced $d \to \tilde{d} = d + D_t - N_t = p + s - t$ in the phase factor to account for the additional phases. This formula is now valid for all branes in Euclidean world-sheet theories.

Taking now into account that the tension is real only for $\tilde{d} \in \{1, 5, 9\}$, it is straightforward to iterate all possible (real) branes for a given space-time signature. In the appendix we present an exhaustive list of all D-branes in all possible Euclidean string theories. Here, let us just discuss two examples of space-time signature $(7, 3)$ and $(5, 5)$.

In the first case there are 3 time directions, thus $p = 3$. Then, $\tilde{d} \in \{1, 5, 9\}$ requires that $s - t$ is either -2, 2 or 6. Moreover s and t count the number of longitudinal dimensions of the brane, which cannot exceed the available dimensions, i.e. in this case $0 \leq t \leq 3$, $0 \leq s \leq 7$. Iterating over all possibilities one finds the allowed branes and tensions as shown on the left in table 6.1. Note that the tensions are given by (6.125), here we just list the signs. Now we turn to the second example with signature $(5, 5)$. As $p = 5$, from $\tilde{d} \in \{1, 5, 9\}$ follows that $s - t$ is either equal to -4, 0 or 4. Moreover, s and t are integers in the interval $[0, 5]$. Iterating over all possibilities we find the brane spectrum listed on the right in table 6.1.

s	t	Tension	Dp	E/L
0	2	−	D1	E
1	3	−	D3	L
6	0	−	D5	E
7	1	−	D7	L
2	0	+	D1	E
3	1	+	D3	L
4	2	+	D5	E
5	3	+	D7	L

s	t	Tension	Dp	E/L
0	4	−	D3	E
1	5	−	D5	L
5	1	−	D5	L
4	0	−	D3	E
0	0	+	D(-1)	E
1	1	+	D1	L
2	2	+	D3	E
3	3	+	D5	L
4	4	+	D7	E
5	5	+	D9	L

Table 6.1: Brane spectrum for signature $(7, 3)$ (left) and signature $(5, 5)$ (right).

As one can see, only even dimensional branes exist, implying that we are in a type IIB setup. Note that this information was not put in by hand, but is enforced by the signature of space-time. These tables agree precisely with the results obtained by a spacetime argument

[12]. Moreover, the tables are consistent with the classification of D-branes obtained by Hull.

As a final remark we note that in our derivation the constraints for the allowed D-branes followed directly from the bosonic normalization factor. We have not explicitly discussed the GSO projections in the fermionic sector, but as usual the constraint on even/odd dimension of the branes follows directly from the Clifford algebra of the fermionic zero modes. This computation does not change in the Euclidean case so that the D-branes obtained from the bosonic normalization are also GSO invariant.

Orientifolds of Euclidean strings

In this section, we will take a look at orientifold projections of the Euclidean exotic superstring theories. As the calculation strongly resembles the usual one, we will be very brief and refer to standard textbooks [195, 197] for more details. Here we only show that in the computation of the loop-channel Klein-bottle and Möbius strip amplitudes, the same phase factors appear as for the corresponding annulus amplitude.

Thus, let us consider a single bosonic direction $X(\sigma_1, \sigma_2)$. The orientifold projection $\Omega : (\sigma_1, \sigma_2) \to (\sigma_1, -\sigma_2)$ acts on the modes as

$$\Omega\, \alpha_n\, \Omega^{-1} = \overline{\alpha}_n\,. \tag{6.126}$$

One can also combine Ω with the reflection $I_1 : X \to -X$ so that

$$(\Omega I_1)\, \alpha_n\, (\Omega I_1)^{-1} = -\overline{\alpha}_n\,. \tag{6.127}$$

Moreover, we choose the action of Ω on the vacuum as $\Omega\,|0\rangle = |0\rangle$. Recall that the Klein-bottle amplitude is defined as

$$Z^{\mathcal{K}}_{\Omega} = \mathrm{Tr}\left(\Omega\, q^{L_0 - c/24}\, \overline{q}^{\overline{L}_0 - c/24}\right) = \mathrm{Tr}_{\mathrm{sym}}\left(e^{-4\pi t (L_0 - c/24)}\right)\,. \tag{6.128}$$

The non-zero mode contribution again agrees with the usual result, while the zero modes contribute a phase due to the additional factor of i in the Gaussian integral. Thus for a single boson we get

$$Z^{\mathcal{K}}_{\Omega} = \frac{e^{-i\pi/4}}{\sqrt{\alpha' t}} \frac{1}{\eta(2it)}\,. \tag{6.129}$$

The Klein-bottle amplitude for the orientifold projection ΩI_1 does not receive any zero mode contribution so that one obtains

$$Z^{\mathcal{K}}_{\Omega I_1} = \mathrm{Tr}\left(\Omega I_1\, q^{L_0 - c/24}\, \overline{q}^{\overline{L}_0 - c/24}\right) = e^{\frac{i\pi}{24}} \sqrt{2} \sqrt{\frac{\eta(2it)}{\theta_2(2it)}}\,. \tag{6.130}$$

Turning to the open string sector, the action of the orientifold on the modes is

$$\Omega\, \alpha^{\mu}_n\, \Omega^{-1} = \pm (-1)^n \alpha^{\mu}_n\,, \tag{6.131}$$

with the plus sign for NN boundary conditions and the minus sign for DD conditions. Again the non-zero modes agree with the usual expressions. As in the DD sector there is no zero mode contribution in the open string channel, the Möbius strip amplitude is as usual

$$Z^{\mathcal{M}(DD)} = e^{\frac{i\pi}{24}}\sqrt{2}\sqrt{\frac{\eta(it+\frac{1}{2})}{\theta_2(it+\frac{1}{2})}}\,. \tag{6.132}$$

The NN amplitude receives an additional phase from the Gaussian integral so that

$$Z^{\mathcal{M}(NN)} = e^{\frac{i\pi}{24}}\frac{e^{-i\pi/4}}{\sqrt{2\alpha' t}}\frac{1}{\eta(it+\frac{1}{2})}\,. \tag{6.133}$$

Therefore, both the former annulus amplitudes and these additional non-oriented one-loop amplitudes differ from the usual ones for Lorentzian signature by the same relative phases. The next step is to introduce the corresponding crosscap states satisfying the usual crosscap gluing conditions and allowing the description of the amplitudes in tree-channel. Moreover, one can add the contributions from the world-sheet fermions. However, also here the only difference to the standard case is the appearance of the same phases as already experienced for the D-brane boundary states. Thus, we refrain from presenting the explicit form.

Performing now a full orientifold projection[7] ΩI_{9-p} of the Euclidean type IIA/B superstring theories, the tadpole cancellation conditions go through as usual, the Op-planes will have tension

$$T_{Op} = -2^{p-4}T_{Dp}\,. \tag{6.134}$$

Introducing time-like directions has the same effect on the phase of the tension as for the corresponding boundary states. To cancel the tadpole induced by the orientifold projection one can introduce stacks of Dp-branes on top of the orientifold planes.

6.2.6 Exotic Brane Phenomenology

The mathematical description of the Euclidean CFTs in the previous sections can now be studied in regards to their phenomenological viability. While the additional time directions necessarily lead to ghost states in the closed string sector, we will study the possibility of a ghost-free gauge subsector. Moreover, we demand the existence of a subspace of signature (3,1). This of course rules out the purely space-like IIA theory with signature (10,0) as well as theories with less than three space dimensions. The absence of massless ghost requires the brane to have negative tension. This can be seen as follows. The DBI action of a brane expanded to low order is given by

$$\begin{aligned} S_{\text{DBI+CS}} =& -T_q\int_{\Sigma_{q+1}} \mathrm{d}^{q+1}x\,\sqrt{|g|}\,e^{-\phi}\left[1+\frac{1}{4}(2\pi\alpha')^2F_{\mu\nu}F^{\mu\nu}+...\right] \\ &+\mu_q\int_{\Sigma_{q+1}}\left[C_{q+1}+F\wedge C_{q-1}+...\right]\,. \end{aligned} \tag{6.135}$$

[7] As already shown in figure 6.4 there will be extra factors of $(-1)^{F_L}$ in certain cases.

To obtain the Euclidean branes from this one can use a map developed in [12]. This map relates a usual type II theory to an exotic theory. Explicitly it is given by

$$\begin{aligned} \det e^a_\mu &\to \omega^{-p} \det e^a_\mu \,, \\ e^a_\mu = \left(e^a_\parallel, e^a_\perp\right) &\to \omega^{\frac{1}{2}} \left(\omega^{-1} e^a_\parallel,\, e^a_\perp\right) \,, \\ G_{(9,1)} &\to \omega\, G_{(10-p,p)} \,, \\ e^{-\phi} &\to \omega^{\frac{p-3}{2}} e^{-\phi} \,, \\ (C_{p+1})|_{\Sigma_{p+1}} &\to -(C_{p+1})|_{\Sigma_{p+1}} \,, \end{aligned} \tag{6.136}$$

where $\omega = \pm i$. Note that under this map the gauge field kinetic terms $|F^2|$ change their sign. We have seen that the branes can have positive as well as negative tension. Thus after applying the map there are two possibilities for the DBI action.

$$S_{\text{DBI}} = \begin{cases} -T_q \int \mathrm{d}^{q+1}x \, \sqrt{|g|}\, e^{-\phi} \left[1 - \frac{1}{4}(2\pi\alpha')^2 F_{\mu\nu}F^{\mu\nu} + ...\right] \pm \mu_q \int \left[C_{q+1} + ...\right] \\ +T_q \int \mathrm{d}^{q+1}x \, \sqrt{|g|}\, e^{-\phi} \left[1 - \frac{1}{4}(2\pi\alpha')^2 F_{\mu\nu}F^{\mu\nu} + ...\right] \pm \mu_q \int \left[C_{q+1} + ...\right] . \end{cases} \tag{6.137}$$

In the upper case the overall sign in front of the kinetic term of the gauge field is positive. As this is the wrong sign, it implies that these are ghost fields. Thus the absence of ghosts requires the brane to have negative tension.

It is now possible to use formula (6.125) in each possible signature to find all theories which have a ghost-free gauge sector. Moreover, to be phenomenological viable they should have a subspace of signature (3,1). The full list of branes satisfying these conditions is

$$\begin{aligned} &\text{type IIB}: \ \mathrm{D9}^{(9,1)}_{(9,1)} \,, \quad \mathrm{D7}^{(7,1)}_{(7,3)} \,, \quad \mathrm{D5}^{(5,1)}_{(5,5)} \,, \quad \mathrm{D3}^{(3,1)}_{(3,7)} \,, \\ &\text{type IIA}: \ \mathrm{D8}^{(8,1)}_{(8,2)} \,, \quad \mathrm{D6}^{(6,1)}_{(6,4)} \,, \quad \mathrm{D4}^{(4,1)}_{(4,6)} \,. \end{aligned} \tag{6.138}$$

Note that these have some common properties. They are all space-filling and only extend in 1 of the time directions. This immediately leads to a problem. The additional time dimensions have to be compactified and the displacements of the brane in these directions would give rise to ghosts. These deformations are absent if the brane wraps a rigid cycle. This condition rules out the compactification on simple tori. Moreover, open strings ending on these branes will only have winding modes in the space-like directions and KK modes in the time-like directions. Thus the spectrum of such a string would be

$$E^2 = \sum_i (p^i)^2 + \sum_s \left(\frac{m_s}{R_s}\right)^2 + \sum_t \left(\frac{n_t R_t}{\alpha'}\right)^2 - \frac{i}{\alpha'}\,(N - a) \,, \tag{6.139}$$

where $s(t)$ indicate space(time)like directions, The N is the mode number and a is the ghost or normal ordering contribution. The winding and KK modes contribute in the

same way, but the oscillator contributions are imaginary. We will not try to interpret this behaviour and will simply focus on the "massless" level $N = a$. Another important consistency condition is the tadpole cancellation. In this case especially the RR tadpole in the transversal directions of the branes. As usual O-planes have the opposite charge relative to the branes, thus they exactly cancel the tadpole. The required orientifold projection in each theory is exactly the projection needed to remove all massless closed string ghosts. But these ghosts are exactly correlated with the existence of dS space solutions. Therefore, for the Euclidean exotic string theories with in general multiple times, there is a strong correlation between the presence of a phenomenologically viable D-brane (gauge theory) sector and the existence of dS solutions, which leads to the conjecture:

> **Conjecture:** *A compactified Euclidean exotic string theory contains a 4D ghost-free gauge theory with signature* $(3, 1)$*, iff the closed string sector does not admit classical dS vacua.*

This conjecture extends the usual dS conjecture to the exotic theories.

6.2.7 Conclusions

In this chapter exotic attempts to construct dS space in string theory have been studied. While it is possible to construct dS spaces in string theory using tachyon condensation, 4 dimensional dS was not constructed yet. The obtained dimensions are in agreement the cobordism conjecture, claiming that compactifications are only possible in certain dimensions. If one allows for more time directions or changes the signature of the world-sheet, it is possible to obtain dS spaces, also in 4 dimensions. The price one has to pay is the existence of massless ghosts. The orientifold projections required to eliminate these ghosts are also eliminating the dS solutions. Even only demanding a ghost-free gauge subsector is impossible, as the orientifold projections needed for the tadpole cancellation are the same as in the closed string sector.

Chapter 7

Outlook

In this final chapter some possible future research directions arising form the work in this thesis are discussed. One of the main results of this thesis are analytic expressions for the transition matrices at the conifold and thereby analytic expressions for the conifold periods. These have been used to realize the first step of the KKLT construction by constructing exponentially small superpotentials close to a warped throat. The next step in the construction would be the explicit stabilization of the Kähler moduli. This requires the computation of the so-called Pfaffians of the CY space. While some expressions for these are known, a method to compute them for a general CY has not been found yet. Especially the simple polynomial expressions in the known examples motivate future research in this direction.

The analytic expressions for the periods can also be used in general studies of string phenomenology close to conifolds. The procedure is in principle general enough to compute the conifold periods for any CICY. In practice the limiting step is the analytic evaluation of certain hypergeometric functions at argument 1. These can be determined numerically to arbitrary precision, but in practice are hard to compute analytically. It is conjectured that the values of these functions at the conifold are always expressible via colored multiple zeta values. Thus machine learning tools could be able to identify closed forms for these values given a basis of CMZVs of different weights, which are known. For the computation of the periods we have mainly used analytical properties of the hypergeometric functions. While this is a powerful approach, implementing it in explicit examples is complicated and prone to errors. It is long known that the periods and the mirror map have many interesting arithmetic and modular properties [198]. One example for this are the mirror maps for elliptic fibers and K3 manifolds, which are known to follow a Schwarzian equation. In the CY 3-fold case this equation is only slightly modified by certain quantum corrections depending on the Yukawa couplings. This allows to rewrite the mirror map and the periods in terms of automorphic forms. These expressions are not only compact, but can speed up computations drastically. Yet, these methods have not seen wide applications, as the determination of the suitable subgroups of $SL(2,\mathbb{Z})$ is difficult in practice and mainly worked out by computing the hypergeometric periods first. A better understanding of these properties could improve the computational control, especially at singular configurations

like the conifold. These properties seem to be related to the observation made in chapter 3 that the elements of the transition matrices are given by L-function values, as these are deeply related to θ-functions which can be used to construct bases of modular forms.

We have also given a review of the state-of-the-art techniques in computing numerical CY metrics. It would be interesting to use these to study the full KK spectrum of a CY in the warped regime. As the Laplace operator depends on the target space metric, this seems to be an obvious application. But most numerical techniques to compute CY metrics are not applicable close to a conifold. Recent developments using machine learning techniques could lead to progress in this area. Also, all techniques applied to this date are based on either optimizing an energy functional or Donaldson's T-operator. These approaches limit the form of the metric to algebraic metrics. While this is well suited for generic points in moduli space, the algebraic metrics do not reproduce the singularities expected at a conifold point. Thus applying more elaborated Ansätze for the metric, enforcing this singularity structure, may improve the convergence in this region as well as perhaps giving a hint of the analytic form. Also, the recent analytic result for K3 metrics could be compared to these methods. As the former is exact, this would give a nice benchmark scenario for numerical tools. At the moment we have only numerical approximations to compare to, it is unclear how far from the real solutions these results are. The best we can do is to use integrated measures like the deviation from Ricci-flatness. Moreover, the numerical metrics can be used to test the results obtained by algebraic geometry. An example is the recent test of the distance conjecture, where an exponential decay of KK states was explicitly seen using the numerical metrics [199]. The distances at which the first states become exponentially light are larger than expected due to level crossings between states.

In the last chapter we have seen that tachyons can lead to very interesting theories, including even dS spaces. The available techniques to study closed string tachyons are restricted to on-shell methods based on exactly solvable CFTs. These processes are fine-tuned to keep the conformal invariance along the whole condensation process. In general one would be interested in the endpoint of zero momentum tachyons, as these represent true vacuum solutions of string theory. The computation of these requires methods of string field theory. But even the computation of the quartic bosonic SFT vertex is a formidable task, which has only been solved numerically. Results beyond the quintic order are not available at all. This renders statements about the true vacuum of string theory impossible, although the results point towards the existence of such a vacuum with non-zero cohomology. The most difficult step in this computation is given by a minimal area problem, which is solved by the Strebel differentials mentioned in chapter 3. If these differentials could be computed analytically, this would also result in analytic expressions for the SFT vertices. While this problem may look daunting at first glance, a surprisingly simple solution in a real co-dimension 1 subspace of the moduli space was found in [88]. The solution on this subspace turns out to be a simple linear function in the fundamental domain. All non-linearities are introduced by mapping this function via Möbius transformations to other domains. While the known examples show that this simple Ansatz does not work when extended to the whole moduli space, it is possible that an analytic solution could be guessed by machine learning techniques, as was the case with the polynomial solutions for the line

bundle cohomologies of hypersurfaces in toric varieties.

Despite all this progress and possible future directions one of the main questions of string phenomenology remains: Are effective theories formulated in 4-dimensional dS space part of the swampland? In all situations where we have complete computational control it turns out to be impossible to construct a stable dS solution. Yet, the KKLT construction of dS also survives every test made so far and more parts of the construction continue to be carried out explicitly without any obvious flaws appearing. It seems that the core step in resolving this contradiction lies in a better understanding of the non-perturbative effects of string theory. This could require a new formulation of string theory and the development of new mathematical tools. But while string theory did not manage to predict our world in the last 40 years, it managed to create a plethora of new areas of mathematics and mathematical results. So maybe this task is not as difficult as it may seem today.

Appendix A

Appendix

A.1 (A)dS Spaces of Signature (p, q)

First we introduce the notion of anti-de Sitter and de Sitter spaces with signature (p, q) where p denotes the number of time-like directions.

$AdS_{p,q}$ **spaces:** This space is defined as the real hypersurface

$$-\sum_{i=0}^{p} t_i^2 + \sum_{j=1}^{q} x_j^2 = -\alpha^2 \tag{A.1}$$

in $\mathbb{R}_{p+1,q}$, where α denotes a real number. A solution to this equation can be written as

$$\begin{aligned} t_0 &= \alpha \cosh(\rho/\alpha) + \frac{e^{\rho/\alpha}}{2\alpha}(-\sum_{i=1}^{p} \hat{t}_i^2 + \sum_{j=2}^{q} \hat{x}_j^2) \\ x_1 &= \alpha \sinh(\rho/\alpha) - \frac{e^{\rho/\alpha}}{2\alpha}(-\sum_{i=1}^{p} \hat{t}_i^2 + \sum_{j=2}^{q} \hat{x}_j^2) \\ t_i &= e^{\rho/\alpha}\hat{t}_i\,, \quad i = 1, \dots p \\ x_j &= e^{\rho/\alpha}\hat{x}_j\,, \quad j = 2, \dots q\,. \end{aligned} \tag{A.2}$$

The metric on $AdS_{p,q}$ is then given as

$$ds^2 = d\rho^2 + e^{2\rho/\alpha}(-\sum_{i=1}^{p} d\hat{t}_i^2 + \sum_{j=2}^{q} d\hat{x}_j^2) \tag{A.3}$$

which is the so-called flat slicing of $AdS_{p,q}$. One can introduce a corresponding $(p+q)$-bein E^A on $AdS_{p,q}$ so that the metric (A.3) takes the simple form $ds^2 = \eta^{(p,q)}_{AB} E^A E^B$. The resulting Ricci-tensor in this frame reads

$$R_{AB} = -\eta^{(p,q)}_{AB} \frac{(p+q-1)}{\alpha^2} \tag{A.4}$$

so that the Ricci-scalar becomes $R = -(p+q)(p+q-1)/\alpha^2$.

$dS_{p,q}$ spaces: Similarly, one can define and describe de Sitter spaces with signature (p,q). It is defined as the real hypersurface

$$-\sum_{i=0}^{p-1} t_i^2 + \sum_{j=1}^{q+1} x_j^2 = \beta^2 \tag{A.5}$$

in $\mathbb{R}_{p,q+1}$ with a solution given as

$$\begin{aligned} t_0 &= \beta \sinh(\tau/\beta) + \frac{e^{\tau/2\beta}}{2\beta}(-\sum_{i=1}^{p-1} \hat{t}_i^2 + \sum_{j=2}^{q+1} \hat{x}_j^2) \\ x_1 &= \beta \cosh(\tau/\beta) - \frac{e^{\tau/2\beta}}{2\beta}(-\sum_{i=1}^{p-1} \hat{t}_i^2 + \sum_{j=2}^{q+1} \hat{x}_j^2) \\ t_i &= e^{\tau/\beta}\hat{t}_i\,, \quad i = 1, \dots p-1 \\ x_j &= e^{\tau/\beta}\hat{x}_j\,, \quad j = 2, \dots q+1 \end{aligned} \tag{A.6}$$

yielding the metric

$$ds^2 = -d\tau^2 + e^{2\tau/\beta}(-\sum_{i=1}^{p-1} d\hat{t}_i^2 + \sum_{j=2}^{q+1} d\hat{x}_j^2)\,, \tag{A.7}$$

from which one can read of a $(p+q)$-bein $\mathcal{E}_A$. The resulting Ricci-tensor reads

$$R_{AB} = \eta_{AB}^{(p,q)} \frac{(p+q-1)}{\beta^2} \tag{A.8}$$

with the Ricci-scalar $R = (p+q)(p+q-1)/\beta^2$.

A.2 First Order Systems

In this appendix we give the used conventions for the first order systems. These represent the ghost systems appearing in the covariant quantization of string theory. These represent interacting conformal field theories. They come in two variants, fermionic as well as bosonic.

A.2.1 Fermionic Systems

The energy momentum tensor of a first order system is given by

$$T = -\lambda b \partial c + (1-\lambda)(\partial b) c\,, \tag{A.9}$$

where λ is the only parameter of the system, fixing the conformal dimensions of the fields. The fields have the conformal dimension of the two fields b and c $h_b = \lambda$ and $h_c = 1 - \lambda$. For $\lambda = 2$ this corresponds to the bc-ghosts arising from gauge fixing the metric. For $\lambda = 1$ this describes ghosts for a U(1) symmetry, e.g. the R-symmetry ghosts of $\mathcal{N} = 2$ superstrings or the additional ghost system obtained by fermionizing a boson. In this case the fields b and c are usually denoted η and ξ. For $\lambda = 1/2$ the system becomes a complex fermion.

Independent of λ the system describes a U(1) symmetry with a background charge of

$$Q = (1 - 2\lambda) \, . \tag{A.10}$$

By computing the OPE between T and itself the central charge is determined to be

$$c = -(12\lambda^2 - 12\lambda + 2) = 1 - 3Q^2 \, . \tag{A.11}$$

For the bc system this results in $c_{bc} = -26$ while for the $\eta\xi$ system in $c_{\eta\xi} = -2$. For the complex fermion the central charge becomes 1. As a complex fermion consists out of 2 free fermions with central charge $c = 1/2$ this is expected.

The U(1) current is not conserved due to the background charge and corresponds to the zero modes of the fields. The number of zero modes follows from the Riemann-Roch theorem and turns out to be

$$N_c - N_b = Q(g - 1) \, , \tag{A.12}$$

where g is the genus of the surface. This non-conservation is the reason why it is necessary to insert c ghost zero modes in the string amplitudes, as they would otherwise vanish.

A.2.2 Bosonic Systems

The bosonic version of a first order system works rather similar to the fermionic. The different spin statistic leads to the appearance of several signs.The energy momentum tensor is the same as in the fermionic case. The most important example of a bosonic first order system is the $\beta\gamma$ ghost system of superstring theory, described by $\lambda = 3/2$. For the bosonic case the following formulas hold

$$Q = -(1 - 2\lambda) \, , \tag{A.13}$$

$$c = 12\lambda^2 - 12\lambda + 2 = -1 + 3Q^2 \, , \tag{A.14}$$

$$N_c - N_b = -Q(g - 1) \, . \tag{A.15}$$

This results in a central charge of $c_{\beta\gamma}$=11. As it is more convenient to work with fermionic fields it is conventional to fermionize this system as

$$b = e^{-\phi}\partial\xi \qquad , \qquad c = \eta e^{\phi} \, , \tag{A.16}$$

where η and ξ form a $\lambda = 1$ fermionic first order system and ϕ is a scalar field with background charge Q. The non conservation of the current then requires the insertion of $e^{-2\phi}$ into the amplitudes.

A.3 Number Theory

A.3.1 The ζ-function

The Riemann ζ-function is defined as

$$\zeta(x) = \sum_{n=1}^{\infty} n^{-x} \,. \tag{A.17}$$

This sum converges only for $x > 1$, but it can be analytically continued to the whole complex plane. Especially, the ζ-function fulfills the functional equation

$$\zeta(1-s) = \frac{2}{(2\pi)^s} \cos(\frac{\pi s}{2}) \Gamma[s] \zeta(s) \,. \tag{A.18}$$

This allows to express the values of $\zeta(x)$ at negative x in terms of the converging series (A.17) with $x > 1$. Especially important for string theory is the value of the zeta function at -1, which can be evaluated as

$$\zeta(-1) = \frac{2}{(2\pi)^2} \cos(\pi) \Gamma[2] \zeta(2) = -\frac{1}{2\pi^2} \zeta(2) \,. \tag{A.19}$$

With Euler's famous solution to the Basel problem, $\zeta(2) = \frac{\pi^2}{6}$ this results in

$$\zeta(-1) = -\frac{1}{12} \,. \tag{A.20}$$

One possible generalization is the Hurwitz ζ-function:

$$\zeta(x, q) = \sum_{n=0}^{\infty} (q+n)^{-x} \,. \tag{A.21}$$

For $q = 0$ or $q = 1$ this function reduces to the usual Riemann ζ-function. Importantly, for $x = -1$ this function has a closed form:

$$\zeta(-1, q) = -\frac{1}{12}(6q^2 - 6q + 1) \,. \tag{A.22}$$

A.3.2 Colored Multiple Zeta Values

The colored multiple zeta values (CMZV) are a generalization of the usual zeta function. They are defined as

$$\mathrm{CMVZ}(\vec{a},\vec{s}) = \sum_{n_1>n_2>\ldots n_d>0} \frac{a_1^{n_1} a_2^{n_2} \ldots a_d^{n_d}}{n_1^{s_1} n_2^{s_2} \ldots n_d^{s_d}} \ . \tag{A.23}$$

The length of the parameter vectors d is usually called the depth of the CMZV. The a_i, $i = 1, \ldots, d$ are N-th roots of unity, with the most important example being N=2, the so-called Euler sums. CMZV fulfill several algebraic relations, known as stuffel and shuffel relations, which allow to reduce the number of basis elements needed at each depth. There are many explicit evaluations of CMZV known, and they represent a useful basis for integer relation algorithms. The elements of the transition matrices, given by parameter derivatives of hypergeometric functions at 1 can be represented in terms of CMZV in the case of elliptic curves.

In the case all $a_i = 1$, the CMZV reduce to multiple zeta values

$$\mathrm{CMVZ}(\vec{1},\vec{s}) = \zeta(\vec{s}) \ . \tag{A.24}$$

The relation between periods (solutions of a Piccard-Fuchs system) and CMZV was used by mathematicians to evaluate new CMZV, see e.g. [200].

A.4 Modularity and L-functions

Modular functions are functions which are defined in the upper half-plane $\mathbb{H}$ and transform under modular transformations, i.e. elements of the modular group $SL(2,\mathbb{Z})$ as

$$f\left(\frac{a\tau+b}{c\tau+d}\right) = (c\tau+d)^k f(\tau) \ . \tag{A.25}$$

The integer k is known as the weight of the function. Another representation of a modular form is given by its q-expansion. There the function is mapped to the unit disc by the coordinate change

$$q = e^{2\pi i\tau} \ . \tag{A.26}$$

q is know as the "nome". The modular function can then be expanded as

$$f(\tau) = \sum_{n=0}^{\infty} a_n q^n \ . \tag{A.27}$$

If the first term in this expansion vanishes, i.e. $a_0 = 0$, the modular form is a cusp-form.

A value $L(f, j)$ is called a critical L-value if $j \in \{1, 2, \ldots, k-1\}$. The Hecke operators T_m are defined by their action on a modular form as

$$T_m f(\tau) = m^{k-1} \sum_{d|m} d^{-k} \sum_{b=0}^{d-1} f\left(\frac{m\tau + bd}{d^2}\right) . \tag{A.28}$$

A modular form which is an eigenfunction of all Hecke operators is called a Hecke eigenform, i.e.

$$T_m f(\tau) = \lambda_m f(\tau) . \tag{A.29}$$

$SL(2, \mathbb{Z})$ is generated by two transformations denoted S and T, corresponding to inversions and translations:

$$S : f(\tau) \to f(-\frac{1}{\tau}), \tag{A.30}$$

$$T : f(\tau) \to f(\tau + 1) . \tag{A.31}$$

Sometimes one is not interested in the full modular group $SL(2, \mathbb{Z})$ but only into subgroups. The most common subgroups are $\Gamma_0(N)$. These are given by the elements of $SL(2, \mathbb{Z})$ for which $c \equiv 0$ mod N.

A.4.1 Examples of Modular Functions

Dedekind η-function

The η function is defined as

$$\eta(\tau) = q^{\frac{1}{24}} \prod_{n=1}^{\infty} (1 - q^n) . \tag{A.32}$$

Equivalently, it can be written as an infinte sum

$$\eta(\tau) = q^{\frac{1}{24}} \sum_{n=-\infty}^{\infty} (-1)^n q^{\frac{3(n^2-n)}{2}} . \tag{A.33}$$

Under modular transformation it transforms as

$$\eta(\tau + 1) = e^{\frac{\pi i}{12}} \eta(\tau), \tag{A.34}$$

$$\eta(-\frac{1}{\tau}) = \sqrt{-i\tau}\, \eta(\tau) . \tag{A.35}$$

It represents a level 1 weight 1/2 modular form. This allows it to be used to construct other modular forms via so-called eta-quotients.

Theta functions

There is a plentora of different conventions in use for the θ-functions. As only the zero values are needed in this thesis, we will use a convention suppressing the second coordinate. I.e. we define the θ functions as

$$\theta_{\alpha\beta}(\tau) = \sum_{n\in\mathbb{Z}} e^{i\pi(n+\alpha)\tau^2+2\pi i(n+\alpha)\beta} \,. \tag{A.36}$$

4 special cases of this function are usually denoted as θ_i, $i = 1, \ldots, 4$

$$\theta_1 = \theta_{1/2,1/2} \,, \tag{A.37}$$
$$\theta_2 = \theta_{1/2,0} \,, \tag{A.38}$$
$$\theta_3 = \theta_{0,0} \,, \tag{A.39}$$
$$\theta_4 = \theta_{0,1/2} \,. \tag{A.40}$$

While θ_1 is identically 0, it is nevertheless important as its derivative is non-vanishing. These can all expressed as eta-quotients as

$$\theta_2(\tau)\theta_3(\tau)\theta_4(\tau) = 2\eta(\tau)^3 \,, \tag{A.41}$$
$$\theta_2 = \frac{2\eta^2(2\tau)}{\eta(\tau)} \,, \tag{A.42}$$
$$\theta_3 = \frac{\eta^2((\tau+1)/2)}{\eta(\tau+1)} \,, \tag{A.43}$$
$$\theta_4 = \frac{\eta^2(\tau/2)}{\eta(\tau)} \,. \tag{A.44}$$

Moreover, the θ functions obey Jacobi's "absurd identity"

$$\theta_3^4 - \theta_2^4 - \theta_4^4 = 0 \,. \tag{A.45}$$

These identities are useful in proving the vanishing of certain superstring partition functions as well as crosschecks for numerical implementations of the functions. The θ functions appear in many places, e.g they can be used to express the j-function as well as its inverse and they appear in the string partition functions.

Harmonic Polylogarithms

In this section we give the basic definitions of the used harmonic polylogarithms (HPL). These as well as a Mathematica package to evaluate them can be found in [201]. HPLs are one-variable functions with a parameter vector $\vec{a}$. The dimension k of the vector a is

called the weight of the HPL. We define the functions

$$\begin{aligned} f_1(x) &= \frac{1}{1-x}, \\ f_0(x) &= \frac{1}{x}, \\ f_{-1}(x) &= \frac{1}{1+x}. \end{aligned} \tag{A.46}$$

The HPL's are defined recursively through integration of these three functions:

$$\mathrm{HPL}(a, a_1, \ldots, a_k; x) = \int_0^x f_a(t)\, \mathrm{HPL}(a_1, \ldots, a_k; t)\, \mathrm{d}t\ . \tag{A.47}$$

For the weight one HPL $\left[-1; \frac{1-x_3}{1+x_3}\right]$ from the main text we have

$$\mathrm{HPL}\left[-1; \frac{1-x_3}{1+x_3}\right] = \int_0^{\frac{1-x_3}{1+x_3}} \frac{1}{1+t}\mathrm{dt} = \log\left(1 + \frac{1-x_3}{1+x_3}\right). \tag{A.48}$$

The modular properties of these functions depend on the parameters. Some example transformations include

$$\mathrm{HPL}[0, \frac{1}{x}] = -\mathrm{HPL}[0, x], \tag{A.49}$$

$$\mathrm{HPL}[1, \frac{1}{x}] = \mathrm{HPL}[1, x] + \mathrm{HPL}[0, x] - i\pi, \tag{A.50}$$

$$\mathrm{HPL}[-1, \frac{1}{x}] = \mathrm{HPL}[-1, x] - \mathrm{HPL}[0, x]. \tag{A.51}$$

$$\tag{A.52}$$

This shows that the HPL itself are not modular forms, but combinations thereof are. Note that harmonic polylogarithms only including weight 0 represent the usual polylogarithms. At x=1 these reduce to multiple zeta values, explaining the appearance of CMZVs in the transition matrices.

A.5 Hypergeometric Functions

Hypergeometric functions are defined by the infinite series

$${}_pF_q\left(\{a_1, a_2, \ldots, a_p\}, \{b_1, b_2, \ldots, b_q\}, x\right) = \sum_{n=0}^{\infty} \frac{\prod_{i=1}^{p} (a_i)_n}{\prod_{i=1}^{q} (b_i)_n} \frac{x^n}{n!}\ , \tag{A.53}$$

where $(x)_n$ denotes the Pochhammer symbol

$$(x)_n = \frac{\Gamma[x+n]}{\Gamma[x]} \,. \tag{A.54}$$

They are annihilated by the differential operator

$$D = x\prod_{n=1}^{p}(x\partial_x + a_n) - x\partial_x\prod_{n=1}^{q}(x\partial_x + b_n - 1) \,. \tag{A.55}$$

The Piccard-fuchs operators for Calabi-Yau periods are of exactly this type. This operator has the important property that a coordinate change $x \to \frac{1}{x}$ results in another hypergeometric differential operator. This relates the solutions at the LCS point to the solutions at the LG point, allowing for analytic expressions for the transition matrices. The continuation to the conifold point leaves the regime of hypergeometric functions and requires other methods, either by extending the function space to Meijer G functions or by rewriting the derivatives of the hypergeometric functions in term of variations of polylogarithms.

The Meijer G functions fulfill the differential equation

$$\left((-1)^{p-m-n}z\prod_{j=1}^{p}(z\partial_z + a_j - 1) - \prod_{j=1}^{q}(z\partial_z + b_j)\right) G^{m,n}_{p,q}(\vec{a};\vec{b},z) = 0 \,. \tag{A.56}$$

Every hypergeometric function is expressible in terms of Meijer G functions as

$${}_pF_q(\vec{a};\vec{b};x) = \frac{\prod_{j=1}^{p}\Gamma[a_j]}{\prod_{j=1}^{q}\Gamma[b_j]} G^{1,p}_{p,q+1}(1-\vec{a};0,\vec{b};-x) \,. \tag{A.57}$$

A.6 Line Bundle Cohomologies

Phase	h^0	h^1	h^2
I	0	0	$-n^2+nm+m^2+2$
II	$-n^2+nm+m^2+2$	0	0
III	$\frac{5m^2}{4}+\frac{7}{4}$	$3n^2-3nm-3n+\frac{3m^2}{4}+\frac{3m}{2}+\frac{3}{4}$	$2n^2-2nm-3n+\frac{m^2}{2}+\frac{3m}{2}+1$
IV	$2n^2-2nm+3n+\frac{m^2}{2}-\frac{3m}{2}+1$	$3n^2-3nm+3n+\frac{3m^2}{4}-\frac{3m}{2}+\frac{3}{4}$	$\frac{5m^2}{4}+\frac{7}{4}$
V	$2n^2-2nm+3n+\frac{m^2}{2}-\frac{3m}{2}+1$	$3n^2-3nm+3n+\frac{3m^2}{4}-\frac{3m}{2}+1$	$\frac{5m^2}{4}+2$
VI	$\frac{5m^2}{4}+2$	$3n^2-3nm-3n+\frac{3m^2}{4}+\frac{3m}{2}+1$	$2n^2-2nm-3n+\frac{m^2}{2}+\frac{3m}{2}+1$
VII	0	$3n^2-3nm-3n+3m$	$2n^2-2nm-3n+m^2+3m+2$
$VIII$	$2n^2-2nm+3n+m^2-3m+2$	$3n^2-3nm+3n-3m$	0

Table A.1: Polynomials for all h^i in the case of $\mathbb{P}^3_{1112}[5]$.

Phase	h^0	h^1	h^2	h^3
I	0	0	0	$\frac{8m^3}{3} - 2m^2n - \frac{2m}{3} - 2n$
II	$-\frac{8m^3}{3} + 2m^2n + \frac{2m}{3} + 2n$	0	0	0
III	$\frac{m^3}{3} - 2m^2 + \frac{11m}{3} + \frac{n^3}{8} + \frac{3n^2}{8} + \frac{5n}{4} - 1$	$-1 + 3m - 2m^2 + 3m^3 - (3n)/4 - 2m^2n + (3n^2)/8 + n^3/8$	0	0
IV	0	0	$-3m^3 + 2m^2n - 2m^2 - 3m - \frac{n^3}{8} + \frac{3n^2}{8} + \frac{3n}{4} - 1$	$-1 - (11m)/3 - 2m^2 - m^3/3 - (5n)/4 + (3n^2)/8 - n^3/8$
V	$\frac{m^3}{3} - 2m^2 + \frac{11m}{3} - 2$	$3m^3 - 2m^2n - 2m^2 + 3m - 2n - 2$	0	0
VI	$\frac{m^3}{3} - 2m^2 + \frac{11m}{3} + \frac{n^3}{8} + \frac{3n^2}{8} + \frac{7n}{8} - \frac{11}{8}$	$3m^3 - 2m^2n - 2m^2 + 3m + \frac{n^3}{8} + \frac{3n^2}{8} - \frac{9n}{8} - \frac{11}{8}$	0	0
VII	0	0	$-3m^3 + 2m^2n - 2m^2 - 3m - \frac{n^3}{8} + \frac{3n^2}{8} + \frac{9n}{8} - \frac{11}{8}$	$-\frac{m^3}{3} - 2m^2 - \frac{11m}{3} - \frac{n^3}{8} + \frac{3n^2}{8} - \frac{7n}{8} - \frac{11}{8}$
$VIII$	0	0	$-3m^3 + 2m^2n - 2m^2 - 3m + 2n - 2$	$-\frac{m^3}{3} - 2m^2 - \frac{11m}{3} - 2$

Table A.2: Polynomials for all h^i in the case of $\mathbb{P}^4_{11222}[8]$.

A.7 Periods of $\mathbb{P}^4_{112812}[24]$

In this appendix we collect some more details about the periods of $\mathbb{P}_{1,1,2,8,12}[24]$. The given periods are local solutions to the PF equations. To obtain the symplectic basis these have to multiplied by the transition matrices given in the main text.

A.7.1 Local Periods at the LCS

A local basis of periods ω_{LCS} around the LCS point is given by

$$\omega_{\text{LCS},1} = w_1\,,$$

$$\omega_{\text{LCS},2} = w_2 - \frac{iw_1\log(x_1)}{2\pi}\,,$$

$$\omega_{\text{LCS},3} = w_3 - \frac{iw_1\log(x_2)}{2\pi}\,,$$

$$\omega_{\text{LCS},4} = w_4 - \frac{iw_1\log(x_3)}{2\pi}\,,$$

$$\begin{aligned}\omega_{\text{LCS},5} = w_5 &+ \frac{w_1\log^2(x_1)}{\pi^2} + \frac{w_1\log^2(x_3)}{4\pi^2} + \frac{w_1\log(x_1)\log(x_2)}{2\pi^2} + \frac{w_1\log(x_1)\log(x_3)}{\pi^2}\\ &+ \frac{w_1\log(x_2)\log(x_3)}{4\pi^2} + \left(\frac{4iw_2}{\pi} + \frac{iw_3}{\pi} + \frac{2iw_4}{\pi}\right)\log(x_1)\\ &+ \left(\frac{2iw_2}{\pi} + \frac{iw_3}{2\pi} + \frac{iw_4}{\pi}\right)\log(x_3) + \left(\frac{iw_2}{\pi} + \frac{iw_4}{2\pi}\right)\log(x_2)\,,\end{aligned}$$

$$\omega_{\text{LCS},6} = w_6 + \frac{w_1\log(x_1)\log(x_3)}{4\pi^2} + \frac{w_1\log^2(x_1)}{4\pi^2} + \left(\frac{iw_2}{\pi} + \frac{iw_4}{2\pi}\right)\log(x_1) + \frac{iw_2\log(x_3)}{2\pi}\,,$$

$$\begin{aligned}\omega_{\text{LCS},7} = w_7 &+ \frac{w_1\log(x_1)\log(x_2)}{4\pi^2} + \frac{w_1\log(x_1)\log(x_3)}{2\pi^2} + \frac{w_1\log^2(x_1)}{2\pi^2}\\ &+ \left(\frac{2iw_2}{\pi} + \frac{iw_3}{2\pi} + \frac{iw_4}{\pi}\right)\log(x_1) + \frac{iw_2\log(x_2)}{2\pi} + \frac{iw_2\log(x_3)}{\pi}\,,\end{aligned}$$

$$\begin{aligned}\omega_{\text{LCS},8} = w_8 &+ \frac{iw_1\log(x_1)\log(x_2)\log(x_3)}{8\pi^3} + \frac{iw_1\log^2(x_1)\log(x_2)}{8\pi^3} + \frac{iw_1\log^2(x_1)\log(x_3)}{4\pi^3}\\ &+ \frac{iw_1\log(x_1)\log^2(x_3)}{8\pi^3} + \frac{iw_1\log^3(x_1)}{6\pi^3} + \left(-\frac{w_2}{\pi^2} - \frac{w_3}{4\pi^2} - \frac{w_4}{2\pi^2}\right)\log(x_1)\log(x_3)\\ &+ \left(-\frac{w_2}{\pi^2} - \frac{w_3}{4\pi^2} - \frac{w_4}{2\pi^2}\right)\log^2(x_1) + \left(-\frac{w_2}{2\pi^2} - \frac{w_4}{4\pi^2}\right)\log(x_1)\log(x_2)\\ &- \frac{w_2\log(x_2)\log(x_3)}{4\pi^2} - \frac{w_2\log^2(x_3)}{4\pi^2} + \frac{iw_5\log(x_1)}{2\pi} + \frac{iw_6\log(x_2)}{2\pi} + \frac{iw_7\log(x_3)}{2\pi}\,,\end{aligned}$$

where the power series terms are

$$w_1 = 1 + 60x_1 + 13860x_1^2 + 27720x_1^2x_3 + \mathcal{O}(x^3)\,,$$

$$\begin{aligned} w_2 = {} & -\frac{156ix_1}{\pi} - \frac{38826ix_1^2}{\pi} + \frac{ix_3}{2\pi} - \frac{30ix_1x_3}{\pi} - \frac{98442ix_1^2x_3}{\pi} + \frac{3ix_3^2}{4\pi} \\ & - \frac{15ix_1x_3^2}{\pi} + \frac{3465ix_1^2x_3^2}{\pi} + \frac{3ix_2x_3^2}{2\pi} - \frac{30ix_1x_2x_3^2}{\pi} + \frac{6930ix_1^2x_2x_3^2}{\pi} + \mathcal{O}(x^3)\,, \end{aligned}$$

$$\begin{aligned} w_3 = {} & -\frac{ix_2}{\pi} - \frac{60ix_1x_2}{\pi} - \frac{13860ix_1^2x_2}{\pi} - \frac{3ix_2^2}{2\pi} - \frac{90ix_1x_2^2}{\pi} - \frac{20790ix_1^2x_2^2}{\pi} \\ & - \frac{27720ix_1^2x_3}{\pi} + \frac{27720ix_1^2x_2x_3}{\pi} + \frac{13860ix_1^2x_2^2x_3}{\pi} + \mathcal{O}(x^3)\,, \end{aligned}$$

$$\begin{aligned} w_4 = {} & -\frac{60ix_1}{\pi} - \frac{20790ix_1^2}{\pi} + \frac{ix_2}{2\pi} + \frac{30ix_1x_2}{\pi} + \frac{6930ix_1^2x_2}{\pi} + \frac{3ix_2^2}{4\pi} \\ & + \frac{45ix_1x_2^2}{\pi} + \frac{10395ix_1^2x_2^2}{\pi} - \frac{ix_3}{\pi} + \frac{60ix_1x_3}{\pi} + \frac{27720ix_1^2x_3}{\pi} \\ & - \frac{13860ix_1^2x_2x_3}{\pi} - \frac{6930ix_1^2x_2^2x_3}{\pi} - \frac{3ix_3^2}{2\pi} + \frac{30ix_1x_3^2}{\pi} - \frac{6930ix_1^2x_3^2}{\pi} \\ & - \frac{3ix_2x_3^2}{\pi} + \frac{60ix_1x_2x_3^2}{\pi} - \frac{13860ix_1^2x_2x_3^2}{\pi} + \mathcal{O}(x^3)\,, \end{aligned}$$

$$\begin{aligned} w_5 = {} & \frac{120x_1}{\pi^2} + \frac{183294x_1^2}{\pi^2} - \frac{x_2^2}{4\pi^2} - \frac{15x_1x_2^2}{\pi^2} - \frac{3465x_1^2x_2^2}{\pi^2} + \frac{169704x_1^2x_3}{\pi^2} \\ & - \frac{13860x_1^2x_2x_3}{\pi^2} + \mathcal{O}(x^3)\,, \end{aligned}$$

$$\begin{aligned} w_6 = {} & \frac{33696x_1^2}{\pi^2} - \frac{78x_1x_2}{\pi^2} - \frac{19413x_1^2x_2}{\pi^2} - \frac{117x_1x_2^2}{\pi^2} - \frac{58239x_1^2x_2^2}{2\pi^2} \\ & - \frac{30x_1x_3}{\pi^2} - \frac{6795x_1^2x_3}{\pi^2} - \frac{x_2x_3}{4\pi^2} + \frac{15x_1x_2x_3}{\pi^2} + \frac{49221x_1^2x_2x_3}{\pi^2} - \frac{x_2^2x_3}{8\pi^2} \\ & + \frac{15x_1x_2^2x_3}{2\pi^2} + \frac{49221x_1^2x_2^2x_3}{2\pi^2} - \frac{x_3^2}{4\pi^2} + \frac{3465x_1^2x_3^2}{2\pi^2} - \frac{13x_2x_3^2}{8\pi^2} + \frac{45x_1x_2x_3^2}{2\pi^2} \\ & - \frac{3465x_1^2x_2x_3^2}{2\pi^2} + \frac{3x_2^2x_3^2}{16\pi^2} - \frac{15x_1x_2^2x_3^2}{4\pi^2} + \frac{3465x_1^2x_2^2x_3^2}{4\pi^2} + \mathcal{O}(x^3)\,, \end{aligned}$$

$$\begin{aligned} w_7 = {} & \frac{67392x_1^2}{\pi^2} - \frac{x_3}{2\pi^2} - \frac{30x_1x_3}{\pi^2} + \frac{84852x_1^2x_3}{\pi^2} - \frac{13x_3^2}{8\pi^2} + \frac{45x_1x_3^2}{2\pi^2} \\ & - \frac{3465x_1^2x_3^2}{2\pi^2} - \frac{7x_2x_3^2}{4\pi^2} + \frac{15x_1x_2x_3^2}{\pi^2} + \frac{3465x_1^2x_2x_3^2}{\pi^2} + \mathcal{O}(x^3)\,, \end{aligned}$$

$$\begin{aligned} w_8 = {} & -\frac{120ix_1}{\pi^3} - \frac{26055ix_1^2}{\pi^3} - \frac{39ix_1x_2^2}{\pi^3} - \frac{19413ix_1^2x_2^2}{2\pi^3} + \frac{ix_3}{2\pi^3} - \frac{91782ix_1^2x_3}{\pi^3} \\ & + \frac{ix_2x_3}{4\pi^3} - \frac{15ix_1x_2x_3}{\pi^3} - \frac{49221ix_1^2x_2x_3}{\pi^3} + \frac{9ix_3^2}{16\pi^3} - \frac{75ix_1x_3^2}{4\pi^3} + \frac{10395ix_1^2x_3^2}{2\pi^3} \\ & + \frac{23ix_2x_3^2}{16\pi^3} - \frac{135ix_1x_2x_3^2}{4\pi^3} + \frac{24255ix_1^2x_2x_3^2}{4\pi^3} - \frac{3ix_2^2x_3^2}{32\pi^3} + \frac{15ix_1x_2^2x_3^2}{8\pi^3} \\ & - \frac{3465ix_1^2x_2^2x_3^2}{8\pi^3} + \mathcal{O}(x^3)\,. \end{aligned}$$

A.7.2 Local Periods at the Conifold

A local basis of periods ω_c around the $(\overline{x},\overline{y},\overline{z}) = (0,0,1)$ conifold is given by

$$\omega_{c,1} = \tilde{w}_1\,,$$

$$\omega_{c,2} = \tilde{w}_2 + \tilde{w}_1 \log(x_1)\,,$$

$$\omega_{c,3} = \tilde{w}_3 + \frac{1}{2}\tilde{w}_1 \log(x_2) + \tilde{w}_1 \log(x_3)\,,$$

$$\omega_{c,4} = \tilde{w}_4\,,$$

$$\omega_{c,5} = \tilde{w}_5 + \tilde{w}_4 \log(x_2)\,,$$

$$\omega_{c,6} = \tilde{w}_6 + \tilde{w}_1 \log^2(x_1) + 2\tilde{w}_2 \log(x_1)\,,$$

$$\begin{aligned}\omega_{c,7} = {} & \tilde{w}_7 + \frac{1}{2}\tilde{w}_1 \log(x_1)\log(x_2) + \tilde{w}_1 \log(x_1)\log(x_3) + \tilde{w}_1 \log^2(x_1) \\ & + (2\tilde{w}_2 + \tilde{w}_3)\log(x_1) + \frac{1}{2}\tilde{w}_2 \log(x_2) + \tilde{w}_2 \log(x_3)\,,\end{aligned}$$

$$\begin{aligned}\omega_{c,8} = {} & \tilde{w}_8 + \frac{3}{4}\tilde{w}_1 \log^2(x_1)\log(x_2) + \frac{3}{2}\tilde{w}_1 \log^2(x_1)\log(x_3) + \tilde{w}_1 \log^3(x_1) \\ & + \left(3\tilde{w}_2 + \frac{3\tilde{w}_3}{2}\right)\log^2(x_1) + \frac{3}{2}\tilde{w}_2 \log(x_1)\log(x_2) + 3\tilde{w}_2 \log(x_1)\log(x_3) \\ & + \frac{3}{4}\tilde{w}_6 \log(x_2) + \frac{3}{2}\tilde{w}_6 \log(x_3) + 3\tilde{w}_7 \log(x_1)\,,\end{aligned}$$

where the power series terms are

$$\tilde{w}_1 = 1 + \frac{5x_1}{36} + \frac{385x_1^2}{3456} - \frac{385x_1^2x_3}{10368} + \mathcal{O}(x^3)\,,$$

$$\tilde{w}_2 = \frac{31x_1}{36} + \frac{15637x_1^2}{20736} - \frac{x_3}{2} - \frac{5x_1x_3}{72} - \frac{2927x_1^2x_3}{10368} - \frac{x_3^2}{4} - \frac{5x_1x_3^2}{144} - \frac{385x_1^2x_3^2}{41472} - \frac{x_2x_3^2}{8} - \frac{5}{288}x_1x_2x_3^2 - \frac{385x_1^2x_2x_3^2}{82944} + \mathcal{O}(x^3)\,,$$

$$\tilde{w}_3 = \frac{385x_1^2}{10368} + x_3 + \frac{5x_1x_3}{36} + \frac{385x_1^2x_3}{5184} + \frac{x_3^2}{2} + \frac{5x_1x_3^2}{72} + \frac{385x_1^2x_3^2}{20736} + \frac{x_2x_3^2}{4} + \frac{5}{144}x_1x_2x_3^2 + \frac{385x_1^2x_2x_3^2}{41472} + \mathcal{O}(x^3)\,,$$

$$\tilde{w}_4 = \sqrt{x_3} - \frac{x_2\sqrt{x_3}}{16} - \frac{15x_2^2\sqrt{x_3}}{1024} + \frac{x_3^{3/2}}{3} + \frac{5}{108}x_1x_3^{3/2} + \frac{1}{16}x_2x_3^{3/2} + \frac{5}{576}x_1x_2x_3^{3/2} + \frac{3x_2^2x_3^{3/2}}{1024} + \frac{5x_1x_2^2x_3^{3/2}}{12288} + \mathcal{O}(x^3)\,,$$

$$\tilde{w}_5 = 2\sqrt{x_3} - \frac{17x_2^2\sqrt{x_3}}{1024} + \frac{10x_3^{3/2}}{9} + \frac{25}{162}x_1x_3^{3/2} - \frac{1}{4}x_2x_3^{3/2} - \frac{5}{144}x_1x_2x_3^{3/2} + \frac{x_2^2x_3^{3/2}}{1024} + \frac{5x_1x_2^2x_3^{3/2}}{36864} + \mathcal{O}(x^3)\,,$$

$$\tilde{w}_6 = \frac{961x_1^2}{1296} - x_3 - \frac{13x_1x_3}{18} - \frac{13727x_1^2x_3}{20736} - \frac{5x_3^2}{12} - \frac{19x_1x_3^2}{48} - \frac{443x_1^2x_3^2}{5184} - \frac{5x_2x_3^2}{24} - \frac{19}{96}x_1x_2x_3^2 - \frac{443x_1^2x_2x_3^2}{10368} + \mathcal{O}(x^3)\,,$$

$$\tilde{w}_7 = \frac{5x_1}{18} + \frac{1045x_1^2}{864} - \frac{5099x_1^2x_3}{20736} - \frac{x_3^2}{4} - \frac{5x_1x_3^2}{144} - \frac{385x_1^2x_3^2}{20736} - \frac{385x_1^2x_2x_3^2}{82944} + \mathcal{O}(x^3)\,,$$

$$\tilde{w}_8 = -\frac{5x_1}{3} - \frac{1313x_1^2}{864} + 3x_3 + \frac{2557x_1^2x_3}{6912} + \frac{2x_3^2}{3} - \frac{7x_1x_3^2}{16} - \frac{719x_1^2x_3^2}{2304} + \frac{31x_2x_3^2}{48} + \frac{5}{64}x_1x_2x_3^2 - \frac{1271x_1^2x_2x_3^2}{13824} + \mathcal{O}(x^3)\,.$$

Bibliography

[1] P. S. Aspinwall, "The Moduli space of N=2 superconformal field theories," in ICTP Summer School in High-energy Physics and Cosmology, pp. 0352–401. 11, 1994. arXiv:hep-th/9412115.

[2] R. Blumenhagen, D. Kläwer, L. Schlechter, and F. Wolf, "The Refined Swampland Distance Conjecture in Calabi-Yau Moduli Spaces," JHEP **06** (2018) 052, arXiv:1803.04989 [hep-th].

[3] J. McNamara and C. Vafa, "Cobordism Classes and the Swampland," arXiv:1909.10355 [hep-th].

[4] R. Dijkgraaf, B. Heidenreich, P. Jefferson, and C. Vafa, "Negative Branes, Supergroups and the Signature of Spacetime," JHEP **02** (2018) 050, arXiv:1603.05665 [hep-th].

[5] J. Kaidi, "Stable Vacua for Tachyonic Strings," arXiv:2010.10521 [hep-th].

[6] **LIGO Scientific Collaboration and Virgo Collaboration** Collaboration, "Observation of gravitational waves from a binary black hole merger," Phys. Rev. Lett. **116** (Feb, 2016) 061102. https://link.aps.org/doi/10.1103/PhysRevLett.116.061102.

[7] H.-C. Kim, H.-C. Tarazi, and C. Vafa, "Four-dimensional $\mathcal{N} = \mathbf{4}$ SYM theory and the swampland," Phys. Rev. D **102** no. 2, (2020) 026003, arXiv:1912.06144 [hep-th].

[8] C. Vafa, "The String landscape and the swampland," arXiv:hep-th/0509212 [hep-th].

[9] H. Ooguri and C. Vafa, "On the Geometry of the String Landscape and the Swampland," Nucl. Phys. B **766** (2007) 21–33, arXiv:hep-th/0605264.

[10] T. Banks and N. Seiberg, "Symmetries and Strings in Field Theory and Gravity," Phys. Rev. D **83** (2011) 084019, arXiv:1011.5120 [hep-th].

[11] R. Blumenhagen, D. Lüst, and S. Theisen, Basic concepts of string theory. Theoretical and Mathematical Physics. Springer, Heidelberg, Germany, 2013.

[12] R. Blumenhagen, M. Brinkmann, A. Makridou, L. Schlechter, and M. Traube, "dS Spaces and Brane Worlds in Exotic String Theories," JHEP **06** (2020) 077, arXiv:2002.11746 [hep-th].

[13] J. Polchinski, String theory. Vol. 1: An introduction to the bosonic string. Cambridge Monographs on Mathematical Physics. Cambridge University Press, 12, 2007.

[14] J. R. David, S. Minwalla, and C. Nunez, "Fermions in bosonic string theories," JHEP **09** (2001) 001, arXiv:hep-th/0107165.

[15] N. Seiberg and E. Witten, "Spin Structures in String Theory," Nucl. Phys. B **276** (1986) 272.

[16] J. Kaidi, J. Parra-Martinez, and Y. Tachikawa, "Classification of String Theories via Topological Phases," Phys. Rev. Lett. **124** no. 12, (2020) 121601, arXiv:1908.04805 [hep-th].

[17] S. Hellerman and I. Swanson, "Charting the landscape of supercritical string theory," Phys. Rev. Lett. **99** (2007) 171601, arXiv:0705.0980 [hep-th].

[18] S. Hellerman and I. Swanson, "Cosmological unification of string theories," JHEP **07** (2008) 022, arXiv:hep-th/0612116.

[19] L. J. Dixon and J. A. Harvey, "String Theories in Ten-Dimensions Without Space-Time Supersymmetry," Nucl. Phys. B **274** (1986) 93–105.

[20] H. Ooguri and C. Vafa, "Geometry of N=2 strings," Nucl. Phys. B **361** (1991) 469–518.

[21] N. Berkovits and C. Vafa, "On the Uniqueness of string theory," Mod. Phys. Lett. A **9** (1994) 653–664, arXiv:hep-th/9310170.

[22] T. Banks, W. Fischler, S. H. Shenker, and L. Susskind, "M theory as a matrix model: A Conjecture," Phys. Rev. D **55** (1997) 5112–5128, arXiv:hep-th/9610043.

[23] C. Vafa, "Evidence for F theory," Nucl. Phys. B **469** (1996) 403–418, arXiv:hep-th/9602022.

[24] R. Blumenhagen, A. Font, M. Fuchs, D. Herschmann, E. Plauschinn, Y. Sekiguchi, and F. Wolf, "A Flux-Scaling Scenario for High-Scale Moduli Stabilization in String Theory," Nucl. Phys. B **897** (2015) 500–554, arXiv:1503.07634 [hep-th].

[25] T. Kaluza, "Zum Unitätsproblem der Physik," Int. J. Mod. Phys. D **27** no. 14, (2018) 1870001, arXiv:1803.08616 [physics.hist-ph].

[26] O. Klein, "Quantentheorie und fünfdimensionale relativitätstheorie," Zeitschrift für Physik **37** no. 12, (Dec, 1926) 895–906. https://doi.org/10.1007/BF01397481.

[27] E. Witten, "Search for a realistic kaluza-klein theory," Nuclear Physics B **186** no. 3, (1981) 412 – 428. http://www.sciencedirect.com/science/article/pii/0550321381900213.

[28] A. Adams, M. Ernebjerg, and J. M. Lapan, "Linear models for flux vacua," Adv. Theor. Math. Phys. **12** no. 4, (2008) 817–852, arXiv:hep-th/0611084.

[29] T. W. Grimm, "The Effective action of type II Calabi-Yau orientifolds," Fortsch. Phys. **53** (2005) 1179–1271, arXiv:hep-th/0507153.

[30] S. Gukov, C. Vafa, and E. Witten, "CFT's from Calabi-Yau four folds," Nucl. Phys. B **584** (2000) 69–108, arXiv:hep-th/9906070. [Erratum: Nucl.Phys.B 608, 477–478 (2001)].

[31] P. Candelas and X. de la Ossa, "Moduli Space of {Calabi-Yau} Manifolds," Nucl. Phys. B **355** (1991) 455–481.

[32] V. V. Batyrev, "Dual polyhedra and mirror symmetry for Calabi-Yau hypersurfaces in toric varieties," J. Alg. Geom. **3** (1994) 493–545, arXiv:alg-geom/9310003.

[33] K. Hori, S. Katz, A. Klemm, R. Pandharipande, R. Thomas, C. Vafa, R. Vakil, and E. Zaslow, Mirror symmetry, vol. 1 of Clay mathematics monographs. AMS, Providence, USA, 2003.

[34] M. Kreuzer and H. Skarke, "Classification of reflexive polyhedra in three-dimensions," Adv. Theor. Math. Phys. **2** (1998) 853–871, arXiv:hep-th/9805190.

[35] M. Kreuzer and H. Skarke, "Complete classification of reflexive polyhedra in four-dimensions," Adv. Theor. Math. Phys. **4** (2002) 1209–1230, arXiv:hep-th/0002240.

[36] P. S. Aspinwall, B. R. Greene, and D. R. Morrison, "The Monomial divisor mirror map," arXiv:alg-geom/9309007.

[37] S. Hosono, A. Klemm, S. Theisen, and S.-T. Yau, "Mirror symmetry, mirror map and applications to Calabi-Yau hypersurfaces," Commun. Math. Phys. **167** (1995) 301–350, arXiv:hep-th/9308122.

[38] L. B. Anderson, F. Apruzzi, X. Gao, J. Gray, and S.-J. Lee, "A new construction of calabi–yau manifolds: Generalized cicys," Nuclear Physics B **906** (2016) 441–496. https://www.sciencedirect.com/science/article/pii/S0550321316001073.

[39] P. Candelas, X. C. De La Ossa, P. S. Green, and L. Parkes, "A pair of calabi-yau manifolds as an exactly soluble superconformal theory," Nuclear Physics B **359** no. 1, (1991) 21 – 74. http://www.sciencedirect.com/science/article/pii/0550321391902926.

[40] P. Candelas, X. De La Ossa, A. Font, S. H. Katz, and D. R. Morrison, "Mirror symmetry for two parameter models. 1.," AMS/IP Stud. Adv. Math. **1** (1996) 483–543, arXiv:hep-th/9308083.

[41] P. Berglund, P. Candelas, X. De La Ossa, A. Font, T. Hubsch, D. Jancic, and F. Quevedo, "Periods for Calabi-Yau and Landau-Ginzburg vacua," Nucl. Phys. B **419** (1994) 352–403, arXiv:hep-th/9308005.

[42] P. Candelas, A. Font, S. H. Katz, and D. R. Morrison, "Mirror symmetry for two parameter models. 2.," Nucl. Phys. B **429** (1994) 626–674, arXiv:hep-th/9403187.

[43] I. Gelfand, M. Kapranov, and A. Zelevinsky, "Generalized euler integrals and a-hypergeometric functions," Advances in Mathematics **84** no. 2, (1990) 255 – 271. http://www.sciencedirect.com/science/article/pii/000187089090048R.

[44] S. Hosono, A. Klemm, S. Theisen, and S.-T. Yau, "Mirror symmetry, mirror map and applications to complete intersection Calabi-Yau spaces," AMS/IP Stud. Adv. Math. **1** (1996) 545–606, arXiv:hep-th/9406055.

[45] R. Altman, J. Gray, Y.-H. He, V. Jejjala, and B. D. Nelson, "A Calabi-Yau Database: Threefolds Constructed from the Kreuzer-Skarke List," JHEP **02** (2015) 158, arXiv:1411.1418 [hep-th].

[46] R. Álvarez-García, R. Blumenhagen, M. Brinkmann, and L. Schlechter, "Small Flux Superpotentials for Type IIB Flux Vacua Close to a Conifold," arXiv:2009.03325 [hep-th].

[47] J. P. Conlon and F. Quevedo, "On the explicit construction and statistics of Calabi-Yau flux vacua," JHEP **10** (2004) 039, arXiv:hep-th/0409215.

[48] N. Cabo Bizet, O. Loaiza-Brito, and I. Zavala, "Mirror quintic vacua: hierarchies and inflation," JHEP **10** (2016) 082, arXiv:1605.03974 [hep-th].

[49] T. Huber and D. Maitre, "HypExp 2, Expanding Hypergeometric Functions about Half-Integer Parameters," Comput. Phys. Commun. **178** (2008) 755–776, arXiv:0708.2443 [hep-ph].

[50] A. Singh Nimbran, "Sums of series involving central binomial coefficients & harmonic numbers," arXiv e-prints (June, 2018) arXiv:1806.03998, arXiv:1806.03998 [math.NT].

[51] J. M. Campbell, "Series containing squared central binomial coefficients and alternating harmonic numbers," Mediterranean Journal of Mathematics **16** no. 2, (2019) 37.

[52] M. Cantarini and J. D'Aurizio, "On the interplay between hypergeometric series, fourier-legendre expansions and euler sums," 2018.

[53] M.-x. Huang, A. Klemm, and S. Quackenbush, "Topological string theory on compact Calabi-Yau: Modularity and boundary conditions," Lect. Notes Phys. **757** (2009) 45–102, arXiv:hep-th/0612125.

[54] W. Zudilin, "A Hypergeometric Version of the Modularity of Rigid Calabi-Yau Manifolds," SIGMA **14** (2018) 086, arXiv:1805.00544 [math.NT].

[55] G. Shimura, "On the periods of modular forms," Mathematische Annalen **229** no. 3, (Oct, 1977) 211–221. https://doi.org/10.1007/BF01391466.

[56] P. Berglund, S. H. Katz, and A. Klemm, "Mirror symmetry and the moduli space for generic hypersurfaces in toric varieties," Nucl. Phys. B **456** (1995) 153–204, arXiv:hep-th/9506091.

[57] E. Scheidegger, "Analytic Continuation of Hypergeometric Functions in the Resonant Case," arXiv:1602.01384 [math.CA].

[58] E. Witten, "Phases of N=2 theories in two-dimensions," AMS/IP Stud. Adv. Math. **1** (1996) 143–211, arXiv:hep-th/9301042.

[59] N. Doroud, J. Gomis, B. Le Floch, and S. Lee, "Exact Results in D=2 Supersymmetric Gauge Theories," JHEP **05** (2013) 093, arXiv:1206.2606 [hep-th].

[60] F. Benini and S. Cremonesi, "Partition Functions of $\mathcal{N} = (2, 2)$ Gauge Theories on S^2 and Vortices," Commun. Math. Phys. **334** no. 3, (2015) 1483–1527, arXiv:1206.2356 [hep-th].

[61] H. Jockers, V. Kumar, J. M. Lapan, D. R. Morrison, and M. Romo, "Two-Sphere Partition Functions and Gromov-Witten Invariants," Commun. Math. Phys. **325** (2014) 1139–1170, arXiv:1208.6244 [hep-th].

[62] D. Erkinger and J. Knapp, "Sphere partition function of Calabi-Yau GLSMs," arXiv:2008.03089 [hep-th].

[63] A. Gerhardus and H. Jockers, "Dual pairs of gauged linear sigma models and derived equivalences of Calabi–Yau threefolds," J. Geom. Phys. **114** (2017) 223–259, arXiv:1505.00099 [hep-th].

[64] O. N. Zhdanov and A. K. Tsikh, "Studying the multiple mellin-barnes integrals by means of multidimensional residues," Siberian Mathematical Journal **39** no. 2, (Apr, 1998) 245–260. https://doi.org/10.1007/BF02677509.

[65] S. Friot and D. Greynat, "On convergent series representations of Mellin-Barnes integrals," J. Math. Phys. **53** (2012) 023508, arXiv:1107.0328 [math-ph].

[66] D. R. Morrison, "Gromov–Witten invariants and localization," J. Phys. A **50** no. 44, (2017) 443004, arXiv:1608.02956 [hep-th].

[67] J.-P. Aguilar, D. Greynat, and E. De Rafael, "Muon Anomaly from Lepton Vacuum Polarization and The Mellin-Barnes Representation," Phys. Rev. D **77** (2008) 093010, arXiv:0802.2618 [hep-ph].

[68] A. B. Givental, Symplectic geometry of Frobenius structures, pp. 91–112. Vieweg+Teubner Verlag, Wiesbaden, 2004. https://doi.org/10.1007/978-3-322-80236-1_4.

[69] S.-T. Yau, "On the ricci curvature of a compact kähler manifold and the complex monge-ampére equation, I," Commun. Pure Appl. Math. **31** no. 3, (1978) 339–411.

[70] S. Kachru, A. Tripathy, and M. Zimet, "K3 metrics from little string theory," arXiv:1810.10540 [hep-th].

[71] S. Kachru, A. Tripathy, and M. Zimet, "K3 metrics," arXiv:2006.02435 [hep-th].

[72] S. Donaldson, "Some numerical results in complex differential geometry," arXiv: Differential Geometry (2005) .

[73] M. R. Douglas, R. L. Karp, S. Lukic, and R. Reinbacher, "Numerical Calabi-Yau metrics," J. Math. Phys. **49** (2008) 032302, arXiv:hep-th/0612075.

[74] M. R. Douglas, S. Lakshminarasimhan, and Y. Qi, "Numerical Calabi-Yau metrics from holomorphic networks," arXiv:2012.04797 [hep-th].

[75] L. B. Anderson, M. Gerdes, J. Gray, S. Krippendorf, N. Raghuram, and F. Ruehle, "Moduli-dependent Calabi-Yau and $SU(3)$-structure metrics from Machine Learning," arXiv:2012.04656 [hep-th].

[76] V. Jejjala, D. K. Mayorga Pena, and C. Mishra, "Neural Network Approximations for Calabi-Yau Metrics," arXiv:2012.15821 [hep-th].

[77] G. Tian, "On a set of polarized kähler metrics on algebraic manifolds," Journal of Differential Geometry **32** (1990) 99–130.

[78] M. Headrick and A. Nassar, "Energy functionals for Calabi-Yau metrics," Adv. Theor. Math. Phys. **17** no. 5, (2013) 867–902, arXiv:0908.2635 [hep-th].

[79] B. Sturmfels, "Solving algebraic equations in terms of a-hypergeometric series," Discrete Mathematics **210** no. 1, (2000) 171 – 181. http://www.sciencedirect.com/science/article/pii/S0012365X99001260.

[80] V. Braun, T. Brelidze, M. Douglas, and B. Ovrut, "Eigenvalues and eigenfunctions of the scalar laplace operator on calabi-yau manifolds," J High Energy Phys **0807** (05, 2008) .

[81] D. Klaewer and L. Schlechter, "Machine Learning Line Bundle Cohomologies of Hypersurfaces in Toric Varieties," Phys. Lett. B **789** (2019) 438–443, arXiv:1809.02547 [hep-th].

[82] R. Blumenhagen, B. Jurke, T. Rahn, and H. Roschy, "Cohomology of Line Bundles: A Computational Algorithm," J. Math. Phys. **51** (2010) 103525, arXiv:1003.5217 [hep-th].

[83] C. R. Brodie, A. Constantin, R. Deen, and A. Lukas, "Index Formulae for Line Bundle Cohomology on Complex Surfaces," Fortsch. Phys. **68** no. 2, (2020) 1900086, arXiv:1906.08769 [hep-th].

[84] M. Saadi and B. Zwiebach, "Closed string field theory from polyhedra," Annals of Physics **192** no. 1, (1989) 213–227. https://www.sciencedirect.com/science/article/pii/0003491689901267.

[85] B. Zwiebach, "Closed string field theory: Quantum action and the B-V master equation," Nucl. Phys. B **390** (1993) 33–152, arXiv:hep-th/9206084.

[86] N. Moeller, "Closed bosonic string field theory at quartic order," JHEP **11** (2004) 018, arXiv:hep-th/0408067.

[87] M. Mulase and M. Penkava, "Ribbon graphs, quadratic differentials on riemann surfaces, and algebraic curves defined over $\overline{Q}$," arXiv preprint math-ph/9811024 (1998) .

[88] J. Song and B. Xu, "Constructing strebel differentials via belyi maps on the riemann sphere," Computational Methods and Function Theory **20** no. 1, (Feb, 2020) 63–83. http://dx.doi.org/10.1007/s40315-020-00302-3.

[89] S. K. Ashok, F. Cachazo, and E. Dell'Aquila, "Strebel differentials with integral lengths and Argyres-Douglas singularities," arXiv:hep-th/0610080.

[90] M. R. Douglas, "Statistics of string vacua," 1, 2004. arXiv:hep-ph/0401004.

[91] W. Lerche, D. Lust, and A. Schellekens, "Chiral Four-Dimensional Heterotic Strings from Selfdual Lattices," Nucl. Phys. B **287** (1987) 477.

[92] W. Taylor and Y.-N. Wang, "The F-theory geometry with most flux vacua," JHEP **12** (2015) 164, arXiv:1511.03209 [hep-th].

[93] P. Candelas, E. Perevalov, and G. Rajesh, "Toric geometry and enhanced gauge symmetry of F theory / heterotic vacua," Nucl. Phys. B **507** (1997) 445–474, arXiv:hep-th/9704097.

[94] D. Klaewer and E. Palti, "Super-Planckian Spatial Field Variations and Quantum Gravity," JHEP **01** (2017) 088, arXiv:1610.00010 [hep-th].

[95] N. Arkani-Hamed, L. Motl, A. Nicolis, and C. Vafa, "The String landscape, black holes and gravity as the weakest force," JHEP **06** (2007) 060, arXiv:hep-th/0601001.

[96] D. Harlow, "Wormholes, Emergent Gauge Fields, and the Weak Gravity Conjecture," JHEP **01** (2016) 122, arXiv:1510.07911 [hep-th].

[97] G. Shiu, P. Soler, and W. Cottrell, "Weak Gravity Conjecture and extremal black holes," Sci. China Phys. Mech. Astron. **62** no. 11, (2019) 110412, arXiv:1611.06270 [hep-th].

[98] S. Hod, "A proof of the weak gravity conjecture," Int. J. Mod. Phys. D **26** no. 12, (2017) 1742004, arXiv:1705.06287 [gr-qc].

[99] Z. Fisher and C. J. Mogni, "A Semiclassical, Entropic Proof of a Weak Gravity Conjecture," arXiv:1706.08257 [hep-th].

[100] W. Cottrell and M. Montero, "Complexity is simple!," JHEP **02** (2018) 039, arXiv:1710.01175 [hep-th].

[101] C. Cheung, J. Liu, and G. N. Remmen, "Proof of the Weak Gravity Conjecture from Black Hole Entropy," JHEP **10** (2018) 004, arXiv:1801.08546 [hep-th].

[102] Y. Hamada, T. Noumi, and G. Shiu, "Weak Gravity Conjecture from Unitarity and Causality," Phys. Rev. Lett. **123** no. 5, (2019) 051601, arXiv:1810.03637 [hep-th].

[103] A. Urbano, "Towards a proof of the Weak Gravity Conjecture," arXiv:1810.05621 [hep-th].

[104] M. Montero, "A Holographic Derivation of the Weak Gravity Conjecture," JHEP **03** (2019) 157, arXiv:1812.03978 [hep-th].

[105] H. Ooguri and L. Spodyneiko, "New Kaluza-Klein instantons and the decay of AdS vacua," Phys. Rev. D **96** no. 2, (2017) 026016, arXiv:1703.03105 [hep-th].

[106] T. Banks and L. J. Dixon, "Constraints on String Vacua with Space-Time Supersymmetry," Nucl. Phys. B **307** (1988) 93–108.

[107] M. Montero, A. M. Uranga, and I. Valenzuela, "A Chern-Simons Pandemic," JHEP **07** (2017) 123, arXiv:1702.06147 [hep-th].

[108] C. Cheung and G. N. Remmen, "Naturalness and the Weak Gravity Conjecture," Phys. Rev. Lett. **113** (2014) 051601, arXiv:1402.2287 [hep-ph].

[109] B. Heidenreich, M. Reece, and T. Rudelius, "Sharpening the Weak Gravity Conjecture with Dimensional Reduction," JHEP **02** (2016) 140, arXiv:1509.06374 [hep-th].

[110] J. Polchinski, "Monopoles, duality, and string theory," Int. J. Mod. Phys. A **19S1** (2004) 145–156, arXiv:hep-th/0304042.

[111] E. Palti, "The Weak Gravity Conjecture and Scalar Fields," JHEP **08** (2017) 034, arXiv:1705.04328 [hep-th].

[112] G. Obied, H. Ooguri, L. Spodyneiko, and C. Vafa, "De Sitter Space and the Swampland," arXiv:1806.08362 [hep-th].

[113] P. Agrawal, G. Obied, P. J. Steinhardt, and C. Vafa, "On the Cosmological Implications of the String Swampland," Phys. Lett. B **784** (2018) 271–276, arXiv:1806.09718 [hep-th].

[114] J. M. Maldacena and C. Nunez, "Supergravity description of field theories on curved manifolds and a no go theorem," Int. J. Mod. Phys. **A16** (2001) 822–855, arXiv:hep-th/0007018 [hep-th]. [,182(2000)].

[115] M. P. Hertzberg, S. Kachru, W. Taylor, and M. Tegmark, "Inflationary Constraints on Type IIA String Theory," JHEP **12** (2007) 095, arXiv:0711.2512 [hep-th].

[116] D. Junghans, "Weakly Coupled de Sitter Vacua with Fluxes and the Swampland," JHEP **03** (2019) 150, arXiv:1811.06990 [hep-th].

[117] H. Ooguri, E. Palti, G. Shiu, and C. Vafa, "Distance and de Sitter Conjectures on the Swampland," Phys. Lett. B **788** (2019) 180–184, arXiv:1810.05506 [hep-th].

[118] A. Bedroya and C. Vafa, "Trans-Planckian Censorship and the Swampland," JHEP **09** (2020) 123, arXiv:1909.11063 [hep-th].

[119] S. Kachru, R. Kallosh, A. D. Linde, and S. P. Trivedi, "De Sitter vacua in string theory," Phys. Rev. D **68** (2003) 046005, arXiv:hep-th/0301240.

[120] J. Polchinski, "Brane/antibrane dynamics and KKLT stability," arXiv:1509.05710 [hep-th].

[121] R. Kallosh, A. Linde, E. McDonough, and M. Scalisi, "de Sitter Vacua with a Nilpotent Superfield," Fortsch. Phys. **67** no. 1-2, (2019) 1800068, arXiv:1808.09428 [hep-th].

[122] S. Kachru and S. P. Trivedi, "A comment on effective field theories of flux vacua," Fortsch. Phys. **67** no. 1-2, (2019) 1800086, arXiv:1808.08971 [hep-th].

[123] J. Moritz, A. Retolaza, and A. Westphal, "Toward de Sitter space from ten dimensions," Phys. Rev. D **97** no. 4, (2018) 046010, arXiv:1707.08678 [hep-th].

[124] S. Sethi, "Supersymmetry Breaking by Fluxes," JHEP **10** (2018) 022, arXiv:1709.03554 [hep-th].

[125] X. Gao, A. Hebecker, and D. Junghans, "Control issues of KKLT," arXiv:2009.03914 [hep-th].

[126] U. H. Danielsson and T. Van Riet, "What if string theory has no de Sitter vacua?," Int. J. Mod. Phys. D **27** no. 12, (2018) 1830007, arXiv:1804.01120 [hep-th].

[127] T. W. Grimm, E. Palti, and I. Valenzuela, "Infinite Distances in Field Space and Massless Towers of States," JHEP **08** (2018) 143, arXiv:1802.08264 [hep-th].

[128] B. Heidenreich, M. Reece, and T. Rudelius, "Emergence of Weak Coupling at Large Distance in Quantum Gravity," Phys. Rev. Lett. **121** no. 5, (2018) 051601, arXiv:1802.08698 [hep-th].

[129] B. Heidenreich, M. Reece, and T. Rudelius, "The Weak Gravity Conjecture and Emergence from an Ultraviolet Cutoff," Eur. Phys. J. C **78** no. 4, (2018) 337, arXiv:1712.01868 [hep-th].

[130] P. Corvilain, T. W. Grimm, and I. Valenzuela, "The Swampland Distance Conjecture for Kähler moduli," JHEP **08** (2019) 075, arXiv:1812.07548 [hep-th].

[131] E. Palti, "The Swampland: Introduction and Review," Fortsch. Phys. **67** no. 6, (2019) 1900037, arXiv:1903.06239 [hep-th].

[132] J. Calderón-Infante, A. M. Uranga, and I. Valenzuela, "The Convex Hull Swampland Distance Conjecture and Bounds on Non-geodesics," arXiv:2012.00034 [hep-th].

[133] P. S. Aspinwall, "Minimum distances in nontrivial string target spaces," Nucl. Phys. B **431** (1994) 78–96, arXiv:hep-th/9404060.

[134] D. Erkinger and J. Knapp, "Refined swampland distance conjecture and exotic hybrid Calabi-Yaus," JHEP **07** (2019) 029, arXiv:1905.05225 [hep-th].

[135] W. Schmid, "Variation of hodge structure: The singularities of the period mapping," Inventiones mathematicae **22** no. 3, (Sep, 1973) 211–319. https://doi.org/10.1007/BF01389674.

[136] R. Álvarez-García and L. Schlechter, "To appear,".

[137] M. Cvetic, R. Donagi, J. Halverson, and J. Marsano, "On Seven-Brane Dependent Instanton Prefactors in F-theory," JHEP **11** (2012) 004, arXiv:1209.4906 [hep-th].

[138] R. Donagi and M. Wijnholt, "MSW Instantons," JHEP **06** (2013) 050, arXiv:1005.5391 [hep-th].

[139] F. Ruehle and C. Wieck, "One-loop Pfaffians and large-field inflation in string theory," Phys. Lett. B **769** (2017) 289–298, arXiv:1702.00420 [hep-th].

[140] L. McAllister, P. Schwaller, G. Servant, J. Stout, and A. Westphal, "Runaway Relaxion Monodromy," JHEP **02** (2018) 124, arXiv:1610.05320 [hep-th].

[141] M. R. Douglas and S. Kachru, "Flux compactification," Rev. Mod. Phys. **79** (2007) 733–796, arXiv:hep-th/0610102.

[142] A. Giryavets, S. Kachru, P. K. Tripathy, and S. P. Trivedi, "Flux compactifications on Calabi-Yau threefolds," JHEP **04** (2004) 003, arXiv:hep-th/0312104.

[143] F. Denef, M. R. Douglas, and B. Florea, "Building a better racetrack," JHEP **06** (2004) 034, arXiv:hep-th/0404257.

[144] M. Demirtas, M. Kim, L. Mcallister, and J. Moritz, "Vacua with Small Flux Superpotential," Phys. Rev. Lett. **124** no. 21, (2020) 211603, arXiv:1912.10047 [hep-th].

[145] M. Demirtas, M. Kim, L. Mcallister, and J. Moritz, "Conifold Vacua with Small Flux Superpotential," arXiv:2009.03312 [hep-th].

[146] R. Kallosh, A. Linde, E. McDonough, and M. Scalisi, "4D models of de Sitter uplift," Phys. Rev. D **99** no. 4, (2019) 046006, arXiv:1809.09018 [hep-th].

[147] F. Gautason, V. Van Hemelryck, and T. Van Riet, "The Tension between 10D Supergravity and dS Uplifts," Fortsch. Phys. **67** no. 1-2, (2019) 1800091, arXiv:1810.08518 [hep-th].

[148] Y. Hamada, A. Hebecker, G. Shiu, and P. Soler, "On brane gaugino condensates in 10d," JHEP **04** (2019) 008, arXiv:1812.06097 [hep-th].

[149] Y. Hamada, A. Hebecker, G. Shiu, and P. Soler, "Understanding KKLT from a 10d perspective," JHEP **06** (2019) 019, arXiv:1902.01410 [hep-th].

[150] F. Carta, J. Moritz, and A. Westphal, "Gaugino condensation and small uplifts in KKLT," JHEP **08** (2019) 141, arXiv:1902.01412 [hep-th].

[151] F. Gautason, V. Van Hemelryck, T. Van Riet, and G. Venken, "A 10d view on the KKLT AdS vacuum and uplifting," JHEP **06** (2020) 074, arXiv:1902.01415 [hep-th].

[152] I. Bena, M. Graña, N. Kovensky, and A. Retolaza, "Kähler moduli stabilization from ten dimensions," JHEP **10** (2019) 200, arXiv:1908.01785 [hep-th].

[153] R. Blumenhagen, M. Brinkmann, D. Kläwer, A. Makridou, and L. Schlechter, "KKLT and the Swampland Conjectures," PoS **CORFU2019** (2020) 158, arXiv:2004.09285 [hep-th].

[154] M. R. Douglas, J. Shelton, and G. Torroba, "Warping and supersymmetry breaking," arXiv:0704.4001 [hep-th].

[155] I. Bena, E. Dudas, M. Graña, and S. Lüst, "Uplifting Runaways," Fortsch. Phys. **67** no. 1-2, (2019) 1800100, arXiv:1809.06861 [hep-th].

[156] R. Blumenhagen, D. Kläwer, and L. Schlechter, "Swampland Variations on a Theme by KKLT," JHEP **05** (2019) 152, arXiv:1902.07724 [hep-th].

[157] I. Bena, A. Buchel, and S. Lüst, "Throat destabilization (for profit and for fun)," arXiv:1910.08094 [hep-th].

[158] E. Dudas and S. Lüst, "An update on moduli stabilization with antibrane uplift," arXiv:1912.09948 [hep-th].

[159] L. Randall, "The Boundaries of KKLT," Fortsch. Phys. **68** no. 3-4, (2020) 1900105, arXiv:1912.06693 [hep-th].

[160] P. Candelas, X. C. De La Ossa, P. S. Green, and L. Parkes, "A Pair of Calabi-Yau manifolds as an exactly soluble superconformal theory," AMS/IP Stud. Adv. Math. **9** (1998) 31–95.

[161] G. Curio, A. Klemm, D. Lüst, and S. Theisen, "On the vacuum structure of type II string compactifications on Calabi-Yau spaces with H fluxes," Nucl. Phys. B **609** (2001) 3–45, arXiv:hep-th/0012213.

[162] R. Blumenhagen, D. Herschmann, and F. Wolf, "String Moduli Stabilization at the Conifold," JHEP **08** (2016) 110, arXiv:1605.06299 [hep-th].

[163] A. Klemm, "CY 3-folds over finite fields, Black hole attractors, and D-brane masses.". in "Simons Collaboration on Special Holonomy in Geometry, Analysis, and Physics," SCGP Stony Brook, September 8-11 2019.

[164] S. B. Giddings, S. Kachru, and J. Polchinski, "Hierarchies from fluxes in string compactifications," Phys. Rev. D **66** (2002) 106006, arXiv:hep-th/0105097.

[165] I. R. Klebanov and M. J. Strassler, "Supergravity and a confining gauge theory: Duality cascades and chi SB resolution of naked singularities," JHEP **08** (2000) 052, arXiv:hep-th/0007191.

[166] S. B. Giddings and A. Maharana, "Dynamics of warped compactifications and the shape of the warped landscape," Phys. Rev. D **73** (2006) 126003, arXiv:hep-th/0507158.

[167] G. Shiu, G. Torroba, B. Underwood, and M. R. Douglas, "Dynamics of Warped Flux Compactifications," JHEP **06** (2008) 024, arXiv:0803.3068 [hep-th].

[168] E. Witten, "Instability of the kaluza-klein vacuum," Nuclear Physics B **195** no. 3, (1982) 481 – 492. http://www.sciencedirect.com/science/article/pii/0550321382900074.

[169] I. n. García Etxebarria, M. Montero, K. Sousa, and I. Valenzuela, "Nothing is certain in string compactifications," JHEP **12** (2020) 032, arXiv:2005.06494 [hep-th].

[170] H. Ooguri and C. Vafa, "Non-supersymmetric AdS and the Swampland," Adv. Theor. Math. Phys. **21** (2017) 1787–1801, arXiv:1610.01533 [hep-th].

[171] B. Freivogel and M. Kleban, "Vacua Morghulis," arXiv:1610.04564 [hep-th].

[172] A. Sen, "Universality of the tachyon potential," JHEP **12** (1999) 027, arXiv:hep-th/9911116.

[173] M. Schnabl, "Analytic solution for tachyon condensation in open string field theory," Adv. Theor. Math. Phys. **10** no. 4, (2006) 433–501, arXiv:hep-th/0511286.

[174] L. Rastelli, A. Sen, and B. Zwiebach, "Vacuum string field theory," 6, 2001. arXiv:hep-th/0106010.

[175] A. Adams, J. Polchinski, and E. Silverstein, "Don't panic! Closed string tachyons in ALE space-times," JHEP **10** (2001) 029, arXiv:hep-th/0108075.

[176] S. Hellerman, "On the landscape of superstring theory in D > 10," arXiv:hep-th/0405041.

[177] S. Hellerman and X. Liu, "Dynamical dimension change in supercritical string theory," arXiv:hep-th/0409071.

[178] S. Hellerman and I. Swanson, "Dimension-changing exact solutions of string theory," JHEP **09** (2007) 096, arXiv:hep-th/0612051.

[179] S. Hellerman and I. Swanson, "A Stable vacuum of the tachyonic E(8) string," arXiv:0710.1628 [hep-th].

[180] V. A. Kostelecky and S. Samuel, "Collective Physics in the Closed Bosonic String," Phys. Rev. D **42** (1990) 1289–1292.

[181] A. Belopolsky, "Effective Tachyonic potential in closed string field theory," Nucl. Phys. B **448** (1995) 245–276, arXiv:hep-th/9412106.

[182] H. Yang and B. Zwiebach, "A Closed string tachyon vacuum?," JHEP **09** (2005) 054, arXiv:hep-th/0506077.

[183] N. Moeller and H. Yang, "The Nonperturbative closed string tachyon vacuum to high level," JHEP **04** (2007) 009, arXiv:hep-th/0609208.

[184] N. Moeller, "Closed Bosonic String Field Theory at Quintic Order: Five-Tachyon Contact Term and Dilaton Theorem," JHEP **03** (2007) 043, arXiv:hep-th/0609209.

[185] P. C. West, "The Spontaneous compactification of the closed bosonic string," Phys. Lett. B **548** (2002) 92–96, arXiv:hep-th/0208214.

[186] D. Lüst, "Covariant fermionic and heterotic strings from the bosonic string," Nuclear Physics B **292** (1987) 381–399. https://www.sciencedirect.com/science/article/pii/0550321387906511.

[187] L. Schlechter, "Closed Bosonic String Tachyon Potential from the $\mathcal{N} = 1$ Point of View," arXiv:1905.09621 [hep-th].

[188] P. Goddard and C. B. Thorn, "Compatibility of the Dual Pomeron with Unitarity and the Absence of Ghosts in the Dual Resonance Model," Phys. Lett. B **40** (1972) 235–238.

[189] C. M. Hull and R. R. Khuri, "Branes, times and dualities," Nucl. Phys. B **536** (1998) 219–244, arXiv:hep-th/9808069.

[190] C. M. Hull, "Timelike T duality, de Sitter space, large N gauge theories and topological field theory," JHEP **07** (1998) 021, arXiv:hep-th/9806146 [hep-th].

[191] C. M. Hull, "Duality and the signature of space-time," JHEP **11** (1998) 017, arXiv:hep-th/9807127 [hep-th].

[192] I. Quiros, "Time-like versus space-like extra dimensions," arXiv:0707.0714 [gr-qc].

[193] P. Di Vecchia and A. Liccardo, "D Branes in String Theory, I," NATO Sci. Ser. C **556** (2000) 1–60, arXiv:hep-th/9912161 [hep-th].

[194] P. Di Vecchia and A. Liccardo, "D-branes in string theory. 2.," in YITP Workshop on Developments in Superstring and M Theory Kyoto, Japan, pp. 7–48. 1999. arXiv:hep-th/9912275 [hep-th].

[195] R. Blumenhagen and E. Plauschinn, "Introduction to conformal field theory," Lect. Notes Phys. **779** (2009) 1–256.

[196] A. Recknagel and V. Schomerus,
Boundary Conformal Field Theory and the Worldsheet Approach to D-Branes.
Cambridge Monographs on Mathematical Physics. Cambridge University Press,
2013. http://www.cambridge.org/9780521832236.

[197] C. Angelantonj and A. Sagnotti, "Open strings," Phys. Rept. **371** (2002) 1–150,
arXiv:hep-th/0204089 [hep-th]. [Erratum: Phys. Rept.376,no.6,407(2003)].

[198] B. H. Lian and S.-T. Yau, "Arithmetic properties of mirror map and quantum
coupling," Commun. Math. Phys. **176** (1996) 163–192, arXiv:hep-th/9411234.

[199] A. Ashmore and F. Ruehle, "Moduli-dependent KK towers and the Swampland
Distance Conjecture on the Quintic," arXiv:2103.07472 [hep-th].

[200] W. Yang, "Double zeta values and Picard-Fuchs equation," arXiv:1910.09576
[math.NT].

[201] D. Maitre, "HPL, a mathematica implementation of the harmonic polylogarithms,"
Comput. Phys. Commun. **174** (2006) 222–240, arXiv:hep-ph/0507152.